

**Exploring the genetics underlying the Zn deficiency  
response in *Arabidopsis thaliana***

Andrea Valeria Ochoa Tufiño

## **Thesis committee**

### **Promotor**

Prof. Dr M.G.M. Aarts

Personal chair at the Laboratory of Genetics

Wageningen University & Research

### **Co-promotor**

Prof. Dr M. Koornneef

Personal chair at the Laboratory of Genetics

Wageningen University & Research

### **Other members**

Prof. Dr G.H. Immink, Wageningen University & Research

Dr H. Schat, VU Amsterdam

Dr A.G.L. Assunção, University of Copenhagen, Denmark

Dr S. Merlot, French National Centre for Scientific Research (CNRS), Gif sur Yvette, France

This research was conducted under the auspices of the Graduate School of Experimental Plant Sciences (EPS).

# Exploring the genetics underlying the Zn deficiency response in *Arabidopsis thaliana*

Andrea Valeria Ochoa Tufiño

## Thesis

submitted in fulfilment of the requirements for the degree of doctor  
at Wageningen University

by the authority of the Rector Magnificus,

Prof. Dr A.P.J. Mol,

in the presence of the

Thesis Committee appointed by the Academic Board

to be defended in public

on Friday 5 October 2018

at 11 a.m. in the Aula.

Andrea Valeria Ochoa Tufiño

Exploring the genetics underlying the Zn deficiency response in *Arabidopsis thaliana*,  
218 pages.

PhD thesis, Wageningen University, Wageningen, the Netherlands (2018)

With references, with summary in English

ISBN 978-94-6343-339-6

DOI <https://doi.org/10.18174/458236>



## Table of Contents

<b>Chapter 1:</b> General Introduction .....	7
<b>Chapter 2:</b> Uncovering Zn transporters induced by Zn deficiency.....	17
<b>Chapter 3:</b> Disruption of N-terminal-acetylation disturbs mineral homeostasis in <i>Arabidopsis thaliana</i> .....	49
<b>Chapter 4:</b> Exploring <i>Arabidopsis thaliana</i> natural genetic variation to identify genes underlying the Zn deficiency response.....	87
<b>Chapter 5:</b> A conserved cluster of tandemly arrayed <i>HIPP</i> genes affects tolerance to Fe and Zn deficiency in <i>Arabidopsis thaliana</i> .....	123
<b>Chapter 6:</b> General Discussion .....	155
<b>References</b> .....	171
<b>Summary</b> .....	207
<b>Acknowledgments</b> .....	211
<b>Curriculum Vitae</b> .....	213
<b>Educational Statement</b> .....	215



# **Chapter 1**

## **General Introduction**

### Zinc is essential for life

Zinc (Zn) is an essential element for all living organisms. It is involved in a wide range of biological processes due to its particular chemistry, which makes biological systems choose Zn, rather than other elements, such as Iron (Fe) or Copper (Cu) in certain biochemical processes. Firstly, the oxidation state (+2) of Zn does not change under physiological conditions, due to the lack of unpaired electrons and its electron configuration with no unfilled d subshells (Barak and Helmke, 1993; Krężel and Maret, 2016). Therefore, I will refer to  $\text{Zn}^{2+}$  simply as Zn in the rest of this thesis. The Zn redox stability favours the role of Zn as the cofactor of enzymes involved in redox reactions. The kind of reactions mentioned above can lead to the generation of damaging radicals in delicate processes, such as DNA or RNA synthesis (Park et al., 1999). Secondly, Zn has low coordination number sites that are strongly acidic. The Zn coordination is specific for Sulphur (S), Nitrogen (N), and Oxygen (O). Consequently, it binds to the side chains of histidine, glutamate, aspartate, and/or cysteine in proteins (Barak and Helmke, 1993). Thirdly, Zn has flexible coordination geometries with different ligands, this feature facilitates the reactions of enzymes of catalysis (Williams, 1984).

Zinc was not considered as an essential element for any living organism until 1869, when J. Raulin, a student of Louis Pasteur, reported that Zn was required for growth of the fungus *Aspergillus niger* (Raulin, 1869). A half-century later, Mazé reported that *Zea mays* (maize) plants required Zn for growth (Mazé, 1914). However, this finding was questioned for inconsistent reproducibility. Fortunately, those results stimulated investigations to obtain more conclusive evidence. In 1926, Zn became generally recognised as essential for higher plants, after Sommer and Lipman showed the effects of Zn deficiency in *Hordeum vulgare* (barley) and *Helianthus annuus* (sunflower), which were grown hydroponically (Sommer and Lipman, 1926). In 1934, Zn was established as essential for higher animals by Todd, Elvehjem and Hart (Todd et al., 1980). In 1961, it was documented that Zn was essential for humans, after Prasad studied cases of Zn deficiency in Iran and Egypt (Prasad et al., 1963).

### Zinc deficiency

An adult human body contains an average of 2.5 grams of Zn, and a person should consume 8 to 15 mg of Zn per day in the diet (Royal Society of Chemistry; U.S. Department of Health & Human Services). Zinc deficiency affects two billion people in the world (Prasad, 2003; Müller and Krawinkel, 2005). Around 2800 human proteins contain zinc-binding domains, corresponding to 10% of the human proteome, 40% of them are transcription factors and the

rest are mainly enzymes (Andreini et al., 2006). Zinc is involved in a multitude of biochemical processes associated with immunity, wound healing, growth, communication among cells, such as cells in the salivary gland or neurons (Roohani et al., 2013). Zn deficiency causes a broad range of symptoms, depending upon the severity of the condition. Mild Zn deficiency is the most important numerically (Roohani et al., 2013), and its symptoms are growth retardation, impaired immunity, cognitive impairment, neurological disorders, and delayed wound healing (Prasad, 2012). Zinc deficiency increases young children's risks to suffer diarrhoeal disease, pneumonia, and malaria (Caulfield and Black, 2004; Black et al., 2008), which accounts for 29% of all deaths of children under five years old (World Health Organisation; Global Health Observatory data).

One of the strategies to improve Zn status in vulnerable human populations is through bio-fortification of crops. This strategy aims to increase the nutrients content of staple food through agronomical practices and genetic improvement (Roohani et al., 2013). In low- and middle-income regions the population diet relies on staple food, such as cereals, if these crops are grown on Zn deficient soils, their edible parts will be Zn deficient, as well. Thus, in low- and middle-income regions, Zn deficiency in humans is strongly correlated with Zn deficiency in soils. (Müller and Krawinkel, 2005; Alloway, 2009; Beal et al., 2017).

After recognising Zn as an essential element for living organisms, people gave attention to Zn deficiency in the soil. In 1990, the FAO published a report on soil samples from around the world indicating that half of them were Zn deficient (FAO, Soils Bulletins). The availability of Zn to plants in soils is affected by factors, such as low Zn concentration, high pH, high organic matter content, high moisture, and high concentrations of calcite, bicarbonate, Phosphorous (P), Magnesium (Mg), Sodium (Na), and Calcium (Ca). The low Zn concentration in soils can be solved by the application of fertilizers, as long as the deficiency is identified. When Zn deficiency is marginal in soils, symptoms of Zn deficiency in the crops are hidden and easily confused with deficiencies in other nutrients, such as Fe. As a result, the crops yield and quality are reduced without a clear reason (Alloway, 2009). In severe, Zn deficient soils, crops visible symptoms are: stunted growth, short internodes, interveinal chlorosis, small leaves, reddish-brown leaves, inward curled leaves and reduced yield (Cakmak, 2008; Alloway, 2009; Marschner and Marschner, 2012; Nielsen, 2012; Yruela, 2013; Mattiello et al., 2015).

### **Zn homeostasis in plants**

Zn homeostasis regulates the acquisition, redistribution and storing of Zn according to internal demands and external conditions (Sinclair and Krämer, 2012). Zn concentration varies in a narrow range within the cell, due to its buffering system, which is based on high-affinity binding to proteins and transport processes (Krężel and Maret, 2016). Zn homeostasis is driven by metal transporters, chelators, transcription factors, and post-transcription regulators (Sinclair and Krämer, 2012; Assunção et al., 2013).

Zn transport begins with the uptake of free  $\text{Zn}^{2+}$  from the soil across the plasma membrane of root cells. Within the symplast, Zn can be chelated (Haydon and Cobbett, 2007), or kept as free Zn (Sinclair and Krämer, 2012) to either be stored in root cell vacuoles or continue with radial transport until the stele (Claus et al., 2013). In the stele, Zn is uploaded into xylem to be translocated to the shoot. In shoot tissues, Zn is immediately used, stored or remobilised to different tissues via phloem to meet the plant requirements (Blindauer and Schmid, 2010; Sinclair and Krämer, 2012).

The Zn deficiency response cascade starts when plants are exposed to low Zn supply. This response is regulated by the transcription factors BASIC-REGION LEUCINE-ZIPPER 19 (bZIP19) and bZIP23. These two transcription factors work together to positively regulate the expression of genes mainly involved in Zn transport (Assunção et al., 2010), which facilitate the acquisition of Zn and its distribution in the plant.

The main transporters involved in the Zn root uptake belong to the ZRT-IRT-like protein (ZIP) family. The members of this ZIP family mainly transport Zn, however, they show variation in substrate range and specificity with other divalent cations, like Fe or Manganese (Mn). The coding sequences of *ZIP1*, *ZIP2*, *ZIP3*, *ZIP4*, *ZIP5*, *ZIP6*, *IRT1*, *IRT2*, or *IRT3* are able to complement the yeast Zn-uptake-defective mutant (Korshunova et al., 1999; Vert et al., 2001; Lin et al., 2009; Assunção et al., 2010; Milner et al., 2013). ZIP proteins are associated with symplast Zn influx (Eide, 2006; Milner et al., 2013). Ten (*ZIP1*, *ZIP3*, *ZIP4*, *ZIP5*, *ZIP9*, *ZIP10*, *ZIP11*, *ZIP12*, and *IRT3*) of the fifteen members of the ZIP family, increase their expression under Zn deficiency with higher levels in roots than in shoots (Wintz et al., 2003; van de Mortel et al., 2006; Campos, 2015; Campos et al., 2017).

For Zn to be translocated to shoots, it first needs to enter into the stele of the root. Roots are complex structures with different types of cells that contribute to nutrients acquisition, sequestration, and delivery to the xylem. Root nutrients, including Zn, move radially from the outer root layers (epidermis, cortex, and endodermis) into the root vasculature for further translocation. Nutrients can move via the apoplastic route through cell walls and spaces between cells, via the symplastic route by transporters, which take them up into the cells and then move from cell to cell through plasmodesmata, or via a combination of both routes. The apoplastic route mainly takes place in younger zones of the root. As long as the root keeps getting older, it starts to develop the Casparian strip, which is a poorly ion-permeable belt that makes the endodermis a barrier to the free diffusion of solutes into the stele, and just allows the symplastic movement of nutrients (Clarkson, 1993; Tester and Leigh, 2001; Geldner, 2013; Barberon and Geldner, 2014). When the root becomes even older, a suberin layer develops around all sides of the endodermis, which just allows the cross of elements through plasmodesmata or passage cells to enter the root stele (Clarkson, 1993; Tester and Leigh, 2001; Geldner, 2013; Barberon and Geldner, 2014).

Within the root stele, the off-loading of Zn from parenchyma cells into the stele apoplast is facilitated by members of the Heavy-Metal-ATPases (HMA) family of cation transporters energised by hydrolysis of ATP. Within the apoplast, Zn can be loaded into xylem vessels for later translocation (Axelsen and Palmgren, 2001; Baxter et al., 2003; Eren and Argüello, 2004). Among the members of the HMA family, *HMA2* is the only one induced by Zn deficiency (van de Mortel et al., 2006), however, only the double *hma2/hma4* mutant shows decreased Zn concentration in shoots. The long-distance Zn transport is also mediated by the PLANT CADMIUM RESISTANCE 2 (PCR2) protein, which is a Zn symplast efflux transporter expressed in the epidermis and xylem parenchyma. It functions in the Zn removal from the roots in a mechanism independent of HMA4 and HMA2 proteins (Song et al., 2010).

Zn transporters mediate the mobilization of free Zn or Zn chelated to ligands as glutathione, citrate, and oligopeptides such as nicotianamine (NA) (Krężel and Maret, 2016). For instance, members of the YELLOW STRIPE-LIKE (YSL) protein family are involved in the metal-NA complex transport. Within shoots, the double *ysl1/ysl3* mutant fails to remobilize Zn from senescing leaves into seeds (Waters et al., 2006). The Zn phloem transport is still poorly investigated, and probably more genes, apart from *YSL1* and *YSL3*, are involved in this process.

Several proteins involved in Zn transport are also able to bind to other divalent cations, such as Cadmium (Cd), Cobalt (Co), Cu, Fe, Mn, Nickel (Ni), and Lead (Pb). (Henriques et al., 2002; Eren and Argüello, 2004; Puig and Peñarrubia, 2009; Sinclair and Krämer, 2012; Milner et al., 2013). The Irving-William series of divalent metal ions ( $\text{Cu} > \text{Zn} > \text{Ni} > \text{Co} > \text{Fe} > \text{Mn} > \text{Mg} > \text{Ca}$ ) shows that micronutrients, such as Cu and Zn have a higher affinity than macronutrients, such as Mg and Calcium (Ca) to a model chelate (Williams, 1984). The overlapping substrate specificities, interactions and relationships among elements can cause large disequilibria in the full plant ionome due to the deficiency of just one of the elements (Huang et al., 2000; Graham, 2008; Nichols et al., 2012; Nishida et al., 2015).

### **Arabidopsis the model plant for research**

*Arabidopsis thaliana* (Arabidopsis) is a very useful organism for the discovery and study of novel gene functions. Arabidopsis is the favourite model organism for plant research (Koornneef and Meinke, 2010). Some of the reasons are: its short life cycle, small size, self-pollination, production of a large number of seeds, ease of crossing (Meinke et al., 1998), small size of the genome (Somerville, 1999; The Arabidopsis Genome, 2000), easy and high efficient plant transformation (Clough and Bent, 1998), and large natural variation (Koornneef et al., 2004). A large number of Arabidopsis resources are available for research, and there is an active exchange of stocks among researches (Koornneef and Meinke, 2010). Arabidopsis stock centres include collections of natural accessions and single mutant lines, available to be ordered. In addition, databases and online tools with sequences information, gene expression, protein-protein interaction, gene networks, gene ontology among others are available to the public (Provar et al., 2016). Arabidopsis intrinsic characteristics, ease of manipulation and availability of resources facilitate researches work at the moment to formulate hypotheses, design experiments and interpret results.

Arabidopsis is widely used to implement and optimise new technologies. It has been extensively used in forward genetics by the generation of randomly mutagenized populations to identify mutants of interest (Page and Grossniklaus, 2002). In reverse genetics, the use of transferred DNA (T-DNA) has been a unique tool for gene functional studies (Page and Grossniklaus, 2002; Meinke et al., 2003). In cell biology, the convergence of Arabidopsis, microscopy and fluorescent proteins has been essential to fulfil genes functional analyses (Tian et al., 2004; Sappl and Heisler, 2013). The high level of variation among Arabidopsis natural accessions (Koornneef and Meinke, 2010) is exploited for the identification of causal polymorphisms. This



can be done for instance by biparental populations or Genome-Wide Associations (GWA) approaches (Nordborg and Weigel, 2008). The GWA approach overcomes the problems of generating a segregating population and the limited resolution of biparental populations (Kim et al., 2007; Nordborg and Weigel, 2008).

Knowledge generated in *Arabidopsis* has illuminated the fundamentals of plant biology and help to improve properties of crops (Koornneef and Meinke, 2010; Provart et al., 2016). Several plant mechanisms, including interaction among genes, regulatory loops, biosynthetic pathways of phytohormones, plant immunity, sensing and response to abiotic stress have been discovered due to the research conducted in *Arabidopsis* (Provart et al., 2016).

### **The scope of the thesis**

The main aim of this thesis is to increase the knowledge of Zn deficiency response in the model plant *Arabidopsis thaliana*. **Chapter 2** describes the functional analyses of Zn transporters induced as a response to Zn deficiency. The gene expression of these transporters is mapped to their location in the root at the cellular level and evaluated through time during Zn deficiency. In addition, the effect of loss of function mutants of Zn transporters is analysed based on the Zn distribution in roots and the sensitivity to Zn deficiency.

After showing in Chapter 2, Zn transporters that belong to Zn deficiency response, I searched for new players involved in Zn homeostasis. In **Chapter 3**, I describe a forward genetic approach to search for regulators of the Zn deficiency response cascade. A mutation in the *N-ALPHA-TERMINAL ACETYLTRANSFERASE 25 (NAA25)* gene, involved in protein acetylation, affected several pleiotropic traits including aberrant regulation of the Zn deficiency response, biotic defence response and enhanced susceptibility to Fe deficiency.

In **Chapter 4**, a different approach is taken to find new Zn deficiency players. In this case, the ionome natural variation in 350 natural accessions of *Arabidopsis* grown under normal and low Zn supply was used in a Genome-Wide Association (GWA) analysis to identify significant loci associated with micronutrients concentrations. Several loci were associated and candidate genes within those loci were selected to validate their role in Zn deficiency tolerance. T-DNA insertion lines disrupting the sequence of the candidate genes showed significant changes in Cu, Fe, Mn, Molybdenum (Mo), and/or Zn concentration due to Zn deficiency.

**Chapter 5**, was the direct result of the GWAS in Chapter 4. In this Chapter, the functional analyses of a cluster of tandemly arrayed *HEAVY METAL-ASSOCIATED ISOPRENYLATED PLANT PROTEINS (HIPP)* genes are described. The functional analyses provided information about the expression regulation, interaction with transcription regulators, and tolerance to adverse Zn and Fe supply due to the loss function of single *HIPPs*.

Finally, in **Chapter 6**, I discuss the main results obtained in my thesis research, their importance for the knowledge of Zn homeostasis, and future research paths to take this research further.





# Chapter 2

## Uncovering Zn transporters induced by Zn deficiency

Valeria Ochoa Tufiño<sup>1,2</sup>, Maria Almira Casellas<sup>1</sup>, Aron van Duynhoven<sup>1</sup> and Mark G.M. Aarts<sup>1</sup>

- 1) Laboratory of Genetics, Wageningen University, Wageningen, The Netherlands
- 2) Current affiliation: Departamento de Ciencias de la Vida, Universidad de las Fuerzas Armadas ESPE, Sangolquí, Ecuador

*In preparation for submission*

### Abstract

Plants are sessile organisms which have developed several strategies to cope with variable nutrients concentrations in soils to avoid either toxicity or nutrients deficiency. One of the most widespread micronutrient deficiencies in soils is Zn deficiency. To cope with Zn deficiency, plants adjust their Zn homeostasis by inducing the expression of Zn transporters. In order to learn more about the role of Zn transporters induced by Zn deficiency, we performed functional analyses on them. We followed their gene expression induction through time by qRT-PCR, mapped their cell layer expression in roots by using their promoter sequenced fused to YFP, and determined the effects of their loss of function by using single and double T-DNA insertion mutants. The Zn transporter genes' expression induction starts after six hours of exposure to Zn deficiency in roots and at day four in shoots, and the highest induction for most of the Zn transporters, in roots and shoots, is at day twelve. The Zn transporter *ZIP1* gene expresses in the endodermis and stele, *ZIP3* and *ZIP5* express in the epidermis and cortex, *IRT3* expresses from the epidermis to stele and *ZIP11* and *HMA2* in xylem parenchyma cells. The loss of function of single Zn transporters does not cause a significant effect in the overall plant performance when compared to wild-type plants. However, the Zn distribution in the root is disturbed in single mutants. Among double mutants, the *zip3/zip5* showed the highest sensitivity to Zn deficiency and was unable to uptake Zn during short periods of time. The lack of strong Zn deficient phenotypes in single mutants suggests that several Zn transporters have redundant functions, especially for the case of *ZIP3* and *ZIP5*.

## Introduction

Zn is an essential micronutrient for life, being the second most abundant transition element in all organisms. Zn deficiency in plants causes symptoms like stunted growth, chlorosis, reduced yield, among others (Cakmak, 2008; Alloway, 2009; Marschner and Marschner, 2012; Yruela, 2013; Mattiello et al., 2015). Luckily, plants are able to sense the shortage of Zn supply and adjust Zn homeostasis. The transcription factors BASIC REGION-LEUCINE ZIPPER 19 and 23 (bZIP19 and bZIP23) induce the expression of genes, among them some Zn transporter genes, to increase the Zn uptake capacity, enabling the plant to adapt to Zn deficiency stress (Assunção et al., 2010; Assunção et al., 2013). The main known Zn transporters belong to the families of the ZRT-IRT-like proteins (ZIP), heavy-metal ATPases (HMA), and cation diffusion facilitators (CDFs) (Eren and Argüello, 2004; Kobae et al., 2004; Eide, 2006; Sinclair and Krämer, 2012). Arabidopsis encodes fifteen ZIPs, most of them have been suggested to transport divalent cations from extracellular space or organelle lumen into the symplast (Eide, 2006). Several members of the ZIP family are associated with Zn transport due to differential gene expression, yeast functional complementation, and sequence similarity (Grotz et al., 1998; van de Mortel et al., 2006; Milner et al., 2013). Zn deficiency strongly induces gene expression in plants of *ZIP1*, *ZIP3*, *ZIP4*, *ZIP5*, *ZIP9*, *ZIP10*, *ZIP12*, and *IRT3* and in a less degree *ZIP2* and *ZIP11* (van de Mortel et al., 2006; Assunção et al., 2010; Campos, 2015). The coding sequences of the Arabidopsis genes *ZIP1*, *ZIP2*, *ZIP3*, *ZIP4*, *ZIP7*, *ZIP11*, *ZIP12*, *IRT1*, *IRT2*, and *IRT3* complement the growth defect of *zrt1zrt2*, a yeast mutant defective in Zn uptake (Grotz et al., 1998; Korshunova et al., 1999; Vert et al., 2001; Lin et al., 2009; Assunção et al., 2010; Milner et al., 2013). Proteins as IRT3 can transport Fe as well (Lin et al., 2009), ZIP1 and ZIP3 are highly specific for Zn transport, but Zn transport can be inhibited by increased concentrations of Mn, Co, Fe, Cd or Cu (Grotz et al., 1998). The gene expression response to Zn deficiency and the specificity for Zn as substrate strongly supports that ZIP1, ZIP3, ZIP4, and IRT3 transport Zn especially during Zn deficiency stress.

The CDFs and P1B ATPases transport cations from the symplast to the outside of the cell or into subcellular compartments. In plants, CDFs are usually called MTP (Metal Tolerance Proteins) (Paulsen and Saier Jr, 1997; Montanini et al., 2007). MTP1 and MTP3 are tonoplast localized and mediate the Zn efflux from the symplast to the vacuole (Kobae et al., 2004; Desbrosses-Fonrouge et al., 2005; Arrivault et al., 2006). The closest homologue of MTP1 and

MTP3 is MTP2 (Dräger et al., 2004) which is the only member of the MTP family induced by Zn deficiency (van de Mortel et al., 2006).

The P1B ATPases are cation transporters energized by hydrolysis of ATP. The sequence of the *HEAVY METAL ATPASE 3 (HMA3)* complements the *ycf1* yeast mutant Cd/Pb-hypersensitive and the Arabidopsis HMA3 loss-of-function mutant is sensitive to high concentrations of Zn and Cd. HMA3 is located in the tonoplast and is likely involved in Zn detoxification by vacuolar sequestration (Morel et al., 2009). HMA4 rescues the *zntA Escherichia coli* mutant sensitive to high Zn (Mills et al., 2003) and Arabidopsis HMA4 loss-of-function mutant accumulates less Zn in shoots than wild-type plants (Hussain et al., 2004). The HMA2 ATPase activity is activated by Zn and Cd and, to a lesser extent by Pb, Ni, Cu, and Co (Eren and Argüello, 2004) and its expression is induced by Zn deficiency (van de Mortel et al., 2006). *HMA2* and *HMA4* are expressed in the vasculature of roots, stems and leaves and promotes Zn translocation from roots to shoots (Hussain et al., 2004) (Sinclair et al., 2007). The double mutant *hma2/hma4* significantly decreases Zn concentration in shoots (Hussain et al., 2004).

Zinc can be transported in complex with organic molecules, such as citrate malate, histidine or nicotianamine (NA) (Beneš et al., 1983; Anderegg and Ripperger, 1989; Scholz et al., 1992). Zn-NA complex can be transported across membranes by members of the Yellow Stripe-Like (YSL) family of oligopeptide transporters, eg. YSL1 and YSL3 (Waters et al., 2006). The Zn-NA complex facilitates the Zn mobilization, by preventing Zn precipitation or binding with cell walls (Deinlein et al., 2012).

The Zn shoot supply depends on how effectively roots obtain Zn and make it available for translocation to other parts of the plant. In the roots, nutrients move radially through epidermis, cortex, and endodermis to enter the stele, where nutrients are loaded into the xylem. This transport can be apoplastic, i.e. by passive transport through cell walls and intercellular spaces, or symplastic, mediated by influx carriers (transporters) and subsequently from cell-to-cell through plasmodesmata, or in a combination of both, the coupled pathway, which combines influx and efflux carriers to transport nutrients from one cell to the other. Transport across the endodermis has to occur symplastically since Casparian strip prevents most of the apoplastic transport (Clarkson, 1993; Tester and Leigh, 2001; Geldner, 2013; Barberon and Geldner, 2014).



Previous studies of Zn transporters have not examined in detail the Zn transport in roots. With the aim of filling this research gap, we followed Zn fluxes using Zinpyr-1 in the roots of wild-type plants and loss-of-function mutants of the most well-known Zn transporters. Based on promoter studies and gene expression studies, we show the root cell layer(s) where each transporter is expressed and how their expression levels change over time. Moreover, we analyzed the general effect on plants of single and double loss-of-function Zn transporter mutants. These approaches provided us with information on how each of the studied Zn transporters contribute to the Zn uptake and transfer.

## Materials and Methods

### Plant material

T-DNA insertion lines for any of the Arabidopsis genes studied were ordered from NASC ([www.arabidopsis.info/BasicForm](http://www.arabidopsis.info/BasicForm)) (**Supplemental Table S1**). Arabidopsis accession Columbia was used for transformation and as a wild-type control.

### Growing conditions

Prior to germination, seeds were stratified for three days at 4°C in the dark. For propagation and genotyping, plants were grown in a greenhouse set at a 16/8 h light/dark cycle at 20/18°C day/night temperatures and 70% humidity. For Zn deficiency treatment, plants were grown hydroponically, in a climate-controlled growth chamber set at a 12/12 h light/dark cycle at 20/15°C day/night temperatures and 70% humidity. Seeds were surface-sterilized using vapor-phase seed sterilization (Clough and Bent, 1998) and sown on 0.55%-agar-filled tubes in trays containing a modified half-strength Hoagland's nutrient solution (Schat et al., 1996). During ten days, plants grew in a fully supplemented medium (containing 2  $\mu\text{M}$   $\text{ZnSO}_4$ ), after that, plants were either treated with Zn deficiency (no Zn added to the medium) or continued to grow at fully supplemented medium. For the Zn uptake experiment, plants were grown for 15 days in garden soil in a greenhouse set at a 16/8 h light/dark cycle at 20/18°C day/night temperatures and 70% humidity. After that, plants were grown hydroponically, in the conditions mentioned above, for 30 days in Zn deficiency (no Zn added to the medium). Then, the plants were placed, for three hours in the morning, in a fully supplemented medium (containing 2  $\mu\text{M}$   $\text{ZnSO}_4$ ). For Zn tracking, surfaced-sterilized seeds were sown on 9-cm circular plates filled with water in a climate-controlled growth chamber set at a 16/8 h light/dark cycle at 22/20°C day/night temperatures and 50% humidity. For gene expression imaging, surfaced-sterilized seeds were

sown on 12-cm square plates containing 1%-agar-solidified 0.5 MS medium (pH 5.8). Plants grew either on a fully supplemented medium (containing 15  $\mu$ M ZnSO<sub>4</sub>) or on medium to which no Zn was added in case of Zn deficiency treatment. Plants were grown in a climate-controlled growth chamber set at a 16/8 h light/dark cycle at 22/20°C day/night temperatures and 50% humidity.

### Genotyping

T-DNA insertion lines were genotyped to confirm or select for homozygote T-DNA insertion plants. Oligonucleotide primers were designed using the Salk Institute website ([signal.salk.edu/tdnaprimers.2.html](http://signal.salk.edu/tdnaprimers.2.html)). Two PCR reactions were performed per plant, the first with the primers combination left border (LB)-T-DNA border (BP) and the second with the primer combination LB-right border (RP) (**Supplemental Table S1**).

### Zn tracking

Five- to seven-day-old seedlings were incubated with 5  $\mu$ M of Zinpyr-1 (Sigma-Aldrich; [www.sigmaaldrich](http://www.sigmaaldrich)) for 3 hours as described in Sinclair et al. (2007). Cell walls were stained with 10 mg /ml Propidium Iodide (PI) for 30 sec. Images were taken with a CLSM (Confocal Laser-Scanning Microscope) Leica SPE DM5500 upright run with the LAS AF 1.8.2 software (Leica; [www.leica-microsystems](http://www.leica-microsystems)). Zinpyr-1 and PI were excited with a 488-nm solid-state laser. The Zinpyr-1 and PI emission were detected at a bandwidth of 540–550 and 700-800 nm respectively. Images were processed using Image J (Schneider et al., 2012).

### Gene expression quantification

The treatment was applied at 8:00 am and samples were collected 15 min, 1 hour, 3 hours, 6 hours, 12 hours, after treatment in day one, then at 8:00 pm in day two, four and twelve. Full root systems and shoots of three plants were collected for each biological replicate. Three biological replicates were collected in each time point and treatment. Total RNA was extracted with Direct-zol™ RNA MiniPrep Kit (Zymo Research, [www.zymoresearch](http://www.zymoresearch)) and cDNA was synthesized with the iScript cDNA Synthesis Kit (Bio-Rad, [www.bio-rad](http://www.bio-rad)). Gene expression was quantified by reverse transcriptase quantitative PCR (RT-qPCR) based on the SYBR® Green mix (Bio-Rad, [www.bio-rad](http://www.bio-rad)). Primers are described in **Supplemental Table S2**.

### Generation of promoter-NLS-YFP transgenic lines

A destination vector based on the Invitrogen Gateway technology was constructed to clone the promoter sequences. For this purpose, pFAST-R07 (Shimada et al., 2010) was digested with EcoRI and NruI to remove the eGFP coding sequence. In parallel, synthetic yellow fluorescent protein 2 (SYFP2) (Kremers et al., 2006) was isolated from pCZN633 (Smaczniak et al., 2012) by PCR using primers containing a short linker including an NruI restriction enzyme site and an overlapping sequence with a nuclear localisation signal (NLS) fragment. The NLS was isolated from pGREEN:GW:NLS-GFP (Horstman et al., 2015) by PCR using primers containing a short linker including an overlapping sequence with the sYFP2 fragment. The NLS and sYFP2 fragments were connected with a double joint PCR (Yu et al., 2004) and subsequently digested with EcoRI and NruI. The digested pFAST-R07 and NLS-sYFP2 fragments were ligated resulting in pFAST-R7-VO (**Supplemental Figure S1**). PCR primers for vector construction are detailed in **Supplemental Table S3**. The different promoter sequences were isolated from Arabidopsis Col-0 genomic DNA. Promoters were selected to be between 435 bp and 1800 bp depending on the distance with the upstream gene. Promoter PCR fragments were cloned into the pDONOR201 vector and subsequently into the expression vector pFAST-R7-VO by standard Gateway BP and LR reactions. Primers for promoter sequences cloning are detailed in **Supplemental Table S4**. Arabidopsis plants were transformed by the floral dip method (Clough and Bent, 1998). Transformed seeds (T1 generation) were selected based on the red fluorescence marker expressed in seeds (Shimada et al., 2010).

### Gene expression imaging

Transgenic Arabidopsis T2 seeds were used. Roots from six- to ten-day-old seedlings were stained with 10 mg /ml PI for 30 s. CSLM images were taken as described above. The 488 nm solid-state laser was used to excite SYFP2 and PI. The SYFP2 and PI emission were detected at a bandwidth of 530–570 and 700–800 nm respectively. Images were processed using Image J (Schneider et al., 2012).

### Metal content analysis

Root and shoot samples were collected to do a metal content analysis as was described by (Assunção et al., 2003). The metal content of Zn was measured in an atomic absorption Spectrophotometry.

### Statistical analysis

Data was log10 transformed prior to any test. Two-sample t-test, one- and two-way ANOVA and Tukey post hoc tests were performed using Genstat 18th edition (VSN International; [www.vsnl.co.uk/software/genstat/](http://www.vsnl.co.uk/software/genstat/)).

## Results

### Zn distribution in Arabidopsis Zn deficient roots

We have used the Zn fluorescent dye Zinpyr-1 to visualize the Zn distribution in roots of young (5-7 days old) Arabidopsis Col-0 seedlings. Zinpyr-1 is a fluorescein-based bright fluorescent Zn<sup>+2</sup> sensor (Woodroffe et al., 2004), its fluorescence intensity indicates relative levels of Zn (Sinclair et al., 2007). Zn sufficiency conditions were not applied due to the strong fluorescence in all root layers, which did not allow the differentiation of Zn distribution patterns. Seedlings are grown in strong Zn deficiency conditions to force the plants to prioritize their Zn distribution. The presence of Zn is examined in the whole root, from the root tip to the transition zone (**Figure 1**). The root tip, lateral root primordia, lateral root tips, and the transition zone show the highest Zinpyr-1 fluorescence, while the elongation zone shows the least fluorescence. In the differentiation zone, the Zinpyr-1 fluorescence is concentrated in the stele and endodermis. In addition, within epidermal and cortex cells, the Zinpyr-1 fluorescence intensity shows a gradient, being higher in the direction of the transition zone than in the direction of the root tip.

In five-day-old seedlings, the closer to the transition zone, the more intense the Zinpyr-1 fluorescence is in the stele (**Figure 1A**). In six-day-old seedlings, fluorescence in the stele close to the transition zone (**Figure 1B**), is lower compared to five-day-old seedlings. In seven-day-old seedlings, the fluorescence concentrated in the stele just until half of the root (**Figure 1C**). From halfway the root to the transition zone, the Zinpyr-1 fluorescence is spread along the epidermis, cortex, and endodermis (**Figure 1D-F**). Therefore, the Zinpyr-1 fluorescence in the stele close to the transition zone decreases when the tissue becomes older. In five-, six-, and seven-day-old seedlings, the high Zinpyr-1 fluorescence is consistently high in root zones with dividing cells, suggesting Zn tends to locate to growing tissues.

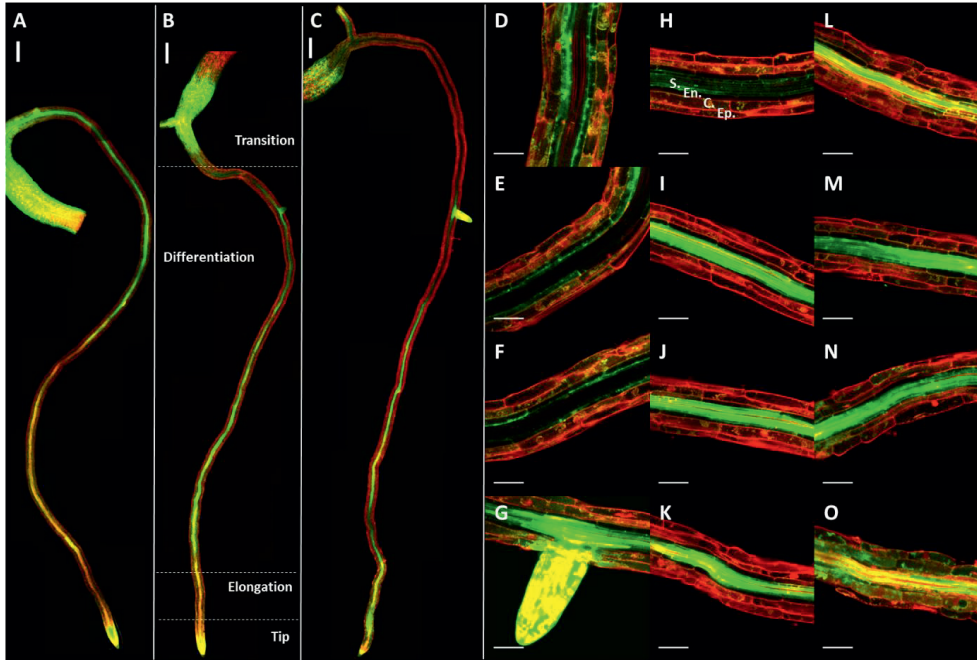


**Figure 1.** Confocal laser-scanning microscope images of Zn distribution in *Arabidopsis* roots. Zn deficient *Arabidopsis* Col-0 roots incubated with Zinpyr-1 to detect Zn (A) in five-, (B) six- or (C) seven-day-old plants covering the root between (D) the transition zone and the (O) root tip. Zinpyr-1 complexed to Zn fluoresces green, while propidium iodide bound to cell wall or DNA fluoresces red. Root cell layers can be differentiated from the outside to inside epidermis (Ep.), cortex (C.), endodermis (En.) and stele (S)) as described in (H). The scale bars indicate 200  $\mu\text{m}$  in A-C, and 50  $\mu\text{m}$  in D-O.

After elucidating the Zn distribution in roots of wild-type plants, we analysed the Zn distribution in roots of Zn transporters loss-of-function mutant plants. Our target were the Zn transporter genes *ZIP1*, *ZIP3*, *ZIP5*, *IRT3*, and *YSL3*, because their expression in roots is induced by Zn deficiency (van de Mortel et al., 2006) thus, we used T-DNA insertion lines of these genes. Of all mutants examined, the five-days-old *zip3* and *zip5* mutants show the strongest difference in Zn distribution compared to wild type (**Supplemental Figure S2**). Both mutants lack the high Zinpyr-1 fluorescence in lateral root primordia and in the stele, similar to the seven-day-old wild-type seedlings (**Figure 2**). In these mutants the Zinpyr-1 fluorescence is seen particularly in pericycle cells within the stele, but not in the whole stele as in wild type. In the differentiation zone close to the transition zone, the Zinpyr-1 fluorescence is seen in cortex and epidermis in *zip3* mutants and in cortex only in *zip5* mutants (**Figure 2**). The Zinpyr-

1 fluorescence pattern in five-day-old *zip3* and *zip5* seedlings resembles seven-day-old wild-type seedlings, suggesting more retention and less translocation to shoots in these mutants.

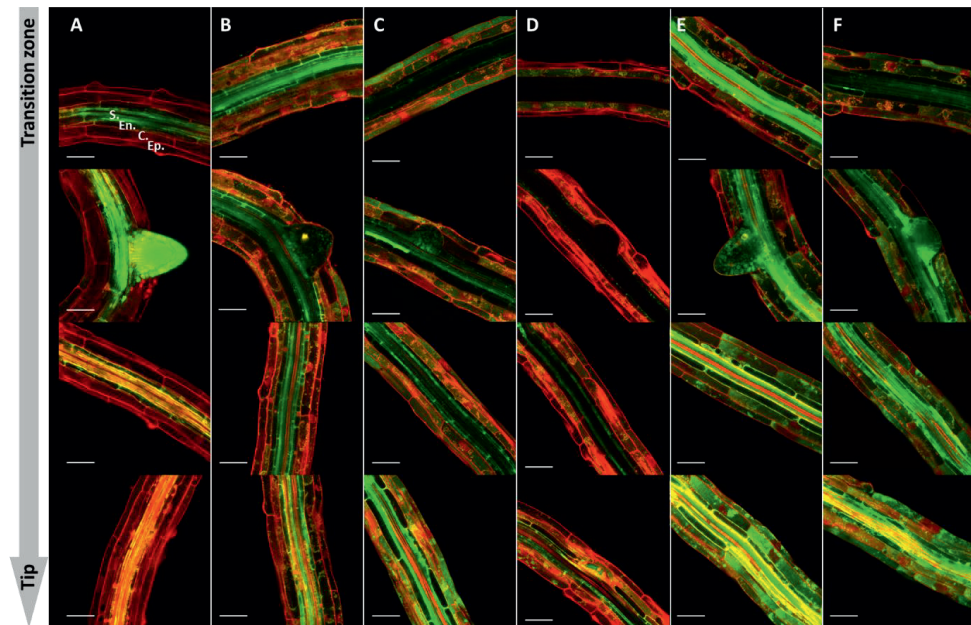


**Figure 2.** Confocal laser scanning microscope images of Zn deficient *Arabidopsis* roots. Sections of different genotypes incubated with Zinpyr-1 to detect Zn. Zinpyr-1 complexed to Zn fluoresces green, while propidium iodide bound to cell wall or DNA fluoresces red. Sections from the younger (bottom) to the older (up) regions of the root differentiation zone of five-day-old (A) Col-0 wild-type, (B) *zip1*, (C) *zip3*, (D) *zip5*, (E) *irt3* and (F) *ysl3* plants. The cell layers can be differentiated from the outside to inside ((epidermis (Ep.), cortex (C.), endodermis (En.) and stele (S.)) as described in (A) top image. The scale bars indicate 50  $\mu$ m.

The Zinpyr-1 fluorescence in *zip1* mutant shows similar intensity in all root layers, while in wild-type roots the fluorescence intensity is higher in the stele (**Figure 2** and **Supplemental Figure S2**). In addition, Zinpyr-1 fluorescence, in *zip1*, is not particularly intense in lateral root primordia, as it is wild-type roots. The Zinpyr-1 fluorescence intensity pattern was similar between the *ysl3* and *zip1* mutants. The five-day-old seedlings of the *zip1*, *zip3*, *zip5* and *ysl3* mutants showed a common Zinpyr-1 fluorescence pattern of less intensity in the stele and lateral primordia compared to the wild type. There is no difference in the Zinpyr-1 fluorescence pattern distribution between the *irt3* mutant and wild type, while the intensity seems higher in *irt3* mutant than in wild type.

### Gene expression patterns in Zn deficiency

We determined Zn transporter genes' expression induction upon Zn deficiency in order to examine their spatial and timely coordination. The Zn deficiency or control treatment was applied to 15-day-old plants. The treatment started at 8:00 am on day one and samples were collected at different time points, ranging between fifteen minutes and twelve days of treatment. On day one, the last sample was collected at 8:00 pm, samples from day two, four and twelve were also collected at 8:00 pm.

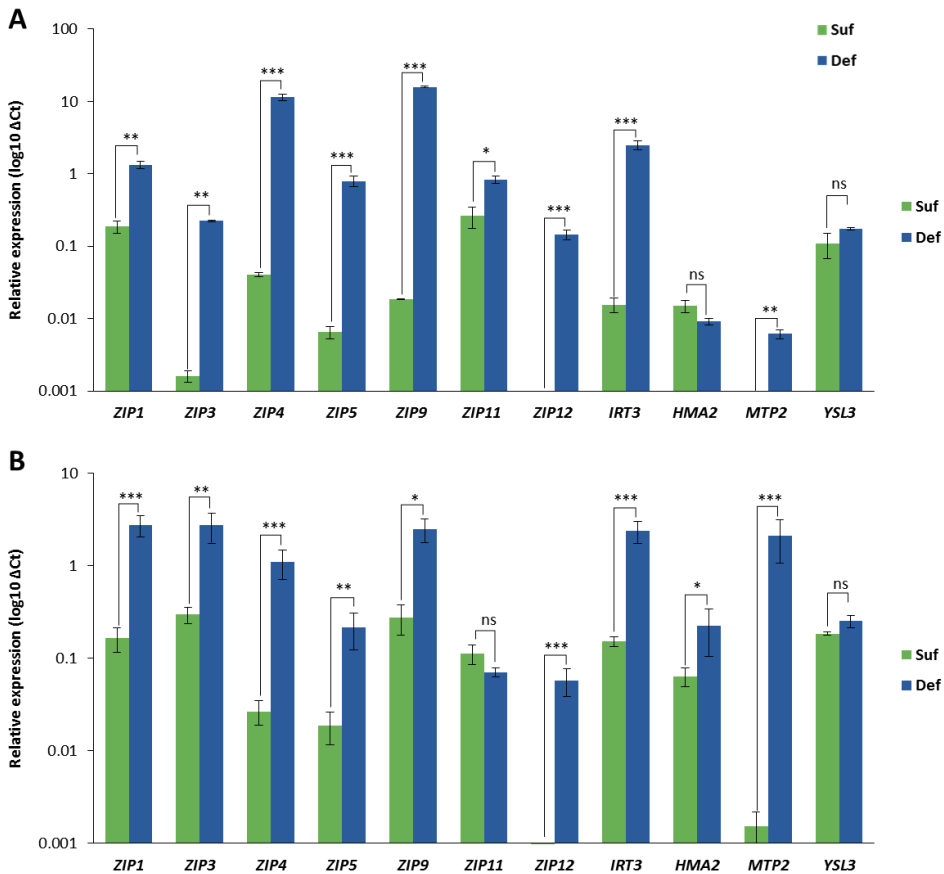


**Figure 3.** Gene expression of Zn transporters in shoots and roots of *Arabidopsis Col-0* after twelve days of Zn deficiency treatment. Gene expression relative to *At5g25760* and *AT2G28390* (A) in shoots and (B) roots of plants grown for ten days in fully supplied medium and then twelve days in either Zn deficiency (Zn def: blue bars) or Zn sufficiency (Zn suf: green bars). Mean  $\pm$  SE,  $n = 3$  of 3 pooled plants. Statistical significance was determined by Student's *t* test (\* $p < 0.05$ , \*\* $p < 0.01$ , and \*\*\* $p < 0.001$ ).

The highest level of gene expression induction was detected at day twelve of exposure to Zn deficiency, for most of the genes (**Table 1 and Supplemental Figure S3**). At day twelve, *ZIP1*, *ZIP3*, *ZIP4*, *ZIP5*, *ZIP9*, *ZIP11*, *ZIP12*, *IRT3*, and *MTP2* in shoots (**Figure 3A**), and *ZIP1*, *ZIP3*, *ZIP4*, *ZIP5*, *ZIP9*, *ZIP12*, *IRT3*, *MTP2*, and *HMA2* in roots (**Figure 3B**) are all significantly higher expressed in response to Zn deficiency when compared to plants grown in Zn sufficiency. The highest expressed genes upon Zn deficiency treatment are *ZIP4* and *ZIP9* in shoots and *ZIP1*, *ZIP3*, *ZIP4*, *ZIP9*, *IRT3*, and *MTP2* in roots at day twelve days of exposure to Zn deficiency. Instead, the highest fold induction by Zn deficiency at day twelve was detected for *ZIP9* and *ZIP12* in shoots and *ZIP12* and *MTP2* in roots was, this effect was largely due to their low expression under Zn sufficiency.

Some genes did not have their highest level of induction at day twelve. In shoots, the highest induction of *HMA2* was after 12 hours and of *YSL3* was at day four of exposure to Zn deficiency, however, their induction does not reach a 3 fold increase. In the roots, the highest induction of *YSL3* was at day four of exposure to Zn deficiency. And the expression of *ZIP11* is not affected by Zn deficiency in roots (**Table 1 and Supplemental Figure S3**). Apart from day twelve when the induction of most of genes peak, the expression profile of Zn transporters changes over time. While in the shoots, there was no significant increase of expression until day four, when *ZIP1*, *ZIP4*, *ZIP5*, *ZIP12*, *IRT3*, *HMA2*, *MTP2*, and *YSL3* significantly increased their expressions. Instead in roots, after six hours of deficiency *ZIP1* and *ZIP4* significantly increase their expression, with a three-fold change, after twelve hours *ZIP3*, *ZIP5* and *IRT3*, at thirty-six hours *ZIP1*, *ZIP3*, and *IRT3*, and at day four *ZIP1*, *ZIP4*, and *YSL3*. Both in the roots and shoots, most of the genes follow the pattern of a first low peak of gene expression induction at twelve hours, a drop of induction after thirty six hours, a second low peak of gene expression induction at day four and a final high peak of gene expression induction at day twelve (**Table 1**).

### **Zn transporters are expressed in different cell layers of the root**

The ZIP family of transporters is able to transport cations (mostly Fe and Zn and some related ions) into the symplast, while the HMA and CDF family transporters are mostly thought to be involved in the export of cations from the symplast, either to the intercellular space, or to the vacuole or other organelles (Eren and Argüello, 2004; Kobae et al., 2004; Eide, 2006; Sinclair and Krämer, 2012). We decided to study the root cell-specific expression of several ZIP, HMA and CDF genes suggested to be implicated in Zn transport. For that purpose, we generated



transgenic Arabidopsis lines expressing a nuclear localized *yellow fluorescent protein* (NLS-SYFP2) of which transcription is controlled by the promoters of *ZIP1*, *ZIP3*, *ZIP5*, *ZIP9*, *ZIP10*, *ZIP11*, *ZIP12*, *IRT3*, *MTP2*, *YSL3*, and *HMA2*. As a rule of thumb, we considered promoter regions of at most 1800 bp upstream of the predicted coding sequence start codon, but depending on the position of the upstream gene, this could be shorter. *ZIP11* has the shortest promoter region, corresponding to 435 bp. Three *ZIP* genes share their promoter regions with other genes: 1) *ZIP1* with an auxin-responsive gene (AT3G12760) (Biswas et al., 2007); 2) *ZIP9* with a sulfolipid synthetase (AT4G33030) (Essigmann et al., 1998; Sanda et al., 2001); and 3) *ZIP10* with a gene of unknown function (AT1G31270)

**Table 1.** Fold changes of gene expression of Zn transporters through time. Fold change means of gene expression relative to At5g25760 and AT2G28390 after increasing times (from 0.25 hours (h) to 12 days (d)) of exposure to Zn deficiency, when compared to plants grown at Zn sufficiency. Colours indicate the highest fold change (red), middle (white) and the lowest fold change (blue) among time points within each gene. Darker numbers indicate statistical significant gene expression induction when comparing between Zn deficiency and Zn sufficiency grown plants at each time points per gene. Statistical significance was determined by Student's *t* test ( $p < 0.05$ ).

Shoot	ZIP1	ZIP3	ZIP4	ZIP5	ZIP9	ZIP11	ZIP12	IRT3	HMA2	MTP2	YSL3
0.25	0.9	0.8	0.8	0.6	0.9	0.8	0.6	0.7	1.0	0.5	0.8
1h	0.7	0.9	1.4	0.4	0.7	0.8	0.1	0.7	0.6	0.8	0.8
3 h	1.0	0.7	1.1	0.7	0.9	1.0	0.6	1.2	0.8	1.3	0.9
6 h	1.4	1.4	1.5	1.3	0.7	0.9	0.9	1.8	2.1	0.6	1.1
12 h	1.5	1.2	1.3	1.4	1.5	1.1	3.0	2.5	1.2	1.1	1.3
36 h	0.4	0.8	0.8	0.7	0.5	0.4	0.5	1.0	0.2	0.7	1.2
4 d	2.0	0.7	1.4	2.3	1.4	1.4	5.8	4.5	1.7	2.2	2.8
12 d	7.4	144	285	125.7	853.3	3.6	886.6	169.5	0.6	8.8	1.9
Root	ZIP1	ZIP3	ZIP4	ZIP5	ZIP9	ZIP11	ZIP12	IRT3	HMA2	MTP2	YSL3
0.25 h	1.1	0.7	0.9	0.8	0.8	2.3	0.3	0.6	1.2	0.3	0.6
1h	2.0	0.9	1.5	0.5	1.2	2.3	3.8	1.1	0.6	0.4	0.2
3 h	1.9	1.1	2.4	1.3	0.9	1.1	1.4	1.7	0.7	0.2	1.2
6 h	3.3	1.6	3.1	1.6	1.0	1.7	0.9	1.9	0.7	1.2	0.4
12 h	2.7	2.1	3.5	3.1	0.9	1.6	4.4	5.9	1.4	0.8	1.8
36 h	2.5	1.8	1.5	1.5	0.6	0.7	0.7	2.3	0.9	0.6	2.8
4 d	3.4	1.7	2.2	1.4	1.3	1.2	0.4	2.4	0.4	2.1	5.0
12 d	17.3	9.3	42.3	12.0	10.1	0.7	1289.5	15.5	3.6	1833.7	1.4

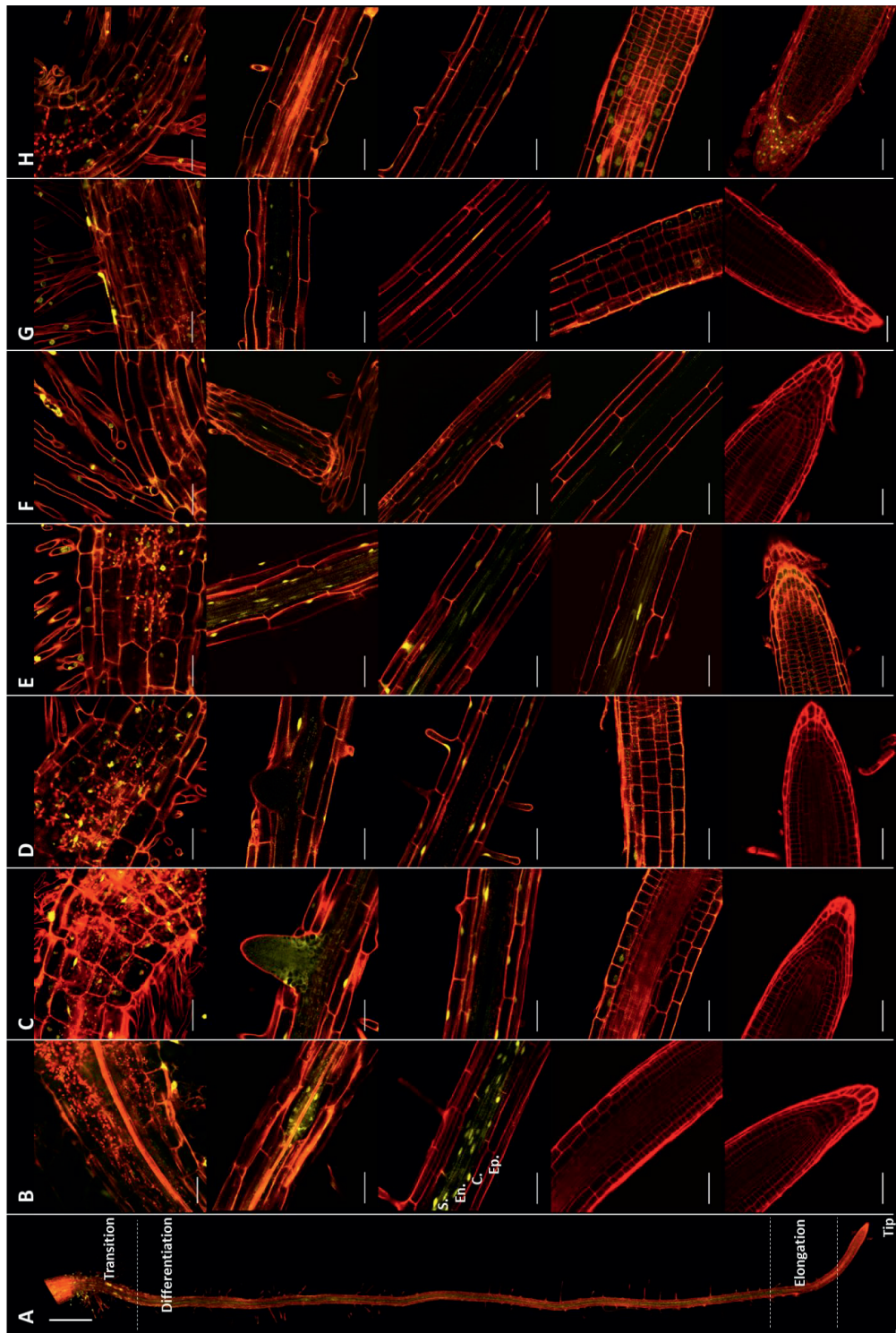


**Figure 4.** Confocal laser scanning microscope images of *Arabidopsis* roots expressing nuclear-localised YFP driven by the promoter regions of Zn transporters. The SYFP2 fluorescent signal (yellow) can be seen in all nuclei of cells expressing the NLS-SYFP2 marker gene. The red fluorescent signal indicates mainly cell walls stained with propidium iodide. (A) Whole *Arabidopsis* root expressing NLS-SYFP2 driven by the promoter regions of ZIP1, including root tip, elongation, differentiation and transition zones from where the more detailed images of (B) ZIP1, (C) ZIP3, (D) ZIP5, (E) ZIP11, (F) IRT3, (G) HMA2, and (H) YSL3 were taken. In panel (B) in the differentiation zone are labelled the cell layers from the outside to inside (epidermis (Ep.), cortex (C.), endodermis (En.) and stele(S.)). Yellow spots bigger than nuclei, in the transition zone, correspond to the autofluorescence of seed fragments. The scale bars indicate 500  $\mu\text{m}$  in A and 50  $\mu\text{m}$  in B-H.

To analyse the cell-specific expression, we examined two independent transgenic lines per construct grown on Zn deficient vertical agar plates. The two transgenic lines showed the same expression pattern per construct. We used T2 seeds which were either homozygous or heterozygous for the insertion, selected based on the seed red fluorescence (Shimada et al., 2010). For all promoters, except for *ZIP10*, expression of YFP is detected by confocal microscopy (**Figure 4** and **Supplemental Figure S4**). *ZIP1* is expressed in the endodermis, stele, and lateral root primordia. *ZIP1* is the gene with the lowest expression detected in the transition zone between root and hypocotyl (**Figure 4B**). *ZIP3* and *ZIP5* had the same expression pattern, both genes are expressed from the elongation to the transition zone of the root. In the differentiation zone, we can clearly see, *ZIP3* and *ZIP5* expression in the epidermis and cortex. The only difference in their expression is that *ZIP3* is highly expressed in lateral root primordia, and in all cell layers of young lateral roots, while *ZIP5* expression was not detected in those cases (**Figures 4C and D**). *ZIP11* is expressed from the elongation to the transition zone. In the young differentiated zone, *ZIP11* is expressed in xylem parenchyma cells, but in the older parts of the root the expression shifts to endodermal cells (**Figure 4E**). This shift occurs abruptly, with hardly any overlap between both *ZIP11* expression sites. The expression of *ZIP9* and *ZIP12* was only detected in the transition zone, where it was not possible to clearly differentiate cell layers (**Supplemental Figure S4**). *IRT3* is expressed in the root tip, the differentiated zone, and the transition zone. In the young differentiated zone, *IRT3* is expressed in the inner stele cells accompanying the xylem parenchyma cells protoxylem vessels. In the older differentiated zone, *IRT3* expressed in all cell types from the epidermis to stele. The shift occurs gradually, with overlap between both *IRT3* expression patterns (**Figure 4F**). Like *IRT3*, *HMA2* is expressed in the inner stele next to xylem vessels, mainly in the young differentiated zone. *HMA2* is also expressed in the transition zone. The *HMA2* expression in the lateral roots is stronger than in the primary root (**Figure 4G**). *YSL3* is expressed in the root cap, the elongation zone, the differentiated zone, and the transition zone. In the differentiated zone, *YSL3* expressed in the epidermis and cortex, however its expression was low and hard to detect (**Figure 4H**). The expression of *MTP2* was only detected in the transition zone, particularly in the root hairs (**Supplemental Figure S4**).

### **ZIP Zn transporters are largely redundant in response to Zn deficiency**

To evaluate the plant response to the loss of one or two *ZIP* transporters, single and double T-DNA insertion lines of these genes are evaluated in response to Zn sufficiency and Zn deficiency. In Zn sufficiency, the shoot phenotype of *zip1*, *zip3*, *zip5*, and *zip9* look smaller

than wild-type shoots (**Figure 5A and B**), but these mutants are not statistically different from the wild type (**Figure 5C and D**). However, *zip3*, *zip5* and *zip9* shoot dry weights are significantly lower than the double mutants *zip1/zip3*, *zip1/zip5*, *zip9/zip12*, and *zip9/mtp2*. The root dry weight of roots of *zip9* is significantly lower than the double mutants *zip1/zip3*, *zip1/zip5*, *zip9/zip12*, and *zip9/mtp2* (**Figure 5C and D**), which is a similar pattern as the one observed in the shoots. In Zn deficiency, the shoot phenotype of most of the genotypes cannot be distinguished from the wild type. However, the exceptions were the double mutants *zip1/zip3* and *zip3/zip5*, which are more yellow, and with more curly leaves than the wild type, in addition *zip3/zip5* is clearly smaller than the wild type (**Figure 5C**). The shoot dry weight of *zip3/zip5* is significantly lower than the wild type and all the other mutants, while the shoot dry weight of *zip1/zip3* is significantly lower than all the other genotypes except for the wild type, *zip5* and *zip9/mtp2*. The root dry weight of roots of any of the mutants was different from the wild type. However, *zip9* and *zip3/zip5* are significantly lower than *zip1/zip5* (**Figure 5D**).

Because the double mutant *zip3/zip5* was the only genotype significantly different from the wild type, we analysed its Zn uptake and translocation capacity compared to wild type and the single mutants *zip3* and *zip5*. In Zn deficient plants, the shoot Zn concentration of *zip3* and *zip5* is not different from the wild type, while that of *zip3/zip5* is higher than wild type (**Figure 6A**). The root Zn concentration of all genotypes tested was similar in Zn deficiency (**Figure 6B**). To analyse the Zn uptake and translocation capacity, Zn deficient plants were supplied Zn for three hours before harvesting. After these three hours, the Zn concentration significantly increased in shoots and roots of all genotypes except in *zip3/zip5*. The response was particularly strong in roots where the increase was approximately nine fold in wild type, *zip3* and *zip5*.

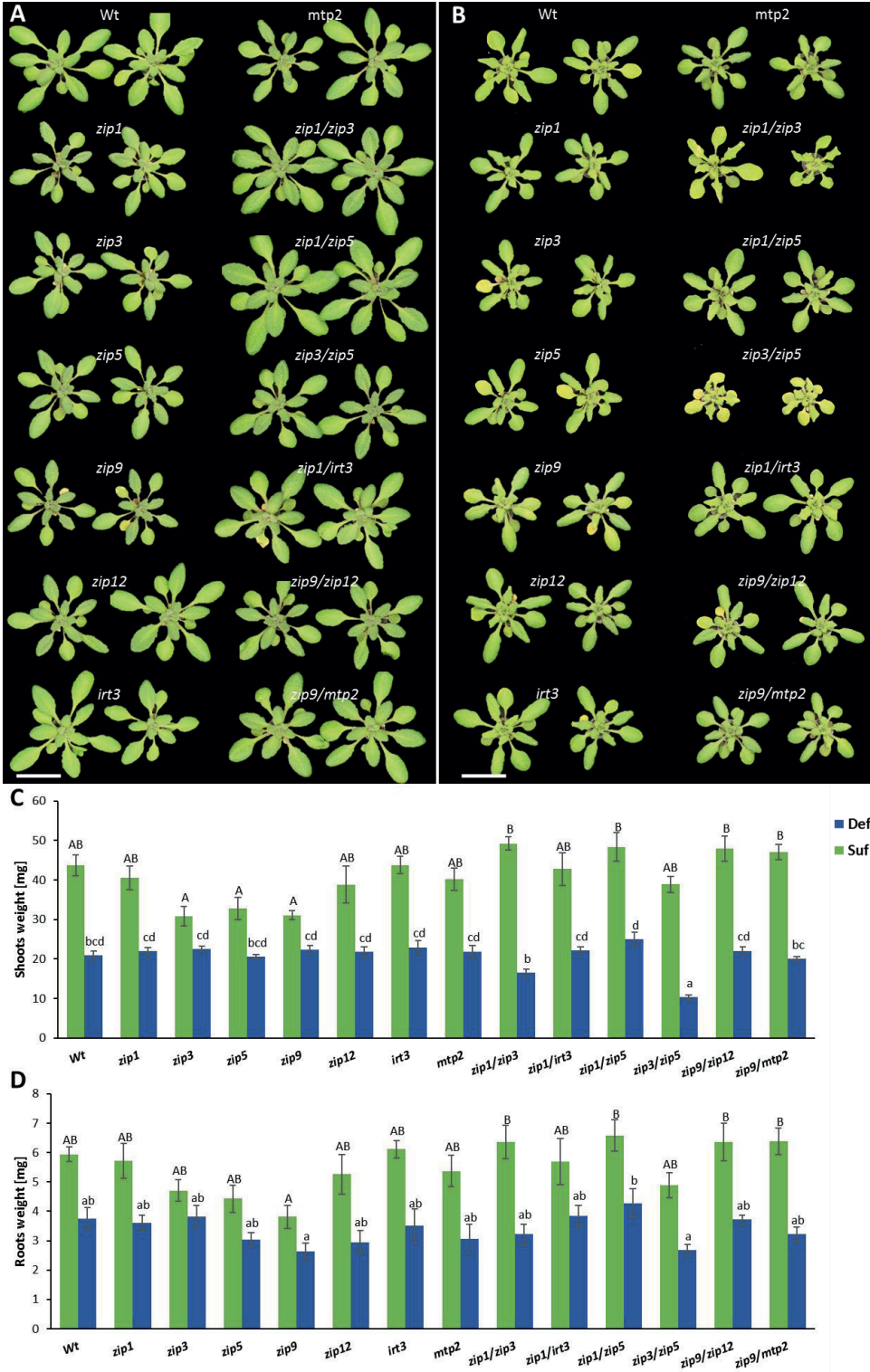




**Figure 5.** Response of single and double Zn transporter T-DNA insertion lines grown under Zn sufficiency and Zn deficiency. Two representative plants of wild-type and single and double Zn transporter T-DNA insertion lines grown hydroponically (A) 25 days under Zn sufficiency and (B) 10 days under Zn sufficiency and 15 days under Zn deficiency are shown. The scale bars indicate 2 cm in A-B. (C) Shoot and (D) root dry weight of wild-type and Zn transporter T-DNA insertion line plants grown hydroponically 25 days under Zn sufficiency (green bars) and 10 days under Zn sufficiency and 15 days under Zn deficiency (blue bars). Mean  $\pm$  SE,  $n = 10$  plants. Upper case letters (Zn sufficiency) and lower case letter (Zn deficiency) above the bars denote statistically different groups, when comparing among genotypes grown under each treatment, obtained with a Tukey post hoc test ( $\alpha=0.05$ ), after a one-way ANOVA ( $p<0.01$ ).

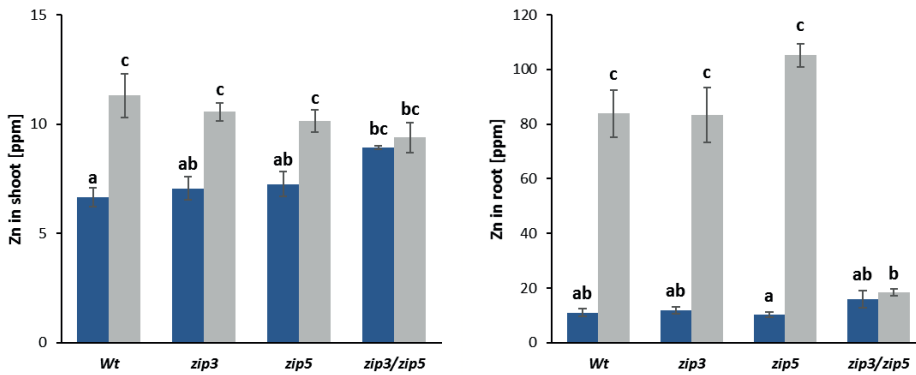


**Figure 6.** Zinc concentration of single and double, *zip3* and *zip5* T-DNA insertion lines. Zn concentration in (A) shoots and (B) roots measured in wild-type (*Wt*) and single and double *zip3* and *zip5* T-DNA insertion lines grown in soil for 15 days and 30 days hydroponically under Zn deficiency (blue bars) plus 3 hours of Zn sufficiency before harvesting (grey bars) are shown. Mean  $\pm$  SE,  $n = 6$  plants. Letters above the bars denote statistically different groups, obtained with a Tukey post hoc test ( $\alpha=0.05$ ), after a two-way ANOVA ( $p<0.01$  genotype  $\times$  treatment interaction).

## Discussion

### Loss-of-function of Zn transporters affects Zn distribution in Arabidopsis Zn roots

When plants face nutrients deficiency, a strategy for survival is to transport the nutrients to metabolic active organs. In aerial parts, micronutrients like Zn can be remobilized from senescent leaves and stems by the phloem to growing organs (Maillard et al., 2015; Diaz-Mendoza et al., 2016). But in roots, the half-hidden of the plant, we do not have a clear knowledge of this process. Therefore, we traced Zn distribution in whole roots of Zn deficient plants by using the Zimpyr-1 fluorescence dye (Woodroffe et al., 2004; Sinclair et al., 2007).

In these roots, Zn concentrates mainly in growing zones such as main root tip, lateral root primordia, secondary root tips, and transition zone, meaning that during shortage, nutrients are still available for younger plant organs (Himmelblau and Amasino, 2001; Avice and Etienne, 2014). In addition, root tips can be an easy access point to the root stele considering the lack of Casparian strip or suberin layer in this root zone. In the root differentiation zone, most of the Zn seems to be concentrated in the stele, which could subsequently be translocated from root to shoot. As we observed when comparing the stele Zinpyr-1 fluorescence among five-, six-, and seven- days-old Arabidopsis seedlings, the concentration of Zn in the stele of the older regions of the differentiation zone disappear when the plant suffer from Zn deficiency for a prolonged period of time. Therefore, the translocation of Zn to the shoot will be affected.

With the use of Zinpyr-1, we found different Zn deficiency distribution patterns through time, thus we decided to use the same approach to study the pattern of Zn distribution in Zn transporter mutants. The Zinpyr-1 fluorescence distribution pattern of five-day-old *zip1*, *zip3*, *zip5*, and in a lesser degree *ysl3* mutants is similar to the pattern observed in five-day-old wild type. This indicates that Zn deficiency appears earlier in these mutants than in wild-type plants. In addition, the Zinpyr-1 fluorescence is less intense in the lateral root primordia of *zip1*, *zip3* and *zip5* than in the wild type. The most similar Zinpyr-1 fluorescence distribution pattern is between *zip3* and *zip5* mutants. In both mutants in the older region of the differentiation zone, the Zinpyr-1 fluorescence is almost absent in the stele, while present in cortex, epidermis, and pericycle. This particular pattern could be explained by a possible increase in expression of other Zn transporter like *ZIP4*, which is expressed in cortex and pericycle (Lin et al., 2016). These observations suggest that the plant machinery shuts down earlier the Zn allocation to the root stele in the mutants *zip1*, *zip3*, *zip5* and *ysl3* than in the wild type. From the five mutant lines analysed, the *irt3* mutant did not show clear differences in the Zinpyr-1 fluorescence distribution pattern when compared to wild type.

### Zn deficiency response cascade starts in roots

One of the strategies to cope with fluctuating availability and concentrations of nutrients relies on changes in genes expression (Maillard et al., 2015). The transcriptome within cells and organisms is very flexible and constitutes a key factor to rapidly respond and adapt to changes in the environment. The dynamics of transcription responses allows for coordinated development and stress response by reshaping metabolic and physiological processes relevant for a given stress like nutrient deficiency (de Nadal et al., 2011). Arabidopsis plants were able



to sense Zn deficiency in the medium and enhance the transcription of Zn transporters in roots after six hours of exposure to Zn deficiency. The first genes to show a significant induction are *ZIP1* and *ZIP4* after six hours, *ZIP3*, *ZIP5* and *IRT3* after twelve hours, and *ZIP1*, *ZIP3*, and *IRT3* after thirteen hours. During the first hours of exposure to Zn deficiency, only genes of the ZIP family are significantly induced and only in the root. Due to the protein topology of the ZIP family, these protein transport metal ions from the apoplast or organellar lumen to the symplast (Eide et al., 1996). Therefore, the first response to Zn deficiency of the plant seems to be to increase the uptake of Zn from the soil in the cell symplast. In the first day of exposure to Zn deficiency, the highest peak of induction was detected after twelve hours, when *ZIP4*, *ZIP3*, *ZIP5*, *ZIP12*, *IRT3* in roots and *ZIP12* in shoots showed above a three-fold induction. This induction could be a Zn deficiency solely or a combined response due to diurnal or circadian clock effect interaction (Grundy et al., 2015; Feeney et al., 2016) interaction. To avoid this combined effects from the twelfth hour of day one to day twelve, all samples were collected at the same time in the evening.

The second day at 8:00 in the evening, the gene expression of transporters in shoots and roots slightly dropped. This response could be the effect of a transient stabilization in the symplastic levels of Zn, due to the initial upregulation (Shalem et al., 2008; Yosef and Regev, 2011) of genes in charge to mobilize Zn into the symplast. Gene expression levels tend to return towards the original levels when cells are close to the unstressed state, even with continuous environmental stimuli (Yosef and Regev, 2011). We took the next sample at day four of exposure to Zn deficiency, when the levels of induction increase again in roots, showing a significant increase in the expression of *ZPII*, *ZIP4*, and *YSL3*. The activity of *YSL3* has been associated with the long distance transport of cations (Waters et al., 2006; Curie et al., 2009). Since day four, we also detected the significant increase in shoots of the expression of *ZIP1*, *ZIP4*, *ZIP5*, *ZIP12*, *IRT3*, *HMA2*, *MTP2*, and *YSL3*. This set of genes includes Zn symplast importers as the ZIP family (Eide, 2006) and Zn symplast exporters as *HMA2* (Eren and Argüello, 2004) and *MTP2* (Eide, 2006). This suggests that at day four, the plant starts to modify its Zn deficiency response cascade. The transcriptome fine tuning will determine the magnitude and duration of the response according to the degree of the environmental stimuli (Lopez-Maury et al., 2008). The highest induction for most of the genes in shoots and root was detected at day twelve. At this time point, *ZIP1*, *ZIP3*, *ZIP5*, *ZIP9*, *ZIP11*, *ZIP12*, *IRT3*, and *MTP2* in shoots, and *ZIP1*, *ZIP3*, *ZIP5*, *ZIP9*, *ZIP12*, *IRT3*, *HMA2* and *MTP2* in roots are significantly induced by Zn deficiency. The only exceptions were *HMA2* in shoots, *ZIP11* in

roots, and *YSL3* in shoots and roots, which showed a different pattern of expression from the rest of the genes tested. These three genes lack the ZDRE motif in their promoter sequences, which is present in the promoter sequences of *ZIP1*, *ZIP3*, *ZIP4*, *ZIP5*, *ZIP9*, *ZIP12*, and *IRT3*. This motif is the target sequence for binding bZIP19 and bZIP23 transcription factors that regulate the adaptation to Zn deficiency (Assunção et al., 2010). When the same transcription factors control a group of genes, these genes will share the same expression pattern (Yosef and Regev, 2011). In addition, *MTP2* and *ZIP12* showed the largest gene expression induction due to Zn deficiency. The expression of both genes was almost not detectable in normal Zn supply. However, *MTP2* promoter only contains two palindromic sequences 80% similar to the ZDRE. So, its high level of induction by Zn deficiency could be regulated by transcription factors different from bZIP19 and bZIP23.

As mentioned before, another gene without a ZDRE domain in its promoter is *HMA2*. This gene is known to be involved in Zn symplast efflux for root to shoot Zn translocation (Hussain et al., 2004; Sinclair et al., 2007). This gene was induced only above a three-fold change at day twelve in roots. *HMA2* and *HMA4* have a combined role in the Zn symplastic efflux and translocation to shoots (Hussain et al., 2004; Sinclair et al., 2007). However, *HMA4* is not induced by Zn deficiency (van de Mortel et al., 2006). Therefore, during Zn deficiency, probably the root to shoot translocation is not prioritized over the Zn root uptake.

### **Zn transporters express in different cell layers**

Water and nutrients move radially through the root concentric cell layers to enter from the soil solution to the xylem where they will be translocated to the shoot. The concentric cell layers from the outer to the most inner layer are: epidermis, cortex, endodermis, and stele which consist of pericycle, xylem, phloem, companion cells and procambium (Barberon and Geldner, 2014). The tested Zn transporters are expressed in different combinations across the root cell layers. A summary of the cell layer where each transporter is expressed is presented in **figure 7**. *ZIP1* expresses in the endodermis and root stele. The *ZIP1* early expression and its putative location in the tonoplast (Milner et al., 2013) indicates that the Zn deficiency response initially promotes the increase of the Zn symplastic concentration by using the vacuole as a nutrient storage compartment, which becomes a side-branch of the symplastic pathway (Tester and Leigh, 2001).

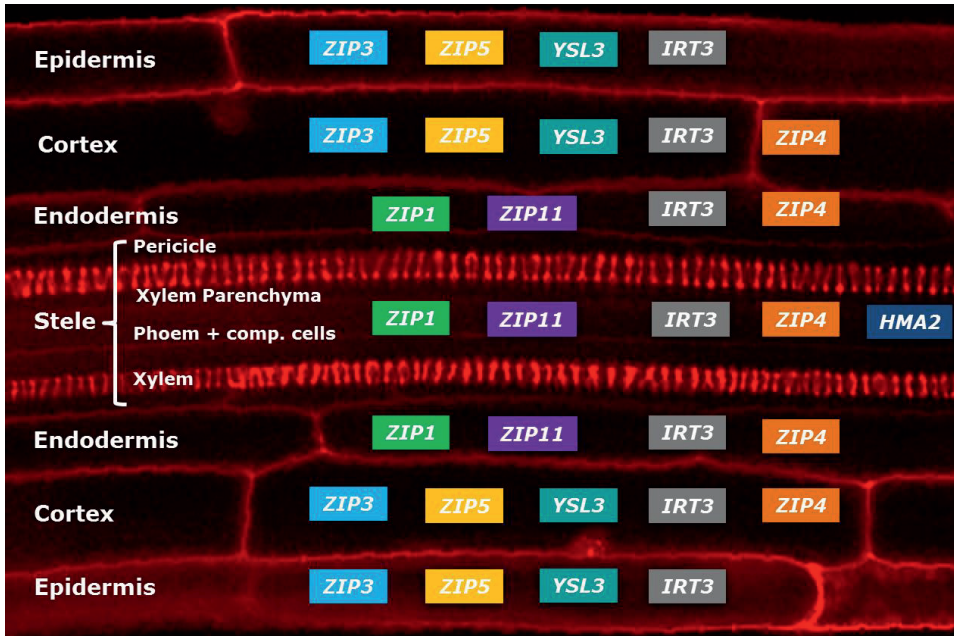


**Figure 7.** Summary of the cell layer where each Zn transporter is expressed. The scheme is based in a confocal laser-scanning microscope image of *Arabidopsis* root. The red fluorescent signal indicates mainly cell walls stained with propidium iodide. The cell layers are label as epidermis, cortex, endodermis and stele, which includes pericycle, xylem, xylem parenchyma, phloem and companion cells. Transporters are represented by different coloured rectangles.

The symplastic pathway starts with the Zn uptake into the symplast. The expression of *ZIP3* and *ZIP5*, which are located in the root outer layers (epidermis and cortex), constitutes the first step for the Zn symplastic pathway. Epidermis and cortex are functionally similar in terms of nutrients absorption (Barberon and Geldner, 2014). The expression of *ZIP3* and *ZIP5* in epidermis and cortex assures the symplastic pathway even in older zones of the root. In these zones, the endodermis becomes a barrier for the apoplastic pathway due to the Casparian strip (Geldner, 2013). The Zn transporter *IRT3*, promotes uptake into the symplast (Lin et al., 2009), in all the root from the epidermis to the stele. The expression of *ZIP4* is mainly in cortex, endodermis, and pericycle, which likely facilitates the Zn entry to the stele (Lin et al., 2016). The role of Zn efflux into the stele apoplast is mainly attributed to the *HMA2* and *HMA4* (Hussain et al., 2004; Sinclair et al., 2007). However, only *HMA2* shows to be induced by Zn deficiency (van de Mortel et al., 2006). We observed *HMA2* expression in an inner-layer of the stele in xylem parenchyma cells. This result differs slightly with Sinclair, 2007, where a *HMA2p-HMA2-GFP* showed expression in pericycle cells. Nonetheless, in both cases, the

expression is detected in stele cells, which can favour the availability of Zn in the stele apoplast. The expression location of *ZIP11* was particularly interesting, due to its expression in xylem parenchyma cells in the young differentiation zone of the roots, and in endodermal cells in the older differentiation zone of the roots. The cell layer where *ZIP9*, *ZIP12* and *MTP2* express could not be defined, because they only showed expression in the transition zone, however, lateral roots were not analysed.

### The function of Zn transporters is redundant

Zn deficiency significantly reduces the biomass production of plants (Campos et al., 2017) either wild-type or Zn transporter mutants. Under normal Zn supply, the biomass of shoots and roots of the single mutants *zip3*, *zip5*, and *zip9* was lower than the biomass of wild-type plants, and the double mutants *zip1/zip3*, *zip1/zip5*, *zip9/zip12* and *zip9/mtp2* was higher than the biomass of wild-type plants, however, the difference is not statistically different. Under Zn deficiency, almost all mutant genotypes have similar weight in shoot and root than the wild type, the only exception is *zip3/zip5*. The double mutant *zip3/zip5*, is the most sensitive genotype to Zn deficiency, with yellow curly leaves and a significant decrease in shoot biomass compared to wild type. The double mutant *zip1/zip3*, also shows to be more sensitive to Zn deficiency than the wild type, but this difference is not statistically different. The lack of reports showing the effect of the loss of function of the Zn transporters here analysed and the small or null effect of single Zn transporters mutants strongly suggest redundant functions among Zn transporters, especially in the case of *zip3* and *zip5*. Both genes are phylogenetically closely related (Mäser et al., 2001), are expressed in the same cell layers in the root, the Zn distribution is similar in their loss-of-function mutants, and their double loss-of-function mutant is highly sensitive to Zn deficiency.

Considering that *zip3/zip5* was the only mutant statistically different from the wild type in Zn deficiency, we analyzed its Zn concentration and uptake capacity. The wild-type, *zip3* and *zip5* single mutants have a similar Zn concentration among them in shoots and roots when plants grown under Zn deficiency conditions. Surprisingly, the double mutant *zip3/zip5* had a significantly higher concentration of Zn in shoots than wild type. After a three hours Zn supply wild-type, *zip3* and *zip5* single mutants significantly increased their Zn concentration in shoot and roots, while *zip3/zip5* shows no increase in Zn concentration. This suggests that *ZIP3* and *ZIP5* are involved in Zn uptake in the roots.

## **Conclusions**

All Zn transporters studied here are induced by Zn deficiency either in shoot or in roots, after hours and/or after days of exposure to Zn deficiency. The Zn deficiency response initiates in the roots and later is induced in shoots. In roots, each Zn transporter gene is expressed in one, or more, specific root cell layer(s), from epidermis till stele. This location may differ, depending on the root region. These transporters showed partial functional redundancy among them because the single or double loss-of-function of Zn transporters do not cause strong sensitivity to Zn deficiency, except for the double mutant *zip3/zip5*. The *ZIP3* and *ZIP5* genes seem to be highly redundant and to be involved in Zn uptake from roots.

## **Acknowledgements**

We thank Prof. Richard Immink, Alice Pajoro, and Tjitske Ricksen (Wageningen University) for facilitating the use of the confocal microscope and providing the technical support. We thank Prof. Henk Schat (VU Amsterdam) for his help in the Zn uptake assay. This work was supported by the Ecuadorian government through SENESCYT (Secretaría de Educación Superior, Ciencia, Tecnología e Innovación) and Universidad de las Fuerzas Armadas-ESPE.

## Supplemental information

**Table S1.** T-DNA insertion lines of Zn transporter genes with their respective LB (left border) and RP (right border) primers to genotype for homozygote T-DNA insertion plants.

Symbol	Locus identifier	T-DNA line	Primer	Sequence (5'-3')
ZIP1	At3g12750	SALK_023634C	LB	CTTGAGGACACTACAGCTGGG
			RB	GAATGCGGATTATTAGCTGG
ZIP3	At2g32270	SAIL_35_B08	LB	GGCTCGTTACTTTCCTTGGAC
			RB	CCATTATTTGGAATGCAATCG
ZIP5	At1g05300	SALK_009007C	LB	AGGGACAAAAACAAATACGGG
			RB	AGGCAATGAAAATTCAGTGAC
ZIP9	At4g33020	SALK_074682C	LB	ACACCGATCGGAGTAGTGATG
			RB	TTTCGGTTATGTCTGACCCAG
ZIP10	At1g31260	SALK_104586C	LB	TTTGCTTTTATTGAGTGACAACC
			RB	TCTGCATTCCATAAATGTCAAG
ZIP11	At1g55910	SALK_120099C	LB	TTGGTTGATCTTCTGTTTGG
			RB	AGGATTTGGATTGAGATCGG
ZIP12	At5g62160	SALK_137184	LB	AATGTCCTTGTGAGGCATGAG
			RB	GATTTCTCCTGGTCGAAGAG
IRT3	At1g60960	WiscDsLox429D04	LB	TGATGTGTGTTTGCTCTTCG
			RB	AGCAATGGATAAGAAATTGCG
MTP2	At3g61940	SALK_003649C	LB	GCTGCAGATGGATTCAAGAAG
			RB	ATGAGAGCATACGAGAAAGCG
YSL3	At5g53550	SALK_045218C	LB	GCCTTTAGGAGTGTGGAACC
			RB	TTTTCTCTCGTCATTTTCC
HMA2	At4g30110	SALK_034393	LB	GGAGAGTGACTCCCTAAAGCC
			RB	TAAACAAGAAATGGCGTCGAAG

**Table S2.** Sequences of primers used for gene expression quantification by qRT-PCR

Symbol	Primer Forward (5'-3')	Primer Reverse (5'-3')
ZIP1	TCTCCCTGGCGGATATGAAGTC	TCCACCATTATTGCCTCTTTGCTC
ZIP3	CTCCTTCTCATCGCCGTCGT	CGAGCTCCGGCTTTGTTTTTC
ZIP4	GGCTGCATCTCTCAGGCACA	GGCCACTGCAGTTCCAATCC
ZIP5	CGTCGCTTAAACCGGAGACG	CATAAACCCGTTGCGAGGA
ZIP9	ACTTGTGTACATGGCGCTTG	TGCAAGAGCAGACATCATCC
ZIP11	TTGGTACACAATTCGCCGGA	AAGCAATGGGTAAAGCCGGA
ZIP12	CCATCTTAATCGCCGAGTA	TCTTCTCAAGGCACGAAC
IRT3	GATTCTGCCACGGGTTTTG	GCAAAGAATCCGGGAAAGG
HMA2	TCCGTCAAGAACCATCATCGTC	AACGATTTGGAAGTGCAGAGG
MTP2	CGAGCTGCTTCAATGCGAAA	AGCACCAACATCAGTGAGCA
YSL3	GGTGGTACAGAGTGCGGTTT	TGATCCCCAAGACAGAACC
SAND	GTTGGGTCACACCAGATTTTG	GCTCCTTGCAAGAACACTCA

**Table S3.** Sequences of primers used to generate the destination vector. Underlined oligoes represent the primers linkers.

Primers description	Sequence (5'- 3')
Forward for NLS	ATTCACATTCTTGCCCGCCT
Reverse for NLS plus a sYFP2 linker	<u>GCCCTTGCTCACCAT</u> AGGTTGAGAAGATGGCTCTATTTTC
Forward for sYFP2 plus a NLS linker	<u>CCATCTTCTCAACCT</u> ATGGTGAGCAAGGGCGAGGAGCTGT
Reverse for sYFP2	CCTTCAACGTTGCGGTTCTG
Forward for the DJ fragment	TCTTGCCCGCCTGATGAATG
Reverse for DJ fragment plus a NRUI linker	TTCT <u>CGCGAT</u> CTAGTAACATAGATGACAC

**Table S4.** Sequences of primers used to clone gene promoters. Forward primers include the attB1 linker (GGGGACAAGTTTGTACAAAAAGCAGGCTTA) and reverse primers include the attB2 linker (GGGGACCACTTTGTACAAGAAAGCTGGGTA)

Promoter	Primer Forward	Primer Reverse
ZIP1	CAGTTATGCAAATACTCCGG	TGAGTTTAAGATATTTATGTTCTTGTT
ZIP3	TATCCAGAAAGATGATGTGTATACA	AATCTCTATCTTATTTAAAAATTAGGG
ZIP5	TATGTTTTTATTTGAGGCACAAATT	CTTATCGATTAGGGTTTGAATTTGA
ZIP9	CAGATATGCCCAAAGCATATTCCT	TAGCTGCGAACTTGAGGGTAA
ZIP10	TTGTCCTCTTTTCCCGCTTC	CTTCTATTTGTTCTTGTGGAGTTTT
ZIP11	GAACTTTGAGAAATTATTGGTTGAAAC	TTTGAATGTTCAAGTGGGTTTGT
ZIP12	GAGTTGTGTACCGTGAGTTGATTATT	TCGTTTACTTTTGACAAAAGTTAGG
IRT3	ACTCTTTTTCATGTTCCATACACAATT	TTGGGGTCTAAGATGTCCTCG
HMA2	CATCTCAAAAGGTAACTTAAAGACAA	CTGCAGCAAAAAAGATTGTAACTTT
MTP2	AACTATTCCAAATGAGGAATCACAC	TCTTGTTTAAGGATTCTGCA
YSL3	CGTCCGAATATAATAGTCCAATTCTAC	TTTTTTCCAAGAACAGAACAAAAAA

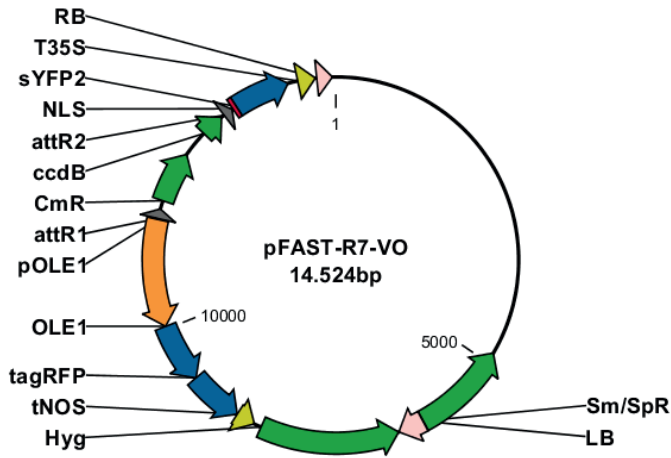


**Figure S1.** Gateway destination vector was generated to clone the promoter sequences. FAST-R07 (Shimada et al., 2010) modified vector.

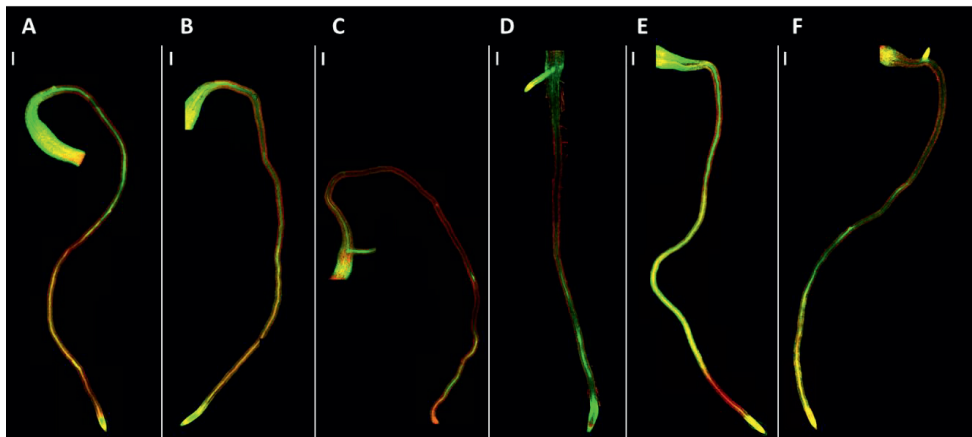


**Figure S2.** Confocal laser scanning microscope images of Zn distribution in Arabidopsis roots of wild-type and T-DNA insertion lines. (A) Zn deficient Arabidopsis roots of five-day-old Col-0 wild-type, *zip1* (B), (C) *zip3*, (D) *zip5*, (E) *irt3* and (F) *ysl3* plants incubated with Zinpyr-1 to detect Zn. Zinpyr-1 complexed to Zn fluoresces green, while propidium iodide bound to cell wall or DNA fluoresces red. The scale bars indicate 200  $\mu$ m.



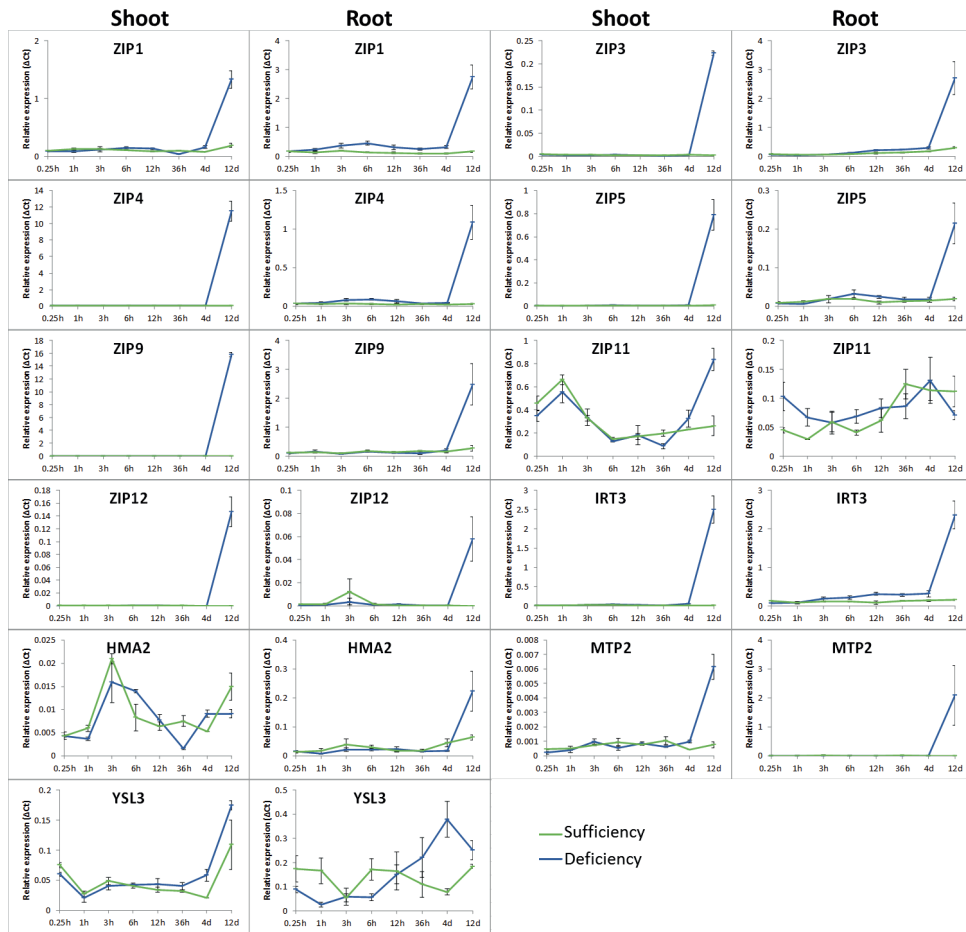


**Figure S3.** Gene expression in shoots and roots of Arabidopsis in response to Zn deficiency. Gene expression relative to *At5g25760* and *AT2G28390* in shoots and roots of plants grown for ten days in fully supplied medium and then in either Zn deficiency (blue lines) or Zn sufficiency (green lines) during 12 days. Samples were taken at several time points from 0.25 hours (h) to 12 days (d) after applying the treatment. Mean  $\pm$  SE,  $n = 3$  of 3 pooled plants.

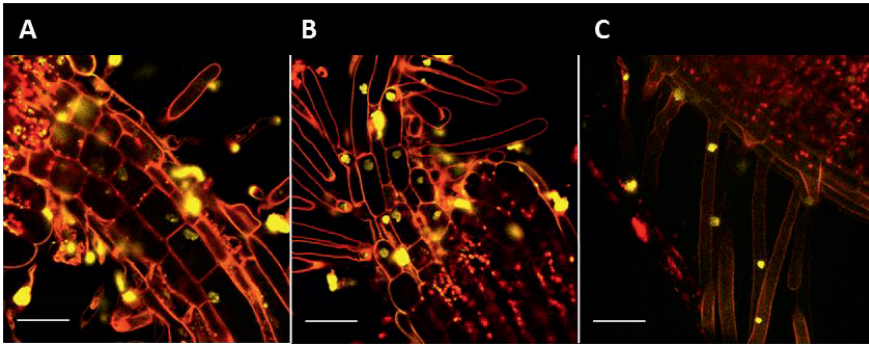


**Figure S4.** Confocal laser scanning microscope images of *Arabidopsis* roots expressing nuclear-localized YFP driven by promoter regions of three Zn transporters. The SYFP2 fluorescent signal (yellow) can be seen in all nuclei of cells expressing the NLS-SYFP2 marker gene. The red fluorescent signal indicates mainly cell walls stained with propidium iodide. *Arabidopsis* root transition zone expressing NLS-SYFP2 driven by the promoter regions of (A) ZIP9, (B) ZIP12, and (C) MTP2. Yellow spots bigger than nuclei, in the transition zone, correspond to the autofluorescence of seed fragments. The scale bars indicate 50  $\mu\text{m}$  in B-H.





# Chapter 3

## **Disruption of N-terminal-acetylation disturbs mineral homeostasis in *Arabidopsis thaliana***

Valeria Ochoa Tufiño<sup>1,3</sup>, Ana Carolina Campos<sup>1,4</sup>, Joost van den Heuvel<sup>1</sup>, Ana G. L. Assunção<sup>1,5</sup>, Eric Linster<sup>2</sup>, Markus Wirtz<sup>2</sup> and Mark G.M. Aarts<sup>1</sup>

- 1) Laboratory of Genetics, Wageningen University, Wageningen, The Netherlands
- 2) Centre for Organismal Studies, University of Heidelberg, Heidelberg, Germany
- 3) Current affiliation: Departamento de Ciencias de la Vida, Universidad de las Fuerzas Armadas ESPE, Sangolquí, Ecuador
- 4) Current affiliation: Dümmer Orange, Leiderdorp, The Netherlands
- 5) Current affiliation: Department of Plant and Environmental Science, University of Copenhagen, Copenhagen, Denmark

*In preparation for submission*

### Abstract

The functional diversity of the plant proteome is large, even larger than the diversity of the plant transcriptome, this is as a result of several types of protein modifications that alter protein activity, lifespan, localization and protein-protein interactions. N-terminal-acetylation (N-t-acetylation) is a protein modification that is widespread among eukaryotes, carried out by N-alpha-terminal-acetyltransferase complexes (Nats). After a mutation mapping approach in *Arabidopsis thaliana* (Arabidopsis) we identified a mutation in the *N-ALPHA-TERMINAL ACETYLTRANSFERASE 25 (NAA25)* gene, which encodes the non-catalytic subunit of NatB, to be responsible for aberrant regulation of the Zn deficiency response. We tested several additional mutants of *NAA25*, all which displayed pleiotropic effects affecting plant morphology, sensitivity to Fe deficiency, and to a lesser degree the deregulation of Zn deficiency response. To further understand the processes involved, we examined the transcriptome of a *naa25* mutant under control, Zn or Fe deficiency medium. The mutant showed differential expression of genes involved in plant defence response under all tested conditions. Several Zn deficiency responsive genes showed a slightly but consistently high expression in *naa25*, under fully supplemented medium, compared to wild-type plants. Upon Fe deficiency, genes involved in Fe distribution and sequestration are higher expressed in the mutant than the wild type. In addition, several genes encoding components of Photosystem I (PSI) and PSII are differentially expressed in *naa25*. Although Zn and Fe deficiency responses are affected in the *naa25* mutant, these appear to be pleiotropic effects of a general de-regulation of protein N-t-acetylation, which affects several other processes involved in plant growth and development.

## Introduction

Proteins can undergo different kinds of co- and/or post-translation modifications (Karve and Cheema, 2011). One of these modifications is N-t-acetylation, which generally occurs during translation. N-t-acetylation is very common in most eukaryotes. Around 80% of mammalian and plant proteins are N-t-acetylated (Pesaresi et al., 2003; Linster et al., 2015; Aksnes et al., 2016). N-t-acetylation can affect protein stability, subcellular location, interaction with membranes, protein-protein interactions, protein folding, and aggregation. It involves the transfer of acetyl groups from acetyl-CoA to the  $\alpha$ -amino group of the protein N-terminal-residue. This process is carried out by ribosome-associated N-alpha-terminal-acetyltransferase (NAA) enzymes (Polevoda and Sherman, 2000; Gibbs, 2015; Aksnes et al., 2016). The NAA proteins form complexes, named as Nats, with catalytic and non-catalytic auxiliary subunits (Polevoda and Sherman, 2003). A total of seven Nats (NatA-NatG) are described in eukaryotes. The most common are the NatA, NatB, and NatC, which are responsible for the majority of N-t-acetylation events (Linster et al., 2015).

Little information is available about NatA, NatB, and NatC in plants. In *Arabidopsis* the disruption of *NAA30*, which encodes for the NatC catalytic subunit, decreases the accumulation of mature proteins in chloroplasts, affecting photosynthesis efficiency (Pesaresi et al., 2003). NatA impairment in *Arabidopsis*, due to the disruption of either *NAA10* or *NAA15*, causes embryo lethality. These genes encode for the catalytic and auxiliary subunit of NatA respectively. Downregulation mutants of *NAA10* or *NAA15* show a decreased sulphate assimilation and increased drought tolerance (Linster et al., 2015). Downregulation of *NAA10* or *NAA15* also increases the stability of the plant immune receptor SUPPRESSOR OF NPR1-1, CONSTITUTIVE 1 (SNC1). On the other hand, the stability of SNC1 decreases due to mutations in *NAA20* or *NAA25*, which encode for the catalytic and auxiliary subunit of NatB (Xu et al., 2015). The phenotypes of *naa10*, *15*, *20*, *25* and *30* single mutants (Linster et al., 2015) suggest a major role of N-t-acetylation in plant growth and adaptation to environmental changes (Gibbs, 2015).

Plants are continuously challenged to biotic and abiotic stresses that reduce plant fitness, crop yield, and food quality. One of these stresses is micronutrient deficiency, that is a shortage of Fe, Zn, Mn, Cu, Mo, B, Co, and/or Se. Micronutrient deficiencies often lead to stunted growth, poor development, small and twisted leaves, chlorosis or necrotic spots. Zn and Fe

micronutrient deficiencies are widespread and occur at many sites worldwide, often associated with calcareous or (slightly) alkaline soils, in which the bioavailability of divalent cations is generally low (Alloway, 2009). Plant responses to mineral deficiencies are often specific for each mineral and involve several physiological adaptations, following the sensing and signalling of the deficiency.

The Fe deficiency response, involving the expression of several genes contributing to Fe acquisition and distribution, is regulated by several transcription factors, such as the FE-DEFICIENCY-INDUCED TRANSCRIPTION FACTOR 1 (FIT1) and basic helix-loop-helix proteins bHLH38, 39, 100, 101, 104, 115 and POPEYE (PYE) (Colangelo and Guerinot, 2004; Wu et al., 2012; Wang et al., 2013; Liang et al., 2017). Compared to the control of Fe deficiency, less is known about the regulation of the Zn deficiency response, even though both elements share an intricate cross-homeostasis system (Shanmugam et al., 2011; Pineau et al., 2012; Briat et al., 2015). So far, the only identified regulators of the Zn deficiency response are the BASIC-REGION LEUCINE ZIPPER 19 (bZIP19) and bZIP23 proteins. Both transcription factors are expressed at low levels in plants and partly redundant, but without their function, plants are not able to induce the expression of several genes essential for a proper Zn deficiency response in mobilizing and acquiring more Zn from the soil (Assunção et al., 2010; Assunção et al., 2013).

We identified an *naa25* mutant in a screen for mutants displaying an aberrant Zn deficiency response. The *naa25* mutation promotes a mild Zn deficiency response under sufficient Zn conditions, but also a strong sensitivity to Fe deficiency. *NAA25* encodes the auxiliary subunit of the NatB in Arabidopsis. We examined additional mutant phenotypes, including *naa25* mutant transcriptome, and analysed the involvement of the *NAA25* gene in the response to Fe and Zn deficiency to further understand the pleiotropic phenotype of the *naa25* mutant.

## Materials and Methods

### Plant material and growth conditions

T-DNA insertion lines were ordered from the Nottingham Arabidopsis Stock Centre (NASC; [www.arabidopsis.info/BasicForm](http://www.arabidopsis.info/BasicForm)), except for *naa20* (Salk-027687), which was provided by Markus Wirtz. Arabidopsis accession Columbia (Col-0) was used for, and depending on the background of T-DNA insertion lines either Col-0 or Col-4 were used as a wild-type control. Prior to germination, seeds were stratified for three days at 4°C in the dark. The plants used for



genetic analysis and transformation were grown in peat-based fertilized potting mixture or rockwool, in a greenhouse set at 16/8 h light/dark cycle at 20/18°C day/night temperatures and 70% humidity. For agar-plate-based phenotypic screens, plants were grown on agar plates in a climate-controlled growth chamber set at a 16/8 h light/dark cycle at 22/20°C day/night temperatures and 50% humidity. Seeds were surface-sterilized using vapor-phase seed sterilization (Clough and Bent, 1998) and sown on 12-cm square petri dishes containing 1% agar-solidified half-strength MS medium (pH 5.8). The control medium contained 15  $\mu\text{M}$   $\text{ZnSO}_4$ , 50  $\mu\text{M}$   $\text{Fe}(\text{Na})_2\text{EDTA}_2$  and 0.05  $\mu\text{M}$   $\text{CuSO}_4$ . The media used for different mineral treatments contained the same concentrations except for: no added Zn in the Zn deficiency treatment, 150  $\mu\text{M}$   $\text{ZnSO}_4$  in the Zn excess treatment, 2.5  $\mu\text{M}$   $\text{Fe}(\text{Na})_2\text{EDTA}_2$  in the Fe deficiency treatment and 40  $\mu\text{M}$   $\text{CuSO}_4$  for the Cu excess treatment. Plant grown in agar plates were collected after three weeks of treatment and dried for three days at 60 °C to determine dry weights.

Plants were also grown hydroponically, in a climate-controlled growth chamber set at 70% humidity, a 12/12 h light/dark cycle, and 20/15°C day/night temperatures. Vapor-phase sterilized seeds were sown on 0.55% agar-filled tubes of which the bottom was cut-off, and grown on a modified half-strength Hoagland's nutrient solution (Schat et al., 1996). The first two weeks plants grew in a control medium (2  $\mu\text{M}$   $\text{ZnSO}_4$  and 20  $\mu\text{M}$   $\text{Fe}(\text{Na})_2\text{EDTA}_2$ ), and thereafter treatments were applied or plants were maintained to grow in the control medium. The treatments contained no added Zn for Zn deficiency or no added Fe for Fe deficiency.

### **Generation of mutagenized population and screening**

Seeds of an *Arabidopsis* transgenic line (Col-0 background), stably transformed with a *pZIP4::GUS* construct (Lin et al., 2016) and containing multiple copies of this construct at one locus was used for  $\gamma$ -ray-mutagenesis. For this, seed batches of 65 mg each were suspended in a solution of 10 mM  $\text{KNO}_3$  and 0.2% agar and exposed to a dose of 300 Grey  $\gamma$ -rays at Isotron (Ede, The Netherlands). One hundred pools of ~100 M1 seeds were sown in 100 trays with peat-based fertilized potting mixture in the temperature-controlled greenhouse. From each tray, a pool of M2 seeds was harvested and ~400 seeds per pool (~40,000 seeds) were screened for GUS expression. Seeds were sown on 15-cm diameter round petri dishes containing 0.6% agar-solidified half-strength MS medium plus 1% sucrose. No Zn was added for Zn deficiency or 30  $\mu\text{M}$   $\text{ZnSO}_4$  was added for Zn sufficiency. A non-destructive GUS-assay was used, which involved the application of 3 ml of reagent mix on the surface of every 15-cm diameter round

petri dish. The reagent mix contained 2 mM X-Gluc (5-Bromo 4-Chloro-3-Indolyl  $\beta$ -D-glucuronic acid cycloheximide salt) in 50 mM NaH<sub>2</sub>PO<sub>4</sub> buffer (pH=7.2) and 0.5% Triton X-100. The plates were incubated at room temperature until staining was visible (around 2-3 hours). Selected plants were rescued by transferring to fresh MS medium and kept there for three days. Thereafter, they were transferred to a peat-based, fertilized potting mixture and grown in the greenhouse.

### Identification of causal mutations

The selected mutants, in Col-0 background, were crossed with Ler-1. A dominance test was performed by GUS staining of the F1 and F2 seedlings. To select the plant pools for map-based-cloning, around 2,000 F2 seeds of each mutant x Ler-1 cross were sown on agar plates containing half-strength MS medium with 20 mg/L Hygromycin. After 5 to 7 days, resistant seedlings containing the *pZIP4::GUS* construct were transferred to medium with or without Zn, depending on their phenotype. After two weeks a small piece of the root of each plant was collected for GUS staining to determine their phenotype. Depending on the mutant, selected plants were not expressing GUS under Zn deficiency (for mutants found not to express GUS under Zn deficiency) or expressing GUS under Zn sufficiency (for mutants expressing GUS under Zn sufficiency). The selected seedlings were transplanted to a peat-based potting soil and kept in the greenhouse. Plant material (3 to 4 flower heads) from all plants of each pool was collected for DNA extraction. The DNA was extracted using the DNeasy 96 Plant Kit (Qiagen [www.qiagen.us/](http://www.qiagen.us/)). The mutant sequences were determined by high-coverage whole-genome sequencing following the SHOREmap method as described by Schneeberger et al. (2009).

### Confirmation of mutations and T-DNA insertion lines

To confirm the mutated sites narrowed down by the SHOREmap, DNA was amplified with the Phusion Flash High-Fidelity PCR Master Mix (Thermo Scientific; [www.thermofisher.nl/en/home.html](http://www.thermofisher.nl/en/home.html)) (**Supplemental Table S1**). PCR products were Sanger-sequenced (GATC-BIOTECH; [www.gatc-biotech.eu/index.html](http://www.gatc-biotech.eu/index.html)). T-DNA insertion lines were genotyped to confirm or select for homozygous insertion plants. Primers were designed using the website of the Salk Institute ([www.signal.salk.edu/tdnaprimers.2.html](http://www.signal.salk.edu/tdnaprimers.2.html)) (**Supplemental Table S2**).

### Quantification of N-terminal protein acetylation

This assay was performed as detailed in Linster et al. (2015).

### Quantitative real-time PCR

Total RNA was extracted from leaves using the Direct-zol™ RNA MiniPrep Kit (Zymo Research, [www.zymoresearch.com](http://www.zymoresearch.com)) and cDNA was synthesized with the iScript cDNA Synthesis Kit. Gene expression was quantified by qRT-PCR with SYBR® Green mix (Bio-Rad, [www.bio-rad.com](http://www.bio-rad.com)). Primers for qRT-PCR are detailed in (Assunção et al., 2010).

### Transcriptome determination

For transcriptome analysis, full root systems and shoots of two plants were collected per biological replicate after growing plants for 12 days in hydroponic conditions. Three biological replicates were sampled in each treatment. Total RNA was extracted as described before. RNA quality was confirmed by capillary electrophoresis on an Agilent 2,100 bioanalyzer (Agilent; [www.agilent.com](http://www.agilent.com)). A 250–300 bp insert cDNA library was prepared and sequenced in a HiSeq-S50 Illumina platform  $Q \geq 90\%$  (Novogen; [en.novogene.com](http://en.novogene.com)). Read quality was checked with FastQC, no trimming was applied, the analysis was done with more than 10 million reads per sample. Reads were aligned to the TAIR 10 version of the Arabidopsis whole genome sequence (Swarbreck et al., 2008) ([www.arabidopsis.org](http://www.arabidopsis.org)) using STAR (Dobin et al., 2013) ([www.genome.gov/encode/](http://www.genome.gov/encode/)). After read alignment, only uniquely aligned reads were kept. Gene expression was quantified using HTSeq (Anders et al., 2015) ([htseq.readthedocs.io/en/release\\_0.9.1/index.html](http://htseq.readthedocs.io/en/release_0.9.1/index.html)) per exon, where all exons of a gene were used to quantify the overall gene expression level. Only genes that were counted more than once in at least six of the 36 samples were included in the analysis. Gene expression was normalized using the voom method (Law et al., 2014). Mean difference plots were made using  $\log_2$  transformed count per million reads. To test for significant differences between treatments we performed linear models comparing control treatment with Fe or Zn deficient treatment for both root and shoot samples. For this analysis, we used eBayes lmFit method (Smyth Gordon, 2004). To test for significant differences between genotypes we performed a pairwise comparison for both root and shoot samples. We denoted genes to be significant if they had a False Discovery Rate (FDR) adjusted p-value lower than 0.05 and an absolute log fold change of 0.5. The sets of genes differentially expressed were analysed for overrepresented Gene Ontology (GO) terms. The GO enrichment analyses were performed using the Database for Annotation, Visualization and Integrated Discovery (DAVID) Bioinformatics Resources 6.8 (Huang et al., 2008, 2009).

### Statistical analysis

One way ANOVA, two way ANOVA and their respective post hoc test were calculated with Genstat 18th edition (VSN International; [www.vsn.co.uk/software/genstat/](http://www.vsn.co.uk/software/genstat/)).

## Results

### Identification of Zn homeostasis mutants

We designed a Zn-deficiency specific marker system to identify mutants disturbed in Zn homeostasis. The marker is based on the activity of the Arabidopsis *ZRT-IRT-LIKE PROTEIN 4* (*ZIP4*) Zn transporter promoter. *ZIP4* expression is very low under Zn sufficiency and strongly induced upon Zn deficiency, mainly in roots, but also in shoots (van de Mortel et al., 2006; Assunção et al., 2010; Lin et al., 2016). The full-length promoter was fused to the coding sequence of the *B-GLUCURONIDASE* (*GUS*) gene to create a *pZIP4::GUS* construct (Lin et al., 2016). One transgenic line containing the *pZIP4::GUS* construct at one locus of insertion, but with multiple T-DNA copies, as determined by Southern hybridization (data not shown), was selected based on stable expression of GUS over at least two generations and exclusively under Zn deficient conditions (**Figure 1**).

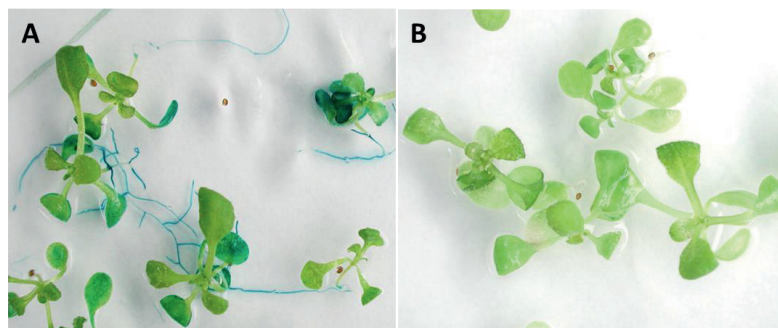


**Figure 1.** *In vivo* GUS staining assay of the Arabidopsis Zn deficiency reporter line carrying the *pZIP4::GUS* reporter construct. Seedlings were grown in MS-agar plates either at (A) Zn deficiency or (B) Zn sufficiency.

The Arabidopsis *pZIP4::GUS* reporter line was used as the genetic background to generate a  $\gamma$ -ray-mutagenized M2 population for mutant screens. From ~10000 irradiated M1 seeds, a large population of ~ 100 pools of M2 progeny was obtained. In total, ~ 35000 M2 seedlings were screened for aberrant GUS staining, either on Zn sufficiency or Zn deficiency MS agar plates (**Supplemental Figure S1**). A total of 81 plants were identified to show an aberrant GUS

staining phenotype. All putative mutant plants were transferred to soil, with 29 M2 plants surviving the transfer and producing M3 progeny by selfing. Since the absence of GUS staining can easily be caused by deletion or mutation of the T-DNA integration, the M3 was tested for hygromycin resistance. Indeed, in 14 out of 29 M3 progenies, the hygromycin resistance was lost. GUS expression in the remaining 15 lines was evaluated on Zn sufficient and Zn deficient medium, confirming the M2 mutant phenotype in only four M3 lines (**Figure 2**), the remaining lines assumed to be false positives. Lines M31 and M68 did not show GUS staining in the Zn deficiency treatment, while lines M22 and M60 expressed GUS in the Zn sufficiency control.

GUS transcript levels were significantly higher under Zn deficiency compared to Zn sufficiency in the *pZIP4::GUS* background control and in the mutant lines M22 and M60, which was consistent with the GUS staining (**Figure 2A and B**). The *ZIP4* transcript levels were significantly higher in all mutants under Zn deficiency compared to Zn sufficiency, with significantly lower transcription in M31, compared to the other lines (**Figure 2C**). Mutant lines M31 and M68 were expected to have low *ZIP4* and GUS transcript levels under Zn deficiency compared to the background control, but this was not the case for the *ZIP4* transcripts in M68. Based on the inconsistent expression in M68, we sequenced the construct in this line and discovered a deletion in the construct removing most of the GUS genes, explaining the absence of GUS staining under Zn deficiency. This line was discarded from further analyses. In contrast to expectations, the *GUS* and *ZIP4* transcript levels in M22 and M60 under Zn sufficiency were only marginally, and not significantly, higher than in the *pZIP4::GUS* background control, even though the GUS staining phenotype was confirmed consistently in at least 60 seedlings per genotype and tested over several generations.

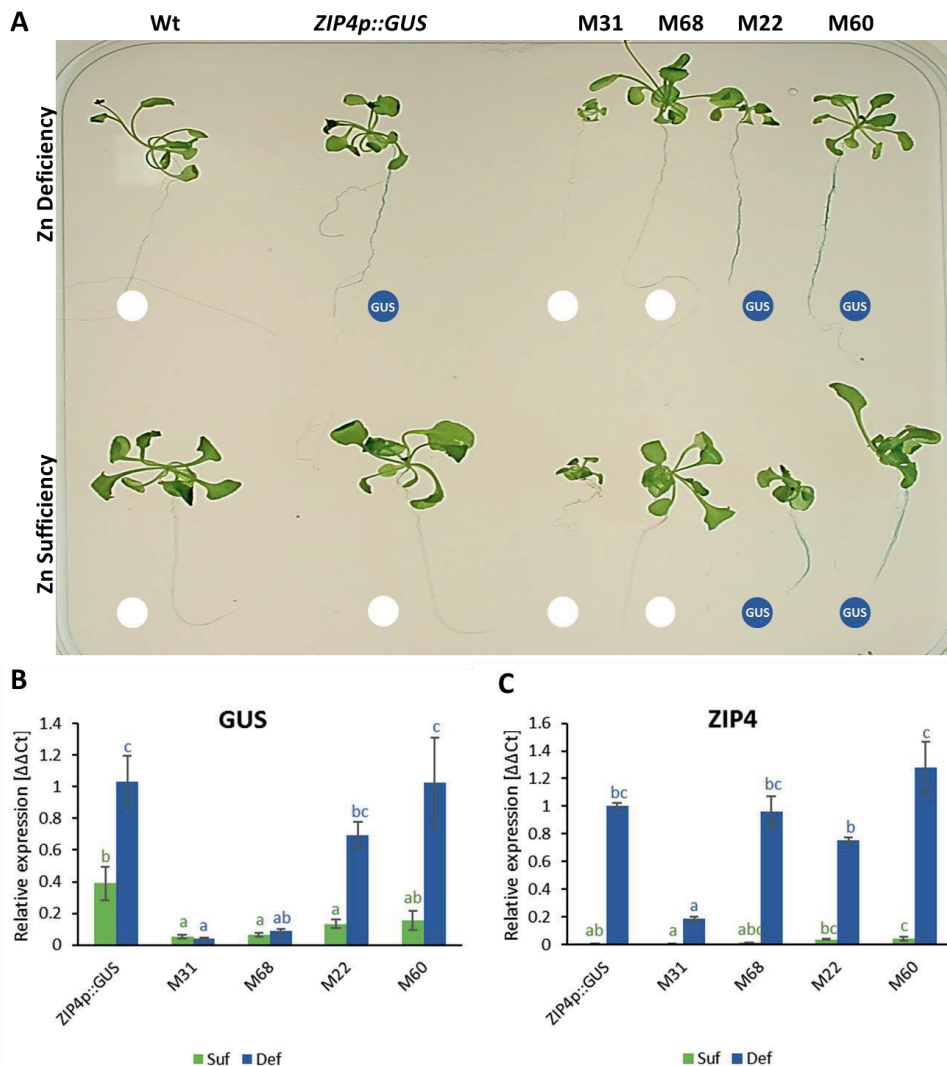


**Figure 2.** Selected mutant lines M31, M68, M22 and M60, displaying an aberrant GUS staining phenotype under either Zn deficiency (M31, M68) or Zn sufficiency (M22, M60). (A) GUS staining phenotypes of wild-type Col-0 (Wt) and the transgenic pZIP4::GUS line used as background for the mutant screen and the four selected mutants grown on vertical MS-agar plates under Zn deficiency (top) and sufficiency (bottom). Expression of (B) GUS and (C) ZIP4 relative to 18S ribosomal RNA in the four mutants and the pZIP4::GUS mutant background, grown under Zn deficiency (Def, blue bars) or Zn sufficiency (Suf, green bars). Means and error bars were calculated from pooled seedlings from three plates. Letters above the bars denote statistically different groups when comparing among genotypes grown under Zn deficiency (blue) or sufficiency (green), obtained with a Tukey post hoc test ( $\alpha=0.05$ ), after a one-way ANOVA (Supplemental Table S3).



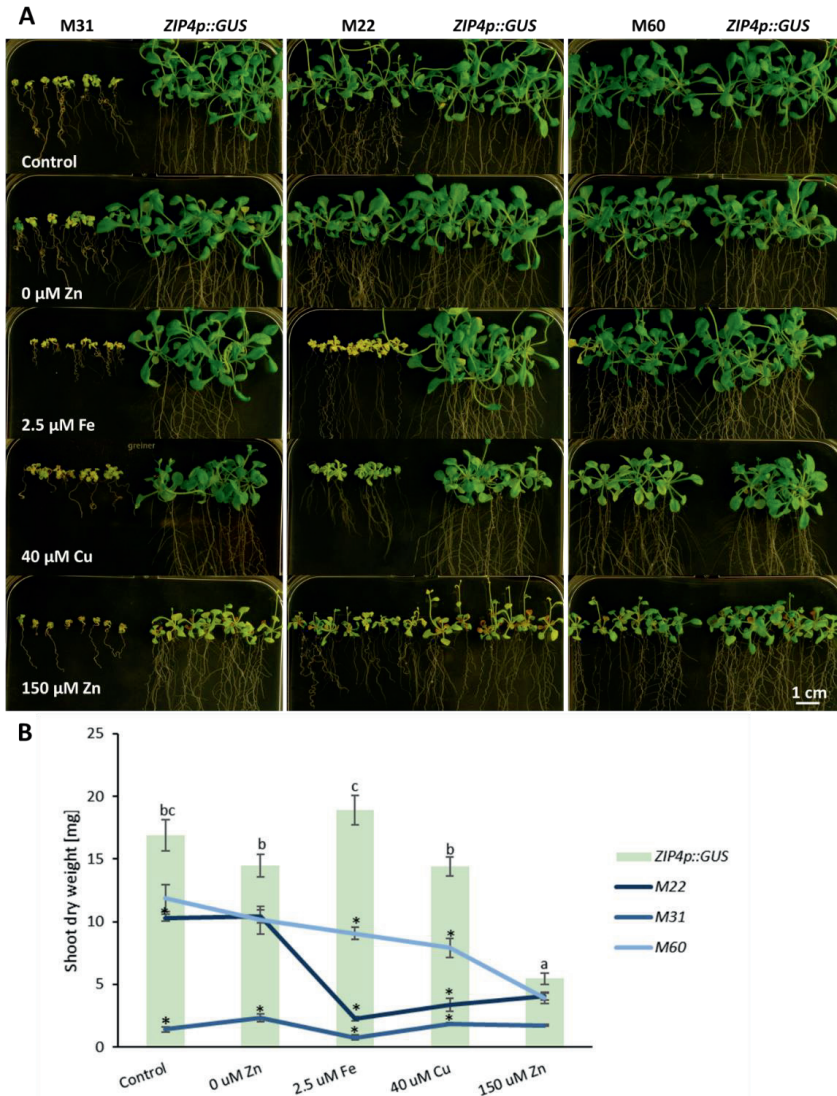


**Figure 3.** Response of mutant lines M31, M22, and M60 to different mineral stress conditions. (A) Three-week-old seedlings grown on vertical half MS-agar plates either at Zn or Fe deficiency or at Cu or Zn excess. (B) Shoot dry weight of the pZIP4::GUS control (green bars), mutant M22 (dark blue line), mutant M31 (medium blue line), and mutant M60 (light blue line). Means and error bars were calculated from pooled seedlings from four plates of each treatment for the mutant lines and from twelve plates of each treatment for pZIP4::GUS control background. Letters above the bars denote statistically different groups of the pZIP4::GUS genotype between treatments, obtained with a Bonferroni post hoc test ( $\alpha=0.05$ ), after a one-way ANOVA. (\*) above error bars indicates significant differences between the mutant and the pZIP4::GUS control, obtained with a Bonferroni post hoc tests ( $\alpha=0.05$ ), after a two-way ANOVA (**Supplemental Table S4**).

### Identification of causal mutations

To identify the causal mutations of the M22, M31 and M60 mutants, we applied a SHOREmap approach (Schneeberger et al., 2009). First, we crossed the mutants to the Landsberg *erecta* (Ler) accession and determined that the mutations in all three lines were recessive, based on the absence of the aberrant GUS staining phenotype in F1 seedlings and the recessive segregation ratio of the phenotype in the F2. Subsequently, we selected all hygromycin resistant F2 plants with the corresponding mutant GUS phenotype of each mutant line. Finally, we pooled these selected mutant plants of each F2 progeny for genome sequence analysis, to determine enrichment of genomic sequences corresponding to Col-0 markers, covering the region of the mutation as well as the region of the *pZIP4::GUS* T-DNA insertion.

The *pZIP4::GUS* construct insertion was mapped to chromosome 5, between positions 19,236,175 and 19,236,228, disrupting the gene At5g47430, which encodes a CCHC-type zinc finger transcription factor of further unknown function. For the M60 mutant, we did not obtain a clear interval within which the mutation would reside, it looks like some of the pooled plants were collected as false-positive mutants, thus disturbing the analysis. The mutations of M22 and M31 were indicating similar regions on chromosome 5. The interval mapping for M31 highlighted the region between positions 22.5-24.5Mb as most enriched in Col-0 markers. However, in this interval, there was not a specific region with strong evidence of being associated with the mutant phenotype. Manual examination of the sequence to identify any possible mutation was not successful. The interval mapping for the M22 mutation candidate identified the region between positions 19.5 to 24.5Mb. By comparing the genome sequence with that of Col-0 and the other mutants, we detected three evident sequence changes. Only one could be confirmed upon resequencing of the specific site. It constitutes an 8-bp deletion in exon 12 of the *NAA25* gene (At5g58450) (**Supplemental Figure S2**). *NAA25* encodes the auxiliary subunit of the acetylation complex NatB. The deletion introduces a premature stop codon, roughly in the middle of the *NAA25* protein coding sequence. A second mutation was confirmed by sequencing, involving a G to A mutation, within the coding sequence of At5g61940, encoding a ubiquitin carboxyl-terminal hydrolase-related protein, however, this change is outside the mapping interval (24.8Mb) and thus considered to be less likely to be causal for the mutant phenotype.



Based on the unambiguous mapping of the M22 mutation, we focused on the two genes in which mutations were found, *NAA25* and AT5G61940. Two independent T-DNA insertion lines, for both *NAA25* and AT5G61940 (**Supplemental Table S2**) were verified and grown to establish their phenotypes. Neither of the two T-DNA insertion lines for At5G61940 showed any similarities to the M22 phenotype. This in contrast to the T-DNA insertion lines for *NAA25*, with insertions in exons 11 (SK24830) and 15 (GK-819A05) of *NAA25* respectively. Both showed similar phenotypes as M22 (**Figure 4**). When compared to wild type, the mutants were shorter; with an increased number of inflorescences originating from the rosette (**Figure 4A**); chlorotic cauline leaves; wider and curly rosette leaves; chlorotic and aborted siliques (**Figure 4B**); and malformed flowers with chlorotic sepals (**Figure 4C**). The two T-DNA insertion lines also showed the same high sensitivity to Fe deficiency as M22 (**Figure 4D**). To confirm allelism, a cross was made between M22 and SK24830 and between *pZIP4::GUS* and SK24830. The F1 plants of the first cross all showed the same sensitivity to Fe deficiency as seen in both parents, while the F1 with *pZIP4::GUS* displayed a normal wild-type phenotype (**Supplemental Figure S3**). This confirms that the M22 and SK24830 mutants are allelic and their mutant phenotypes are the result of mutations in the same gene, *NAA25*. In addition to the similar phenotypes, we checked if our three *naa25* mutant lines (SK24830, GK-819A05 and M22) were truly affecting the N-terminal acetylation of proteins. We used as a positive control *naa20*, a mutant for the catalytic subunit of NatB, and compared to the three *naa25* mutant lines (**Figure 5**). The four mutants behave very similar showing around a 30% decrease in protein N-terminal acetylation. From this point on we continue only with the SK24830 mutant, which has the disruptive T-DNA insertion in *NAA25* very close to the M22 mutation, and is genetically cleaner than M22, as the latter is shown to contain additional mutations and may carry many more, which are not related to the Zn and Fe homeostasis phenotype, but which may disturb the analysis of the *NAA25* gene function.

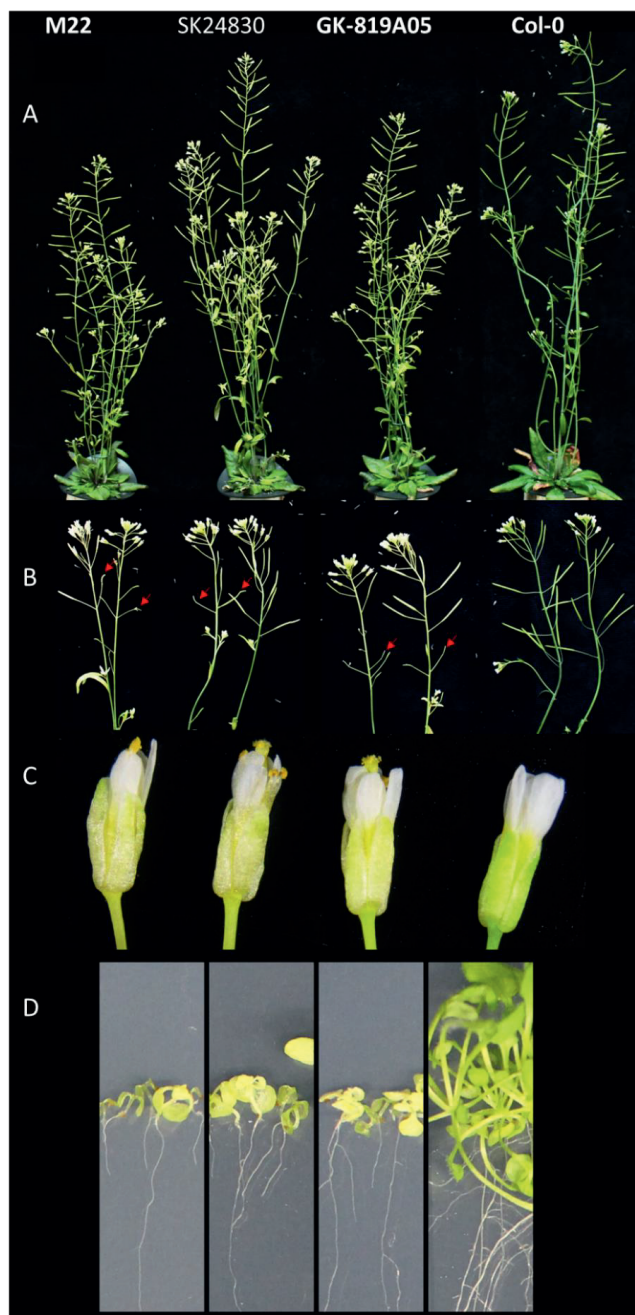


**Figure 4.** Phenotype of M22, two homozygous *NAA25* T-DNA insertion lines carrying the T-DNA in resp. exon 11 and 15 of *NAA25* (SK24830 and GK-819A05), and *Arabidopsis* wild-type plants (Col-0). (A) Fully developed, two-month-old plants, (B) close up of inflorescence, (C) nearly opened flowers, and (D) seedlings grown for three weeks on vertical half MS-agar plates under Fe deficiency.

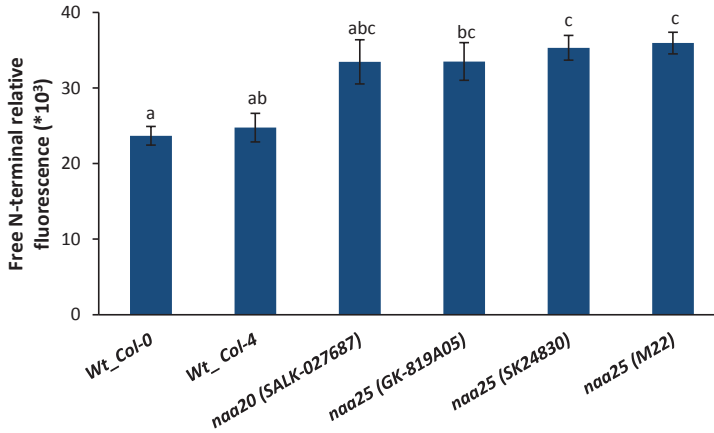


**Figure 5.** Quantification of free N termini in soluble protein fraction of wild-type, *naa20* mutant (Salk-027687), a three different *naa25* mutant (GK-819A05, SK24830 and m22) plants. Mean  $\pm$  SE,  $n = 4$  replicates. Letters above the bars denote statistically different groups, obtained with a Bonferroni post hoc test ( $\alpha=0.05$ ), after a one-way ANOVA ( $p<0.001$ ).

### Disruption of *NAA25* affects expression of genes in a range of biological processes

The disruption of *NAA25* causes several morphological defects, as well as the disturbance of Zn and Fe homeostasis. To gain insights into all biological processes that may be disturbed in the *naa25* mutant, we determined the whole transcriptome gene expression profile of *naa25* mutant SK24830 and its Col-4 wild-type genetic background by RNA-seq. The *naa25* mutant did not show *NAA25* transcripts after exon eleven (**Supplemental Figure S4**). Gene expression was quantified in roots and shoots independently, and denoted to be significantly different between mutant and wild type at a False Rate Discovery (FRD) adjusted  $p < 0.05$  and an absolute log<sub>2</sub> Fold Change (FC) of 0.5 (which corresponds to a  $FC \geq 1.4$ , either up or down). We found 436 genes to be differentially expressed in shoots and 99 differentially expressed genes in roots. Most of the differentially expressed genes were higher expressed in *naa25* (**Figure 6 and Table 1**). From all the genes differentially expressed in *naa25*, only 14 genes were differentially expressed in both shoots and roots.

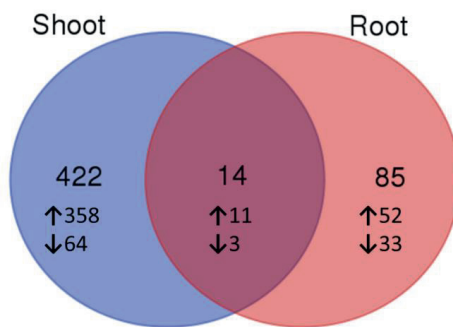


**Figure 6.** Differential gene expression between the *naa25* mutant and the *Col-4* wild type (*Wt*). Venn diagram of the number of differentially expressed genes in roots and shoots between both genotypes (↑ and ↓ indicating higher and lower expression in *naa25* vs *Col-4*).

**Table 1.** Differentially expressed genes in *naa25* mutant compared to the *Col-4* wild type in both shoots and roots. All differentially expressed genes found in both shoots and roots are shown organized from the ones with higher FC (Fold Change) to the ones with the lower FC.

Locus identifier	Symbol	Description	FC Shoot	FC Root	Expression trend
At2g01422		Expressed RNA	21.9	25.6	high
At5g35935		Copia-like retrotransposon gene	10.7	4.6	high
At2g27550	<i>ATC</i>	Homologue of FT and TFL1 involved in initiation of flowering	4.0	1.8	high
At5g01900	<i>WRKY62</i>	Transcription factor involved in biotic defence	3.7	2.2	high
At3g12220	<i>SPL16</i>	Serine carboxypeptidase-like 16	2.7	1.7	high
At4g11320	<i>CP2</i>	Cysteine protease involved in biotic stress response	2.3	2.0	high
At3g61198		Expressed RNA	2.3	2.3	high
At2g14560	<i>LURP1</i>	Factor involved in biotic defence response	2.2	2.6	high
At1g19960		Hypothetical transcription factor	1.9	2.0	high
At1g21520		Hypothetical transcription factor	1.5	2.1	high
At1g43700	<i>SUE3</i>	Transcription factor involved in biotic and abiotic stress	1.9	1.9	low
At1g31850		S-adenosyl-L-methionine-dependent methyltransferase	2.0	1.9	low
At5g58450	<i>NAA25</i>	NatB complex non catalytic subunit	2.5	2.7	low
At1g13710	<i>CYP78A5</i>	Cytochrome P450 involved in controlling seed or organ growth	2.9	3.1	low/high

(low/high) low in shoot and high in root

Among the fourteen *naa25* differentially expressed genes found in both roots and shoots (**Table 1**), several are involved in plants defence. The transcription factor VIRE2-INTERACTING PROTEIN (VIP1) is also known as SULPHATE UTILIZATION EFFICIENCY 3 (*SUE3*), because *sue3* plants with a non-functional allele of this gene are efficient in sulphate uptake (Wu et al., 2010). *SUE3* is also a regulator of osmosensory signaling and regulates *PATHOGENESIS-RELATED PROTEIN 1* (*PR1*) expression (Djamei et al., 2007; Tsugama et

al., 2012). WRKY62 is a negative regulator of plant basal defence, by reducing the expression of *PRI* (Kim et al., 2008). *LATE UPREGULATION IN RESPONSE TO HYALOPERONOSPORA PARASITICA* (*LURPI*) gene shares promoter sequences with the *PRI* regulon. *LURPI* is induced by fungal infections and salicylic acid (SA), and it is a negative regulator of cell death during hypersensitive response (HR) (Knoth and Eulgem, 2008; Lee et al., 2017). CP2 is a cysteine protease induced by wounding and involved in plant-mediated RNAi against herbivorous insects (Mao et al., 2013). The transcript of AT1G21520 is induced in response to SA and correlates with genes expressed in plant defence responses and systemic acquired resistance (SAR) (Meier et al., 2008). The transcript of AT3G61198 is down-regulated in light-treated seedlings and shows a negative correlation with transcript levels of *SUE3* and a positive correlation with transcript levels of *SCN1*. The transcript AT2G01422 is upregulated by fungal infections and down-regulated by ABA (Hruz et al., 2008). In total, eight of the fourteen genes differentially expressed in both roots and shoots of *naa25* are related with biotic defence responses in plants.

**Table 2.** Gene Ontology (GO) terms enrichment of differentially expressed genes in the *naa25* mutant compared to *Col-4* wild-type plants grown in control medium. Top five GO terms enriched within shoots (upper panel) and all GO terms enriched within roots (lower panel) based on higher (high) and lower (low) expressed genes in *naa25* compared to wild type. The percentage of query genes over the total number of genes of each biological process is indicated as (%). Go terms identified using DAVID Bioinformatics Resources 6.8 ([david.ncifcrf.gov/](http://david.ncifcrf.gov/)).

Biological process	GO code	Expression trend	p value	%	Fold enrichment
<b>Shoot</b>					
Anthocyanin-containing compound biosynthetic process	0009718	high	6.5E-06	1.7	21.4
Oxidation-reduction process	0055114	high	2.9E-04	10.2	1.9
Response to salicylic acid	0009751	high	4.9E-04	2.8	4.4
Phloem or xylem histogenesis	0010087	high	7.1E-04	1.4	12.1
Response to jasmonic acid	0009753	high	2.2E-03	2.5	3.9
Cytokinin-activated signalling pathway	0009736	low	8.0E-04	6.0	21.6
Response to chitin	0010200	low	5.9E-03	6.0	10.7
Cell wall biogenesis	0042546	low	1.2E-02	4.5	17.8
Cellular zinc ion homeostasis	0006882	low	1.4E-02	3.0	142.3
Regulation of transcription	0006355	low	2.7E-02	17.9	2.0
<b>Root</b>					
Salicylic acid mediated signalling pathway	0009863	high	1.2E-03	4.9	57.7
Metal ion transport	0030001	high	1.9E-02	4.9	13.9
Oxylipin biosynthetic process	0031408	high	4.6E-02	3.3	41.7
Aromatic compound biosynthetic process	0019438	low	3.0E-04	7.9	112.1
Response to osmotic stress	0006970	low	1.9E-02	7.9	13.8

To obtain a general overview of the biological processes affected in *naa25*, we performed a GO term enrichment analyses on all differentially expressed genes of plants grown in control medium. Several of the biological processes, for which enrichment was found, are related with biotic defence (**Table 2**). In addition, genes involved in cellular Zn homeostasis in shoots and metal ion transport in roots were also differentially expressed in *naa25*. Enrichment was also found for plant hormone signal transduction (**Table 2 and Supplemental Figure S5**). Most of the genes enriched in this pathway were lower expressed in *naa25*.

### **Mutation of *NAA25* alters nutrients homeostasis regulation**

The M22 mutant line was initially selected based on the observed *ZIP4* promoter-mediated GUS misexpression under Zn sufficiency, and three independent *naa25* mutants were highly sensitive to Fe deficiency. Differentially expressed genes are also enriched for cellular Zn homeostasis in shoots and metal ion transport in roots, which was why we also examined the whole transcriptome gene expression profile of the *naa25* mutant and its Col-4 genetic wild-type background under Fe and Zn deficiency conditions. In *naa25* mutant and wild type, both treatments triggered the known deficiency response. The Fe deficiency causes the differential expression of 821 genes in shoots and 512 in roots of both genotypes. This growing conditions upregulated the expression of genes encoding for the transcription factors which regulate the Fe deficiency cascade response. Also, genes encoding for Fe transporters, Fe chelators, and Fe chelate reductases were upregulated in both genotypes in response to Fe deficiency (**Supplemental Table S6**). The Zn deficiency causes the differential expression of 54 genes in shoots and 811 in roots in both genotypes. The genes that were strongly induced upon Zn deficiency encoded for Zn transporters and Zn chelators (**Supplemental Table S7**). This confirmed the effectiveness of the Fe and Zn deficiency treatments. Large-scale differences between genotypes (*naa25* and wild type), treatments (Fe deficiency, Zn deficiency, and control medium), and organs (roots and shoots) were visualized with a multidimensional scaling of all expressed genes. The largest difference was found between root and shoot, then between treatments, and the smallest differences were between genotypes (**Supplemental Figure S6**). To identify which genes were differentially expressed between the *naa25* mutant and the wild-type in each condition tested, we applied a pairwise comparison. As a result, more genes were upregulated in the *naa25* mutant compared to the wild type (**Table 3**).

**Table 3.** Number of genes differentially expressed per genotype, treatment, and tissue. Genes differentially expressed in *naa25* each grown condition are indicated as the total number, higher (high) or lower (low) expressed genes in *naa25* compared to wild type in the column of genotype. Genes differentially expressed in Fe deficiency or Zn deficiency, in both genotypes, compared to control conditions are indicated as the total number, upregulated (up) or downregulated (low) genes in deficiency compared to control medium in the column of treatment. Only the number of significantly differentially expressed genes are shown, based on a False Discovery Rate (FDR) adjusted  $p > 0.05$  and an absolute  $\log_2$  fold change of 0.5.

Sample	Genotype (high/low)	Treatment (up/down)
Control (shoot)	436 (369/67)	
Control (root)	99 (61/38)	
Fe deficiency (shoot)	10 (4/6)	821 (598 / 223)
Fe deficiency (root)	289 (213/76)	512 (425 / 87)
Zn deficiency (shoot)	54 (46/8)	456 (279 / 177)
Zn deficiency (root)	811 (30/510)	238 (173 / 65)

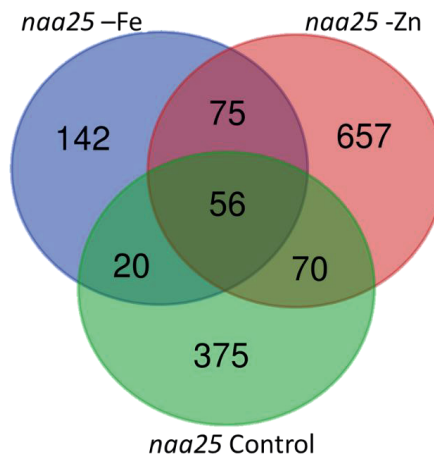


**Figure 7.** Differentially expressed genes in *naa25* mutant upon control, and Zn deficiency treatments. Venn diagram of number differentially expressed genes in *naa25* mutant compared to wild type upon control, Zn deficiency (Zn-) or Fe deficiency (Fe-) medium in shoots and roots. Only the number of significantly differentially expressed genes are shown, based on a False Discovery Rate (FDR) adjusted  $p > 0.05$  and an absolute  $\log_2$  fold change of 0.5.

The *naa25* mutant differentially expressed, in at least two of the three conditions tested, several genes involved in nutrients homeostasis as *SUE3*, *SULFATE TRANSPORTER 2;1* (*SULTR2;1*), *RESPONSE TO LOW SULFUR 3* (*LSU3*), *LSU4*, *SULPHUR DEFICIENCY-INDUCED 1*

(*SDI1*), *BUSH-AND-CHLOROTIC-DWARF 1 (BCD1)*, *HIGH AFFINITY K<sup>+</sup> TRANSPORTER 5 (HAK5)*, *CATION EXCHANGER 3 (CAX3)*, *CATION/H<sup>+</sup> EXCHANGER 16 (CHX16)*, *MAGNESIUM TRANSPORTER CORA-LIKE*, *PHOSPHATE 1 (PHO1)*, *NITRATE TRANSPORTER 2.1 (NRT2.1)*, *HEAVY METAL-ASSOCIATED ISOPRENYLATED PLANT PROTEIN 14 (HIPP14)*, *HIPP29*, and *HEAVY METAL-ASSOCIATED PLANT PROTEIN 10 (HPP10)*. All of them are higher expressed in *naa25* compared to wild type, except for *SUE3*, *PHO1*, *HAK5*, and *CAX3*.

A total of 293 genes were differentially expressed in *naa25* mutant compared to wild type upon Fe deficiency (**Figure 7**). From these 293 genes, 215 genes were higher expressed and 78 lower expressed in *naa25* mutant compared to wild type upon Fe deficiency. The first GO term enriched by the genes higher expressed was photosynthesis and by the genes lower expressed was cellular response to Fe (**Table 4**). Among some of the genes involved in transition metal homeostasis differentially expressed in *naa25* compared to wild type exclusively due to Fe deficiency are *FE SUPEROXIDE DISMUTASE 1 (FSD1)*, *IRT3*, *ZIP3*, *ZIP8*, *VACUOLAR IRON TRANSPORTER-LIKE 5 (VTL5)*, *FERRIC REDUCTION OXIDASE 1 (FRO1)*, *B-GLUCOSIDASE 42 (BGLU42)*, *MYB72*, *WRKY46*, and *HIPP2*. A total of 858 genes were differentially expressed in *naa25* mutant compared to wild type upon Zn deficiency (**Figure 7**). From these 858 genes, 301 genes were higher expressed and 515 lower expressed in *naa25* mutant compared to wild type upon Zn deficiency. Among some of the genes involved in transition metal homeostasis differentially expressed in *naa25* compared to wild type exclusively due to Zn deficiency are *HMA2*, *IRT2*, *ZIP10*, *PLANT CADMIUM RESISTANCE 1 (PCR1)*, *FRO4*, *FRO5*, *FRO8*, *HPP11*, *HPP13*, *HIPP3*, and *HIPP13*. In general, several GO terms enriched among genes differentially expressed in *naa25* compared to wild type in Fe or Zn deficiency consistently include biological processes involved in biotic defence and mineral homeostasis as also observed in control conditions (**Table 2**).

The M22 mutant was selected in a control medium not in Zn deficiency. For this reason, we went back to the *naa25* in control conditions and looked there for the gene expression patterns of Zn deficiency responsive genes. In control medium, the Zn deficiency responsive genes (van de Mortel et al., 2006) *ZIP1*, *ZIP4*, *ZIP5*, *IRT3*, *PCR1*, *YSL3*, *NAS1*, and *NAS4* showed a consistent higher number of transcripts in shoots and roots of *naa25* mutant compared to wild type, while *ZIP9*, *ZIP11*, *FRD3*, and *Cadmium Sensitive 1 (CAD1)* showed only in shoots (**Supplemental Figure S7**). These genes are 0.7 times higher expressed in *naa25* mutant than



in the wild type on the average and due to the samples variation, they do not appear to be significantly different.

**Table 4.** Gene Ontology (GO) terms enrichment of differentially expressed genes in the *naa25* mutant compared to *Col-4* wild-type plants grown under Zn or Fe deficiency. Top five GO terms enriched within Fe deficiency (upper panel) and Zn deficiency (lower panel) based on higher (high) and lower (low) expressed genes in *naa25* compared to wild type. The percentage of query genes over the total number of genes of each biological process is indicated as (%). Go terms identified using DAVID Bioinformatics Resources 6.8 ([david.ncifcrf.gov/](http://david.ncifcrf.gov/)).

Biological process	GO code	Expression difference	P value	%	Fold enrichment
<b>Fe deficiency</b>					
Photosynthesis	0015979	high	1.3E-04	3.8	7.1
Metal ion transport	0030001	high	2.5E-04	3.3	7.9
Defense response to bacterium	0042742	high	1.9E-03	4.3	4.0
Response to chitin	0010200	high	4.6E-03	2.9	5.5
Regulation of stomatal movement	0010119	high	5.8E-03	1.9	10.9
Cellular response to iron ion	0071281	low	2.6E-09	9.7	54.9
Response to hypoxia	0001666	low	8.9E-06	6.9	37.3
Oxidation-reduction process	0055114	low	7.3E-04	18.1	3.1
Response to osmotic stress	0006970	low	6.6E-03	5.6	10.3
Regulation of flower development	0009909	low	2.3E-02	4.2	12.7
<b>Zn deficiency</b>					
Response to toxic substance	0009636	high	8.5E-06	2.4	10.8
Cellular transition metal ion homeostasis	0046916	high	2.1E-05	2.4	9.4
Oxidation-reduction process	0055114	high	6.0E-05	10.2	2.1
Response to oxidative stress	0006979	high	2.2E-04	3.9	3.7
Response to wounding	0009611	high	7.1E-04	3.0	4.1
Plant-type cell wall organization	0009664	low	1.8E-13	3.8	10.5
Receptor protein tyrosine kinase signalling	0007169	low	3.0E-07	3.0	5.8
(1->3)-beta-d-glucan biosynthetic process	0006075	low	2.1E-06	1.2	25.2
Cell wall organization	0071555	low	4.9E-06	4.2	3.4
Protein phosphorylation	0006468	low	2.5E-05	7.4	2.1

### Zn and Fe deficiency response regulators as possible targets of NatB complex

The NatB complex is not known to directly regulate the expression of genes. However, it could modify proteins responsible for regulating gene expression. For that reason, we performed a transcription factor prediction based on the genes differentially expressed upon Fe or Zn deficiency compared to control conditions. The transcription factors predicted for Fe deficiency were PIF1, PIF4, ELONGATED HYPOCOTYL 5 (HY5), bHLH34, bHLH104, PYE, and WRKY53. For Zn deficiency, PIF4, HY5, and SEPALLATA 3 (SEP3) were the predicted

transcription factors. For these transcription factors, we analysed their N-t to determine if they could be targets of acetylation by the NatB complex. The transcription factors bHLH104, WRKY53, PIF1, and PIF4 have putative NatB complex N-t targets. Another major known Fe deficiency regulator is FIT which did not appear in our prediction, but it has the sequence to be a target of the NatB complex. In addition, even bZIP23 and bZIP19 did not appear in our prediction either, they are the only known Zn deficiency regulators. The N-t of bZIP23 and bZIP19 are putative targets for NatB acetylation.

## Discussion

### Pleiotropic effects of *NAA25* disruption

In plants and animals, around 80% of proteins are N-t-acetylated and about 20% of those acetylations can be carried out by the NatB complex (Linster et al., 2015; Aksnes et al., 2016). The NatB complex is composed of the catalytic subunit NAA20 and the auxiliary subunit NAA25. The non-catalytic subunit is required for protein-protein interactions and protein-ribosome interactions (Liszczyk et al., 2013). The M22 mutant, and the T-DNA insertion lines in which *NAA25* is disrupted showed a range of morphological mutant phenotypes. These effects are expected due to the large number of putative substrates of NatB, which infer major and widespread effects in the cells (Linster et al., 2015; Aksnes et al., 2016).

Most of the biological processes with differentially expressed genes in *naa25* mutant were related with stress response, and mainly biotic stress (**Table 2**). The first biological process upregulated in *naa25* mutant was anthocyanins biosynthesis. Anthocyanins are synthesised in response to biotic or abiotic stress conditions and serve as antioxidants that quench reactive oxygen species (ROS). ROS can severely damage cells, but they are also signalling molecules to activate defence response cascades for instance to nutrient deficiency, mechanical disturbance, or pathogen attack (Mittler, 2002; Koinich et al., 2014). In the *naa25* mutant, several biological processes related with plant defence response against wound and pathogen attack have differentially expressed genes. The pathogen resistance regulator SNC1 is the only confirmed substrate of the NatB complex. One of the splice variants of SNC1 is acetylated by NatB, which modifies its stability (Xu et al., 2015). The *snc1* mutant plant is small with curly leaves and enhanced autoimmune response (Zhang et al., 2003). Common autoimmune phenotypes are dwarfism and elevated salicylic acid levels (van Wersch et al., 2016). Some of the pleiotropic effects observed in *naa25* mutants as curly leaves, increased number of basal

branches, and decrease height of the primary inflorescence, resemble plants with either autoimmune response or pathogen infections (Korves and Bergelson, 2003; Stes et al., 2015). However, *naa25* mutant did not show resistance to *Hyaloperonospora arabidopsidis* colonization compared to wild type (data not shown).

The cytokinin signalling pathway was the main lower expressed biological process in *naa25* mutants when compared to wild type. Cytokinins are plant hormones associated with plant immunity, growth, development and Fe homeostasis (Choi et al.; Mathilde et al., 2008). In addition, to the cytokinin signalling pathway to the *naa25* mutant shows to be affected at several levels of the general plant hormone signal transduction (**Supplemental Figure S7**). The misregulation of genes in these pathways can affect processes related with cell division and cell enlargement, therefore shoot initiation and plant growth. This would be in line with some of the pleiotropic phenotypes of the *naa25* mutants, such as branching, and dwarfism. Genes involved in transport tissue histogenesis were higher expressed in *naa25* mutant compared to wild type. Members of this biological process are *DOT1* and *DOT3*, mutations on them cause aberrant venation patterns in leaves. The *dot3* plants are small with problems with fertility (Petricka et al., 2008) and their leaf phenotype resembles the leaf phenotype seen in the *naa25* mutant (Ferrández-Ayela et al., 2013). Therefore, some of the morphologic defects observed in *naa25* mutants could be a consequence of the interferences with the plant hormone signalling pathways.

### **The disruption of *NAA25* affects the regulation of nutrients homeostasis**

Several genes in charge of nutrient homeostasis are misregulated in *naa25* mutant, in both control and Fe/Zn deficiency conditions. These genes have functions related to both macro (S, P, Mg, K and Ca) and micronutrient transport (Zn, Cu, B, and Fe). Particularly, several genes involved S homeostasis are differentially expressed across all the conditions tested. The down-regulation of genes involved in S assimilation was also reported for NatA impaired mutants (Linster et al., 2015). This could be due to the differential expression of *SUE* in *naa25* compared to wild type, which is likely to be involved in low S sensing (Wu et al., 2010). Furthermore, *SUE3* is a putative target of NatB.

In the case of Zn homeostasis, the increased expression of *ZIP4* in control conditions was a common pattern across several Zn deficiency transporter genes in *naa25* mutant. Within this genes, we had several members of the ZIP family and genes from other families which are

mainly expressed under Zn deficiency conditions (van de Mortel et al., 2006). This supports the initial notion on which the M22 mutant was selected, that the *naa25* mutants display a weak Zn deficiency response under sufficient Zn supply. The Zn deficiency response in Arabidopsis is regulated by two transcription factors, bZIP19 and bZIP23 (Assunção et al., 2010). The N-terminus of both bZIP19 and bZIP23 contain sequences that are putative targets of NatB. If bZIP19 and 23 are indeed acetylated by NatB, their regulatory function could be affected by the lack of acetylation in the *naa25* mutant. The role of bZIP19 and 23 does not depend on their transcription levels (Assunção et al., 2010). However, their stability, activity, function and/or localization may depend on post-transcriptional modification such as N-t-acetylation, possibly even affected by the Zn status of the plant. In the case of Fe, the Fe deficiency response regulators bHLH104 and FIT (Yuan et al., 2008; Zhang et al., 2015; Li et al., 2016) are also putative targets of NatB.

### Fe deficiency and biotic defence response signalling

The pathogen defence response and the Fe deficiency response share common processes in plants, such as hormone signalling and the secretion of phenolic compounds. Ethylene, nitric oxide, jasmonic acid and salicylic acid regulate the plant immune response and are also important factors in Fe homeostasis. Several phenolic compounds, production of which is induced upon Fe starvation, have strong antimicrobial properties, next to Fe solubilizing and binding properties. Fe deficiency and biotic defence responses are also evolutionarily linked as soil microorganisms release siderophores (high-affinity iron-chelating compounds) for Fe scavenging, and their perception by the plant triggers both the Fe deficiency and immune responses (Aznar et al., 2014).

Several genes implicated in this link between Fe homeostasis and immunity, are differentially expressed in the *naa25* mutant when compared to wild type. For instance, the *MYB72* gene was lower expressed in the *naa25* mutant upon Fe deficiency compared to wild type. It plays a dual role, by regulating some of the early steps in the Fe deficiency response (Palmer et al., 2013) and its involvement in Induced Systemic Resistance (ISR) (Zamioudis et al., 2015) (Martínez-Medina et al., 2017). The MYB72 transcription factor induces the expression of *BGLU42* which encodes a component of the ISR signalling pathway that is required for the secretion of iron-mobilizing phenolic compounds into the rhizosphere under Fe deficiency (Zamioudis et al., 2014). Like *MYB72*, also the expression of *BGLU42* was lower in the *naa25* mutant upon Fe deficiency compared to wild type. The transcription *WRKY53*, which was predicted to be one

of the regulators the differential gene expression in Fe deficiency for both *naa25* and wild type, is also a putative target of NatB. This transcription factor is involved in pathogen-associated molecular pattern-triggered immunity (Nie et al., 2017). WRKY53 is involved in the salicylic signalling pathway, in which it cross-regulate with WRKY46. The expression of WRKY46 was higher in *naa25* compared to wild type. Its expression significantly affects the root-to-shoot Fe translocation, (Yan et al., 2016). The Fe deficiency response and the biotic defence response are linked through regulators, interestingly the genes making this link are particularly differentially expressed in *naa25* mutant compared to wild type.

### **Photosynthesis and *naa25* mutant sensitivity to Fe deficiency**

One of the most Fe demanding plant processes is photosynthesis, which is why chloroplasts contain around 80% of the Fe in leaves. Iron is a crucial element in the electron-transport chains of photosynthesis and respiration, due to its ability to readily accept and donate electrons (Varotto et al., 2002) (Connolly and Gueriot, 2002; Kessler and Papenbrock, 2005; Yruela, 2013). Several genes encoding proteins of the Photosystem II (PSII) complex were differentially expressed upon Fe deficiency. Even more, genes encoding components of PSI and PSII were differentially expressed in the *naa25* mutant under Fe deficiency (**Supplemental Table S8**).

The photosynthetic activity of a plant drastically decreases under Fe deficiency due to severely photodamaged PSII (Araki and Shikanai, 2014). The PIF1 and PIF4 were predicted as some of the regulators of genes differentially expressed due to Fe deficiency in our study. In addition, the sequences of both proteins are putative targets of acetylation by NatB. In general, PIFs link light signals to the pathway of the phytohormones ethylene, gibberellin, and cytokinin signaling pathways (Zhang et al., 2017) (Liu et al., 2017). Therefore, the lack of acetylation of any of PIF1 or PIF4 could further compromise photosynthesis in the *naa25* mutant, especially under Fe deficiency.

### Conclusions

Although not all targets of N-t-acetylation by the NatB complex are determined as yet, it potentially modifies many proteins involved in many biological processes. Transcript profiling allowed us to get a glimpse of the biological processes which are altered in the *naa25* mutant. The major processes that are affected in the *naa25* mutant relate to plant defence response, which is closely linked with Fe deficiency response. This could be the reason of the high sensitivity to Fe deficiency. However, Fe homeostasis does not seem to be the only mineral homeostasis affected. The Zn deficiency response is slightly induced under Zn sufficiency conditions, which could be either a pleiotropic effect of the reduced acetylation in the *naa25* mutant or the lack of acetylation in a Zn homeostasis regulator. Regulators controlling the homeostasis of Fe and Zn are putative substrates of NatB N-t-acetylation.

### Acknowledgements

We thank Dr. Korbinian Schneeberger (Max Planck Institute) for performing the SHOREmap analysis. We thank Prof. Guido van den Ackerveken and Annemiek Andel (Utrecht University) for performing the disease assay with *Hyaloperonospora*. This work was supported by the Ecuadorian government through SENESCYT (Secretaría de Educación Superior, Ciencia, Tecnología e Innovación) and Universidad de las Fuerzas Armadas-ESPE.

## Supplemental information

**Table S1.** Primers for verification of mutations in *AT5G58450* and *AT5G61940*.

Symbol	Locus identifier	Primer	Sequence (5'-3')
<i>NAA25</i>	<i>At5g58450</i>	Forward	GGCAGAACTGGAAATTGAGA
		Reverse	GCTTCAGCAAGATAGCCAAA
	<i>At5g61940</i>	Forward	AAGTGTGTCAGGCCATAGAC
		Reverse	GAAACTGGCCATTGAGGTACT

**Table S2.** T-DNA insertion lines for *AT5G58450* and *AT5G61940* and primers flanking the left border (LB) and right border (BP) of the insertion, used for their genotyping.

Symbol	Locus identifier	T-DNA line	Primer	Sequence (5'-3')
<i>NAA25</i>	<i>At5g58450</i>	SK24830	LP	AGCCAAAATCTCGAGTTCTCC
			RB	GGCTGTCTGCTTGAAGATGAC
		GK-819A05	LP	TGTATTAGGTTGCATCCGTCC
			RB	TTTTGGCTATCTTGCTGAAGC
	<i>At5g61940</i>	GK_348D02	LP	AAGGGAGAGCTTGGTAACTCG
			RB	GACGTTTAGCTCAAGCTCTGC
		SALK_053216C	LP	TCTTGCTGGTTGGTTTGAAAC
			RB	TGGTTGGTTCAGCAAATCTTC

**Table S3.** Results of one-way ANOVA performed for relative gene expression of *ZIP4* and *GUS* transcripts for mutant lines *M31*, *M22*, and *M60*, and their *pZIP4::GUS* control background grown at Zn sufficiency (*Suf*) or Zn deficiency (*Def*).

Variable	Variance ratio	F probability
<i>ZIP4</i> - <i>Suf</i>	5.62	0.006
<i>GUS</i> - <i>Suf</i>	5.86	0.005
<i>ZIP4</i> - <i>Def</i>	17.27	<.001
<i>GUS</i> - <i>Def</i>	10.57	<.001

**Table S4.** Results of two-way ANOVA performed for dry shoot weight, for each mutant line (M31, M22, and M60) and it respectively pZIP4::GUS control background grown at control medium, Zn or Fe deficient or at Cu or Zn excess. Letters between brackets denote statistically different groups, when comparing grown medium and genotypes, obtained with a Bonferroni post hoc test ( $\alpha=0.05$ ), after a two-way ANOVA.

Mutant line	Factor	Variance ratio	F probability	Groups
M22	Genotype	496.5	<.001	M22 2.5 uM Fe (a), M22 40 uM Cu (ab), M22 120 uM Zn (ab),
	Treatment	75.56	<.001	ZIP4p::GUS 120 uM Zn (b), M22 Control (c), M22 0 uM Zn (c),
	Interaction	59.26	<.001	ZIP4p::GUS 0 uM Zn (cd), ZIP4p::GUS 40 uM Cu (d), ZIP4p::GUS Control (e), ZIP4p::GUS 2.5 uM Fe (e)
M31	Genotype	497.6	<.001	M31 2.5 uM Fe (a), M31 2.5 uM Fe (a), M31 Control (a), M31 120
	Treatment	20.43	<.001	uM Zn (a), M31 40 uM Cu (a), M31 0 uM Zn (a), ZIP4p::GUS 120
	Interaction	23.55	<.001	uM Zn (a), ZIP4p::GUS 40 uM Cu (b), ZIP4p::GUS Control (bc), ZIP4p::GUS 0 uM Zn (bc), ZIP4p::GUS 2.5 uM Fe (c)
M60	Genotype	60.45	<.001	M60 120 uM Zn (a), ZIP4p::GUS 120 uM Zn (ab), M60 40 uM Cu
	Treatment	23.47	<.001	(abc), M60 2.5 uM Fe (bcd), M60 0 uM Zn (bcde), M60 Control
	Interaction	2.4	0.079	(cdef), ZIP4p::GUS 0 uM Zn (def), ZIP4p::GUS 40 uM Cu (ef), ZIP4p::GUS Control (f), ZIP4p::GUS 2.5 uM Fe (f)



**Table S5.** Most differentially expressed genes between the *naa25* mutant and the *Col-4* wild type under control growing conditions. Top ten genes with the highest FC Fold Change) either in shoots (top) or in roots (bottom)

Locus identifier	Symbol	Description	FC	Expression trend
<b>Shoots</b>				
At3g47050		Glycosyl hydrolase protein	7.2	high
At4g22517		Protease inhibitor/seed storage	5.0	high
At2g00340		Expressed RNA	4.2	high
At2g39030	<i>NATA1</i>	N- $\Delta$ -acetyltransferase, induced in response to MeJA and ABA	3.7	high
At5g64810	<i>WRKY51</i>	Transcription factor involved in JA mediated responses	3.6	high
At4g22513		Protease inhibitor/seed storage	3.6	high
At4g22475		Transmembrane protein	3.3	high
At4g19030	<i>NLM1</i>	Aquaporin regulated by ABA, NaCl, desiccation, and arsenite	3.2	high
At4g15660	<i>GRXS8</i>	Thioredoxin superfamily protein	3.4	low
At1g04660		Glycine-rich protein	4.0	low
<b>Roots</b>				
At2g43920	<i>HOL2</i>	Methyltransferase involved in biotic defence	4.3	high
At3g12230	<i>SPL14</i>	Serine carboxypeptidase-like 14	3.4	high
At5g22570	<i>WRKY38</i>	Transcription factor involved in biotic defence response	3.3	high
At1g15610		Transmembrane protein	3.2	high
At1g15620		Transmembrane protein	3.1	high
At3g30260	<i>AGL79</i>	AGAMOUS-like 79	2.8	low
At5g51870	<i>AGL71</i>	Transcription factor involved in floral transition	3.0	low
At4g13420	<i>HAK5</i>	Potassium channel	3.1	low
At1g76210	<i>SCPL14</i>	DUF241 domain protein	3.4	low
At3g42658	<i>SADHU3-2</i>	Member of Sadhu non-coding retrotransposon family	4.1	low

**Table S6.** Differentially expressed genes of both shoot and roots when comparing control conditions to Fe deficiency treatment in *naa25* and *Col-4*. Only genes upregulated (up) or downregulated (down) in Fe deficiency with at least a Fold Change (FC) >3 in one organ (shoots or roots) and at least a FC >1.5 in the second organ with a significance level of  $p < 0.001$  are listed.

Locus identifier	Symbol	Description of encoded proteins	FC shoot	FC root	Expression trend
At3g56970	<i>bHLH38</i>	Transcription factor involved in Fe homeostasis	23.5	6.2	up
At3g56980	<i>bHLH39</i>	Transcription factor involved in Fe homeostasis	21.7	4.7	up
At2g41240	<i>BHLH100</i>	Transcription factor involved in Fe-deficiency responses	20.4	10.6	up
At1g13609		Defensin-like (DEFL) family protein	14.0	22.9	up
At5g04150	<i>BHLH101</i>	Transcription factor involved in Fe-deficiency responses	10.8	8.4	up
At2g14247		Expressed protein	10.1	3.4	up
At1g13608		Defensin-like	9.6	2.8	up
At1g12030		Phosphoenolpyruvate carboxylase	7.7	6.1	up
At1g74770	<i>BTSL1</i>	Zinc ion binding	5.5	2.2	up
At4g19690	<i>IRT1</i>	Iron transporter	5.0	7.1	up
At1g24580		RING/U-box superfamily	4.8	2.3	up
At1g23020	<i>FRO3</i>	Ferric chelate reductase	3.8	2.3	up
At5g53450	<i>ORG1</i>	OBP3-responsive protein 1	3.4	2.5	up
At3g02480	<i>ABR</i>	Late embryogenesis abundant	3.0	2.6	up
At1g56430	<i>NAS4</i>	Nicotianamine synthase	3.0	2.9	up
At5g67370	<i>CGLD27</i>	DUF1230 family protein	2.8	5.3	up
At4g16370	<i>OPT3</i>	Iron transporter that loads iron into the phloem	2.3	4.1	up
At1g01580	<i>FRO2</i>	Ferric chelate reductase involved in Fe reduction at the root surface	2.2	6.9	up
At3g12820	<i>MYB10</i>	R2R3 factor	1.6	3.1	up
At5g59520	<i>ZIP2</i>	Metal ion transporter regulated by copper	2.4	11.2	down
At1g68650		Uncharacterized protein family (UPF0016)	3.2	1.8	down
At2g21650	<i>MEE3</i>	Member of MYB transcription factors	3.4	2.3	down
At2g40300	<i>FER4</i>	Ferritins protect against oxidative damage	3.6	2.6	down
At1g21140	<i>VTL1</i>	Nodulin-like1	4.7	3.7	down
At4g25100	<i>FSD1</i>	Fe-superoxide dismutase	17.8	16.3	down

**Table S7.** Differentially expressed genes of both shoot and roots when comparing control conditions with a Zn deficiency treatment in *naa25* and *Col-4*. Only genes upregulated (up) or downregulated (down) in Zn deficiency with at least a Fold Change (FC) >3 in one organ (shoots or roots) and at least a FC >1.5 in the second organ with a significance level of  $p < 0.05$  are listed.

Locus identifier	Symbol	Description of encoded proteins	FC shoot	FC root	Expression Trend
At4g33020	<i>ZIP9</i>	ZIP family protein induced in response to Zn deficiency	43.8	6.0	up
At2g03445	<i>MIR398A</i>	MicroRNA that targets both CSD and CytC	23.7	23.0	up
At1g09155	<i>PP2-B15</i>	Phloem protein 2-B15	13.9	3.5	up
At5g61320	<i>CYP89A3</i>	Member of CYP89A	10.4	9.0	up
At1g20380		Prolyl oligopeptidase	9.3	6.9	up
At5g60060		F-box SKIP23-like	8.6	3.5	up
At1g10970	<i>ZIP4</i>	ZIP family protein induced in response to Zn deficiency	8.0	4.7	up
At3g08040	<i>FRD3</i>	Transporter involved in root xylem loading of Fe chelator	7.3	2.5	up
At1g56242		Potential natural antisense gene	7.1	15.5	up
At1g56240	<i>PP2-B13</i>	Phloem protein 2-B13	7.1	4.8	up
At1g60960	<i>IRT3</i>	Plasma membrane zinc/iron transporter	7.0	3.1	up
At2g37810		Cysteine/Histidine-rich C1 domain family protein	6.4	2.7	up
At1g05300	<i>ZIP5</i>	ZIP family protein induced in response to Zn deficiency	6.0	3.3	up
At5g50400	<i>PAP27</i>	Purple acid phosphatase 27	4.5	3.0	up
At1g09240	<i>NAS3</i>	Nicotianamine synthase	3.4	19.2	up
At3g12750	<i>ZIP1</i>	ZIP family protein induced in response to Zn deficiency	2.6	3.4	up
At1g56430	<i>NAS4</i>	Nicotianamine synthase	2.2	6.4	up
At3g05790	<i>LON4</i>	Lon protease-like	2.1	5.3	up
At4g30110	<i>HMA2</i>	P1B-type ATPases transport zinc	1.6	3.0	up
At3g04450		Homeodomain-like superfamily protein	1.6	5.1	up
At2g44290		Lipid-transfer protein/seed storage 2S albumin	1.5	3.5	up
At3g01500	<i>CA1</i>	Carbonic anhydrase	2.3	6.8	up/down

(up/down) upregulated in shoots and downregulated in roots

**Table S8.** Genes involved in photosynthesis that are differentially expressed due to Fe deficiency. Genes differentially expressed upon Fe deficiency in wild type and *naa25* (Wt, *naa25*) compared to control medium, upon Fe deficiency in *naa25* (*naa25*) but not in wild type compared to control medium, upon Fe deficiency in wild type and in *naa25* and even more in *naa25* (Wt, *naa25*).

AGI	Gene Name	Genotype
At1g76570	Chlorophyll A-B binding family protein(AT1G76570)	Wt, <i>naa25</i>
At1g29920	Chlorophyll A/B-binding protein 2(CAB2)	Wt, <u><i>naa25</i></u>
At5g08410	Ferredoxin/thioredoxin reductase subunit A (variable subunit) 2(FTRA2)	Wt, <i>naa25</i>
At5g01600	Ferritin 1(FER1)	Wt, <i>naa25</i>
At3g56090	Ferritin 3(FER3)	Wt, <i>naa25</i>
At2g40300	Ferritin 4(FER4)	Wt, <i>naa25</i>
At4g10340	Light harvesting complex of photosystem II 5(LHCB5)	Wt, <i>naa25</i>
At1g15820	Light harvesting complex photosystem II subunit 6(LHCB6)	Wt, <i>naa25</i>
At2g34430	Light-harvesting chlorophyll-protein complex II subunit B1(LHB1B1)	Wt, <i>naa25</i>
At5g13630	Magnesium-chelatase subunit chlH, chloroplast, putative (CHLH)(GUN5)	Wt, <i>naa25</i>
At3g14940	Phosphoenolpyruvate carboxylase 3(PPC3)	Wt, <i>naa25</i>
At5g64040	Photosystem I reaction center subunit PSI-N, chloroplast, putative (PSAN)(PSAN)	Wt, <i>naa25</i>
At1g03130	Photosystem I subunit D-2(PSAD-2)	Wt, <i>naa25</i>
At1g31330	Photosystem I subunit F(PSAF)	Wt, <i>naa25</i>
At2g05100	Photosystem II light harvesting complex protein 2.1(LHCB2.1)	Wt, <i>naa25</i>
At2g05070	Photosystem II light harvesting complex protein 2.2(LHCB2.2)	Wt, <i>naa25</i>
At3g27690	Photosystem II light harvesting complex protein 2.3(LHCB2.3)	Wt, <u><i>naa25</i></u>
At4g05180	Photosystem II subunit Q-2(PSBQ-2)	Wt, <i>naa25</i>
At1g79040	Photosystem II subunit R(PSBR)	Wt, <u><i>naa25</i></u>
At3g21055	Photosystem II subunit T(PSBTN)	Wt, <i>naa25</i>
At2g06520	Photosystem II subunit X(PSBX)	Wt, <i>naa25</i>
At1g44575	Chlorophyll A-B binding family protein(NPQ4)	<i>naa25</i>
At3g01500	Carbonic anhydrase 1(CA1)	<i>naa25</i>
At1g29910	Chlorophyll A/B binding protein 3(CAB3)	<i>naa25</i>
At1g30380	Photosystem I subunit K(PSAK)	<i>naa25</i>
At2g30570	Photosystem II reaction center W(PSBW)	<i>naa25</i>

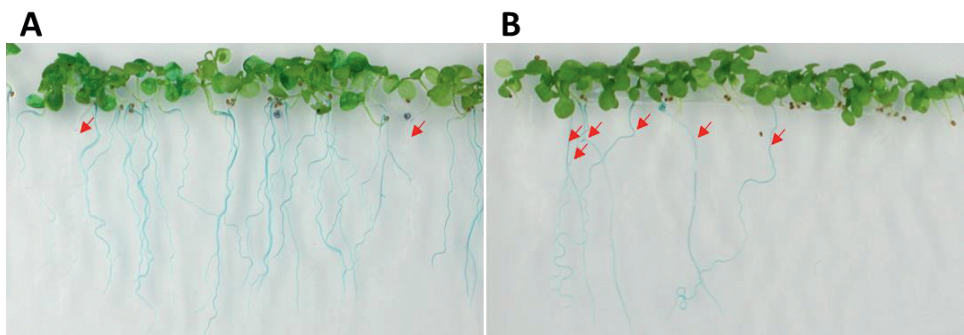


**Figure S1.** *In vivo* GUS staining assay of the pZIP4::GUS M2 mutant screen. Seedlings are grown in MS-agar plates either at (A) Zn deficiency or (B) Zn sufficiency. Arrows indicate mutants with an aberrant GUS staining phenotype, showing no staining in (A) and staining in (B).

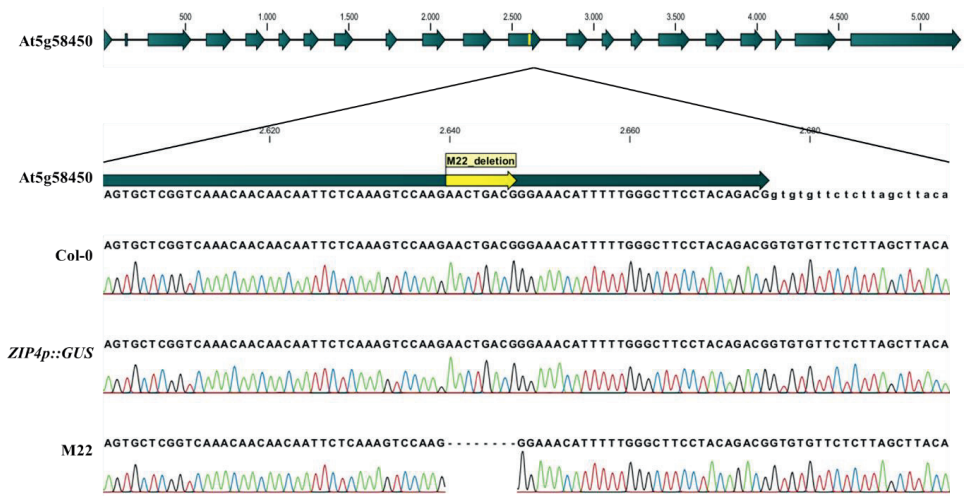


**Figure S2.** Sequence deletion in *naa25* of the M22 mutant. NAA25 (At5g58450) sequence alignment of Col-0, pZIP4::GUS and M22 around the mutation found in M22. Numbers above the sequence represent the base number counting from the translation start. Blue arrows represent exons, lines connecting them introns, and the yellow arrow indicates the 8-bp deletion in M22.



**Figure S3.** F1 seedlings grown under Fe deficiency. Seedlings of mutant line M22, T-DNA insertion line SK24830, pZIP4::GUS background control, F1 of M22xSK24830, and F1 of SK24830xpZIP4::GUS grown for three weeks on Fe deficiency vertical, half MS-agar plates.

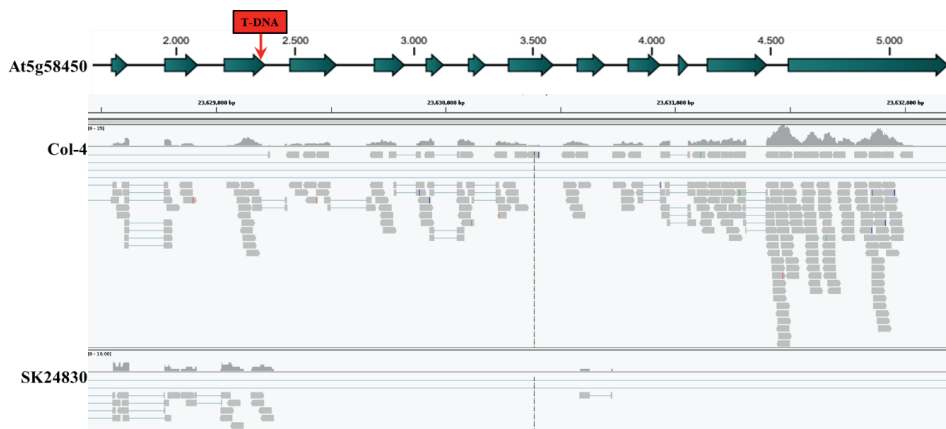


**Figure S4.** NAA25 (*At5g58450*) transcripts sequence reads from exon nine to twenty-one of Col-4 and of SK24830. Red arrow shows the position of the T-DNA insertion in SK24830. NB, there are no reads of NAA25 downstream of the T-DNA insertion, indicating the insertion to disrupt transcription of the gene.

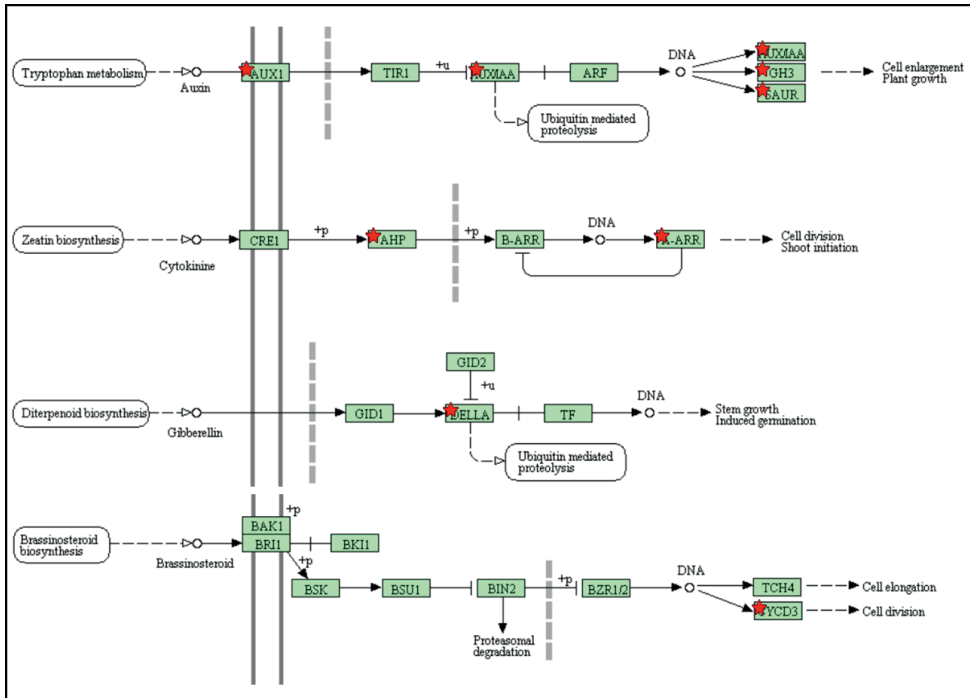


**Figure S5.** Plant hormone signal transduction pathway from Kyoto Encyclopedia of Genes and Genomes Pathways (KEGG). Red stars represent points where genes differentially expressed in *naa25* play a role. Generated through DAVID Bioinformatics Resources 6.8 ([david.ncicrf.gov/](http://david.ncicrf.gov/)).

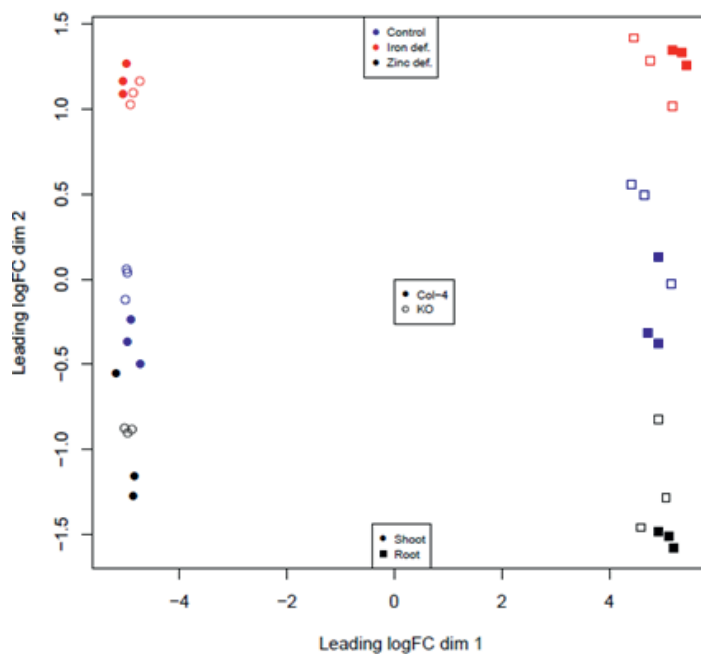


**Figure S6.** Multidimensional scaling transcriptome data of *naa25*. All expressed genes in roots (squares) and shoots (circles) of the *naa25* mutant (KO: unfilled) and wild type (Col-4: filled) under Fe deficiency (red), Zn deficiency (black), or control medium (blue).



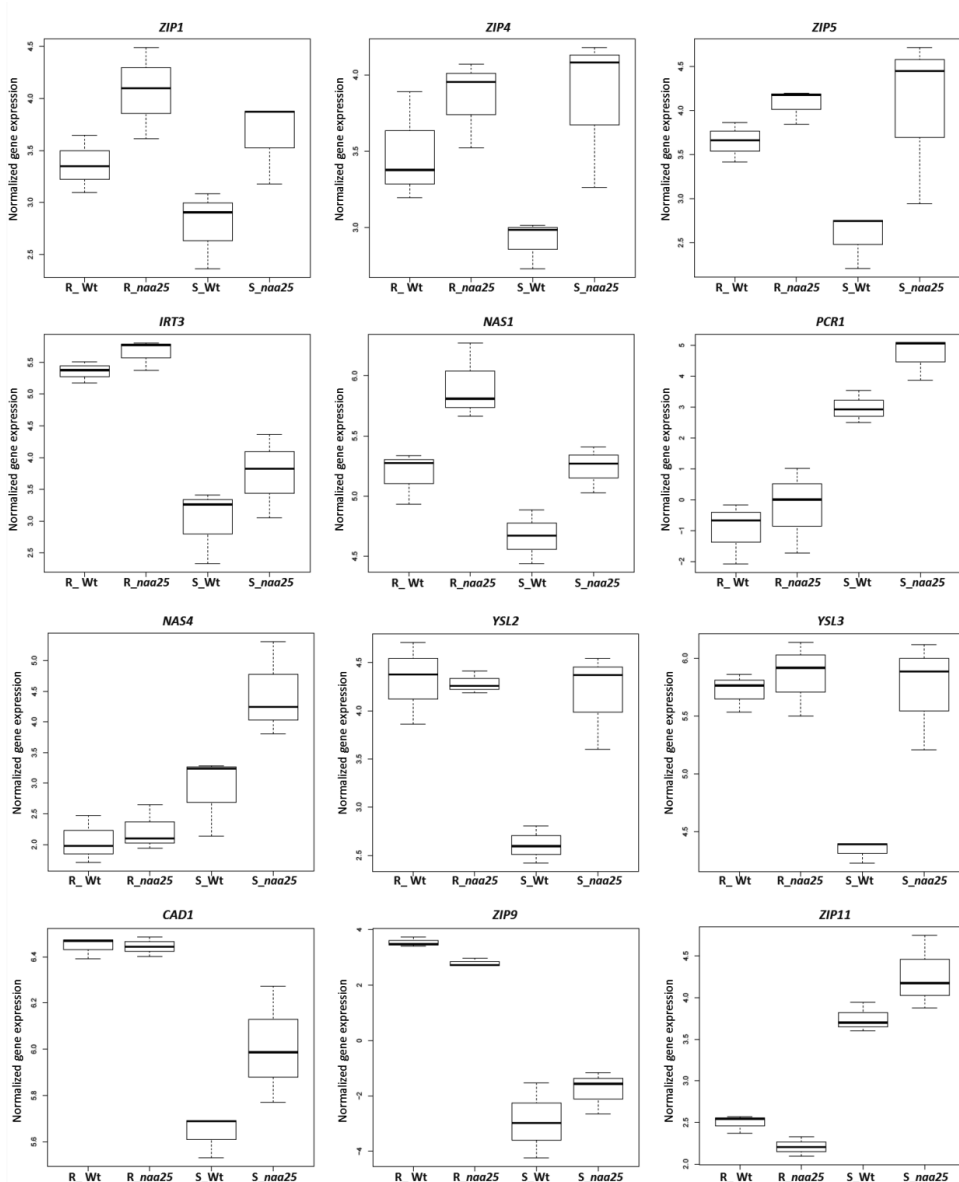


**Figure S7.** Normalized gene expression of Zn transporter genes. Gene expression in shoots (S\_) and roots (R\_) in *naa25* and wild type (Wt) under control conditions. Data from RNA-seq reads.



# Chapter 4

## **Exploring *Arabidopsis thaliana* natural genetic variation to identify genes underlying the Zn deficiency response**

Valeria Ochoa Tufiño<sup>1,3</sup>, Ana Carolina Campos<sup>1,4</sup>, Joost van den Heuvel<sup>1</sup>, Jeroen Wolkamp<sup>1</sup>, John Danku<sup>2</sup>, David E. Salt<sup>2</sup> & Mark G.M. Aarts<sup>1</sup>

- 1) Laboratory of Genetics, Wageningen University, Wageningen, the Netherlands
- 2) School of Biosciences, University of Nottingham, Sutton Bonington, England, United Kingdom
- 3) Current affiliation: Departamento de Ciencias de la Vida, Universidad de las Fuerzas Armadas ESPE, Sangolquí, Ecuador
- 4) Current affiliation: Dümme Orange, Leiderdorp, The Netherlands

*In preparation for submission*

### Abstract

Zn deficiency is a common micronutrient deficiency, affecting yield and nutritional quality of crops around the world. Selection due to environmental conditions and genetic drift promote genetic variation within a species, which can be used to identify the genetic factors contributing to natural variation for a trait. We used a set of 350 natural accessions of *Arabidopsis thaliana* (Arabidopsis) to perform a Genome-Wide Association Study (GWAS) to identify candidate genes underlying natural variation plant ionome profile upon Zn deficiency. Zn deficiency leads to an increased concentration of most of the elements analysed. Ionome profiles have been used to identify genomic regions associated with variation in Cu, Fe, Mn, Mo, and Zn concentration in response to Zn deficiency. Upon screening T-DNA insertion mutant lines for candidate genes, seven genes are confirmed to be involved in the Zn deficiency response, affecting the shoot concentrations of Cu, Fe, Mn, Mo, or Zn. These genes are involved in microtubules organization during cell division, defence mechanisms against pathogens, circadian clock, Fe transport, Fe storage and phosphorylation of carbohydrates. Thus, genes with diverse functions play a role in the plant response to Zn deficiency by a direct or mediated influence on the ionome homeostasis.

## Introduction

Natural genetic variation describes the phenotypic differences within a species due to genetic differences, within or between natural populations, as a result of genetic drift or selection pressure of specific environments. *Arabidopsis thaliana* (*Arabidopsis*) occupies habitats like sandy areas (beaches and river banks), roadsides, rocky mountains in a wide range of climates, which makes it a subject of wide variety of selection factors (Al-Shehbaz and O'Kane, 2002; Koornneef et al., 2004; Alonso-Blanco et al., 2009; Horton et al., 2012). Local adaptation of *Arabidopsis* populations, meaning local enrichment for alleles that provide optimal fitness to specific conditions in the area, can be found (Baxter et al., 2010; Fournier-Level et al., 2011).

The concentrations of elements in plant organs, also known as the ionome, is a complex of traits for which extensive genetic variation is found among *Arabidopsis* accessions (Buescher et al., 2010; Chao et al., 2014). The ionome can be affected by the environment and developmental stage, and it depends on several plant processes ranging from uptake, translocation, and storage. The regulation of maintaining a stable ionome is known as mineral homeostasis. Often, the mineral homeostasis of one element is affected by the concentration of others, and alteration of the concentration of one element often has consequences for the concentrations of several other elements, reflecting the complex physiological responses on changes in nutrient supply (Baxter et al., 2008; Buescher et al., 2010; Baxter et al., 2012).

The elemental concentrations of the soil have a strong effect on the plant ionome and the physiological state of the plant (Marschner and Marschner, 2012). Mineral supply can range from deficient to toxic levels for essential nutrients, while non-essential elements only have an effect when supplied at toxic levels. Among micronutrients, Zn deficiency is the most widespread in the world. 49% of the agricultural soils of the world are deficient in Zn. Crops affected by Zn deficiency produce a lower yield and reduced nutritional quality (Graham, 2008). Zn deficiency in soil often leads to Zn deficiency in humans, which is a widespread problem in most of the developing world (Alloway, 2009). Zn deficiency has serious implications for human health, leading to a decrease in learning capability (IQ) and growth retardation in developing children, while it also affects the immune system, and delays wound healing (Evans, 1986; Graham, 2008; Ackland and Michalczyk, 2016). The World Health Organisation (WHO) estimates that around three billion people suffer from some degree of Zn deficiency, making it a major public health problem. Better knowledge on the plant Zn

homeostasis network can improve the selection for, or genetic engineering of, new crop varieties, which are more efficient with low Zn availability from poor Zn soils, and are better in the partitioning of Zn into harvested plant parts (Ghandilyan et al., 2006; Cakmak, 2008).

Increasing our knowledge on the natural variation for the Arabidopsis ionome is important to further understand the genetics and physiology of mineral homeostasis in plants (Salt et al., 2008; Alonso-Blanco et al., 2009). Genome-Wide Association Studies (GWAS) provide a powerful tool to identify genes and variant alleles that relate to genetic variation of a trait (Korte and Farlow, 2013), by associating genotyped markers (mainly SNPs, Single Nucleotide Polymorphisms) with their contribution to a given trait across a large set of individuals. These associated SNPs are easily identified as long as the alleles they are closely linked to are sufficiently frequent in the population and contribute sufficiently to the trait variation (Korte and Farlow, 2013). GWAS thus shows the best results for traits affected by a small number of loci with large effect sizes, with a few loci explaining most of the phenotypic variance (Atwell et al., 2010). GWAS already detected allelic variation on ionome composition, identifying relevant genes for the concentration of Na, the *HIGH-AFFINITY K<sup>+</sup> TRANSPORTER 1* (*HKT1.1*) gene, encoding a Na transporter (Baxter et al., 2010); for as, the *HIGH ARSENIC CONTENT 1* (*HAC1*) gene, encoding an arsenate reductase (Chao et al., 2014); and Cd, the *HEAVY-METAL ATPASE 3* (*HMA3*) gene, encoding a Cd transporter (Chao et al., 2012).

In this study, we used GWAS analysis of the root and shoot ionomes of 350 natural accessions of Arabidopsis ionomics to explore the genetic variation in Zn deficiency response. We observed that most of the element concentrations increased significantly upon Zn deficiency when compared to a Zn sufficiency control treatment. We also identified several candidate genes that are potentially involved in Arabidopsis ionome homeostasis. Some of these were validated through the phenotypic analysis of T-DNA insertion lines in their response to Zn deficiency.

## Materials and Methods

### Plant material and growth conditions

A set of 350 natural accessions of Arabidopsis (Li et al., 2010) was used in this study. Seeds were surface-sterilized using chlorine vapor-phase (Clough and Bent, 1998). Seeds were sown on 0.8 ml bottomless tubes filled with 0.55% agar-solidified modified half-strength Hoagland

nutrient solution at pH 5.8 (Schat et al., 1996). Prior to germination, seeds were stratified for three days at 4°C in the dark. Upon germination, plants were hydroponically grown in the same nutrient solution in a climate-controlled growth chamber set at 70% humidity, a 12/12 h light/dark cycle, and 20/15°C day/night temperatures. Plants grew in a fully supplemented medium (containing 2  $\mu\text{M}$   $\text{ZnSO}_4$ ) for two weeks. Thereafter, two Zn treatments were applied, continued growth on 2  $\mu\text{M}$   $\text{ZnSO}_4$ , for Zn sufficiency, or growth on medium containing only 0.05  $\mu\text{M}$   $\text{ZnSO}_4$ , imposing a mild Zn deficiency (Campos et al., 2017). Plants grew in trays with the capacity for 70 plants. In each treatment, two replicates per genotype were grown.

*Arabidopsis* T-DNA insertion lines of candidate genes were ordered from the Nottingham *Arabidopsis* Stock Centre (NASC; [www.arabidopsis.info/](http://www.arabidopsis.info/)) (**Supplemental Table S1**). To multiply and genotype these lines, seeds were stratified for three days at 4°C in the dark, and then transferred to grow on nutrient-supplied rockwool in a greenhouse set at 70% humidity, 16/8 h light/dark cycle, and 20/18°C day/night temperatures. T-DNA insertion lines were genotyped to select or confirm homozygote plants. Primers for T-DNA insertion lines genotyping were designed using the website of the Salk Institute ([www.signal.salk.edu/tdnaprimers.2.html](http://www.signal.salk.edu/tdnaprimers.2.html)). Confirmed homozygous T-DNA insertion mutants were grown hydroponically as described above, with the only difference that no Zn was added in the medium for the Zn deficiency treatment.

### **Ionome analyses**

Shoot and roots of *Arabidopsis* plants were collected four weeks after germination. Roots and two young but fully-expanded leaves were washed with 1 mM EDTA (pH 8) and MQ water. Plant material was collected in paper bags and dried for 3 days at 60°C. Element concentrations (ionome composition) was determined by ICP-MS as described by Baxter et al. (2008).

### **Statistical analyses**

Ionome data from natural accessions was log<sub>10</sub>-transformed. Thereafter, we initially perform a principal component analyses using Pearson correlations and two-way ANOVA scripts within R package. Software used for GWAS was written in pure R code (**Script in Supplemental data file 1**) (Kruijer et al., 2015). For each element, two traits were used. first, the concentration of each element in each biological repetition within treatments, and second the residuals of the means. The residuals were calculated from the regression of each element concentration in plants grown under Zn deficiency and the concentration in plants grown with sufficient Zn

supply, using Genstat (18th edition) (VSN International; [www.vsnl.co.uk/software/genstat/](http://www.vsnl.co.uk/software/genstat/)). To ensure that the data were normally distributed, they were log<sub>10</sub>-transformed. For most traits, the strict Bonferroni correction (Bonferroni, 1935) threshold was not met for any locus, which is why a second, arbitrary threshold of significant loci of  $-\log_{10}(p) \geq 4$  was used, which had to be met by several closely linked SNPs. Candidate genes were selected based on their Linkage Disequilibrium (LD) with the associated SNPs with a cut-off of 0.4, the presence of non-synonymous SNPs in the coding region (Weigel and Mott, 2009), a predicted or putative function related to mineral homeostasis, and gene expression upon Zn deficiency (Campos, 2015).

Ionome data obtained from the first test of T-DNA insertion lines of the candidate genes was ln-transformed to generate Biplots (Gabriel, 1971) using Genstat (18th edition) (VSN International; [www.vsnl.co.uk/software/genstat/](http://www.vsnl.co.uk/software/genstat/)). For each element, biplots graphs were generated for four variables (element concentrations in shoots and roots of plants grown under Zn sufficiency and deficiency).

For T-DNA insertion lines test, we fitted mixed effects models with a Gaussian error distribution (lmer function, lme4 package). Treatment and genotype were used as fixed variables, trays as random variables. We fitted first a full factorial model, a model with the two main effects and separately two models with one main effect. With the obtained p-values for the main effects and interaction terms, a likelihood ratio test (Chi-square test using the ANOVA function) was performed between the models with one and two main effects (for main effect significance) and between the full factorial model and the model with two main effects (for the interaction term). All p-values were corrected for multiple testing (p.adjust function) using the Benjamini and Hochberg (1995) method. An alpha value of 0.05 was used as significant for the False Discovery Rate (FDR)-transformed p-values. To ensure that the residuals were normally distributed and that their variances were not heterogeneous between treatment levels, we square-root-transformed the biomass data and ln-transformed the ionome data. To visualize the differences between treatment levels, heatmaps were produced (heatmap function from the heatmap package). Fold changes were calculated of element concentrations as follows for genotype  $(Y_{TDNA,DEF} + Y_{TDNA,SUF}) / (Y_{WT,DEF} + Y_{WT,SUF})$  and for interaction  $(Y_{TDNA,DEF} / Y_{WT,DEF}) / (Y_{TDNA,SUF} / Y_{WT,SUF})$  where Y stands for the mean of a trait value for a specific combination of a genotype and treatment value (WT = control genotype, TDNA = T-DNA line genotype, DEF = deficiency treatment, SUF=sufficiency treatment). For the calculation of these



fold change values, also the biomass data were square-root-transformed and the ionome data were ln-transformed.

## Results

### Zinc deficiency effects on the Arabidopsis ionome

In this study, we grew a set of 350 natural accessions of Arabidopsis on hydroponic medium with sufficient or mild deficient Zn supply. Root and shoot ionome profiles were determined by ICP-MS for B, Ca, Co, Cu, Fe, K, Mg, Mn, Mo, Na, P, S, and Zn. Most of the variation of the ionome of the natural accession was explained by two principal components (PCs) in a PC analysis (PCA) (**Figure 1** and **Supplemental Figure S1**). These two PCs separated the data according to the tissue (PC1: shoot or root) and to the treatment (PC2: sufficiency or deficiency). The elements with the highest relative contribution to PC1 were Zn>Ca>Fe>Na>Cu and for PC2 were Zn>Ca>Na>Mg>Mo. Elements that accumulated more in roots than in shoots were Co, Cu, Fe, Mo, Na, and Zn. Elements that accumulated more in shoots than in roots were Ca and Mg. Elements B, K, Mn, P, and S are found at similar concentrations in roots and shoots (**Supplemental Figure S2**).

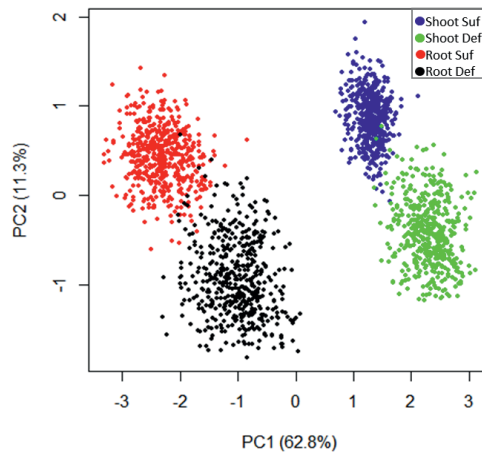


**Figure 1.** Principal component analyses of 13 essential elements (B, Ca, Co, Cu, Fe, K, Mg, Mn, Mo, Na, P, S and Zn) in 350 natural accessions of Arabidopsis. Data correspond to the ionome of shoots (blue dots) and roots (red dots) of plants grown hydroponically in Zn sufficiency and shoots (green dots) and roots (black dots) of plants grown hydroponically in Zn deficiency. For the elements with the highest relative contribution in: PC1 the positive loadings were for Ca and negative ones for Zn, Fe, Na, Cu; and PC2 the positive loadings were for Zn, Ca, and Mg and negative loadings for Na and Mo.

Due to the different ionome compositions in roots and shoots, we analysed both parts independently. In shoots, most of the element concentrations correlated positively with each other over accessions, when comparing the two treatments, with the exception of B. In roots the number of negative correlations was higher than in shoots, with the Ca concentrations mostly negatively correlated with the other element concentrations (**Figure 2**).

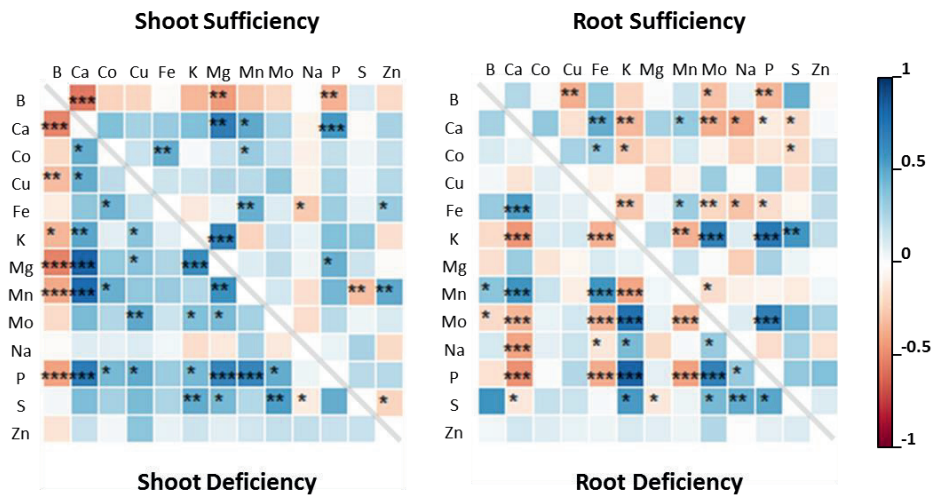


**Figure 2.** Pearson correlations of ionome profiles in 350 natural accessions of *Arabidopsis*. Element concentration in shoots and roots of plants grown hydroponically in Zn sufficiency or deficiency are compared. Elements are in alphabetic order. Positive and negative correlations are indicated by colours as shown in the sidebar. The significance level is represented with \* $p < 0.05$ , \*\* $p < 0.01$ , \*\*\* $p < 0.001$ .

The Zn deficiency treatment affects the direction of just a few correlations among elements. Negative correlations that became positive due to Zn deficiency were Fe-Na, Mn-S, and Zn-S in shoots and B-Cu, Co-K, Co-S, Mg-Mn, and Na-P in roots. Positive correlations that became negative due to Zn deficiency were S-Na in shoots and S-Mg in roots. Overall, the shoot to root concentration ratios did not change much due to Zn deficiency. The correlation coefficient for element concentrations in shoot sufficiency and shoot deficiency was 0.78 and for roots, it was 0.80 ( $p < 0.001$ ). While correlations remain largely similar, the concentrations of most elements were significantly affected by Zn deficiency. In shoots, Zn deficiency increased the B, Ca, Co, Fe, Mg, Mn, Mo, P, and S concentrations and decreased the Cu and Na concentrations (**Table 1**). In roots, Zn deficiency increased the B, Ca, K, Na, and S concentrations and decreased the Cu, Fe, Mg, and P concentrations (**Table 1**). The concentration of K in shoots and the

concentrations of Co, Mn, and Mo in roots were not altered due to Zn deficiency. The mean Zn concentration decreased in shoots from 81 ppm to 14 ppm in Zn deficiency and in roots from 288 ppm to 65 ppm, which is translated to 82% reduction in shoots and 77% reduction in roots. The element with the strongest changes after Zn was Fe, with a 35% increase in shoots and 67% reduction in roots due to Zn deficiency (**Supplemental Figure S3**).

**Table1.** Ionome profiles of shoots and roots of 350 natural *Arabidopsis* accessions grown hydroponically in Zn sufficient and Zn deficient conditions. Data include mean, standard deviation, Coefficient of Variation (CV) and broad sense heritability ( $H^2$ ). ANOVA  $p$  values are represented: \* $p < 0.05$ , \*\* $p < 0.001$ , \*\*\* $p < 0.001$ . Shadow indicates interaction of genotype (Gen)  $\times$  treatment (Trt).

	Control				Deficiency				ANOVA	
	Mean [ppm]	Std dev	C.V [%]	$H^2$ [%]	Mean [ppm]	Std dev	C.V [%]	$H^2$ [%]	Trt	Acc
<b>Shoot</b>										
<b>B</b>	148.7	60.66	41	41	185.6	88.8	48	49	***	
<b>Ca</b>	36319	7280	20	43	46230	14478	31	42	***	
<b>Co</b>	0.15	0.03	20	46	0.16	0.03	21	42	***	
<b>Cu</b>	3.048	0.615	20	45	2.475	0.596	24	53	***	***
<b>Fe</b>	113.8	18.13	16	41	153.1	38.18	25	45	***	
<b>K</b>	28248	7920	28	48	28123	9384	33	48		*
<b>Mg</b>	3577	698.9	20	48	4165	1038	25	51	***	*
<b>Mn</b>	66.3	18.05	27	47	87.61	36.48	42	49	***	***
<b>Mo</b>	16.84	6.14	36	65	22.04	8.58	39	61	***	***
<b>Na</b>	622.1	195.7	31	39	545	257.7	47	45	***	
<b>P</b>	5923	1679	28	44	6479	1674	26	54	***	**
<b>S</b>	9386	1587	17	42	10077	2142	21	47	***	
<b>Zn</b>	81.58	22.33	27	50	14.48	6.37	44	44	***	
<b>Root</b>										
<b>B</b>	142	69	49	40	191.4	87.64	46	45	***	
<b>Ca</b>	6371	1459	23	44	7408	1940	26	59	***	***
<b>Co</b>	0.29	0.13	44	44	0.38	0.46	120	43		
<b>Cu</b>	10.95	3.35	31	50	7.93	2.01	25	53	***	***
<b>Fe</b>	972.5	339.6	35	47	318.9	117.6	37	57	***	***
<b>K</b>	25584	9796	38	50	25821	14963	58	61	***	***
<b>Mg</b>	1583	269.3	17	56	1358	291.9	21	56	***	***
<b>Mn</b>	69.89	33.47	48	48	65.62	23.88	36	48		**
<b>Mo</b>	55.49	32.37	58	57	54.06	33.79	63	56		***
<b>Na</b>	1820	570	31	38	2253	867	38	55	***	***
<b>P</b>	7919	1863	24	54	6537	2462	38	58	***	*
<b>S</b>	7919	2114	27	43	9198	3060	33	56	***	**
<b>Zn</b>	288.1	106.6	37	53	65.26	39.21	60	57	***	***

### Genome-Wide Association Mapping

The processes that influence ionome homeostasis in plants are complex and likely to be driven by a large number of loci with small effects. To expand our knowledge of the genetic architecture underlying ionome homeostasis, with a focus on Zn deficiency tolerance, we performed a GWAS. We narrowed the analyses to the micronutrients with concentrations that were positively correlated with the Zn concentration, irrespective of the treatment and plant part, which meant using the concentration of Co, Cu, Fe, Mn, Mo, and Zn of the 350 natural accessions of *Arabidopsis*. In addition to each element concentration, we used the residuals, of the regression of the element concentrations means, of plants grown under Zn deficiency on plants grown under sufficient Zn supply.

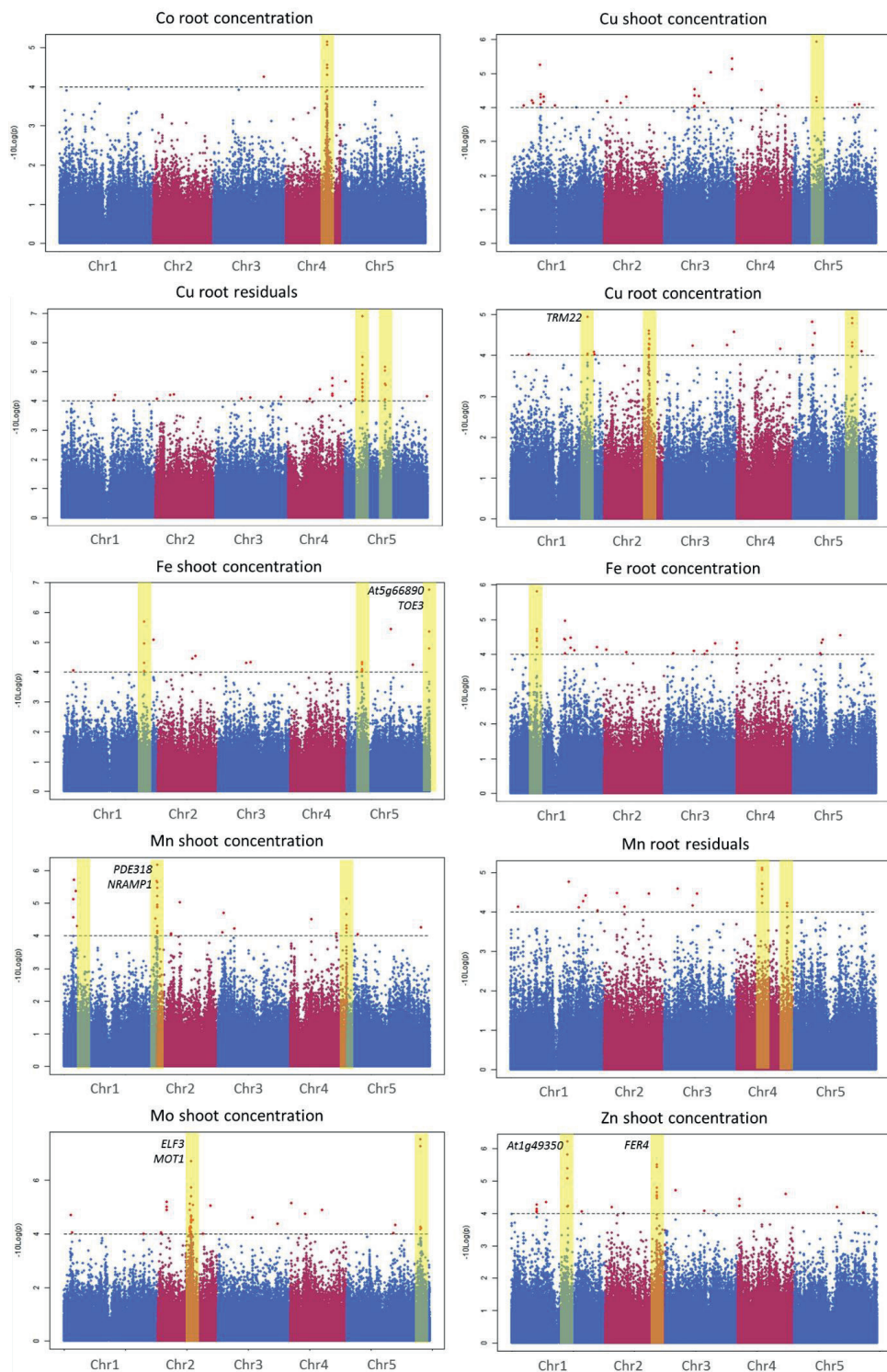
Among the *Arabidopsis* accessions, large variation in ionome profile was observed, especially in roots. We expressed the relative variability of each element in terms of Coefficient of Variation (CV), which is the ratio of the standard deviation to the mean. This is useful to compare the variation of elements with highly different means. The variation was higher in roots than in shoots and in deficiency than in sufficiency (**Table 1**). In shoots, the elements with the highest variation were B>Na>Mo>Zn>Mn and in roots Co>Mo>Zn>K>Mn. Broad-sense heritability was calculated for all element concentrations, as the ratio between estimated genetic variance and total phenotypic variance, which itself is composed of genetic variance and non-genetics, or environmental, variance. This is a measure of how much of the phenotypic variation is due to genetic variation. Heritability ranged from 39% to 66% depending on the element, plant part, and treatment. In shoots, the elements with the highest heritability were Mo>Mg>Cu>P>Mn and in roots Mo>P>Zn>Mg>K. With the exception of B and Co, all elements showed a significant effect of genotype on element concentrations (**Table 1**), which also indicates the genetic control of elements accumulation in the plant. For Ca, Fe, K, Mo, P, and Zn concentration in roots, a significant genotype x treatment interaction was found (**Table 1**).

For all these element concentrations or their residuals, one or more associated SNP markers were found for at least one locus (**Supplemental data file 2**). Based on the criteria mentioned in the materials and methods section, we selected the loci more likely to contain genes involved in the ionome homeostasis (**Figure 3**). For Co, one locus was selected, which was detected in roots either using Co concentration or residuals. For Cu, five loci were selected: three associated with root concentration and two associated with the residuals for root. For Fe, we selected four

loci: one associated with Fe root concentration and Mn root concentration; one associated with Fe shoot concentration; and two associated with Fe shoot concentration and residuals. For Mn, we selected six loci: two associated with Mn root residuals and four associated with Mn shoot concentration. For Mo, we selected two loci associated with Mo shoot concentration, the loci (in chromosome two) was also associated with Mo shoot residuals and Mo root concentration. For Zn, we selected four loci: two associated with Zn shoot concentration; one associated with Zn shoot residuals; and one associated with Zn shoot residuals. The average length of each region covered by the associated SNPs was of 39 Kb. Possible candidate genes residing at those loci were selected, based in the level of significance of associated SNPs, and consistency due to the presence of several associated SNPs on LD.

### Candidate genes with previously described roles in ionome homeostasis

Several of the candidate genes encode for proteins with putative functions related to the ionome homeostasis. In the selected loci (**Figure 3**), are genes encoding for *K UPTAKE PERMEASE 11* (*KUP11*), *HEAVY METAL-ASSOCIATED ISOPRENYLATED PLANT PROTEIN 21* (*HIPP21*), *PURPLE ACID PHOSPHATASE 26* (*PAP26*), and *TONOPLAST INTRINSIC PROTEIN 2;3* (*TIP2;3*) (all for Cu); *CASPARIAN STRIP MEMBRANE PROTEIN 5* (*CASP5*) (Fe); *NATURAL RESISTANCE-ASSOCIATED MACROPHAGE PROTEIN 1* (*NRAMP1*) (Mn); *MOT1* (Mo); and *FERRITIN 4* (*FER4*), and *HIPPs 10, 11, 12, 13, 14* (Zn). Of these genes, only *NRAMP1* (Mn) (Cailliatte et al., 2010; Castaings et al., 2016) and *MOT1* (Mo) (Tomatsu et al., 2007; Baxter et al., 2008) have previously been implicated in Mn and Mo homeostasis respectively. Thus we did not further test these two genes. The other genes are not known to control homeostasis of the element with which they are associated. Of them, *KUP11* was not tested because we lacked a homozygous T-DNA insertion line for this gene.



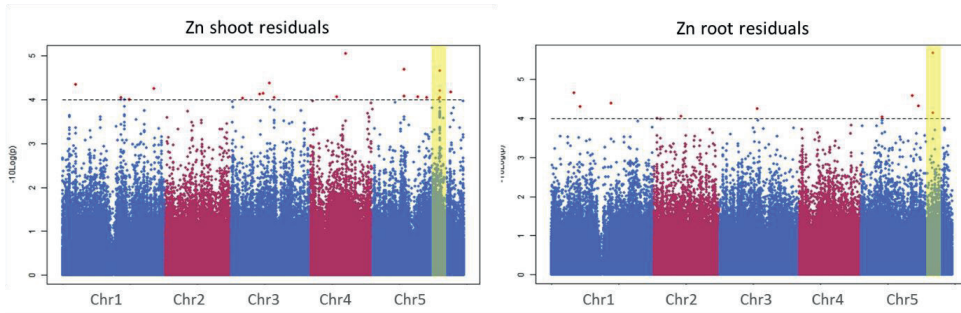


**Figure 3.** Manhattan plots of a GWAS based on 250k SNPs across 350 natural accessions of *Arabidopsis*. SNPs (blue and red dots) above the arbitrary threshold of  $-\log(p)=4$  (dashed line) are considered to be associated with the trait. Yellow bars indicate the selected loci per trait, associated SNPs and genes within each selected loci are listed in Supplemental data file 2. Names of genes positively validated for the trait associated are written next to the locus they are located.

### Validation of novel candidate genes

In order to evaluate the role of these candidate genes in affecting the associated element concentration in response to Zn deficiency, T-DNA insertion mutants were studied. Unfortunately, not all candidate genes could be evaluated, as not for all, a relevant homozygous T-DNA insertion mutant was available. A total of 38 T-DNA insertion mutants, corresponding to thirty-four genes, were examined (**Table 2**). These mutant lines were grown hydroponically in Zn sufficiency or Zn deficiency medium and their shoot and root ionome profiles were determined (**Supplemental Figure S4**). For each element, a PCA Biplot was performed (**Figure 4**), to identify lines with an exceptional ionome profile. In this way, eleven mutants were identified with an aberrant ionome profile. These are mutants T-082 and T-083, both mutated in *TON1 RECRUITING MOTIF 22 (TRM22)*, associated with Cu; mutants T-104, T-108, and T-113, respectively mutated in *At5g66890* (encoding a leucine-rich repeat protein), *TARGET OF EARLY ACTIVATION TAGGED 3 (TOE3)*, and *CASP5*, associated with Fe; mutants T-091, T-122, respectively mutated in *MAJOR FACILITATOR SUPERFAMILY 1 (MSF1)* and *PIGMENT DEFECTIVE 318 (PDE318)*, associated with Mn; mutant T-128, mutated in *EARLY FLOWERING 3 (ELF3)*, associated with Mo; and mutants T-093, T-094, T-132, T-135 and T-141, respectively mutated in *HIPP10*, *HIPP11*, *B-BOX DOMAIN PROTEIN 8 (BBX8)*, *At1g49350* (encoding a pfkB-like carbohydrate kinase protein), and *FER4*, associated with Zn.



**Table 2.** Candidate genes identified upon GWAS of element concentrations under Zn sufficiency and Zn deficiency treatments and selected for further phenotypic analysis, and their respective T-DNA insertion mutant. For each candidate gene is detailed its locus identifier, symbol, Linkage Disequilibrium (LD) with the SNP associated, position of the SNP associated in the respective chromosome (Chr), level of significance of the association ( $-\log_{10}(p)$ ), and the associated element either in concentration (con) and/or residuals (res).

Trait	Chr	Position	$-\log_{10}(p)$	LD	Locus identifier	Symbol	T-DNA
Co res, Co con root	4	13503272	4.4	0.8	At4g26850	VTC2	T-067
Co res, Co con root	4	13551025	4.4	0.8	At4g26970	ACO2	T-068, 69
Co res, Co con root	4	13551025	4.4	1.0	At4g26990		T-070
Cu con root	1	25017792	4.0	1.0	At1g67040	TRM22	T-082, 83
Cu con root	2	14699246	4.6	1.0	At2g34830	WRKY35	T-084, 85
Cu con root	5	19248527	4.9	1.0	At5g47450	TIP2;3	T-087
Cu res root	5	5737381	6.9	1.0	At5g17420	CESA7	T-073
Cu res root	5	5737381	6.9	0.4	At5g17450	HIPP21	T-074
Cu res root	5	13111080	5.1	1.0	At5g34850	PAP26	T-078
Fe con, Mn con root	1	8530152	5.8	1.0	At1g24120	ARL1	T-089
Fe con shoot	5	4966992	4.3	1.0	At5g15290	CASP5	T-113
Fe con, Fe res shoot	1	26154033	5.7	1.0	At1g69550		T-111
Fe con, Fe res shoot	1	26154033	5.7	0.4	At1g69600	ZFHD1	T-112
Fe con, Fe res shoot	5	26714464	4.4	1.0	At5g66890		T-104
Fe con, Fe res shoot	5	26806136	5.2	1.0	At5g67180	TOE3	T-108
Mn con shoot	1	4382479	4.3	0.5	At1g12950	RSH2	T-119, 120
Mn con shoot	1	30358428	6.2	1.0	At1g80770	PDE318	T-122
Mn con shoot	1	30358428	6.2	1.0	At1g80780		T-123
Mn con shoot	4	18442698	4.1	0.9	At4g39700	HIPP23	T-126
Mn con	1	3917803	5.4	0.4	At1g11670		T-117
Mn res root	4	8390639	5.1	1.0	At4g14630	GLP9	T-90
Mn res root	4	16640140	4.1	0.6	At4g34950	MFS1	T-91
Mo con shoot	2	11032027	4.7	1.0	At2g25930	ELF3	T-128
Mo con shoot	5	23904706	7.5	1.0	At5g59250	HP59	T-129
Zn con shoot	1	18264724	5.4	1.0	At1g49350		T-135
Zn con shoot	1	18379245	4.2	1.0	At1g49660	CXE5	T-138
Zn con shoot	2	16851432	4.5	0.7	At2g40300	FER4	T-141
Zn con shoot	2	16852617	4.7	0.6	At2g40435		T-143
Zn con shoot	2	16896465	5.4	1.0	At2g40460		T-144
Zn res root	5	21383803	5.8	0.4	At5g52720	HIPP10	T-093



Zn res root	5	21383803	5.8	0.4	At5g52730	<i>HIPP11</i>	T-094
Zn res root	5	21383803	5.8	0.5	At5g52740	<i>HIPP12</i>	T-096
Zn res root	5	21383803	5.8	1.0	At5g52760	<i>HIPP14</i>	T-098
Zn res shoot	5	19569570	4.0	0.9	At5g48250	<i>BBX8</i>	T-132

In addition to an aberrant ionome profile, these nine mutant lines showed significant changes in biomass due to the Zn deficiency treatment effect when compared to wild-type plants, especially mutant T-090 which is remarkable here. This line is mutated in *GERMIN-LIKE PROTEIN 9 (GLP9)*, and showed the largest increase of all tested mutants, in both shoot and root biomass due to the Zn deficiency treatment, compared to its wild-type background (**Supplemental Figure S5**).

Based on these preliminary results, eight of the tested mutant lines were selected for confirmation of their observed Zn deficiency phenotype. These lines, (T-083, T-090, T-104, T-108, T-122, T-128, T-135, and T-141) were regrown in a second phenotyping experiment, under comparable conditions (**Figure 5**). In this experiment, 12 replicate plants were used per mutant, which meant all biomass differences, when compared, the treatment effect between wild-type Col-0 and the mutants were significantly different (**Supplemental Figure S5**). Mutants T-083, T-122, T-128, T-135, and T-141 showed a significant decrease in root and shoot biomass, due to the Zn deficiency treatment, compared to their wild-type background. Instead, and as found in the initial experiment, mutant T-090 showed an increase in root and shoot biomass. For line T-104, only root biomass was decreased.

Ionome concentrations were determined for shoots and roots of these mutant and wild-type plants. All mutant lines showed significant differences for at least one element when compared to their wild type (**Figure 6**). Six of them showed significant differences, due to genotype x treatment interaction, in the element to which each T-DNA line candidate gene was associated with in the GWAS (**Figure 6**). Those lines were: T-083 associated with Cu in roots, T-104 and T-108 associated with Fe in shoots, T-128 associated with Mo in shoots and roots, and T-135 and T-141 associated with Zn in shoots (**Supplemental Figure S6**). Five of the eight T-DNA lines also showed a significant decrease in Zn concentration either due to genotype or interaction (genotype x treatment). That was the case with lines T-083, T-122, T-128, T-135, and T-141.

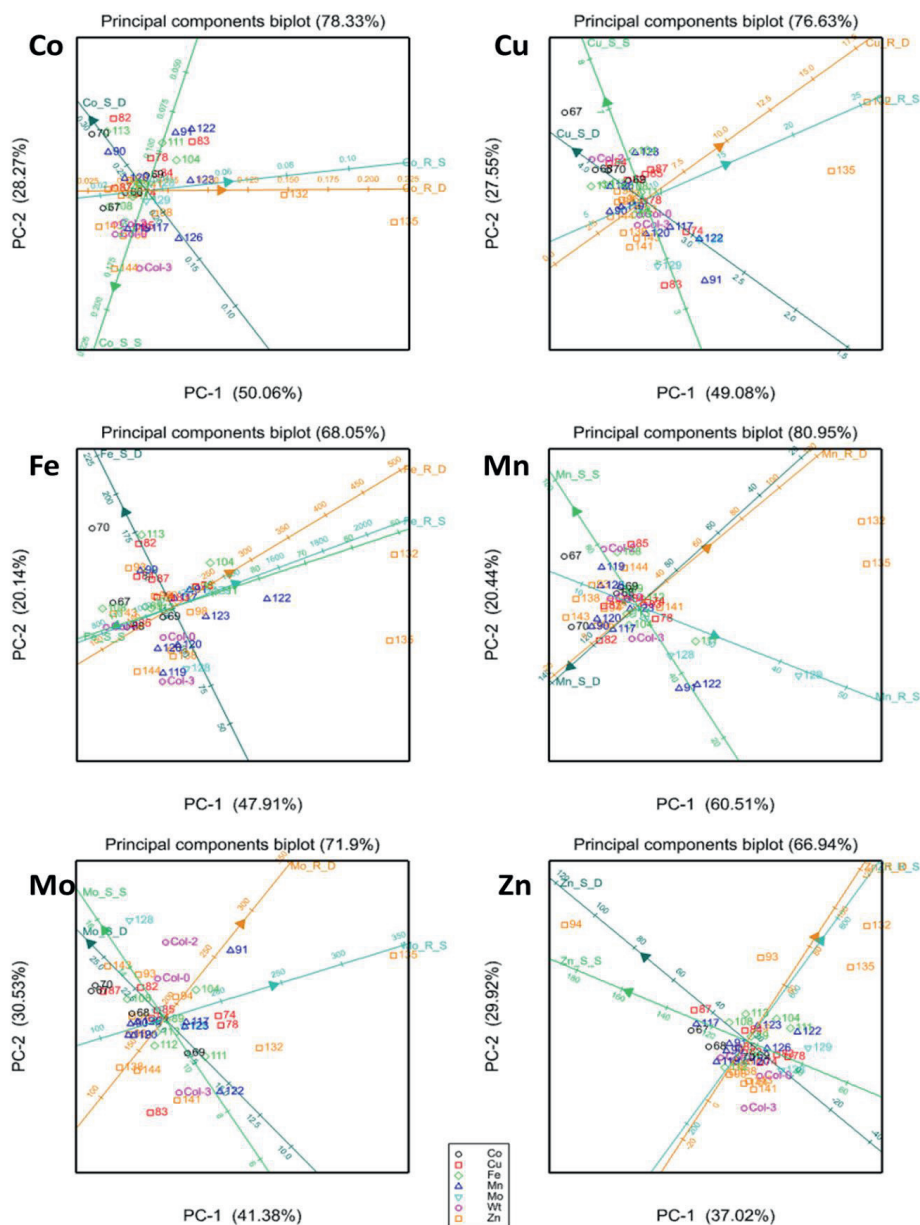


**Figure 4.** PCA Biplot of element concentrations of T-DNA insertion mutant lines. Concentrations of Co, Cu, Fe, Mn, Mo, or Zn in shoots (\_S\_) and roots (\_R\_) of T-DNA insertion mutant lines and wild-type plants grown in Zn sufficiency (S) or Zn deficiency (D). Each mutant is grouped according to the element (symbol with different colour and shape next to the mutant number) to which each candidate gene was associated with in the GWAS. Wild-type (Wt) backgrounds are grouped together and represented with magenta circles.

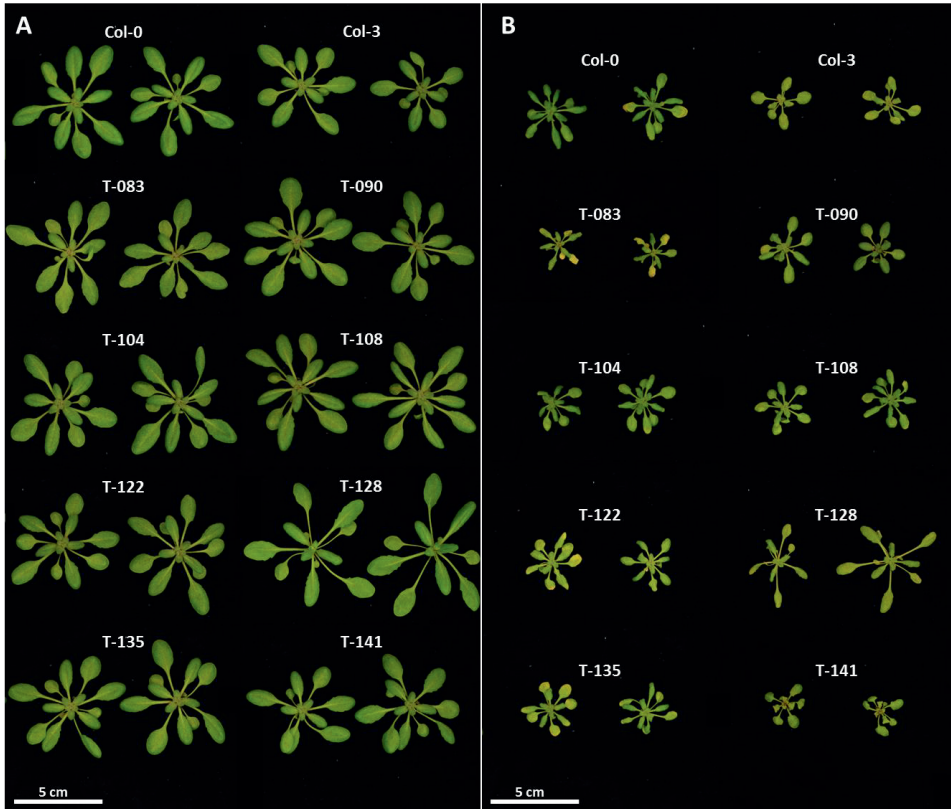


**Figure 5.** Shoot phenotypes of wild-type Col-0/Col-3 and eight GWAS candidate gene T-DNA insertion mutant lines (T-083, T-090, T-104, T-108, T-122, T-128, T-135 and T-141) grown hydroponically in (A) Zn sufficiency for three weeks, or (B) for one week in Zn sufficiency plus two weeks in Zn deficiency. Mutant T-141 was grown for two additional days in Zn deficiency.

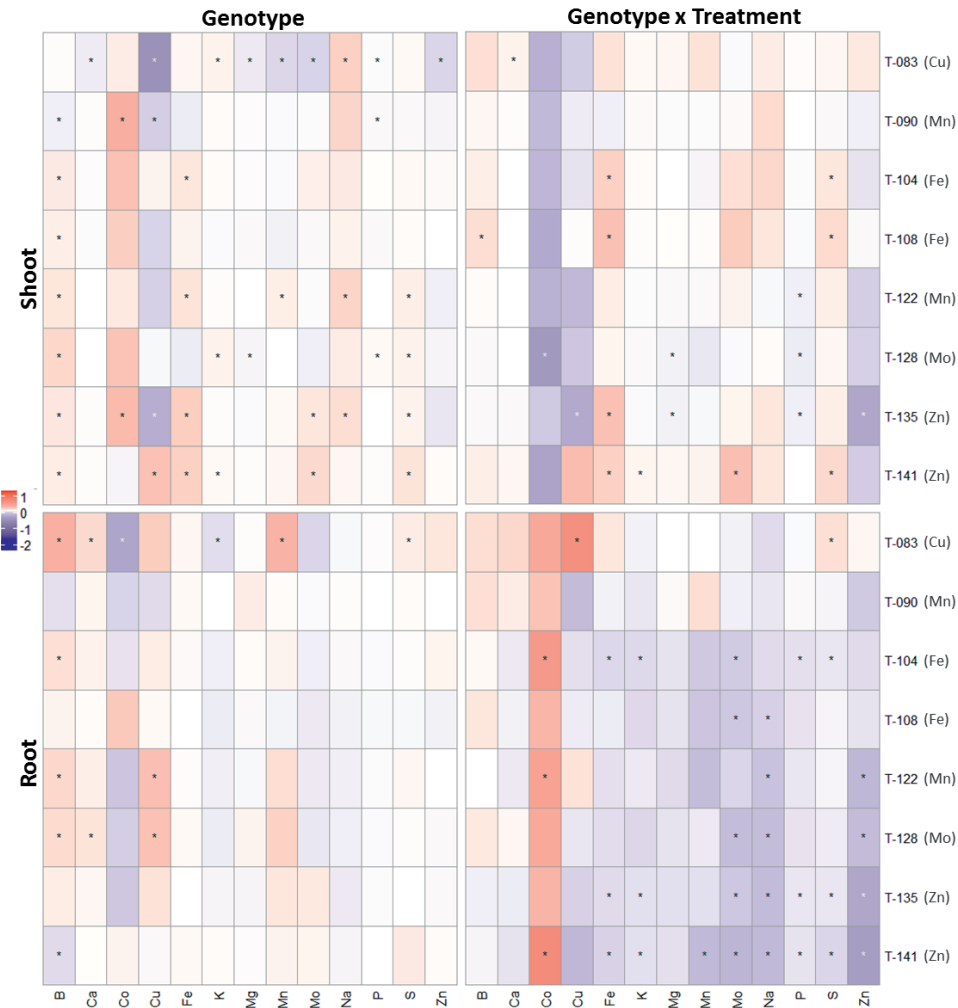


**Figure 6.** Heatmap of shoot and root element concentration fold-changes of T-DNA insertion mutant lines (T-083, T-090, T-104, T-108, T-122, T-128, T-135, and T-141) compared to wild-type plants. Plants were grown hydroponically in Zn sufficiency or Zn deficiency. First the fold-change due to genotype was calculated  $(Y_{TDNA,DEF} + Y_{TDNA,SUF}) / (Y_{WT,DEF} + Y_{WT,SUF})$ , second the fold-change due to the genotype and treatment interaction was calculated  $(Y_{TDNA,DEF} / Y_{WT,DEF}) / (Y_{TDNA,SUF} / Y_{WT,SUF})$  where  $Y$  stands for the mean of a trait value,  $WT$  = control genotype,  $TDNA$  = T-DNA line genotype,  $DEF$  = deficiency treatment,  $SUF$ =sufficiency. \* indicates significant concentration fold-changes with a FDR (False Discovery Rate) adjusted p-value lower than 0.05. Colours indicate positive (red) or negative (blue) fold-changes. The element next to each T-DNA insertion mutant line indicates to which element each candidate gene was associated with in the GWAS.

## Discussion

### Ionome

The ionome was defined by David Salt in 2008 as “the mineral nutrient and trace element composition of an organism, and represents the inorganic component of cellular and organismal systems”. The ionome works as a coordinate network where the disequilibrium of one element concentration is reflected in changes in concentrations of several elements of the ionome (Buescher et al., 2010; Baxter et al., 2012; Huang and Salt, 2016) .

The Arabidopsis ionome analyses illustrated that from the thirteen elements quantified, Zn deficiency increased the concentration in shoots of B, Ca, Co, Fe, Mg, Mn, Mo, P, and S, and in roots of B, Ca, K, Na, and S. Also the relative change of Zn concentrations due to Zn deficiency indicates a decrease 5% higher in shoots than in roots. On the other hand, the relative change of Mn, Mg, Mo, and Fe concentrations due to Zn deficiency shows a decrease in roots and an increase in shoots. The changes in element concentrations and allocations are due to competition among elements with similar chemical characteristics, crosstalk regulation processes, and transporters with overlapping substrate specificities (Huang et al., 2000; Graham, 2008; Nichols et al., 2012; Nishida et al., 2015). Some transporters with overlapping substrate specificities among Zn and other elements are Iron-Regulated Transporter 1 (IRT1: Fe, Zn, Mn, Cd, Co), Zinc Transporter 1 Precursor (ZIP1: Zn, Mn), ZIP4 (Zn, Cu), Ferric Reductase Defective 3 (FRD3: Fe, Zn), NRAMP3/4 (Fe, Zn, Mn, Cd), Heavy Metal Atpase 1 (HMA1: Ca, Cu, Cd, Zn, Co), and HMA2 (Cd, Ni, Co, Cu, Pb, Zn) (Henriques et al., 2002; Eren and Argüello, 2004; Grotz and Guerinot, 2006; Puig and Peñarrubia, 2009; Sinclair and Krämer, 2012; Milner et al., 2013). In Zn deficiency, several of these transporters such as ZIP1, ZIP4, FRD3, and HMA2 increase their expression (van de Mortel et al., 2006; Campos, 2015). For instance, Fe and Zn may compete for root to shoot transport by FRD3 and could transport more Fe to shoots as consequence of Zn deficiency (Durrett et al., 2007; Pineau et al., 2012). The shortage of Zn ions, during Zn deficiency, can increase the transport of other divalent cations present in the plant instead of Zn. This process could lead to toxicity problems in the plant. Consequently, changes in the concentration of other elements, are also indicators of the level of tolerance to Zn deficiency in a plant.

### GWAS

The heritabilities for element concentrations, as determined for the HapMap population of *Arabidopsis* natural accessions, varied from 0.38 to 0.65, and was higher for roots than for shoots, and higher in Zn deficiency than in Zn sufficiency. Ionomer heritabilities vary widely in *Arabidopsis*, ranging from 0.18 to 0.96 according to the sampled plant part, the growth conditions and the type of population (Ghandilyan et al., 2009; Atwell et al., 2010; Baxter et al., 2012; Ghandilyan et al., 2012; Campos et al., 2017). The observed heritabilities suggest that this population is amenable for genetic analysis, with a good prospect that genetic loci can be identified, provided there are not too many loci involved, each with a minor effect on the phenotype, in determining the element concentrations. In those cases, polymorphisms do not cause a phenotypic effect large enough to be detected (Manolio et al., 2009; Gibson, 2010; Yang et al., 2010; Korte and Farlow, 2013).

In the relatively few GWAS that have been performed for *Arabidopsis* ionomes, very few known micronutrient transporters have been detected. In our study, only for two of the analysed elements, a known micronutrient transporter gene was among the candidates. The first was *NRAMP1*, which was found to be associated with the Mn concentration. It is a known Mn transporter, involved in Mn uptake from the soil (Cailliatte et al., 2010; Castaings et al., 2016), also able to transport Fe and Cd (Curie et al., 2000; Takahashi et al., 2011). The second was *MOT1*, associated with Mo concentration, and encoding a known molybdate transporter (Tomatsu et al., 2007; Baxter et al., 2008). The same locus has been detected by GWAS before to affect the Mo concentration in *Arabidopsis* (Atwell et al., 2010). The Mo concentration also had the highest heritability in our study and other genetic studies (Baxter et al., 2012; Campos et al., 2017).

Zn homeostasis has been investigated in detail in *Arabidopsis* and several genes encoding Zn transporters have been identified so far, belonging to the *ZIP*, *MTP/CDF*, *YSL* and *HMA* families (Grotz et al., 1998; Korshunova et al., 1999; Vert et al., 2001; Hussain et al., 2004; Eide, 2006; van de Mortel et al., 2006; Waters et al., 2006; Sinclair et al., 2007; Lin et al., 2009; Deinlein et al., 2012; Milner et al., 2013). These genes do not give Zn deficiency related phenotypes, probably due to their genetic redundancy. Although we were expecting to find at least a few of these genes among the candidates associated with Zn concentration, this was not the case. This confirms the general observation for GWAS of mineral concentrations in plants, that natural genetic variation in mineral transporters rarely contributes to phenotypic variation.

The main reasons for these results could be the multigenic character of the Zn deficiency tolerance and redundancy among transporters. This means several loci with small effects each one, including epistatic interactions as the one reported between *bZIP19* and *bZIP23* (Assunção et al., 2010).

On the other hand, GWAS has been successful to identify genes in Arabidopsis that favour tolerance to high concentrations of non-essential, toxic elements, such as Cd and As. Similar populations as the one we used were grown upon Cd or As supply. In this way, variation at the *HMA3* gene was identified, encoding a P-type ATPase involved in Zn and Cd translocation, to be important for Cd accumulation and tolerance (Chao et al., 2012). It also led to the discovery of the *HAC1* gene, encoding a novel arsenate reductase involved in plant tolerance to As (Chao et al., 2014). The tolerance to non-essential elements requires mainly exclusion of the element from the plant or internal sequestration to detoxify it, instead of maintaining essential elements homeostasis, which is much more about maintaining a steady supply of the element, to keep the internal concentration well between toxicity and deficiency levels. This likely requires functional alleles and often does not favour loss-of-function alleles, as were discovered for the *HMA3* and *HAC1* genes, which contribute with large effect sizes to the phenotype and are easily detected by GWA (Atwell et al., 2010).

Nevertheless our inability to identify known metal transporters as candidates underlying loci affecting the concentration of the same element, we did identify several known genes encoding proteins involved in homeostasis of another element. Examples of those were *KUP11* (Ahn et al., 2004; Bradshaw, 2005), *HIPP21* (Tehseen et al., 2010), *PAP26* (Robinson et al., 2012), *MGT10* (Li et al., 2001) *TIP2;3* (Loqué et al., 2005), *CASP5* (Tester and Leigh, 2001; Gasber et al., 2011), *MOT2* (Gasber et al., 2011), *NIP6;1* (Tanaka et al., 2008), *MGT1* (Ishijima et al., 2012), *bZIP23* (Assunção et al., 2010), *FER4* (Arosio et al., 2009; Tarantino et al., 2010), *HIPP10/11/12/13/14/23/46* (de Abreu-Neto et al., 2013). Since most of these genes were not further examined with respect to their effect on the particular element concentration with which they were found to be associated, it could still be that they are false positives (Korte and Farlow, 2013) or they could be also affecting the homeostasis of the element they were associated with in the GWAS.

### Validation of candidate genes

A total of 38 T-DNA insertion mutants disrupting 34 candidate genes were initially tested for any relevant phenotypic effect under Zn deficiency. Almost half of these mutants showed a difference with wild type either in ionome profile or in biomass production (**Supplemental figure S4 and S5**). The lack of detectable phenotype in the other half could be for several reasons. First and most likely is that the gene is not involved in the trait, because either the associations were false positives or another gene in the LD region of the locus associated is responsible for changes in the ionome. The selection criteria favour the selection of genes with known functions related with nutrients homeostasis. Thus, genes with unknown function could be missed. Second, variants of other genes can play an important role in the effect of a gene due to epistatic interactions, which may not be present in the genetic background of the T-DNA line tested (Weigel, 2012). Third, the evaluated mutants were all generated in the Col-0 or Col-3 background, in which the phenotypic effect may not be very striking, simply because it does not carry a strong wild-type allele of the gene, or it may even carry a natural null allele, in which case the T-DNA insertion allele will not alter the gene function and will not lead to a different phenotype (Koornneef et al., 2004). Therefore, the phenotypic effect of a gene can only be detected in a specific genetic background, which may not always be Col, and this is the common background of T-DNA insertion lines are available.

For a second validation experiment, we selected eight T-DNA insertion mutants, seven based on their differential ionome profile and one based on the observed Zn deficiency-related changes in biomass, as observed in the first experiment. The *TRM22* gene was selected based on associations with Cu concentrations, the *trm22* mutant showed the strongest Zn deficiency symptoms of all mutants and wild-type plants and a significant increase of root Cu concentration due to Zn deficiency treatment when compared to wild-type plants (**Figure 4, 5 and Supplemental Figure S6**). The expression of *TRM22* is induced in roots and repressed in shoots due to Zn deficiency (Campos, 2015). The protein encoded by this gene belongs to the TONNEAU1 Recruiting Motif (TRM) protein family (Drevensek et al., 2012). Members of this family are involved in microtubules array organization during cell division (Azimzadeh et al., 2008; Spinner et al., 2010; Mach, 2012). Initially, we tested two *trm22* mutants (T-082 and T-083). However, T-082 did not show the same ionome profile as T-083 in the initial screen. The reason could be that T-082 disrupts not just *TRM22* but also *ATIG24822*, a non-described gene.



The T-104 and T-108 mutants, for *At5g66890* and *TOE3* respectively, which were selected based on associations with Fe concentrations, had a higher shoot Fe concentration than wild type upon Zn deficiency. The gene *At5g66890* encodes a protein which belongs to LRR (Leucine-Rich Repeat) protein family and is a probable disease resistance protein (Meyers et al., 2003). The gene *TOE3* encodes a transcription factor of the APETALA 2/Ethylene Responsive Factor (AP2/ERF) superfamily and appears to be a conserved paralogue of the *AP2* gene (Zumajo-Cardona and Pabón-Mora, 2016). Both *AP2* and *TOE3* are involved in controlling flowering time and meristem identity (Jung et al., 2014). It is not directly obvious why mutation of either the LRR-family gene or *TOE3* would affect Fe homeostasis. Flowering time and plant defence mechanisms can indirectly affect the Fe homeostasis considering that plant defence mechanisms against pathogens and Fe deficiency response share common features (Zamioudis et al., 2014; Aznar et al., 2015; Martínez-Medina et al., 2017) and that the hypersensitive iron deficiency *bhlh100/bhlh101* double mutant displays a late flowering phenotype (Sivitz et al., 2012).

Candidate genes found to be associated with Mn concentration in shoots, were *NRAMP1*, *PDE318*, and *GLP9*. The *NRAMP1* gene was not further validated due to its already known function in Mn transport (Cailliatte et al., 2010; Castaings et al., 2016). The PDE318 protein is part of the P-loop containing NTP-ase superfamily. Members of this family hydrolyze nucleoside triphosphates and are involved in diverse cellular functions such as root growth (Yu et al., 2016), assembly of F/S proteins (Hausmann et al., 2005), negative regulator of plant defense responses (Cheung et al., 2016). In addition, PDE318 has sequence similarities with Fe transport protein B (FeoB) involved in the Fe transmembrane (tilacoid) transporter (Kammler et al., 1993; Kwon and Cho, 2008). The T-122 *pde318* mutant had higher Fe and Mn concentrations in shoots than the wild type, while in roots, Zn concentration was significantly lower than the wild type upon Zn deficiency. The *GLP9* encodes a germin-like protein. The gene is mainly expressed in roots and can be induced by abiotic stress conditions (Winter et al., 2007) and the defence responses to nematodes (Jammes et al., 2005; Velloso et al., 2007). The T-090 *glp9* mutant produced more biomass than the wild type, but we did not observe any effect on the Mn concentration when compared to wild type, however, *glp9* produced more biomass than the wild type.

The *MOT1* gene was found to be associated with the Mo concentrations. It encodes a Mo transporter (Tomatsu et al., 2007; Baxter et al., 2008). The *ELF3* gene also was associated with

Mo concentrations. It encodes a component of the circadian clock (Covington et al., 2001). The T-128 *elf3* mutant plants were clearly different from the rest of the genotypes analysed due to its characteristic elongated petioles (Reed et al., 2000) and its insensitivity to photoperiod signals (Song, 2012). There is not a clear link between this gene and Mo concentrations, however, the circadian clock regulates the transcription of Mg, Fe, Mn, and Cu transporters (Haydon et al., 2011). Moreover, element concentrations show circadian oscillations (Johnson et al., 1995; Haydon et al., 2015) and concentrations of Cu, Fe, and Mg affect the period length of circadian rhythm (Andrés-Colás et al., 2010; Chen et al., 2013; Hong et al., 2013; Feeney et al., 2016).

Mutants T-135 and T-141, respectively mutated in *Atlg49350* and *FER4*, associated with Zn concentrations, showed decreased shoot and root Fe, P, and Zn concentrations when compared to wild type, due to the effect of the Zn deficiency treatment. *Atlg49350* encodes a pfkB-like carbohydrate kinase with an unknown function. Members of the PfkB family of carbohydrate kinases have diverse carbohydrate substrates as fructose, ribose, adenosine, myo-inositol, and others. The few members of this family characterized are involved in the accumulation of photosynthetic transcripts in chloroplasts, ribose accumulation in both the roots and leaves, and plant growth (Ogawa et al., 2009; Gilkerson et al., 2012; Riggs and Callis, 2016). For instance, the Fe deficiency response requires the accumulation of sugars to induce the expression of Fe acquisition-related genes (Lin et al., 2016). *FER4* gene was associated with Zn concentrations, and encodes a ferritin protein, which acts as Fe storage protein involved in buffering Fe by sequestering intracellular Fe (Arosio et al., 2009; Murgia and Vigani, 2015; Rey et al., 2015). The Fe concentration was lower in roots and higher in shoots of *ferr4* compared to wild type due to the Zn deficiency treatment, alterations in the Fe concentration is characteristic of *ferr4* (Tarantino et al., 2010). In wild type, upon Zn deficiency, the Fe concentration decreases in shoots and increased in roots. Therefore, the effect of the *ferr4* is an augmented effect of Zn deficiency. Its loss-of-function deregulates the expression of several element transporters in the plant stem, for instance, several Zn transporters in the plant stem (Ravet et al., 2009). Apart from it, there is significant decrease in the concentration of K, Mn, Mo, Na, P, S and increase in Co.

The analysis of the *trm22*, *at5g66890*, *toe3*, *elf3*, *atlg49350* and *ferr4* mutants confirmed a difference with wild type, in the concentration of the same element with which this gene was associated with in the GWAS, in response to Zn deficiency. In addition to the target element,

the concentration of several elements was altered in these mutants when compared to wild type, due to the Zn deficiency treatment. Although genetic complementation has not yet been performed, these results suggest that variation at these loci is likely to contribute to variation in the respective mineral concentrations they are implicated in, in response to Zn deficiency.

### **Conclusions**

Discovering the molecular basis of complex traits, like micronutrient homeostasis, is a challenge due to the large number of genes involved in the process and the small effect they have on the phenotype, in addition to their redundant functions, epistatic interactions and pleiotropic effects. Zn deficiency does not only affect the plant Zn concentration, or even Zn homeostasis, there appear to be several physiological consequences for the homeostatic mechanisms balancing other mineral concentrations in *Arabidopsis*. Thus, maintaining the balance in the ionome of Zn deficient plants is also a key point in Zn deficiency tolerance. As shown in this thesis, the loss of function of seven genes causes an increase in the misbalance of the ionome due to Zn deficiency. A deep study of these genes is needed to analyse their potential in Zn deficiency tolerance by maintaining the balance of the ionome.

### **Acknowledgements**

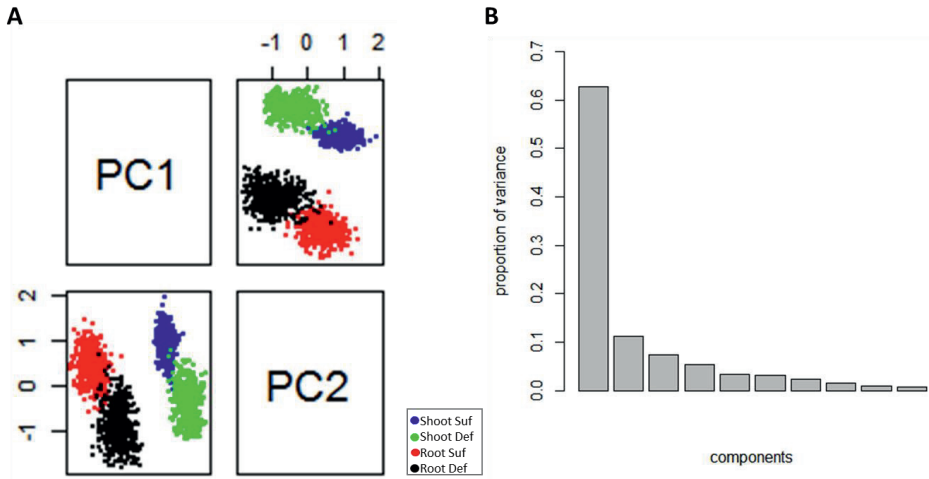
We thank Dr. Tânia Serra for the help in setting the large scale phenotyping of T-DNA insertion lines. This work was supported by the Ecuadorian government through SENESCYT (Secretaría de Educación Superior, Ciencia, Tecnología e Innovación) and Universidad de las Fuerzas Armadas-ESPE.

## Supplemental information

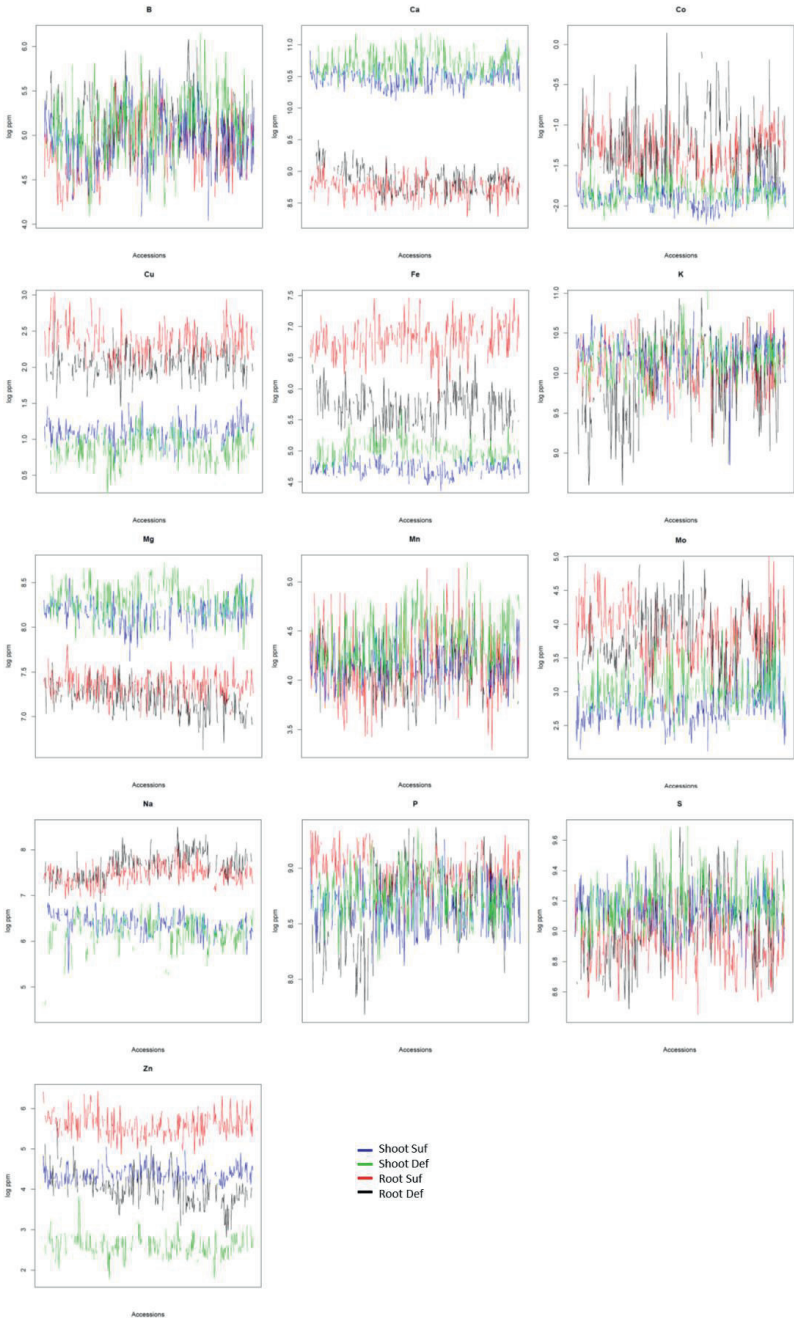
**Supplemental files link:** [https://drive.google.com/open?id=12ixp5aiAX8DxrpuW3d-93N-KetWvmze\\_](https://drive.google.com/open?id=12ixp5aiAX8DxrpuW3d-93N-KetWvmze_)

**Table S1.** Description of T-DNA insertion mutants used to validate GWAS candidate genes. The description includes Line ID used as a code in our the experiments, wild-type background, NASC identification (ID) and donor numbers, and locus identifier.

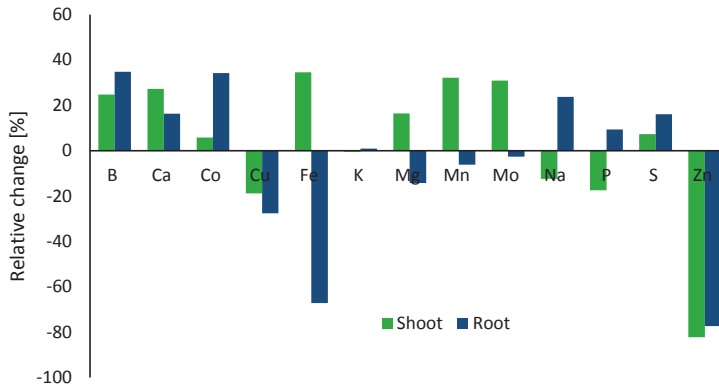
Line ID	NASC ID	Background	Donor Number	Locus identifier
T-067	N656047	Col-0 (N60000)	SALK_146824C	At4g26850
T-068	N671601	Col-0 (N60000)	SALK_079922C	At4g26970
T-069	N671156	Col-0 (N60000)	SALK_009537C	At4g26970
T-070	N403166	Col-0 (N60000)	GK-033H10	At4g26990
T-073	N669529	Col-0 (N60000)	SALK_029940C	At5g17420
T-074	N655731	Col-0 (N60000)	SALK_092415C	At5g17450
T-078	N413741	Col-0 (N60000)	GK-144B01	At5g34850
T-082	N663352	Col-0 (N60000)	SALK_093331C	At1g67040
T-083	N673019	Col-0 (N60000)	SALK_098466C	At1g67040
T-084	N655835	Col-0 (N60000)	SALK_111141C	At2g34830
T-085	N648777	Col-0 (N60000)	SALK_148777 (BX)	At2g34830
T-087	N866736	Col-0 (N60000)	SALK_010974	At5g47450
T-089	N863910	Col-2	WiscDsLox262B01	At1g24120
T-090	N872707	Col-3	SAIL_270_D05	At4g14630
T-091	N662797	Col-0 (N60000)	SALK_066841C	At4g34950
T-093	N684026	Col-0 (N60000)	SALK_049083C	At5g52720
T-094	N438279	Col-0 (N60000)	GK-399F11	At5g52730
T-096	N667786	Col-0 (N60000)	SALK_012334C	At5g52740
T-098	N667818	Col-0 (N60000)	SALK_013684C	At5g52760
T-104	N845057	Col-0 (N60000)	SAIL_1231_B01	At5g66890
T-108	N863162	Col-0 (N60000)	SAIL_603_B01	At5g67180
T-111	N673799	Col-0 (N60000)	SALK_010456C	At1g69550
T-112	N877090	Col-0 (N60000)	SAIL_818_D10	At1g69600
T-113	N542116	Col-0 (N60000)	SALK_042116 (AI)	At5g15290
T-117	N685506	Col-0 (N60000)	SALK_025900C	At1g11670
T-119	N859621	Col-0 (N60000)	SALK_103884 (BD)(BO)	At1g12950
T-120	N677058	Col-0 (N60000)	SALK_136631C	At1g12950
T-122	N645367	Col-0 (N60000)	SALK_145367 (BL)(BX)	At1g80770
T-123	N669178	Col-0 (N60000)	SALK_142773C	At1g80780
T-126	N817417	CS8846	SAIL_378_B11	At4g39700
T-128	N471954	Col-0 (N60000)	GK-750E02	At2g25930
T-129	N862551	Col-0 (N60000)	SAIL_335_F05	At5g59250
T-132	N662685	Col-0 (N60000)	SALK_061961C	At5g48250
T-135	N859815	Col-0 (N60000)	Salk_006361	At1g49350
T-138	N853035	Col-2	WiscDsLox366A7_052	At1g49660
T-141	N662835	Col-0 (N60000)	SALK_068629C	At2g40300
T-143	N661589	Col-0 (N60000)	SALK_015121C	At2g40435
T-144	N660899	Col-0 (N60000)	SALK_058919C	At2g40460



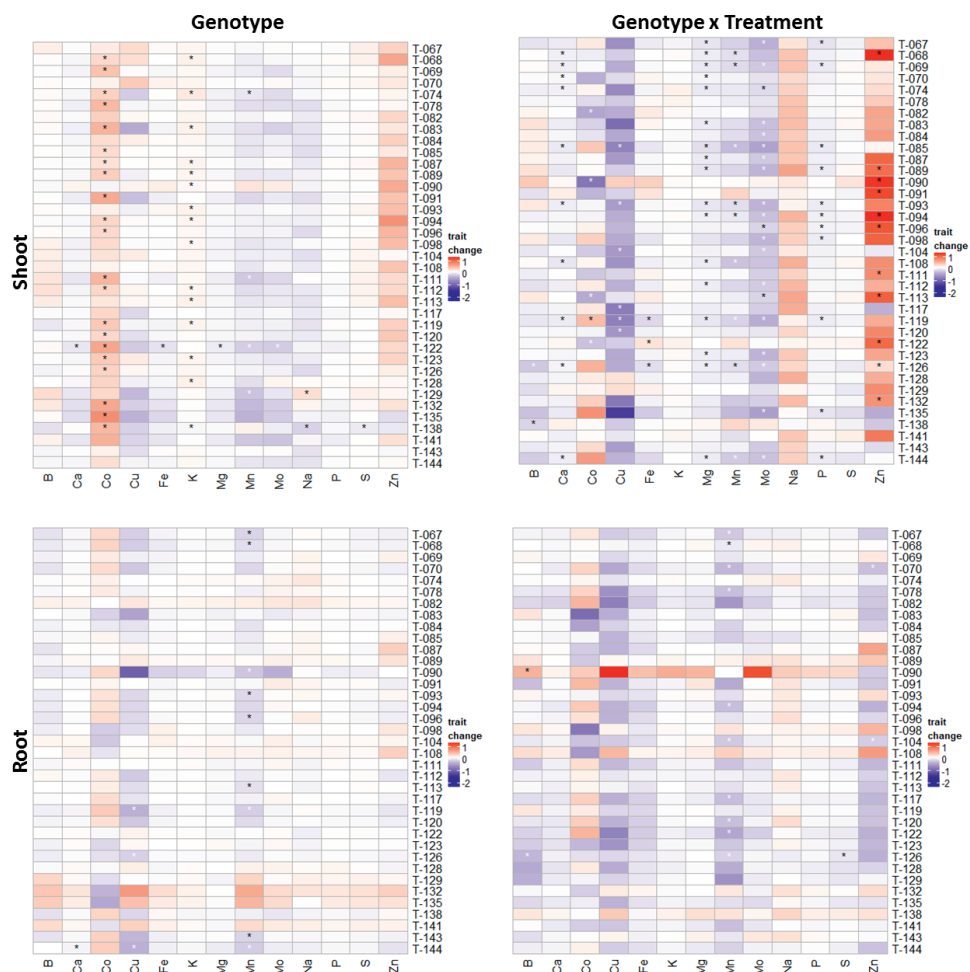
**Figure S1.** Principal component analyses of the concentrations of 13 essential elements in 350 natural accessions of *Arabidopsis*. (A) Distribution of accessions based on element concentrations in shoots (Shoot Suf, blue dots) and roots (Root Suf, red dots) of plants grown hydroponically in Zn sufficiency and shoots (Shoot Def, green dots) and roots (Root Def, black dots) of plants grown hydroponically in Zn deficiency, for different combinations of principal components (PCs). (B) Proportion of variance explained by each one of the principal components.



**Figure S2.** Concentrations of 13 essential elements across 350 natural accessions of *Arabidopsis*. Element concentrations in shoots (Shoot Suf, blue) and roots (Root Suf, red) of plants grown hydroponically in Zn sufficiency and shoots (Shoot Def, green) and roots (Root Def, black) of plants grown hydroponically in Zn deficiency.

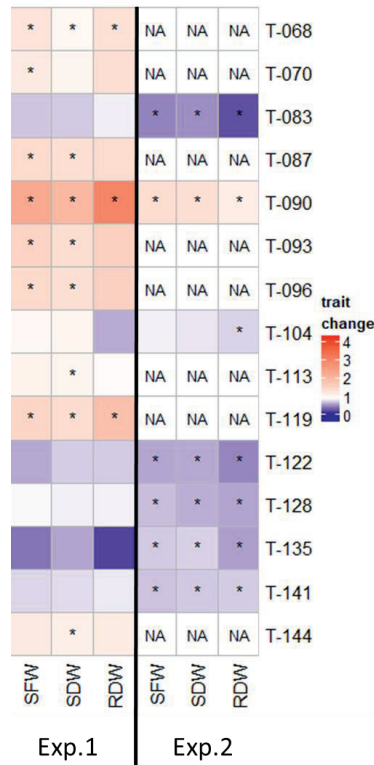


**Figure S3.** Relative change of the concentrations means of 13 essential elements across 350 natural accessions of *Arabidopsis*. Relative change in shoots (green) and roots (blue) of plants grown hydroponically in Zn deficiency vs plants grown hydroponically in Zn sufficiency.

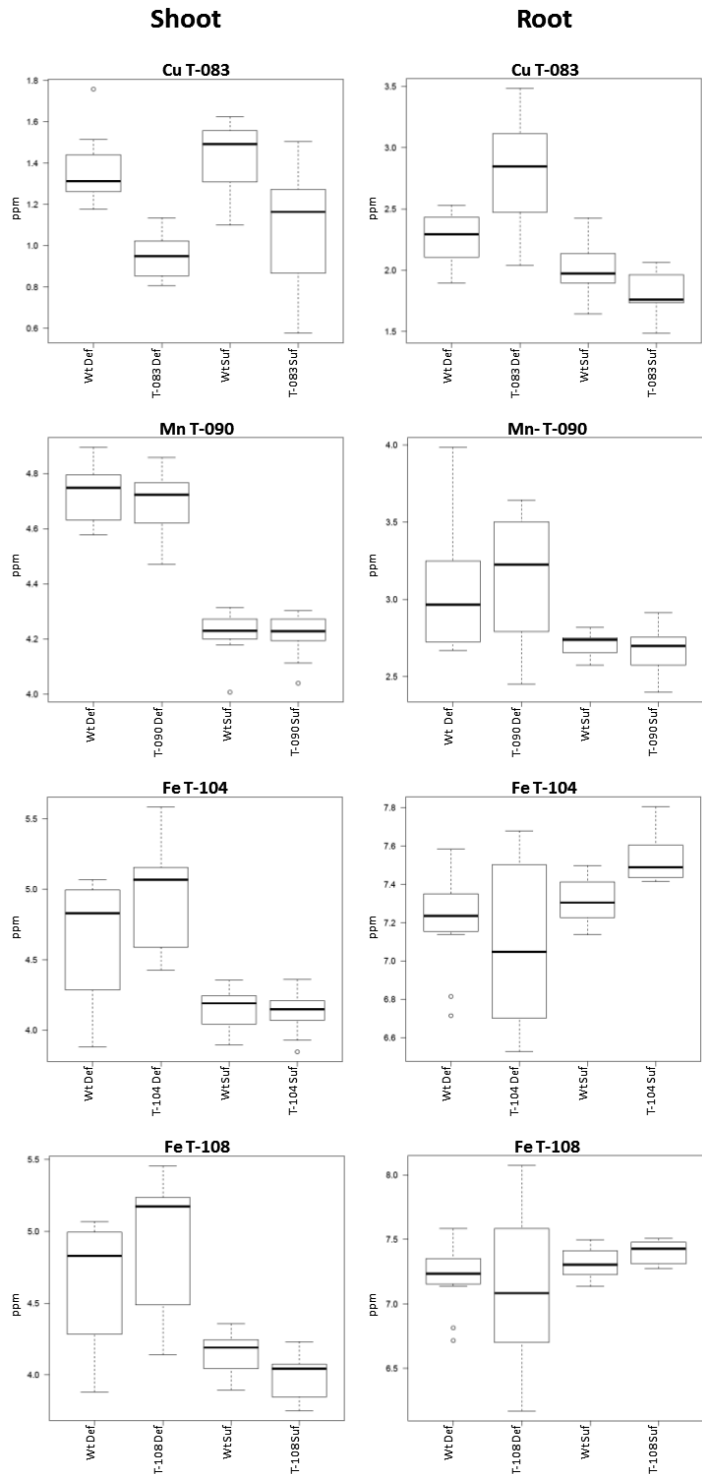


**Figure S4.** Heatmap representing the ionome profile changes of T-DNA insertion mutant lines. Ionome profile changes of T-DNA insertion mutant lines compared to wild-type plants grown hydroponically in Zn sufficiency or Zn deficiency, from test with the initial 38 T-DNA lines of candidate genes. Significant changes between mutant and wild-type plants denoted with (\*) if they had a FDR (False Discovery Rate)-adjusted p-value lower than 0.05. Colours indicate positive (red) or negative (blue) fold changes. First the fold-change due to genotype was calculated  $(Y_{TDNA,DEF} + Y_{TDNA,SUF}) / (Y_{WT,DEF} + Y_{WT,SUF})$ , second the fold-change due to the genotype and treatment interaction was calculated  $(Y_{TDNA,DEF} / Y_{WT,DEF}) / (Y_{TDNA,SUF} / Y_{WT,SUF})$  where Y stands for the mean of a trait value, WT = control genotype, TDNA = T-DNA line genotype, DEF = deficiency treatment, SUF=sufficiency.





**Figure S5.** Heatmap of the biomass of T-DNA insertion mutant lines compared to wild-type plants. Plants grown hydroponically in Zn sufficiency or Zn deficiency, as investigated in experiment 1 (Exp.1: initial 38 T-DNA lines) and experiment 2 (Exp.2: selected 8 T-DNA lines). The traits represented are shoot fresh weight (SFW), shoot dry weight (SDW) and root dry weight (RDW). Only mutants with significant differences in biomass when compared to wild type and the effect of the treatment in both experiments. Significance denoted with (\*) if they had a FDR (False Discovery Rate)-adjusted p-value lower than 0.05. Colours indicate positive (red) or negative (blue) fold changes when compared the mutant to the wild type. The fold-change due to the genotype and treatment interaction was calculated  $(Y_{TDNA,DEF} / Y_{WT,DEF}) / (Y_{TDNA,SUF} / Y_{WT,SUF})$  where Y stands for the mean of a trait value, WT = control genotype, TDNA = T-DNA line genotype, DEF = deficiency treatment, SUF=sufficiency.



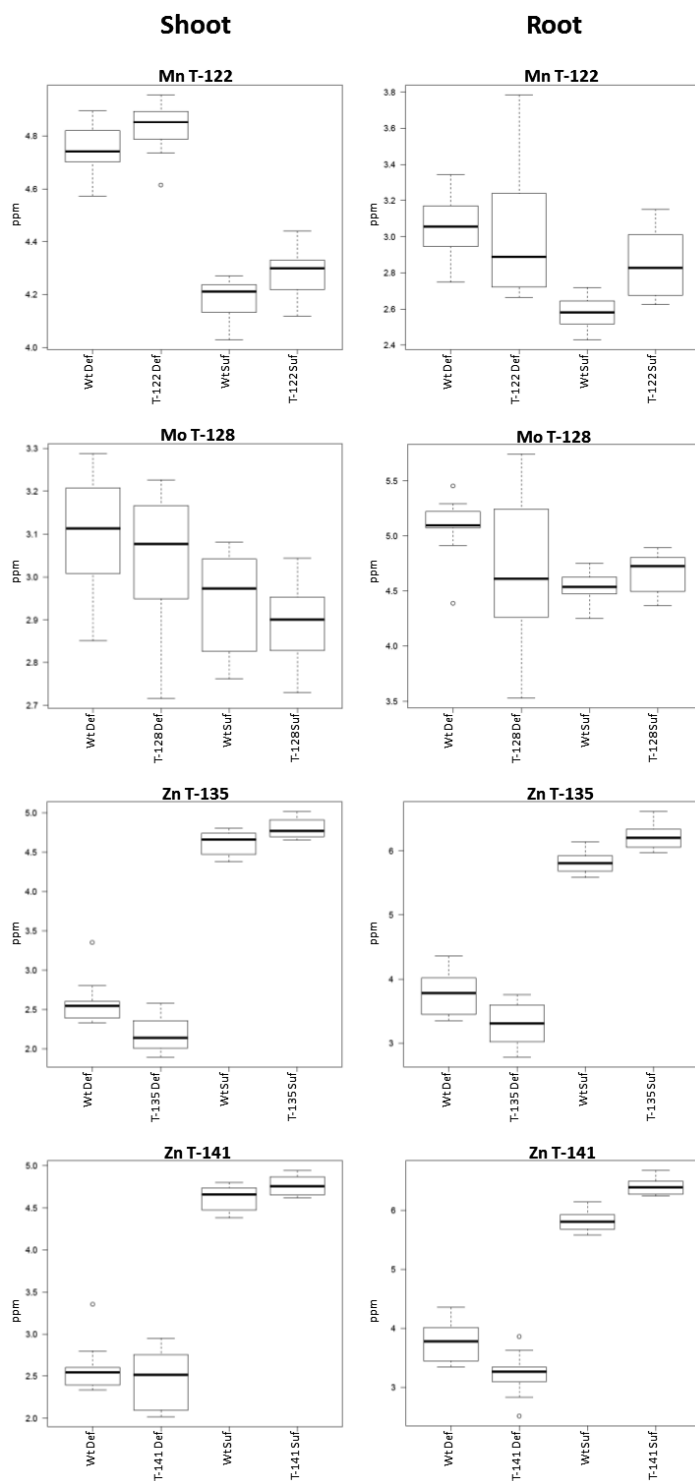


**Figure S6.** *Boxplots of element concentrations of T-DNA insertion mutant lines compared to wild-type plants. Per mutant is plotted the concentrations of the element the mutated gene was associated with in the GWAS. Data represent the  $\log^e$  of element concentration of 12 replicate plants per genotype.*





# Chapter 5

## **A conserved cluster of tandemly arrayed *HIPP* genes affects tolerance to Fe and Zn deficiency in *Arabidopsis thaliana***

Valeria Ochoa Tufiño<sup>1,2</sup>, Khadija Aaliya<sup>1,3</sup>, Jos Meeussen<sup>1</sup> and Mark G.M. Aarts<sup>1</sup>

- 1) Laboratory of Genetics, Wageningen University, Wageningen, The Netherlands
- 2) Current affiliation: Departamento de Ciencias de la Vida, Universidad de las Fuerzas Armadas ESPE, Sangolquí, Ecuador
- 3) Current affiliation: Institute of Agricultural Sciences, University of the Punjab, Lahore, Pakistan

*In preparation for submission*

### Abstract

Abiotic stresses decrease the growth and productivity of plants. Stress-tolerant crops are required for agriculture, and the identification of stress-related genes which increase plants tolerance to abiotic stress is important to achieve such. Previously, by a Genome-Wide Association Study (GWAS) we identified a cluster of tandemly arrayed Heavy Metal-Associated Isoprenylated Plant Proteins (HIPPs) to be associated with Zn deficiency tolerance in *Arabidopsis thaliana* (Arabidopsis). In this study, we explored the relevance of the *HIPP10*, *HIPP11*, *HIPP12*, *HIPP13* and *HIPP14* genes of this cluster for the Fe and Zn deficiency response. The expression of these five *HIPPs* is induced in plants upon Fe or Zn deficiency and single mutant lines *hipp10*, *hipp11*, *hipp12* and *hipp14* are less sensitive to Fe and Zn deficiency treatments compared to wild-type plants. In these *hipp* mutants, the expression of the other *HIPP* genes in the cluster was not induced by Fe deficiency. The five *HIPPs* interact with several transcription factors involved in stress response and plant development. Altogether, these *HIPPs* appear to be negative regulators of plant growth, especially under Fe and Zn deficiency stress.



## Introduction

The bottom of chromosome 5 of *Arabidopsis thaliana* (Arabidopsis) (coordinates 21363486 to 21390189 bp) contains a cluster of 11 tandemly arrayed genes (from *At5g52670* to *At5g52770*) of which six encode for HEAVY METAL-ASSOCIATED PLANT PROTEINS (HPPs; resp. HPP6, 8, 9, 10, 11 and 12) and five for HEAVY METAL-ASSOCIATED ISOPRENYLATED PLANT PROTEINS (HIPPs; resp. HIPP10, 11, 12, 13 and 14). The region comprising HIPP10-14 was previously identified in a Genome-Wide Association Study (GWAS) for response to Zn deficiency to be associated with the root Zn concentration (Chapter 4). HIPPs and HPPs are predicted to be metallochaperone-like proteins, based on sequence similarities. Arabidopsis encodes for 67 metallochaperone-like proteins, 45 HIPPs, and 22 HPPs, containing a predicted Heavy Metal-Associated (HMA) domain. These 67 proteins are classified into two main branches, the first branch contains 46 proteins and the second one 21 proteins (Tehseen et al., 2010). The cluster of 11 tandemly arrayed genes on chromosome 5 encodes proteins that are all found in this second branch, suggesting that these proteins are phylogenetically related and perhaps even derived from one ancestral HIPP/HPP gene. These 11 proteins contain domains with similarity to the HMA domain, even though they lack the CysXXCys motif associated with the metal binding affinities (Tehseen et al., 2010).

All Arabidopsis HIPPs characterized to this moment, have a function related with environmental stress responses. Cold induces the expression of *HIPP24/26/23/25* and represses the expression of *HIPP27*, while *HIPP26* expression is also induced by drought and salt exposure (Barth et al., 2009). *HIPP26* is also expressed upon Cd stress, its protein can bind Cd, Cu and Pb, and its overexpression confers Cd tolerance to Arabidopsis (Gao et al., 2009). The triple mutant *hipp20/21/22* has increased sensitivity to high concentration of Cd, but accumulates less Cd than wild-type plants. The Cd-sensitive *ycf1* yeast mutant is rescued by expressing either *HIPP20*, *HIPP21*, *HIPP22* or *HIPP27* through binding Cd or facilitating its transport into the vacuoles or out of the cells, either way, making Cd not available in the cytosol (Tehseen et al., 2010). *HIPP6* expression is induced by Cd, Hg, Fe, and Cu, and its overexpression confers tolerance to Cd (Suzuki et al., 2002). *HIPP3* expression is repressed by drought and ABA, and induced by *Pseudomonas* infection. Its overexpression affects the regulation of genes involved in biotic and abiotic stress and seed and flower development, and as a consequence *HIPP3*-overexpressing lines flower later than wild type (Zschiesche et al., 2015). So, in general, HIPPs seem to play a role in regulatory networks important for stress

response and development, and their capacity to bind transition metal ions could be important in the response to metal stress, though their function is clearly not limited to metal-exposure-related responses.

Exposure of plants to environmental stress conditions affect their physiology in many different aspects. To ensure their survival, plants need to coordinate growth and stress responses. Most commonly, plants shut down growth under stress (Huot et al., 2014; Haina and Uwe, 2017). Phytohormones such as gibberellic acids (GAs) and brassinosteroids (BRs) are implicated in stress-responsive plant growth. Vegetative growth, in general, is promoted by GA. GA signalling can be repressed by DELLA proteins, which are transcription factors that restrict plant growth (Silverstone et al., 1997; Sun, 2010). The growth-repressing effects of DELLAs are enhanced by stress signals (Achard et al., 2008; Achard and Genschik, 2009) such as the ones induced by salt stress. The growth reduction observed upon salt stress depends on a GA-DELLA-mediated mechanism, based on reduced GAs accumulation, which causes the increased DELLA accumulation. Arabidopsis encodes five DELLA proteins, which act redundantly, with the DELLA quadruple mutant *gai/rga/rgl1/rgl2* showing lower sensitivity to salt stress compared to wild-type plants (Achard et al., 2006). The other group of growth-promoting phytohormones comprises the BRs. One of the final steps in the BR signal transduction pathway is the activation of BRI1-EMS-SUPPRESSOR 1 (BES1) (Clouse, 2011). This transcription factor is a master regulator of the BR pathway, promoting plant growth through the regulation of transcription of several downstream genes. BES1 is degraded upon drought and carbon starvation, which slows down plant growth, while the constitutive activation of BR responses increases the susceptibility to drought. The degradation of BES1 under stress conditions is required for the plant survival (Nolan et al., 2017).

Growth repression upon stress does not depend solely on phytohormones that promote growth but also on the crosstalk with phytohormones that mediate stress responses, such as abscisic acid (ABA), salicylic acid (SA), jasmonic acid (JA) and ethylene (Verma et al., 2016). Disruption of the ethylene signalling pathway promotes vegetative growth (Gagne et al., 2004), while ethylene, JA, and ABA can act together to induce the expression of the *ETHYLENE-RESPONSIVE ELEMENT BINDING FACTOR 4* (*ERF4*) (Yang et al., 2005). The expression of *ERF4* induces the expression of genes involved in biosynthesis and degradation of chlorophyll. *ERF4* is also known to be involved in inhibiting plant growth under Fe deficiency and in the control of the expression of Fe uptake transporter genes (Liu et al., 2017).

In this study, we further investigated the role of *HIPP10-HIPP14* in the response of Arabidopsis to Zn deficiency. We found the regulation and activity of these *HIPPs* to be related to plant growth upon Zn and Fe deficiency. The loss of function of either *HIPP10*, *HIPP11*, *HIPP12* or *HIPP14*, promotes tolerance to unfavourable supply of both Zn and Fe, especially to Fe deficiency. CaMV 35S-mediated overexpression of *HIPPs* led to smaller plants, with delayed flowering and increased sensitivity to unfavourable supply of both Zn and Fe, when compared to wild-type plants. We used the *HIPPs* for yeast two-hybrid (Y2H) screens and identified several transcription factors as interacting partners involved in plant growth, plant development, and stress response. Our results thus provide the first functional analyses of this type of clustered *HIPPs*, which appear to be negative regulators of plant growth, especially under Fe and Zn deficiency stress.

## Materials and Methods

### Plant material

The T-DNA insertion mutant lines for *HIPP10* (At5g52720: SALK\_049083C), *HIPP11* (At5g52730: GK-399F11), *HIPP12* (At5g52740: SALK\_012334C) and *HIPP14* (At5g52760: SALK\_013684C) were ordered from NASC ([www.arabidopsis.info/BasicForm](http://www.arabidopsis.info/BasicForm)) (Chapter 4 Table S1). Arabidopsis accession Columbia (Col-0) was used for transformation and as a wild-type control.

### Growth conditions

Prior to germination, seeds were stratified for three days at 4°C in the dark. The plants were grown on rockwool, in a growth chamber set at 70% humidity, a 16/8 h light/dark cycle and 20/18°C day/night temperatures. For agar-plate-based phenotypic screens, plants were grown on vertical agar plates in a climate-controlled growth chamber set at 50% humidity, a 16/8 h light/dark cycle and 22/20°C day/night temperatures. Seeds were surface-sterilized using vapor-phase seed sterilization (Clough and Bent, 1998) and sown on 12-cm square petri dishes containing 1% agar-solidified half-strength MS medium (pH 5.8). The Zn and Fe concentrations in the medium varied from 15  $\mu\text{M}$   $\text{ZnSO}_4$ , and 50  $\mu\text{M}$   $\text{Fe}(\text{Na})_2\text{EDTA}_2$  in control medium to no added Zn for deficiency and 150  $\mu\text{M}$   $\text{ZnSO}_4$  for Zn excess; and no added Fe for deficiency and 250  $\mu\text{M}$   $\text{Fe}(\text{Na})_2\text{EDTA}_2$  for Fe excess. Plants were also grown hydroponically, in a climate-controlled growth chamber set at 70% humidity, a 12/12 h light/dark cycle and 20/15°C day/night temperatures. Vapor-phase-sterilized seeds were sown on 0.55% agar-filled tubes, of

which the bottom was cut off, and grown on a modified half-strength Hoagland's nutrient solution (Schat et al., 1996). During two weeks, plants were grown in a control medium (2  $\mu$ M ZnSO<sub>4</sub>), thereafter, plants continued to grow on the control medium, or they were transferred to the same medium to which no Zn was added, to induce Zn deficiency.

### RNA isolation and qRT-PCR

Total RNA was extracted from shoots (from petri dishes ~10 plants per sample, from hydroponics two fully expanded opposite leaves from 3 plants per sample) using the Direct-zol™ RNA MiniPrep Kit (Zymo Research; [www.zymoresearch.com](http://www.zymoresearch.com)). cDNA was synthesized with iScript cDNA Synthesis Kit (Bio-Rad, [www.bio-rad.com](http://www.bio-rad.com)). Gene expression was quantified by real-time monitored quantitative reverse transcriptase PCR (qRT-PCR) using a SYBR® Green mix (Bio-Rad, [www.bio-rad.com](http://www.bio-rad.com)). Primers for *HIPP* and housekeeping genes are described in **table S1**.

### Plasmid Constructs and Generation of Transgenic Plants

Coding sequences of *HIPP10*, *11*, *12*, *13* and *14* were PCR-amplified from Arabidopsis Col-0 cDNA with the Phusion Flash High-Fidelity PCR Master Mix (Thermo Scientific; [www.thermofisher.com](http://www.thermofisher.com)) using the primers described in **table S2**. Fragments were cloned into the pDONR201 vector and subsequently into the expression vector pFAST-R2 (Shimada et al., 2010) using standard Gateway technology (Invitrogen, [www.thermofisher.com](http://www.thermofisher.com)). Constructs were Sanger-sequenced to confirm correct cloning (GATC-BIOTECH; [www.gatc-biotech.com](http://www.gatc-biotech.com)). Arabidopsis plants were transformed following the method described in Clough and Bent (1998). Transformed seeds were selected based on their red fluorescence (Shimada et al., 2010). Experiments were performed with transgenic T2 (homo- and heterozygous) seeds.

### Yeast two-hybrid

The bait expression vectors pDEST32, containing the coding sequences of either *HIPP10*, *11*, *12*, *13* or *14* were constructed from the pDONR201 clones as described in the previous section. Yeast strain PJ49-4 $\alpha$  was transformed with each bait vector and the Y2H screening assay was performed based on the GAL4 TF reporter system, using the methods described by de Folter and Immink (2011). The transformed PJ49-4 $\alpha$  strain was mated with the PJ49-4A strains of the Arabidopsis TF library (Pruneda-Paz et al., 2014). An autoactivation test was performed on Synthetic Defined -Leucine/-Histidine (SD -LH) medium supplemented with 1, 5, or 10 mM of 3-amino-1,2,4-triazole (3-AT). The library was screened on SD glucose-Leucine/-Tryptophan/Histidine (SD glu-LWH) medium supplemented with 1, 5, and 10 mM 3-AT; and

SD glu-Leucine/-Tryptophan/-Adenine (SD glu-LWA) medium. Positive interactions were scored after 3 to 5 days of growth, with a threshold of at least five colonies per diploid yeast. For all steps, including the library screen, yeast was grown at 30 °C. The network of positive interactions was built with Cytoscape (Shannon et al., 2003).

### Domain search and interaction prediction

*HIPP* DNA sequences were retrieved from The Arabidopsis Information Resource (TAIR) (Berardini et al., 2015) ([www.arabidopsis.org](http://www.arabidopsis.org)). MotifScan (Pagni et al., 2007) was used to search for protein motifs, using all possible motif sources and only taking strong matches into account. C-terminal prenylation motifs were predicted using Prenylation Prediction Suite (PrePS) (Maurer-Stroh and Eisenhaber, 2005). Disordered binding regions were predicted using ANCHOR (Dosztányi et al., 2009). Illustrator for Biological Sciences (IBS) 1.0.2 (Liu et al., 2015) was used to make the visual representation.

### Statistical analysis

Student's t-test, one way ANOVA, two way ANOVA and post hoc test were calculated with Genstat 18th edition (VSN International; [www.vsn.co.uk/software/genstat/](http://www.vsn.co.uk/software/genstat/)).

## Results

### Variation in Arabidopsis root Zn concentration upon Zn deficiency is associated with a cluster of five tandemly arrayed *HIPP* genes

To investigate the genetics underlying the Zn deficiency tolerance natural variation, we performed a GWAS of Zn concentration in a set of natural accessions of Arabidopsis exposed to Zn sufficient and Zn deficient conditions (Chapter 4). One of the loci associated with the Zn concentration in roots upon Zn deficiency, is characterized by the presence of a cluster of eleven tandemly arrayed genes encoding for proteins described as metallochaperone-like (Tehseen et al., 2010). Five genes from this cluster annotated as *HEAVY METAL-ASSOCIATED ISOPRENYLATED PLANT PROTEIN (HIPP)* genes encode a protein with an isoprenylated domain, while the other six genes, annotated as *HEAVY METAL-ASSOCIATED PLANT PROTEIN (HPP)*, lack this domain. The *HIPP* genes (*HIPP10*, *11*, *12*, *13* and *14*) are in linkage disequilibrium (LD;  $r^2 = 0.4$ ) with the Zn-concentration-associated SNPs (**Figure 1**).

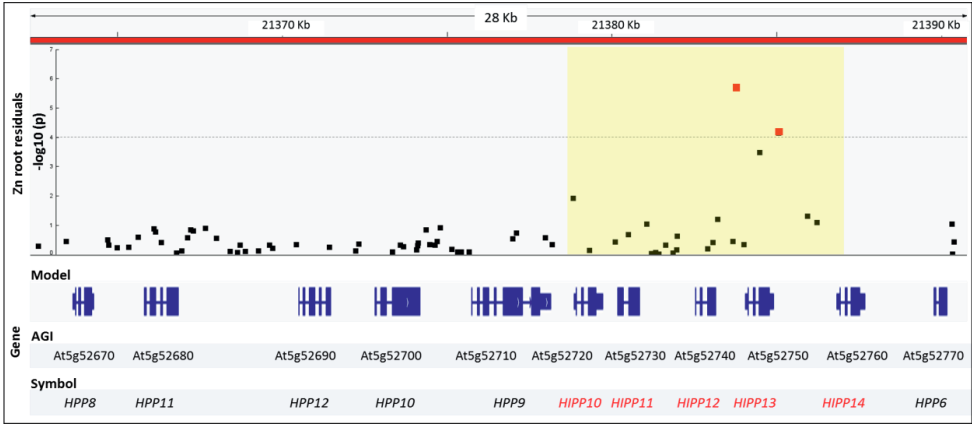


**Figure 1.** Locus associated with the residuals of the root Zn concentration when comparing plants grown under Zn deficiency, with plants grown under Zn sufficiency, as obtained by GWAS (Chapter 4). The “Manhattan” plot of a 28-Kb region on chromosome 5 (scale shown on top) shows two SNPs (red squares) with association  $-\log_{10}(p)$  values above an arbitrary significance threshold set at  $-\log_{10}(p) = 4$  (dashed line), the region in linkage disequilibrium ( $LD \geq 0.4$ ) with the two SNPs is inside the yellow area. The gene structures, with gene locus identifier (AGI: Arabidopsis Genome Initiative) and gene symbol (HPP and HIPP) are shown for all genes in this area (tall blue boxes indicating exons, short blue boxes indicating untranslated transcribed regions, and blue lines indicating introns). HIPP genes found in LD with the associated SNPs are indicated in red.

To validate the role of the five *HIPP* genes in this locus we used *hipp10*, *hipp11*, *hipp12*, and *hipp14* mutants (**Figure 2A**). T-DNA insertion lines *hipp10*, *hipp11*, *hipp12* and *hipp14* were identified ([www.arabidopsis.org](http://www.arabidopsis.org)) ordered, grown and gene expression was determined (**Supplemental Figure S1**). The *hipp10* and *hipp14* lines did not produce any detectable levels of *HIPP10* and *HIPP14* transcripts, respectively. The *hipp11* line does not include the first exon in the transcript but overexpresses the second exon. All three of these lines are considered to be non-functional, null mutants. The *hipp12* line, with a T-DNA insertion in the promoter region, showed similar levels of *HIPP12* transcript as the wild type when plants are grown on Fe-sufficient medium, however, the *HIPP12* expression is significantly lower in *hipp12* mutant compared to wild type on Fe deficient medium. Unfortunately, no suitable T-DNA insertion line for *HIPP13* was available. Previous analysis already showed that the *hipp10*, *hipp11*, and *hipp12* mutants had a higher Zn concentration in shoots and higher shoot biomass than wild-type plants upon Zn deficiency (**Chapter 4; Figure 4, Supplemental Figures S4, and S5**). Moreover, based on transcriptomic data (**Chapter 3**), transcription of *HIPP10*, *HIPP12*, *HIPP13* and *HIPP14* increases upon exposure to Zn or Fe deficiency (**Supplemental Figure S2**). Based

on these results, we decided to further investigate the role of the five *HIPP* genes not just for their involvement in Zn homeostasis, but also in Fe homeostasis.

### **Single HIPPs loss of function promotes growth in stressful Zn and Fe supply conditions**

To investigate the relationship between the *HIPPs* and mineral homeostasis, we evaluated the response of *hipp10*, *hipp11*, *hipp12*, *hipp14* mutants and 35Sp::*HIPP10* plants to Zn and Fe deficiency and excess supply concentrations (**Figure 2**). When *hipp10* and *hipp12* mutants were grown on control medium, almost no discernible differences from the wild type were observed, while the *hipp14* mutant was larger than the wild type. Instead, *hipp11* and the 35Sp::*HIPP10* plants were smaller than the wild type (**Figure 2B and C**), although, in a subsequent experiment, there was no longer a significant difference between *hipp11* and the other *hipp* mutants (**Supplemental Figure S3**). When Zn was left out of the nutrient supply or provided in excess, while keeping Fe supply optimal, wild-type plants showed a decrease in shoot size and slight chlorotic leaves, when compared to plants grown under control conditions. Under Zn deficiency and Zn excess conditions, *hipp10*, *hipp11*, *hipp12* and *hipp14* mutants showed no signs of stress and grew very similar to the plants on control medium, while the 35Sp::*HIPP10* plants showed the same Zn deficiency symptoms as wild-type plants (**Figure 2B and C and Supplemental table S3**). When plants were grown under Fe deficiency, at optimal Zn supply, both wild-type and 35Sp::*HIPP10* plants showed an extreme inhibition of root and shoot growth with chlorotic cotyledons compared to plants grown under control conditions. Again, the *hipp10*, *hipp11*, *hipp12* and *hipp14* mutants showed no symptoms of Fe deficiency. Under Fe excess conditions, all genotypes showed inhibition of root and shoot growth and senescing leaves. The *hipp10* and *hipp14* mutants were the least affected by this treatment. There was a significant effect of genotype, treatment, and genotype x treatment on plant growth in the different Zn and Fe deficiency and excess conditions, as calculated by a two-way ANOVA ( $p < 0.001$  for Zn excess, Fe deficiency, and Fe excess;  $p < 0.05$  for Zn deficiency). Altogether these results indicate that single mutants of either *hipp10*, *hipp11*, *hipp12* or *hipp14* causes an increased tolerance to unfavourable supply of both Zn and Fe, but are not notably affected in growth under control (optimal) nutrient supply.



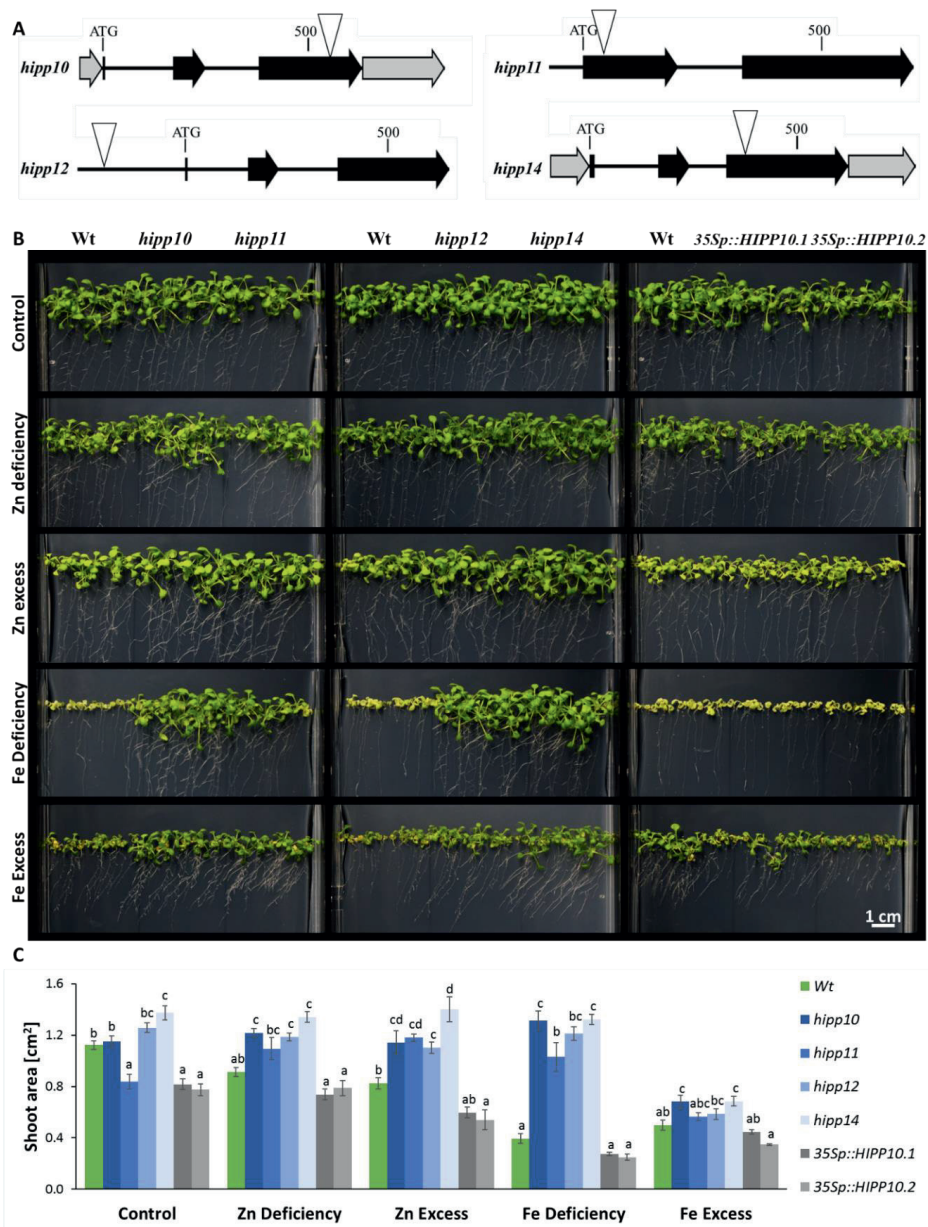


**Figure 2.** HIPPs mutants are tolerant to unfavourable Zn and Fe supply. (A) Schematic drawings of the HIP10, HIP11, HIP12 and HIP14 gene sequences illustrating exons (black arrows), UTRs (grey arrows), untranscribed regions (including introns; black line), and the positions of the T-DNA insertions (white triangle). Distance to the start codon (ATG) is indicated above each gene; (B) Wild-type (Wt), *hipp* mutants and 35Sp::HIP10 plants grown for three weeks on vertical agar plates with control medium (containing 15  $\mu$ M ZnSO<sub>4</sub> and 50  $\mu$ M Fe(Na)<sub>2</sub>EDTA<sub>2</sub>), or medium imposing Zn deficiency (no



added Zn), Zn excess (15  $\mu$ M ZnSO<sub>4</sub>), Fe deficiency (no added Fe) and Fe excess (250  $\mu$ M Fe(Na)<sub>2</sub>EDTA<sub>2</sub>) conditions; (C) Projected shoot area of wild-type (green bars), hipp mutant (blue bars palette), and 35Sp::HIPP10 (grey bars) plants was measured with Image J from plants grown on vertical agar plates (as shown in B). Mean  $\pm$  SE, n = 6 of ~ 4 plants each. Letters above the bars denote statistically different groups, when comparing among genotypes grown in the same treatment, obtained with a Bonferroni post hoc test ( $\alpha=0.05$ ), after a one-way ANOVA ( $p<0.001$ ).

### **HIPP gene expression is induced by Zn and Fe deficiency**

Transcriptome data (**Supplemental figure S2**) showed that the expression of *HIPP12*, *HIPP13* and *HIPP14* was higher in shoots than in roots, while the expression of *HIPP10*, as well as the expression of the closely linked *HPP8*, *HPP9*, *HPP10*, *HPP11* and *HPP12* genes (as shown in figure 1), was highest in roots. Expression of *HPP6* and *HIPP11* could not be detected in this dataset. The transcription of *HIPP12*, *HIPP13* and *HIPP14* was increased in shoots upon exposure to Fe or Zn deficiency, the expression of *HIPP10* was only induced in shoots by Zn deficiency. The expression of *HPP9* was not affected by Fe or Zn variations in the medium, while the expression of *HPP8*, *HPP10*, *HPP11*, *HPP12* and *HIPP10* was slightly induced in roots by Fe deficiency. This initial analysis suggested that while the expression of *HIPP12*, *13* and *14* was very similar, it was different from the expression of *HIPP10*. To confirm the effect of Zn and Fe deficiency on the expression of the *HIPP* genes, wild-type plants, grown on agar plates (control and Fe deficient) or hydroponically (control and Zn deficient), were used for qRT-PCR. This confirmed the higher expression of *HIPP10*, *HIPP11*, *HIPP12*, *HIPP13*, and *HIPP14* in shoots of plants grown on Zn deficient medium, when compared to Zn sufficient medium (**Figure 3A**). Expression of *HIPP10* and *HIPP11* was very low and was only detected upon Zn deficiency. When plants were grown on Fe deficient medium, only the expression of *HIPP10*, *HIPP12*, *HIPP13* and *HIPP14* was higher than under control conditions (**Figure 3B**). Differences in expression of *HIPP11* were not significant, while the expression of *HIPP10* and *HIPP12* was mainly detected upon Fe deficiency. There are differences in *HIPP* expression between the hydroponically grown plants and the agar-plate plants, the latter were generally younger than the former.

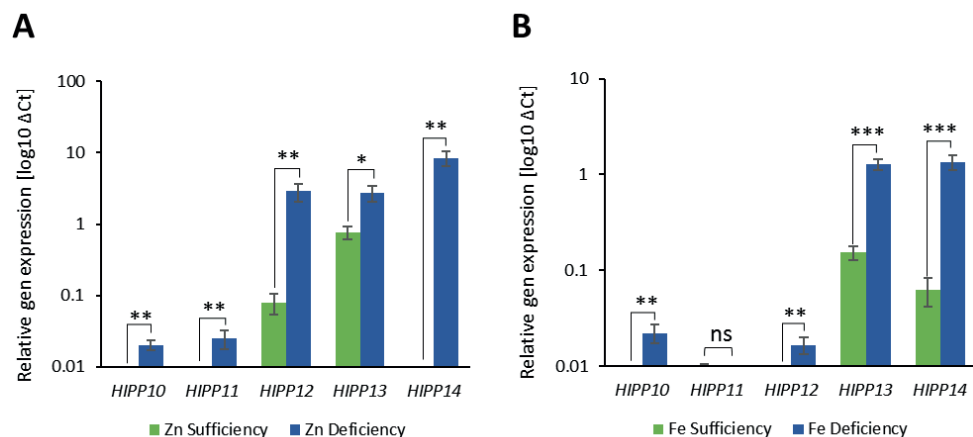


**Figure 3.** Expression of *HIPP10*, *HIPP11*, *HIPP12*, *HIPP13* and *HIPP14* genes is induced by Zn and Fe deficiency. *HIPP* transcription levels relative to the transcription of two stably transcribed reference genes (*At5g25760* and *At2g28390*) are presented of (A) plants grown hydroponically under Zn sufficient (2  $\mu$ M  $\text{ZnSO}_4$ ; green bars) or Zn-deficient (no added Zn; blue bars) conditions; and of (B) plants grown on vertical agar plates under Fe sufficient (50  $\mu$ M  $\text{Fe}(\text{Na})_2\text{EDTA}_2$ ; green bars) or Fe deficient (no added Fe; blue bars) medium. Mean  $\pm$  SE,  $n = 3$  replicates of 3 pooled plants each, for the Zn treatment, and  $n = 6$  replicates of ~10 pooled plants each, for the Fe treatment. Statistical significance was determined by Student's *t* test (ns  $p > 0.05$ , \*  $p < 0.05$ , \*\*  $p < 0.01$ , and \*\*\*  $P < 0.001$ ).

### Disruption of individual *HIPP* genes affects the expression of several other *HIPP* genes under Fe deficiency

To further investigate the function of the five *HIPPs*, we focused our research on the Fe deficiency, rather than the Zn deficiency response, due to the high tolerance to Fe deficiency of the *hipp* mutants (**Figure 2B and C**). We were most interested to understand why every single *hipp* mutant was similarly tolerant to Fe deficiency. Therefore, we determined the expression of the *HIPP10*, *HIPP11*, *HIPP12*, *HIPP13*, and *HIPP14* genes in the four *hipp* mutants (*hipp10*, *hipp11*, *hipp12*, and *hipp14*) grown on Fe deficient medium. The expression of all genes but *HIPP11*, was induced by Fe deficiency in the wild type (**Figure 3B**). Under control conditions, the *HIPP* genes were expressed at comparable levels in the mutants as in the wild type (**Figure 4**), except for the genes which were mutated in the respective line (**Supplemental Figure S1**). There were a few additional exceptions, *HIPP10* and *HIPP12* were much higher expressed in the *hipp11* mutant than in the wild type, and *HIPP13* was lower expressed in the *hipp10* mutant.

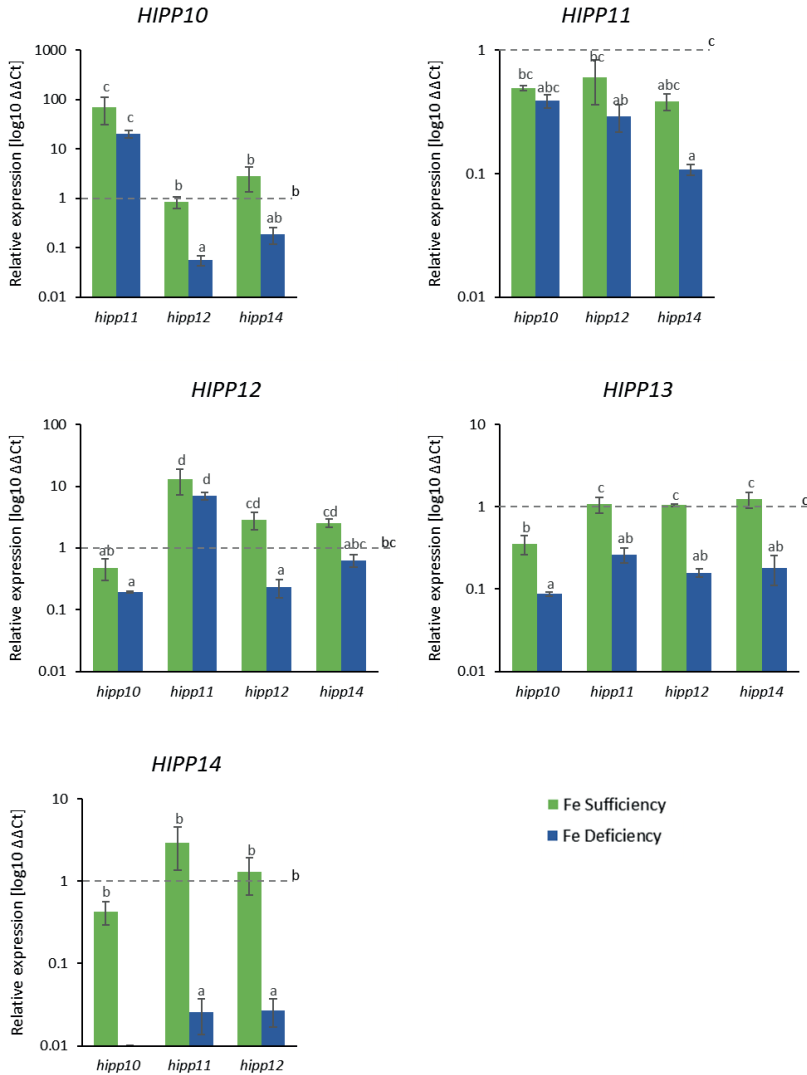


**Figure 4:** Relative expression of HIPP10, HIPP11, HIPP12, HIPP13 and HIPP14 in shoots of *hipp* mutants grown in control conditions (Fe sufficiency) and under Fe deficiency. Transcript levels were normalized relative to reference genes *At5g25760* and *At2g28390* and to the expression in wild-type plants. Plants were grown on agar vertical plates under control conditions (medium containing 50  $\mu$ M  $\text{Fe}(\text{Na})_2\text{EDTA}_2$ ; green bars) or Fe deficiency (the same medium, without Fe added; blue bars). Mean  $\pm$  SE,  $n = 3$  replicates of  $\sim 10$  pooled plants each. Letters above the bars denote statistically different groups, obtained with a Bonferroni post hoc test ( $\alpha=0.05$ ), after a one-way ANOVA ( $p<0.001$ ). The dashed line indicates the mean relative expression in wild type, and the letter at the end of the line indicates to which statistical group the wild type belongs.

Under Fe deficiency, most *HIPP* genes are lower expressed in the *hipp* mutants compared to wild type, again with some exceptions, and often also lower expressed than under control conditions. *HIPP10* and *HIPP12* are again higher expressed in *hipp11* under Fe deficiency, and the expression of *HIPP11* was not significantly different between *hipp10* and wild type, nor was the expression of *HIPP12* different between *hipp14* and wild type. Taken together, disruption of individual *HIPP* genes did not only affect the expression of the mutated gene, but also that of several of the other *HIPP* genes, with the most prominent effects on expression of *HIPP13* and *HIPP14*. This suggests that expression of *HIPP* genes may depend on *HIPP* interactions with transcription factors, which are different under Fe deficiency when compared to control conditions.

### The *HIPP* protein structures favour protein-protein interactions

To infer a putative function of the HPPs and HIPPs encoded by the eleven genes in the cluster protein structures, active sites and biochemical functions were determined. Tehseen et al., (2010) predicted that HIPPs and HPPs contain HMA domain, using MotifScan (Pagni et al., 2007) we confirmed that five HIPPs and two HPPs are predicted to contain one HMA domain, while the remaining four HIPPs were predicted to have two HMA domains (**Supplemental Figure S4**). However, all HMA domains predicted in these proteins lack the M/LXCXXC core sequence of other known HMA domains (Tehseen et al., 2010). Therefore, rather than calling them HMA domains, we prefer to refer to them as HMA-like (HMAL) domains. Using Prenylation Prediction Suite (PrePS) (Maurer-Stroh and Eisenhaber, 2005) the C-terminal end of four HIPPs (*HIPP10*, *11*, *13* and *14*) was predicted to be the target of isoprenylation by farnesyltransferase (FT) or geranylgeranyltransferase 1 (GGT1), while *HIPP12* was predicted to only be a target of FT. An isoprenylated C-terminus can mediate the attachment to other proteins or membranes (Konstantinopoulos et al., 2007). Using ANCHOR (Dosztányi et al., 2009), multiple disordered regions were detected in *HPP9*, *HPP10*, *HIPP10*, *HIPP11*, *HIPP13* and *HIPP14*. Only *HIPP12* was not predicted to contain disordered regions. Disordered regions also contribute to protein-protein interactions due to the flexibility they provide to the protein structure (van der Lee et al., 2014).

### HIPPs interact with nuclear-localized proteins

Given the potential of HIPPs to suppress plant growth under Fe deficiency, to affect the expression of each other, and of the HIPP protein to favour protein-protein interactions, we performed a dedicated Y2H analysis to identify HIPP-interacting transcription factors. This revealed several of such potentially interacting transcription factors (**Table 1**). Several of these transcription factors were found to interact with more than one HIPP (**Table1 and Supplemental Figure S5**).

**Table 1.** Transcription factors that interact with HIPPs in a yeast-two-hybrid assay. Positive interactions were scored after 3 to 5 days of growth with a threshold of at least 5 colonies per diploid yeast on selective media.

HIPP10	HIPP11	HIPP12	HIPP13	HIPP14	Locus identifier	Symbol	Description
yes					At1g01010	NAC001	
yes					At1g32870	NAC13	Induced by high levels of B
yes					At1g34180	NAC016	Induced by salt and oxidative stress
yes					At2g27300	NTL8	Induced by salt stress
yes					At4g01550	NAC69	Mutants are resistance to salt
yes					At4g35580	NTL9	Induced by osmotic stress
yes					At5g22290	NAC89	Promotes cell death
yes			yes	yes	At1g15720	TRFL5	
yes			yes	yes	At1g54060	ASIL1	Repressing seed maturation
yes			yes	yes	At3g21270	DOF2	
	yes				At1g61660	BHLH112	Induced by salinity and drought
		yes			At2g02540	HB21/ZFHD4	
		yes			At2g20350	ERF120	Ethylene response factor
		yes			At3g25790	HHO	Involved in N and P signaling
		yes			At3g49690	MYB84/RAX3	Regulates meristem formation
		yes	yes		At5g41410	BEL1	Involved in ovule morphogenesis
		yes		yes	At2g20570	GLK1	Regulates photosynthesis
		yes		yes	At5g44190	GLK2	Regulates photosynthesis
		yes		yes	At5g60142		
			yes		At3g04420	NAC48	
			yes	yes	At2g28510	DOF2.1	
			yes	yes	At3g11100	ENAP1/VFP3	Involved in ethylene signaling
			yes	yes	At3g04930		
			yes	yes	At3g54390		
			yes	yes	At3g58630		
			yes	yes	At5g05550	ENAP2/VFP5	Interacts with EIN2
				yes	At1g59810	AGL50	
				yes	At3g45610	DOF6	Negative regulator of germination
				yes	At4g13480	MYB79	

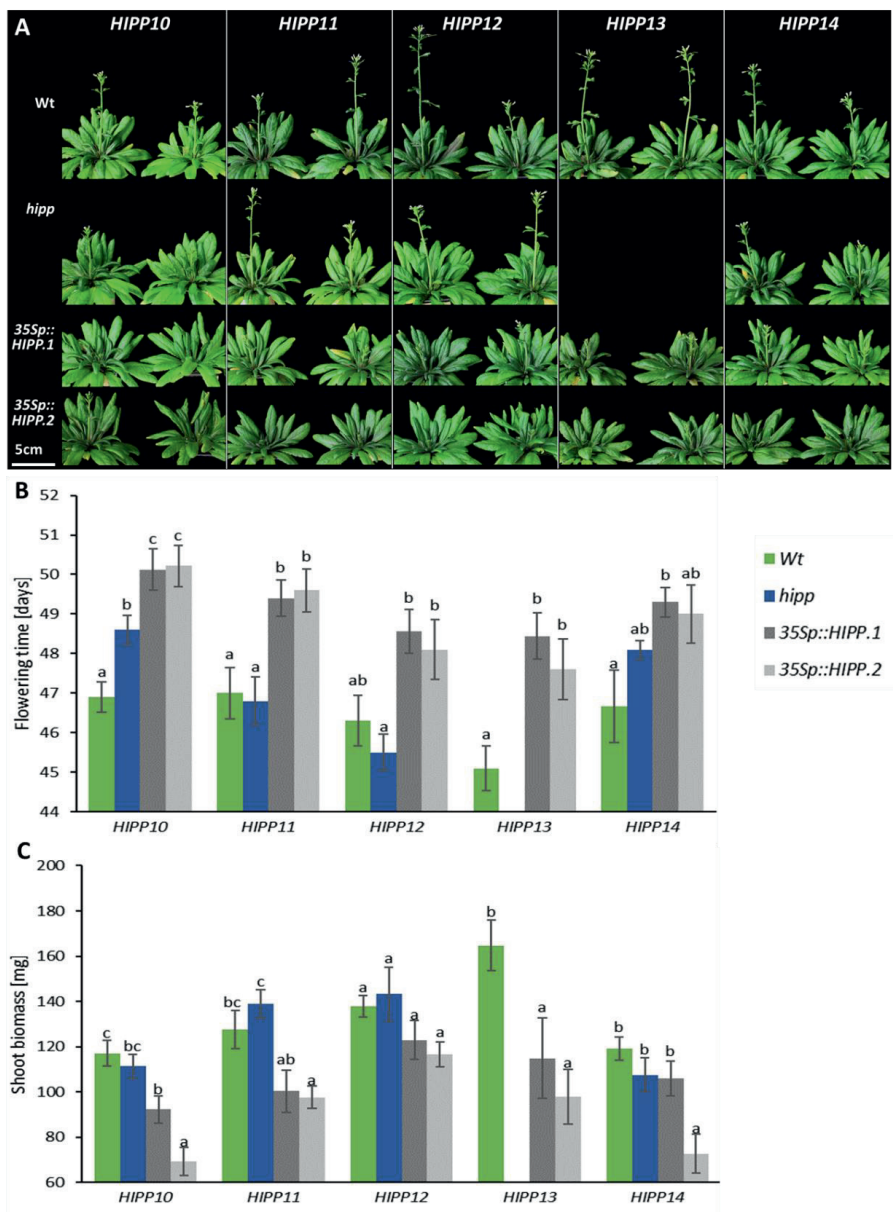


**Figure 5.** Phenotypes of *hipp* mutants and 35S-mediated HIPP overexpression lines grown until flowering upon sufficient Fe supply. (A) Plants grown for 48 days in a climate controlled greenhouse set at a 12h light/dark regime. (B) Flowering time (C) biomass of wild type (Wt, green bars), *hipp* mutant (blue bars), and 35Sp lines (35Sp::HIPP.1 or .2; dark and light grey bars) plants. Mean  $\pm$  SE,  $n = 5$  replicate plants per genotype. Letters above bars denote statistically different groups, comparing Wt, mutant and two 35Sp genotypes for each HIPP gene, grown together, as obtained with a Bonferroni post hoc test ( $\alpha=0.05$ ), after a one-way ANOVA ( $p<0.001$ ).

### **HIPPs affects flowering time**

Since the *HIPP* genes appear to act as negative regulators of plant growth in response to Fe and, to a lesser extent, Zn deficiency, we grew the *hipp* mutants and 35Sp::*HIPP* lines under Fe sufficient and mild Fe deficient conditions in the greenhouse to investigate any possible negative fitness trade-offs, especially under Fe deficiency. Next to the previously used 35Sp::*HIPP10* lines, also 35Sp lines of *HIPP11*, *HIPP12*, *HIPP13* and *HIPP14* were generated and grown. All genotypes growing on Fe deficient medium developed chlorotic leaves, however, no genotype by treatment interaction effect was found for shoot biomass or flowering time. Seven of the ten 35Sp::*HIPPs* lines showed a consistent delay in flowering, and six on the ten 35Sp::*HIPPs* lines showed less biomass compared to the wild type and *hipp* mutant lines, independent of the treatment (**Figure 5**).

## **Discussion**

Plasticity is the physiological or morphological change of an organism in response to environmental clues (Schlichting, 1986). Stress conditions elicit a wide variety of plant responses, ranging from differences in gene expression to differences in growth and morphology. Environmental stress imposed on plants forces them to find a balance between growth and survival, which prompts some species or genotypes to invest in reproduction and quickly finish their life cycle, and others to cease growth and promote survival, often depending on the type and severity of the stress. Stress responses need to be tightly regulated due to antagonistic pleiotropic effects (Des Marais and Juenger, 2010; Todesco et al., 2010; Huot et al., 2014).

### **Loss of function of each one of five HIPPs confers tolerance to unfavourable Fe and Zn supply**

The five *HIPP* genes studied here, were already described in Chapter 4, to reside at a quantitative locus on chromosome 5, associated with fluctuations in the root Zn concentration in response to Zn deficiency. The *hipp10*, *hipp11* and *hipp12* T-DNA insertion mutants were found to be more tolerant to Zn deficiency, in terms of biomass and higher Zn concentration in shoots. Here, we showed that single *hipp10*, *hipp11*, *hipp12* and *hipp14* mutants are not only more tolerant than wild types to Zn deficiency, but also to Zn excess, Fe excess and especially to Fe deficiency. The *hipp9* mutant also showed tolerance to excess of heavy metals (Sanz-

Fernández et al., 2017), the *HPP9* is part of the cluster of 11 tandemly arrayed HPP/HIPP genes located in chromosome 5.

The homeostasis of both Zn and Fe are linked. Zn deficiency causes Fe concentration increase in shoots and decrease in roots (Chapter 4) and the Zn excess induces the expression Fe **deficiency-responsive** genes (van de Mortel et al., 2006) for instance. The most outstanding difference between the *hipps* mutants and wild type were detected upon Fe deficiency. The *hipp10*, *hipp11*, *hipp12*, and *hipp14* mutant plants did not show any Fe deficiency symptom when growing on Fe deficient medium, plants were big and green as on Fe sufficient medium, while wild-type and 35Sp::*HIPP10* plants grown on Fe deficient medium showed severe leaf chlorosis and inhibition of root and shoot growth, as is known to be the normal response to Fe deficiency (Varotto et al., 2002; Li et al., 2016). The decrease in growth due to stress is a common plant response to maximize survival, it is carried out by proteins involved in stress-induced growth modulation (Wolters and Jürgens, 2009). For instance, DELLA proteins integrate environmental and phytohormone signals, and repress plant growth under adverse conditions as salt stress (Achard et al., 2006).

An unexpected finding of this study was that single *hipp* mutants showed similar levels of tolerance to Zn deficiency, Zn excess and Fe deficiency. For instance, neither the single nor the double mutants for *HIPP20*, *HIPP21*, and *HIPP22* exhibited any aberrant phenotype under any of the abiotic stress conditions tested, while only the *hipp20/21/22* triple mutant was Cd sensitive (Tehseen et al., 2010). This suggests that despite their structural similarity, the *HIPP10*, *HIPP11*, *HIPP12*, and *HIPP14* proteins are not functionally redundant, but instead appear to may have complementary functions in the Fe/Zn excess/deficiency stress response.

### **HIPPs gene expression is determined by stress and auto-regulation**

Changes in gene expression are crucial for the organism adaptation to maximize survival under stress conditions (de Nadal et al., 2011). In eukaryote genomes, genes with similar expression may be clustered (Hurst et al., 2004). Here, we have shown that plants encountering limited Zn or Fe in their growth medium increase the expression of *HIPP10*, *HIPP11*, *HIPP12*, *HIPP13*, and *HIPP14*. Changes in gene expression in response to environmental clues are a common characteristic among Arabidopsis *HIPP* genes. Abiotic stresses caused by drought, salt, cold, exogenous ABA, and/or heavy metal affects the expression *HIPP3* (Zschiesche et al., 2015), *HPP9* (Sanz-Fernández et al., 2017), *HIPP22*, *HIPP23*, *HIPP24*, *HIPP25*, *HIPP26*, *HIPP27*



and *HIPP31* (Barth et al., 2009). The response deficiency of Zn or Fe can now be added to the list of environmental stresses that induce HIPPs expression.

The lower expression of the *HIPP10*, *HIPP11*, *HIPP12*, *HIPP13* and *HIPP14* genes in the *hipp10*, *hipp11*, *hipp12*, and *hipp14* mutants, in comparison to the wild type, particularly under Fe deficiency, suggests that these HIPP proteins, directly or indirectly, regulate the expression of the other genes in the *HIPP* gene cluster. This regulation is normally positive, meaning that HIPP expression enhances the expression of its neighbors, upon Fe deficiency, in what may be a positive feedback loop. Transcription regulatory feedback loops contribute to the efficiency of a transcriptional regulatory system, which may consist of a single component or may include several components and interactions among them (Mitrophanov and Groisman, 2008). Such regulation is specially necessary to balance trade-offs between stress response and fitness (Kasuga et al., 1999; Miller et al., 2015). Genes involved in similar processes can be controlled in an auto-regulatory loop. Proteins which interact with each other are known to be co-ordinately regulated in a positive feedback loop (Gómez-Mena et al., 2005). This also seems to be the case of the *HIPP10-14* gene cluster. The result of their action is the high tolerance to adverse Zn and Fe nutrient by the loss of only one of them. We have not investigated the loss of several of these, which is not trivial to do, as it will require multiple CRISPR-Cas9-mediated mutations. Due to their close physical linkage, the regular way to generate double, triple or higher order combined mutations, by crossing single mutants, will not be practically feasible.

### **HIPPs domains promote interactions**

HIPPs are classified as metallochaperone-like proteins due to their predicted HMA domain. The functional core motif of the HMA domain is characterized by CysXXCys or CysCysXXGlu (Tehseen et al., 2010). Some HIPPs containing this motif and experimentally confirmed to bind metals are HIPP26, which binds Pb, Cd and Cu (Gao et al., 2009); HIPP7, which binds Cu, Ni, or Zn (Dykema et al., 1999); and HIPP3, which binds Zn, Ni, Cu, and Fe (Achard et al., 2006). The HMA domain could be an allosteric switch that promotes changes in protein structure, as a response to stress, related with cellular location or binding affinity with different interactors. The resulting allosteric change upon binding a metal ion can affect the interaction with other proteins, such as transcription factors, and thus regulate gene expression (Guerra and Giedroc, 2012). For the mentioned HIPPs containing a functional HMA domain, enhanced or reduced binding to metals may be the way these HIPPs exert their function in response to heavy metal stress.

However, out of 67 metallochaperone-like proteins in Arabidopsis, 45 HIPPs and 22 HPPs, 23 lack the functional core motif of the HMA domain (Tehseen et al., 2010). Among these are the six HPP and five HIPP proteins encoded by the *HPP/HIPP* gene cluster on chromosome 5 (Tehseen et al., 2010). Therefore, it is not clear if the predicted HMA-like (HMAL) domain of these eleven proteins is able to bind metals. We have not examined this any further, as it is not at all trivial, but considering their role in Zn or Fe deficiency response, it will be important for further understanding of their function and mode of action, to verify at least their ability to bind Zn or Fe. It could well be of course that this HMAL domain has taken a different evolutionary trajectory and acquired a new function. Significant changes in domain architecture are frequently observed upon tandem gene duplication (Buljan and Bateman, 2009; Jin et al., 2009), which is likely to be a reason of their remarkable clustering, as is evident from their phylogenetic relationship (Tehseen et al., 2010).

All HIPP sequences contain a C-terminal tetrapeptide recognition motif called the CAAX box. This box serves as a substrate for isoprenylation (Tehseen et al., 2010), which is the attachment of an isoprenoid lipid to the C-terminus (Scott Reid et al., 2004; Konstantinopoulos et al., 2007). After isoprenylation, the C-terminus becomes a hydrophobic domain, which mediates the attachment to other proteins or membranes (Konstantinopoulos et al., 2007). Isoprenylation is most prominent for proteins involved in signal transduction pathways (Roskoski, 2003). For instance, the isoprenylated C-terminus of HIP26 interacts with ACYL-COA-BINDING PROTEIN 2 (ACBP2), which is associated with post-stress membrane repair and itself interacts with an ethylene-responsive element-binding protein (EBP), mediating stress response (Li and Chye, 2004; Gao et al., 2009), through interaction with DELLA proteins (la Rosa et al., 2014).

Additionally, several intrinsically disordered regions (IDRs) were predicted in the HIP10-14 sequences. These regions lack the hydrophobic core of structured regions and favour protein-protein interactions, as flexible linkers between structured regions, specially required for the assembly of multiprotein complexes. Proteins with IDRs are common in protein interaction networks, acting as interaction hubs (Dunker et al., 2001; Fong et al., 2009; van der Lee et al., 2014). The plasticity that IDRs provide to proteins allows them to play key roles in cell signalling and regulation mechanisms (Wright and Dyson, 1999; Uversky et al., 2000; Iakoucheva et al., 2002; Galea et al., 2008; Van Roey et al., 2012). In addition, IDRs at the C-terminus are associated with transcription factor repressors, while internal or N-terminus IDR are associated with transcription factor activators (van der Lee et al., 2014). HIP10, 11, 13 and

14 contain predicted internal and C-terminus IDRs, thus a hypothetical activation or repression activity is not clear. The isoprenylation motif and the IDRs suggest the ability of HIP10-14 to interact with other proteins with the potential to link different pathways.

### **The HIP10-14 proteins interact with multiple nuclear-localized proteins**

Protein interacting partners provide clues about the pathways in which unknown proteins are involved. All proteins encoded by the *HIP10-14* cluster showed interaction with several transcription factors. Therefore, HIPs seem to be highly connected proteins which could work as hubs of protein complexes to interconnect pathways, as is observed for APETALA1 (AP1) and FRUITFULL (FUL) involved in floral meristem identity and floral organ determination (de Folter et al., 2005).

HIP10 showed interaction with seven NAM, ATAF1/2, and CUC2 (NAC) proteins, which have regulatory functions in plant growth, development, and stress responses (Li et al., 2010; Nakashima et al., 2012). Among them NAC13 is induced by high B concentrations (Kasajima and Fujiwara, 2007), and is involved in the cross-talk between ROS signaling (De Clercq et al., 2013), hormone signaling and plant development (O'Shea et al., 2015). Salt and oxidative stress promote *NAC16* gene expression. The *nac16* mutant stays green under salt and oxidative stress, while overexpression *NAC16* senesced rapidly (Kim et al., 2013). NAC16 induces the transcription of STAYGREEN1 (SGR1), which promotes chlorophyll degradation during abiotic stress or plant senescence (Sakuraba et al., 2016). NAC69 integrates salt and auxin signals during germination and *nac69* mutants are resistant to salt stress (He et al., 2015). NAC89 positively regulates programmed cell death, while it negatively regulates chloroplast antioxidant defence system (Klein et al., 2012). *NTM1-Like 8* (*NTL8*) is induced by salinity, the *ntl8* mutant seeds are resistant to high salinity during germination (Kim et al., 2008) and the overexpression of *NTL8* shows reduced growth and delayed flowering (Kim et al., 2007). *NTL9* is induced by osmotic stress and mediates osmotic stress signaling during senescence (Kim et al., 2007). The potential interactors of HIP10 have as a common pattern to be induced by stress conditions such as high concentration of boron, salinity and osmotic stress, their overexpression promotes senescence or reduces growth and their loss of function promotes tolerance to the stress that induces their expression. The *HIP10-14* have a similar behaviour, as these interactors, being induced by the stress conditions of Zn and Fe deficiency, their overexpression reduces growth, and their loss of function promotes tolerance to Zn and Fe deficiency. The

difference between the HIPP10 interactors and HIPP10-14 is the stress factor studied that triggers the response.

For HIPP11, we found one interaction with bHLH112, a transcription factor induced by salinity, drought, and ABA. It positively regulates salt and drought tolerance (Liu et al., 2015). Among the HIPP12 interactors, *ZFHD4* is highly expressed in floral tissues (Tan and Irish, 2006) and also interacts with HIPP26 (Barth et al., 2009). HHO1 represses primary roots growth under P deficiency, its mutants are insensitive to P deficiency (Medici et al., 2015). RAX3 regulates axillary meristem initiation (Müller et al., 2006). HIPP12 and HIPP14 interact with GLK1 and GLK2, which coordinate the expression of photosynthetic genes to regulate chloroplast development and optimize photosynthesis (Fitter et al., 2002; Waters et al., 2009; Murmu et al., 2014). Some proteins that showed interaction with more than one HIPP of the cluster also interact with other HIPPs. Among them are ASIL1 which also interacts with HIPP3 (Zschiesche et al., 2015), HIPP21 and HIPP27 (Provart et al., 2016); DOF2 also interacts with HIPP26 (Provart et al., 2016); and AT3G54390 interacts with HIPP20 as well (Provart et al., 2016).

HIPP13 and HIPP14 have six common interactors, among them, *ENAP1* inhibits the transcription of ethylene-repressed genes in the presence of ethylene. Seedlings overexpressing of *ENAP1* are hypertensive to ethylene and smaller than wild type, while the down-regulation of *ENAP1* makes plants less sensitive to the ethylene with even bigger size than wild type (Zhang et al., 2016; Zhang et al., 2017; Zhang et al., 2018). Ethylene is produced by Fe deficient plants and regulates the expression of several Fe acquisition genes (Lucena et al., 2006; García et al., 2010; Liu et al., 2017).

The hypothesis of complementary functions among HIPP10-14 is supported by the presence of common interactors among them (**Supplemental Figure S5**). The functions of the HIPPs interactors reinforce the responses observed for the *HIPP10-14* genes in relation to induction by stress, stress tolerance and late flowering and give hints to study the relation of ethylene and salt with the *HIPPs* cluster. In addition, all the interactions detected in a Y2H assay should be confirmed by *in vivo* FRET–FLIM (Long et al., 2017) assays.

### Flowering time

The overexpression of HIPP10-14 resulted in a delay of flowering (**Figure 5**). In addition, the overexpression of the HIPPs interactors NTL8, NAC89, and ARABIDOPSIS 6B-

INTERACTING PROTEIN 1-LIKE 1 (ASIL1) also showed delayed flowering (Kim et al., 2007; Li et al., 2010; Park et al., 2011). Furthermore, HIPPI2 and HIPPI3 interact with BEL1, which is important to maintain the indeterminacy of the inflorescence meristems (Bellaoui et al., 2001). Thus the action of the HIPPI0-14 proteins may also involve the indirect control of flowering time, upon Fe and Zn deficiency, as part of the plant survival mechanism. Flowering is known to be regulated by internal and environmental stimuli to ensure plant reproduction under the most favourable conditions. Biotic and abiotic stress factors play a role in the transition to flowering (Riboni et al., 2014; Kazan and Lyons, 2016). For instance, drought stress accelerates the flowering process (Franks, 2011; Schmalenbach et al., 2014), while salt stress delays flowering time (Kim et al., 2013). Nutrient availability, including Zn and Fe supply, also regulates the onset of flowering (Sivitz et al., 2012; Przedpelska-Wasowicz and Wasowicz, 2013; Lin and Tsay, 2017; Chen and Ludewig, 2018; Weber and Burrow, 2018).

### Conclusions

Our findings reveal that HIPPIs are part of the Zn and Fe deficiency response. The mutation of *HIPPI0*, *11*, *12* or *14* generates a similar level of tolerance to Zn and Fe deficiency and their expression is induced by Zn and Fe deficiency. Moreover, the constitutive expression of these genes represses growth and delays flowering time. It places the *HIPPI0-14* genes in pathways connecting Zn/Fe deficiency stress with plant growth and development. In these pathways, HIPPIs can interact directly among them or through common interaction partners. Further research is required to understand the role of HIPPI0-14 in mediating stress-induced growth inhibition for stress tolerance. These genes can be useful candidates to engineer stress tolerant crops, considering that we did not find any trade-offs in the *hippi*s mutants.

### Acknowledgements

We thank Prof. Richard Immink and Marco Busscher (Wageningen University) for facilitating the Y2H cDNA library and the technical support in the Y2H assay respectively. This work was supported by the Ecuadorian government through SENESCYT (Secretaría de Educación Superior, Ciencia, Tecnología e Innovación) and Universidad de las Fuerzas Armadas-ESPE.

## Supplemental information

**Table S1.** Sequences of primers used for quantification of gene expression by qRT-PCR

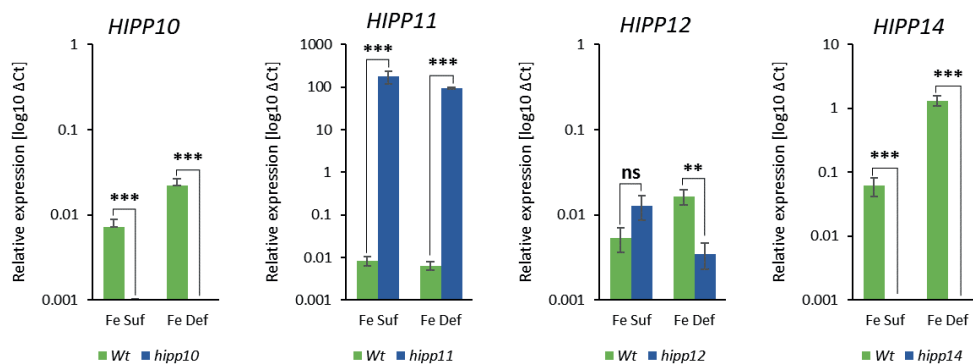
Locus identifier	Gene	Primer	5'→3' sequence
At5g52720	<i>HIPP10</i>	Forward	GCAGGAGACGGTTGTATTCG
At5g52720	<i>HIPP10</i>	Reverse	CCTCTTTCCTTCACGTCTATCAC
At5g52730	<i>HIPP11</i>	Forward	GTTACAAGGCGTGAACCCAA
At5g52730	<i>HIPP11</i>	Reverse	GAGGTATGGACGGACGAGAG
At5g52740	<i>HIPP12</i>	Forward	TCGGTGGAGGTGAAAGATGG
At5g52740	<i>HIPP12</i>	Reverse	TCGTTTCAGGCTTCTTCGGA
At5g52750	<i>HIPP13</i>	Forward	TGAACCAGAGAAACCGGCTC
At5g52750	<i>HIPP13</i>	Reverse	GGCAGGATTGTATTGGTAAGGG
At5g52760	<i>HIPP14</i>	Forward	TGTACCAGCTGTCGTGATGA
At5g52760	<i>HIPP14</i>	Reverse	GGTACGCGTAGTTCATCGGA
At2g28390	<i>SAND</i>	Forward	GTTGGGTACACCAGATTTTG
At2g28390	<i>SAND</i>	Reverse	GCTCCTTGCAAGAACACTTCA
At5g25760	<i>PEX4</i>	Forward	TCCTGAGCCGGACAGTCCTC
At5g25760	<i>PEX4</i>	Reverse	CATAGCGGCGAGGCGTGTAT

**Table S2.** Sequences of primers used to clone *HIPP* gene coding sequences from cDNA. Forward primers include the *attB1* linker (GGGGACAAGTTTGTACAAAAAGCAGGCTTA) and reverse primers include the *attB2* linker (GGGGACCACTTTGTACAAGAAAGCTGGGTA) at their 5' ends. The ATG start codons are underlined.

Locus identifier	Gene	Primer	5'→3' sequence
At5g52720	<i>HIPP10</i>	Forward	<u>ATG</u> CAGGAGACGGTTGTATTC
At5g52720	<i>HIPP10</i>	Reverse	TCACAGGATGATACACTCATCCG
At5g52730	<i>HIPP11</i>	Forward	CGG <u>ATG</u> TATATAAAATACACATGACAGT
At5g52730	<i>HIPP11</i>	Reverse	TTACATGATGATACAACCATCCG
At5g52740	<i>HIPP12</i>	Forward	<u>ATG</u> CAGGTAGTTGTAAGAAATTAGAT
At5g52740	<i>HIPP12</i>	Reverse	TCAAGAGGTGACGCAAGC
At5g52750	<i>HIPP13</i>	Forward	<u>ATG</u> CCTCCAATGAAAGCTGT
At5g52750	<i>HIPP13</i>	Reverse	TCACATAATCACACAATTTGATTCTG
At5g52760	<i>HIPP14</i>	Forward	<u>ATG</u> ACCGCAAAGAACGCT
At5g52760	<i>HIPP14</i>	Reverse	TCACATAATCACACAATTTGGTTC

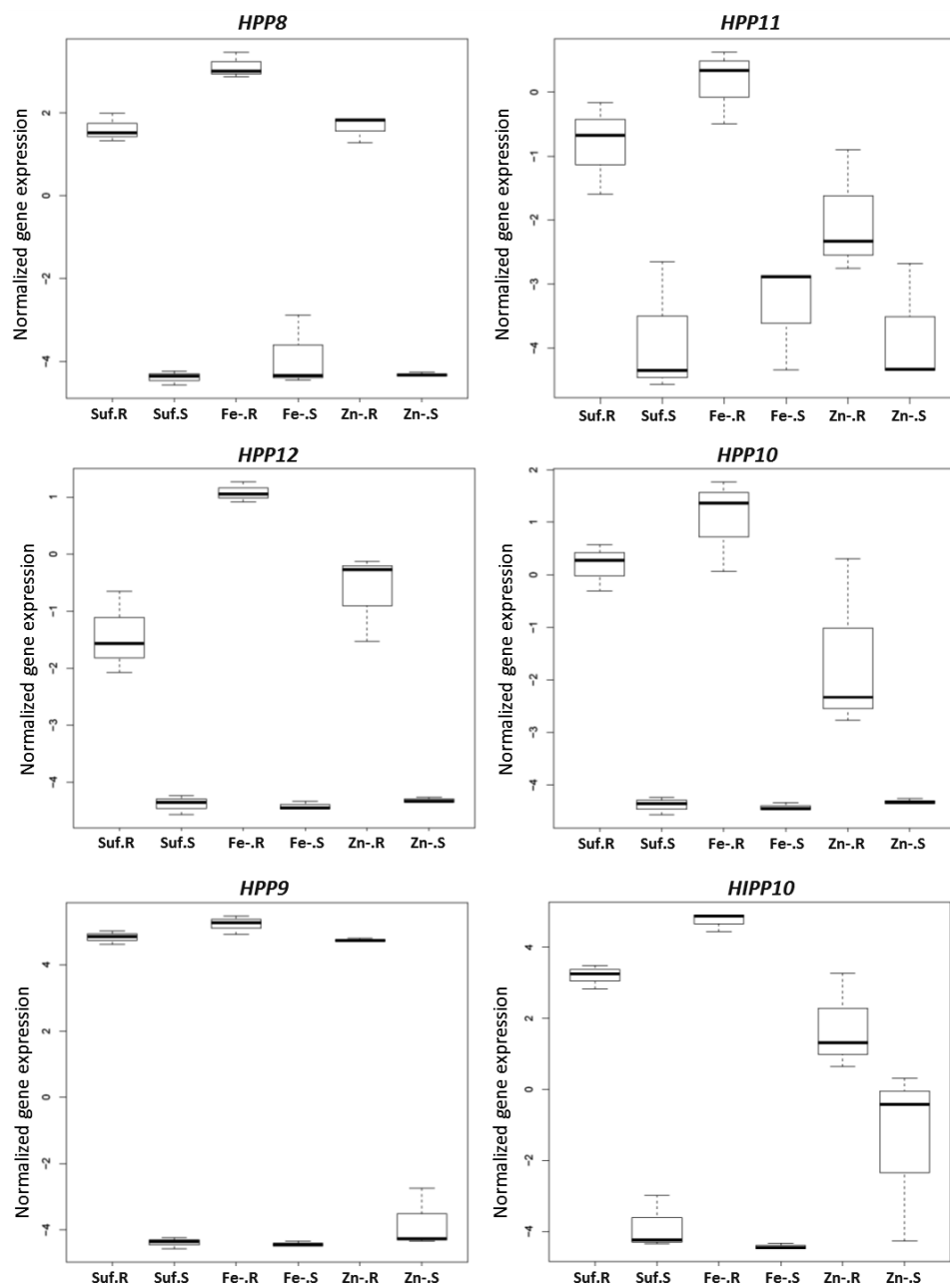
**Table S3.** One-way ANOVA of projected leaf area of wild-type, *hipp* mutants and 35Sp::*HIPP10* plants, grown under Zn deficient, Zn excess, Fe deficient and Fe excess conditions, and compared to control conditions. Significant effects are indicated in bold.

Treatment	Genotype	Variance ratio	F probability
Zn deficiency	Wild type	17.93	<.001
Zn deficiency	<i>hipp10</i>	1.39	0.266
Zn deficiency	<i>hipp11</i>	6.11	<b>0.033</b>
Zn deficiency	<i>hipp12</i>	2.12	0.176
Zn deficiency	<i>hipp14</i>	0.21	0.655
Zn deficiency	35Sp:: <i>hipp10.1</i>	0.03	0.865
Zn deficiency	35Sp:: <i>hipp10.2</i>	1.9	0.198
Zn excess	Wild type	29.28	<.001
Zn excess	<i>hipp10</i>	0.01	0.927
Zn excess	<i>hipp11</i>	27.63	<.001
Zn excess	<i>hipp12</i>	6.93	<b>0.025</b>
Zn excess	<i>hipp14</i>	0.06	0.817
Zn excess	35Sp:: <i>hipp10.1</i>	6.76	<b>0.027</b>
Zn excess	35Sp:: <i>hipp10.2</i>	14.88	<b>0.003</b>
Fe deficiency	Wild type	134.53	<.001
Fe deficiency	<i>hipp10</i>	3.15	0.106
Fe deficiency	<i>hipp11</i>	1.63	0.23
Fe deficiency	<i>hipp12</i>	0.54	0.48
Fe deficiency	<i>hipp14</i>	0.54	0.48
Fe deficiency	35Sp:: <i>hipp10.1</i>	92.64	<.001
Fe deficiency	35Sp:: <i>hipp10.2</i>	234.85	<.001
Fe excess	Wild type	137.33	<.001
Fe excess	<i>hipp10</i>	50.44	<.001
Fe excess	<i>hipp11</i>	17.27	<b>0.002</b>
Fe excess	<i>hipp12</i>	106.22	<.001
Fe excess	<i>hipp14</i>	106.22	<.001
Fe excess	35Sp:: <i>hipp10.1</i>	84.64	<.001
Fe excess	35Sp:: <i>hipp10.2</i>	73.96	<.001



**Figure S1.** Expression of HIPP10, HIPP11, HIPP12, and HIPP14 genes in their respective T-DNA insertion lines. HIPP transcription levels relative to the transcription of two stably transcribed reference genes (*At5g25760* and *At2g28390*) are presented of wild-type plants (green bars) and hipp mutants (blue bars) grown on vertical agar plates under Fe sufficient (50  $\mu$ M  $\text{Fe}(\text{Na})_2\text{EDTA}_2$ : Fe Suf) or Fe deficient (no added Fe: Fe Def) medium. Mean  $\pm$  SE, and  $n = 6$  replicates of  $\sim 10$  pooled plants each, for the Fe treatment. Statistical significance was determined by Student's  $t$  test ( \*\*  $p < 0.01$ , and \*\*\*  $P < 0.001$ ).





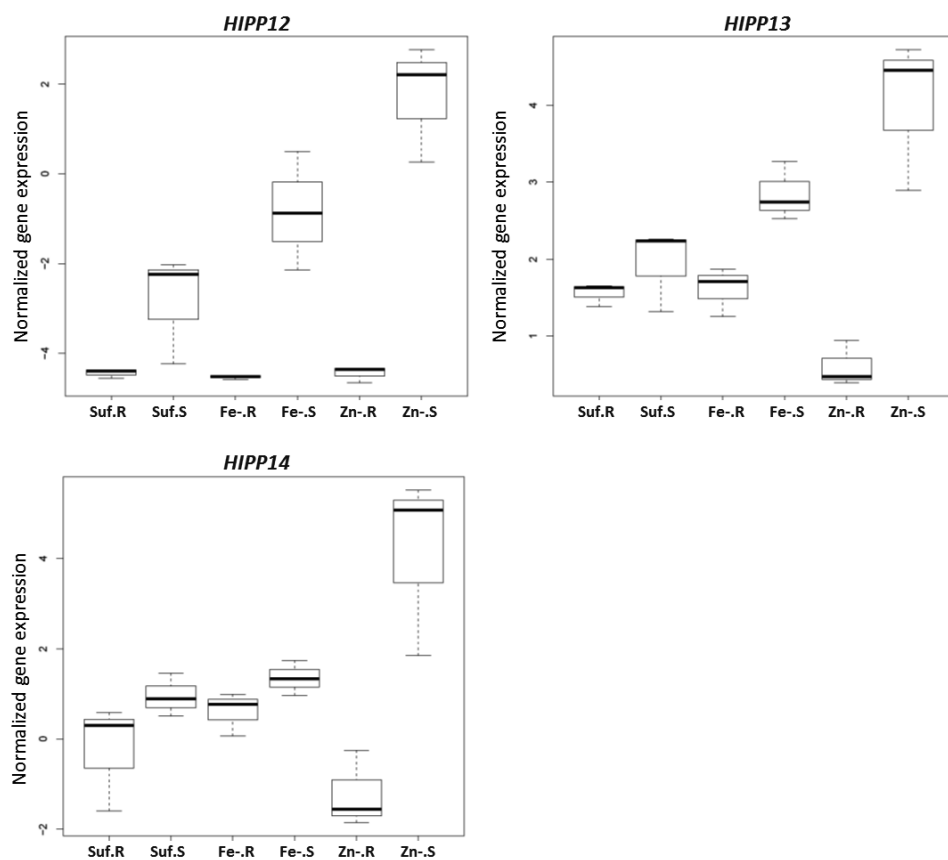


**Figure S2.** Expression of HPP and HIPP genes in shoots (S) and roots (R) of wild-type plants grown on control (Suf), Zn deficient (Zn) and Fe deficient (Fe) medium. Data from RNA-seq reads (Chapter 3).

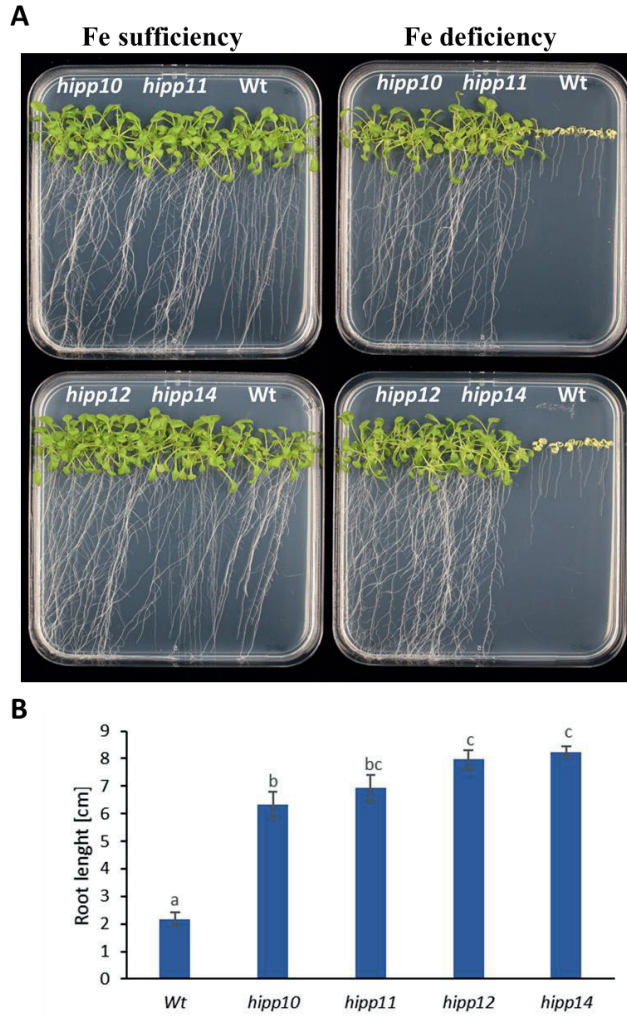


**Figure S3.** *hipp* mutants have increased tolerance to Fe deficiency. (A) Wild-type, *hipp* and 35Sp::HIP10 plants grown for three weeks on control (50  $\mu$ M Fe(Na)<sub>2</sub>EDTA<sub>2</sub>) and Fe-deficient (no added Fe) medium. (B) Root lengths of wild-type and *hipp* mutant plants grown on Fe-deficient medium. Mean  $\pm$  SE,  $n = 22$ . Letters above the bars denote statistically different groups when comparing genotypes, obtained with a Bonferroni post hoc test ( $\alpha=0.05$ ), after a one-way ANOVA ( $p<0.001$ ).

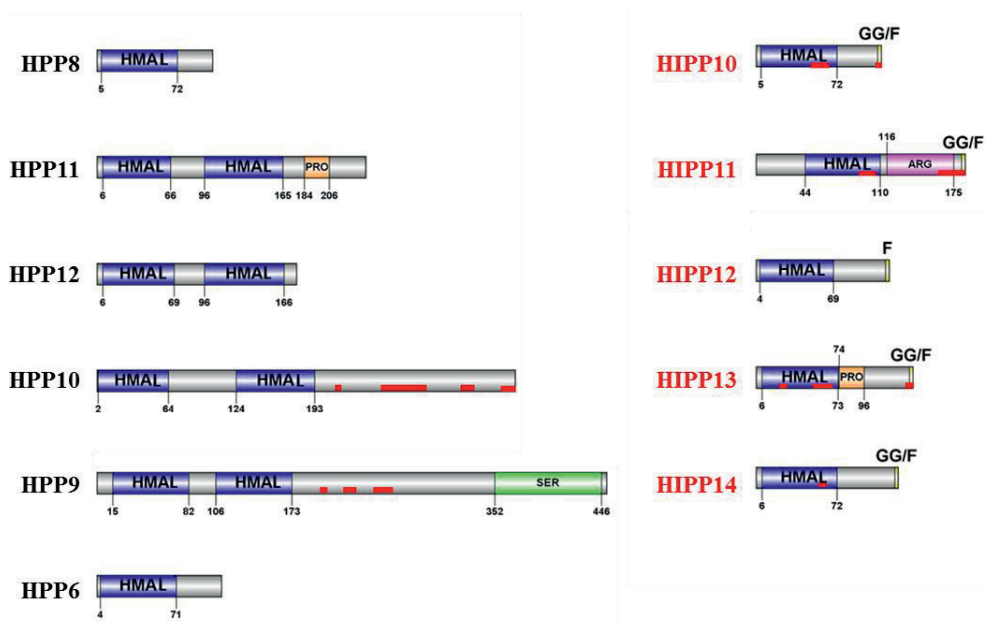


**Figure S4.** Annotated domains and regions in the proteins encoded by the eleven clustered HPP and HIPP genes. Amino acid positions are indicated by the numbers below the bars. HMA (blue) = Heavy Metal Associated domain; PRO (orange) = proline-rich region; SER (green) = serine-rich region; ARG (pink) = arginine-rich region; F (yellow) = farnesylation motif; GG (yellow) = geranylgeranylation motif. Disordered regions are indicated in a separate (lower) bar in red.

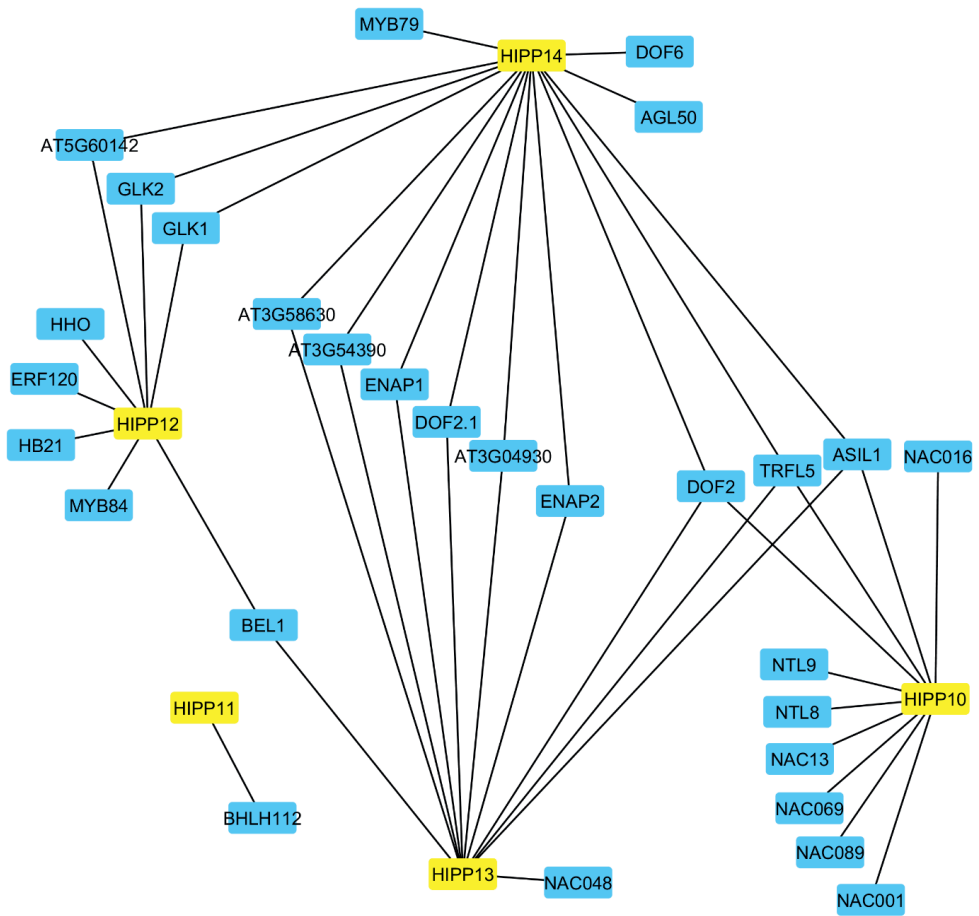


**Figure S5.** Network of HIPP10-14 and their interactors obtained by Y2H assay. Proteins are indicated by rectangles (HIPPs are yellow, and their interactors are blue) and protein interactions with lines.



# **Chapter 6**

## **General Discussion**

### Introduction

In my thesis, I have used forward and reverse genetics approaches to learn more about the genetic architecture of Zn homeostasis, especially under Zn deficiency conditions, in the model species *Arabidopsis thaliana* (Arabidopsis). The results obtained in my thesis research provide enlightening information about the Zn homeostasis, but also show all the challenges of untangling the genetic architecture of Zn homeostasis. Zn homeostasis requires the concert of several processes, molecules, and genes. This is the reason why the study of Zn homeostasis took me through different paths focusing on Zn transporters (Chapter 2), proteins modification as acetylation (Chapter 3), natural variation (Chapter 4), negative-growth regulators (Chapter 5) and homeostasis of other elements as Fe (Chapters 3, 4, and 5).

### Sneaky Zn transporters function

The Zn homeostasis consists of tight control of the Zn cellular concentration to keep the proper physiological concentrations avoiding toxicity or deficiency, regardless of Zn supply (Krężel and Maret, 2006; Sinclair and Krämer, 2012; Krężel and Maret, 2016). Along the years of study of Zn homeostasis, Zn transporters have been the ‘stars’ of this process (Eide, 2006), even more players are involved in it. To understand better the Zn homeostasis, we can start to disentangle it in terms of an isolated cell. Firstly, the cell should contain genes that codify Zn transporters able to scavenge Zn from the surroundings and transport it into the cell, exclude excess Zn from the symplast of the cell, or store Zn into cellular compartments (Regalla and Lyons, 2006). Secondly, the expression of these transporters should be regulated by at least one protein able to sense Zn concentration in the cell (Bird et al., 2003). Thus, in this ideal unicellular system, the cell will need at least four genes driving the Zn homeostasis. However, even in a unicellular organism, such as yeast, the Zn homeostasis is not so simple. Yeast encodes for more than ten proteins directly involved in Zn homeostasis (Regalla and Lyons, 2006; Eide, 2009). Yeast was the organism, in which the first Zn transporter was described (Eide et al., 1996; Zhao and Eide, 1997).

When we move to a more complex organism like a plant, we will find organs, tissues, and cell layers. Each one of them with specialised functions, which are coordinated by cell-cell signalling (Zhu, 2016). For instances, upon exposure to high Zn concentrations, Zn is not sequestered in every single cell of the plant. High concentrations of Zn have been found in non-photosynthetic tissues such as epidermal cells (Kuepper et al., 1999). One of the genes responsible for driving this selective Zn storage is *METAL TRANSPORTER PROTEIN 1*



(*MTP1*), whose protein remobilizes Zn from the symplast into the vacuole (Dräger et al., 2004; Kobae et al., 2004; Gustin. et al., 2009). In another case, upon exposure to Zn deficiency conditions, the *HEAVY METAL ATPASE 2 (HMA2)* expresses in the vasculature to favour the Zn root to shoot translocation (Hussain et al., 2004; Sinclair et al., 2007). Therefore, in complex organisms apart from keeping the Zn equilibrium in only one cell, the processes need to be coordinated to keep the equilibrium in all cell types, which perform different functions. This level of complexity increases the degree of difficulty to find all genes involved in Zn homeostasis and discern their functions.

All the genes that we know to be involved in Zn deficiency in Arabidopsis come from studies either of gene homology with other organisms (Mäser et al., 2001), induction of gene expression due to Zn deficiency (Wintz et al., 2003; van de Mortel et al., 2006), or restoration of the normal growth of the *Saccharomyces cerevisiae zrt1zrt2* mutant defective in Zn uptake (Grotz et al., 1998; Assunção et al., 2010; Milner et al., 2013). The results of these studies correlate with each other supporting the role of these genes in Zn transport.

Almost, after 20 years of the discovery of the first Zn transporter in Arabidopsis, there have not been reports showing an increase in Zn deficiency sensitivity due to the loss of function of any known Zn transporters induced by Zn deficiency. No specific Zn transporter stands out in genetic studies during the analyses of plant extreme phenotypes or during the screening of mutant populations. This suggests that there are redundancies among Arabidopsis Zn transporters and/or Zn transporters have small effects over the Zn deficiency phenotype.

Due to the lack of reports on this topic, I decided to fill this gap in knowledge by studying the Zn deficiency sensitivity in single Zn transporters loss of function mutants. As expected, the loss of function mutants of *zip1*, *zip3*, *zip5*, *zip9*, *zip12*, *irt3*, and *mtp2* did not show a significant increase in the sensitivity to Zn deficiency (Chapter 2) compared to wild-type plants. Still these genes have been shown to be able to transport Zn (Grotz et al., 1998; Assunção et al., 2010; Milner et al., 2013). The expression of these genes is induced after six hours of exposure to Zn deficiency in roots and after more than two days in shoots. However, mutations in them do not give an increased effect on the plant Zn deficiency sensitivity (Chapter 2). The lack of phenotype strongly suggests the presence of the functionally redundant genes (Pickett and Meeks-Wagner, 1995) involved in the Zn deficiency response.

Still encouraged by all the information supporting the Zn transport function of these genes, I continued to search for increased sensitivity to Zn deficiency. So, I generated several combinations of double mutants of these transporters. Most of the double mutant combinations did not show an increased sensitivity to Zn deficiency (Chapter 2). Thus, it could be that the genes selected for each combination are not redundant pairs or that there are more than two redundant genes able to fulfil the same function. Partial or total functional redundancy has been encountered when more than one gene needs to be mutated to observe a phenotype (Pickett and Meeks-Wagner, 1995). The metal transport proteins HMA2 and HMA4 show partial functional redundancy for Zn transport for example. Single *hma2* and *hma4* mutants exhibit no apparent phenotype, while the double mutant *hma2/hma4* is highly sensitive to Zn deficiency (Hussain et al., 2004).

In the case of the Zn transporters, the double mutant combinations of *zip1/zip3* and *zip3/zip5* showed increased sensitivity to Zn deficiency. The double mutant *zip3/zip5* showed the strongest sensitivity to Zn deficiency, which is a synergistic effect on the Zn deficiency phenotype considering the lack of phenotype of the single mutants. Their coding sequences are highly similar (Mäser et al., 2001) and both genes have similar induction timing and location patterns of expression, except in lateral root primordia, indicating similarities between their promoter sequences (Chapter 2).

The Zn concentration in wild-type plants was neither different from the single mutants *zip3* and *zip5* nor from the double mutant *zip3/zip5* upon Zn deficiency supply. However, differences in Zn concentration were possible to be detected after Zn supply during a short period of time (Chapter 2). The double mutant was unable to uptake Zn, as did the wild type and single mutants. This collection of results suggest that *ZIP3* and *ZIP5*, have a redundant function in a subset of Zn homeostasis processes, but have independent functions in other subset of Zn homeostasis processes. The absence of a detectable phenotype, such as increased Zn sensitivity to Zn deficiency or decreased Zn concentration in single mutants of Zn transporters induced by Zn deficiency, is evidence of why alleles of these genes or single mutants have not been detected in forward genetic studies.

To better understand the function this set of Zn transporters induced by Zn deficiency, new combinations of double or triple mutants should be generated to identify groups of redundant genes. In addition, the phenotypes of Zn transporters mutants can be detected with targeted

approaches, such as the use of fluorescein-based bright fluorescent Zn sensor Zinpyr-1 to detect Zn (Woodrooffe et al., 2004). With the use of this fluorescent dye, I observed that in the root differentiation zone, most of the Zn concentrates in the stele, which could subsequently be translocated from root to shoot. Instead, in the Zn transporter mutants *zip1*, *zip3*, *zip5* and *ysl3*, Zn is less concentrated in the stele. Thus, this targeted approach allows phenotypes in Zn transporters mutants to be detected (Chapter 2) (Sinclair et al., 2007). Another targeted approach could be the quantification of Zn concentration on specific cell layers by combining flow cytometry (Evrard et al., 2012; Galbraith, 2014) with Inductively Coupled Plasma Mass Spectrometry (ICP-MS) (Weis-Garcia et al., 2013). For this approach, the transgenic lines that I developed during my research thesis are useful. These lines express a nuclear localized Yellow Fluorescent Protein (NLS-SYFP2), of which, transcription is controlled by the promoters of Zn transporters. These lines could be used directly or after crosses with Zn transporter mutants. The cells in which these transporters are expressed can be isolated and their ionome analysed independently of the rest of the cellular population. Due to this fluorescent tags, we could identify that *IRT3* expresses from the epidermis to stele, *ZIP1* gene expresses in endodermis and stele, *ZIP3* and *ZIP5* express in the epidermis and cortex, and *ZIP11* and *HMA2* express in xylem parenchyma cells (Chapter 2).

### **Zn deficiency regulation at several levels**

Plants are sessile organisms that have developed different regulatory mechanisms to cope with acute stress. These mechanisms maximize their survival by rapid modifications of the physiology of the cells due to changes at the proteome level. The stress signalling networks responses can include targets regulating chromatin structure, transcription, post-transcription, translation and post-translation (Floris et al., 2009; Vert and Chory, 2009; de Nadal et al., 2011).

To search for Zn deficiency response, regulation components is a tempting option, considering the hidden nature of the phenotype of Zn transporters mutants. Up to this moment, the BASIC LEUCINE ZIPPER 19 (bZIP19) and bZIP23 are the only transcription factors known to regulate the Zn deficiency response in *Arabidopsis* (Assunção et al., 2010). However, the way how these two proteins sense Zn deficiency and respond to it to regulate the transcription of Zn transporters is not known (Assunção et al., 2013).

At the same time, that these two regulators were being discovered, the same group of researchers was running a project that identified the mutant studied in Chapter 3. The first goal

of the research described in Chapter 3 was to find regulators involved in the Zn deficiency response. The strategy consisted in using the promoter sequence of *ZINC TRANSPORTER PROTEIN 4 (ZIP4)* gene, a Zn deficiency highly induced gene (Chapter 2 and 3) (Wintz et al., 2003; Assunção et al., 2010) fused to the coding sequence of the *B-GLUCURONIDASE (GUS)* gene (Lin et al., 2016). The Zn deficiency screenable line created in this way, was subject to random mutation. Mutants were screened for a Zn deficiency response suppressed or constantly activated in the plant. The mutant line obtained in this research showed the Zn deficiency response upon Zn deficiency and Zn sufficiency. The mutation responsible for this effect is localized in the *N-ALPHA-TERMINAL-ACETYLTRANSFERASE 25 (NAA25)* gene, which encodes for the non-catalytic subunit of N-alpha-terminal-acetyltransferase complex B (NatB). This complex carries out the N-t-acetylation of proteins during translation (Polevoda and Sherman, 2000; Gibbs, 2015; Aksnes et al., 2016).

The gene found in the mutant screening does not encode for a transcription regulator as originally expected. Instead, the NatB complex is responsible for the acetylation of around 15% of the Arabidopsis proteome (Linster et al., 2015; Aksnes et al., 2016). This result significantly complicated the discovery of a Zn deficiency response regulator, because of the large number of NatB targets in the proteome prone to modification. Protein modifications can affect stability (Schrader et al., 2009), subcellular location, interaction with membranes, protein-protein interactions, protein folding and aggregation (Friso and van Wijk, 2015).

Among the putative targets of NatB are regulators of the Zn deficiency response, such as *bZIP19* and *bZIP23*. Assunção et al. (2010, 2013) hypothesized that these proteins can modify their function by sensing Zn in the medium, because their expression is not significantly increased due to Zn deficiency. If indeed, these two proteins are acetylated by the NatB, the disturbed acetylation in the *naa25* mutant lines, could affect their function causing the expression of Zn transporters even upon Zn sufficiency. Zn transporters induced by Zn deficiency show a slightly but consistently high expression in the *naa25* mutant upon Zn sufficiency compared to wild type. In addition, the *naa25* mutant lines were highly sensitive to Fe deficiency. The Fe deficiency cascade regulators, *BASIC HELIX-LOOP-HELIXE 104 (bHLH104)* and *FER-LIKE IRON DEFICIENCY-INDUCED TRANSCRIPTION FACTOR (FIT)* (Yuan et al., 2008; Zhang et al., 2015; Li et al., 2016) are putative targets of NatB as well. Thus, the effects of the *naa25* loss of function in the Zn and Fe homeostasis can be as a result of the lack of acetylation of their regulators or by pleiotropic effects for the disturbance of other

processes in the plant. The plant immunity is disturbed by mutations in the genes encoding the catalytic and auxiliary subunit of NatB, which decreases the stability of the plant immune receptor *SUPPRESSOR OF NPR1 CONSTITUTIVE 1 (SNCI)* (Xu et al., 2015).

Little is known about how co- and post-translational modifications affect the regulation of elements homeostasis in plants. Several element transporters are target co- and post-translational modifications that affect their stability and specificity. High concentration of Boron (B) induces ubiquitination of the BORON TRANSPORTER 1 (BOR1), this ubiquitination is crucial for the protein sorting and degradation in the vacuole (Kasai et al., 2011). The heavy metal transporter receptor IRON-REGULATED TRANSPORTER 1 (IRT1) is degraded by phosphorylation to avoid the heavy metal accumulation of unspecific substrates such as Zn to ensure proper Fe uptake (Dubeaux et al., 2018). The phosphorylation of the HIGH-AFFINITY K TRANSPORTER 5 (HAK5), K TRANSPORTER 1 (AKT1), and the nitrate transporter NITRATE TRANSPORTER 1 (NTR1) increases the affinity to their respective substrates, upon low supply, while the de-phosphorylated state has a lower affinity (Xu et al., 2006; Ho et al., 2009; Ragel et al., 2015). In the case of Zn homeostasis, there is still a long way to go learning about co- and post-translational modifications that suffer the Zn homeostasis players at the protein level. The aberrant Zn deficiency response in the *naa25* mutant is a hint to test the *in vivo* bZIP19 and bZIP23 N-t-acetylation, and its possible effects over their regulatory function.

### **Natural variation to uncover tolerance to Zn deficiency**

Mining the natural variation of a species is a way to discover new allele variants that are useful to uncover the function of genes. For that reason, I explored the ionome natural variation of Arabidopsis in search of genes involved in the Zn deficiency tolerance. Arabidopsis natural accessions have a high level of variation for several traits (Koornneef and Meinke, 2010) including the responses to Zn deficiency (Campos et al., 2017). The analyses of the variation of specific traits can be done in several ways, for instance by constructing biparental populations with extreme phenotypes or by using large populations in Genome-Wide Association studies (GWAS) (Nordborg and Weigel, 2008).

I followed the GWAS approach inspired in the successful examples where allelic variation was detected for the *HIGH-AFFINITY K TRANSPORTER 1 (HKT1)* gene (Baxter et al., 2010), for the arsenate reductase *HIGH ARSENIC CONTENT 1 (HAC1)* gene (Chao et al., 2014), and the

Cd transporter *HEAVY-METAL ATPASE 3 (HMA3)* gene (Chao et al., 2012). At this point, we need to keep in mind that the homeostasis of essential nutrients requires a tight control of the symplast concentration of each nutrient to meet the physiological requirements and avoid toxicity (Hindt and Guerinot, 2012; Sinclair and Krämer, 2012; Hermans et al., 2013; Printz et al., 2016). Therefore, in the homeostasis of essential nutrients a large number of players will be involved (Hindt and Guerinot, 2012; Sinclair and Krämer, 2012; Hermans et al., 2013; Bashir et al., 2016; Printz et al., 2016) with redundant functions (Chapter 2). Homeostasis of essential nutrients likely requires functional alleles and often does not favour loss-of-function alleles, as were discovered for the *HMA3* and *HAC1* genes. In addition, the tolerance to non-essential elements requires the exclusion of the element from the cells symplast, which likely requires a lower number of genes than the ones involved in essential nutrients homeostasis.

The best results obtained by GWAS are in traits driven by a small number of loci with large effect sizes (Atwell et al., 2010). This implies several current problems in working with complex traits. As mentioned in the infinitesimal model of inheritance of Fisher (Fisher, 1919), traits are driven by many loci with small effects on each one. Large-effect variants are low frequent (Rockman, 2012; Marjoram et al., 2014) and the effect of specific SNPs needs to be sufficiently frequent in the population to be easily identified (Korte and Farlow, 2013). In addition, causal variants can be poorly tagged with makers, the reason why they will not be detected (Gusev et al., 2013). Due to the polygenic nature of Zn homeostasis (Sinclair and Krämer, 2012) and presence of Zn transporters being functionally redundant (Chapter 2), a low success was expected in finding associated SNPs in genes encoding for Zn transporters when Zn concentration was the trait analysed.

Plants suffering from Zn deficiency show a significant decrease in Zn concentration and a generalized disequilibrium of the plant ionome (Chapter 4) (Campos et al., 2017). Thus, in addition to Zn concentration, I also used in the GWAS the concentrations of Co, Cu, Mn, Mo, and Fe, which are micronutrients related to Zn. Associations were detected between Mn concentrations and SNPs in the Mn transporter *NATURAL RESISTANCE-ASSOCIATED MACROPHAGE PROTEIN 1 (NRAMP1)* gene (Cailliatte et al., 2010; Castaings et al., 2016) and between Mo concentrations and SNPs in the *MOLYBDATE TRANSPORTER 1 (MOT1)* (Tomatsu et al., 2007; Baxter et al., 2008). Apart from these two genes, there was not any other micronutrient homeostasis player associated with the element its homeostasis is involved in. Thus, most of the candidate genes selected in Chapter 4 do not have a known function related

with micronutrients homeostasis, but their mutants showed significant changes in element concentrations.

The analyses of the candidate genes mutants *ton1 recruiting motif 22 (trm22)*, *at5g66890*, *pigment defective 318 (pde318)*, *target of early activation tagged (toe3)*, *early flowering 3 (elf3)*, *at1g49350*, and *ferritin 4 (fer4)* showed a significant difference with the wild type, in the concentration of the element, each gene was associated with in the GWAS. Zinc deficient plants show a decrease in the Zn concentration and significant changes in the concentration in most of the elements of the ionome (Ghandilyan et al., 2012; Campos et al., 2017). Therefore, the tolerance to Zn deficiency could be reflected in the lesser changes in the ionome due to Zn deficiency. The changes in the element concentrations due to Zn deficiency intensify in the mutants *trm22*, *at5g66890*, *pde318*, *toe3*, *elf3*, *at1g49350*, and *fer4* when compared to wild type. Some of the elements related to Zn with significant changes in these mutants are Fe, Mn, and Cu. And these elements are required for essential plant process like photosynthesis (Varotto et al., 2002; Kessler and Papenbrock, 2005; Yruela, 2013). The changes in concentration in non-targeted elements, as observed in the mutants studied, could be either a biological pleiotropy or a mediated pleiotropy. In a biological pleiotropy, the gene has a direct biological influence on more than one trait. In a mediated pleiotropy, one phenotype is itself causally related to a second phenotype (Solovieff et al., 2013). Therefore, by using the ionome of plants grown upon Zn sufficiency or Zn deficiency, I could identify genes, in which loss of function increases the ionome disequilibrium in the plant due to Zn deficiency. Probably, these genes were associated with micronutrients concentration due to their effect in several traits, which caused major disequilibrium in the ionome of the plant (Chapter 4).

To identify genetic variants of genes directly involved in Zn homeostasis, more specific questions, and targeted approaches should be applied. A good example of a specific question and targeted approach in applying GWAS was performed for developmental cell-type traits, in which the length of the root meristematic zone was associated with F-box gene *KURZ UND KLEIN (KUK)* that was confirmed to regulate meristem length (Meijón et al., 2014). Thus, in Zn homeostasis, we should try to isolate the process, as much as possible to be able to disentangle their players one-by-one. In this way, we can avoid the effects of genes controlling other processes. For instance, if we are looking to find Zn homeostasis players in roots, probably individual cell layers should be analysed for Zn concentration. In this case, cell sorting by flow cytometry plus ICP-MS (Weis-Garcia et al., 2013), laser micro-dissection, plus ICP-MS or laser

ablation-inductively coupled plasma-mass spectrometry (Persson et al., 2016) could be applied. The analysing of the Zn distribution in the root cellular layers with Zn dyes as Zinpyr-1 can be useful because individual Zn transporter mutants can be spotted in this way (Chapter 2) (Sinclair et al., 2007). Also, the analyses of Zn uptake in short periods of time as shown in Chapter 2 could be suitable to detect basal uptake mechanisms.

### Tolerance to abiotic stress

Plants either in natural or agricultural environments occupy a wide range of ecological niches, to which they are exposed to biotic and abiotic stresses. The defence or tolerance response to stress requires the reallocation of resources to cope with the environmental challenge. The activation of responses to stress often leads to an overall reduced plant growth, for instance, mutant plants with enhanced autoimmune response are small. Thus, plants need to effectively fine-tune the trade-offs between response to the stress and the developmental process in a cost-efficient manner to deal with stress and coordinate growth (Zhang et al., 2003; Vinocur and Altman, 2005; Lozano-Durán and Zipfel, 2015; Haina and Uwe, 2017).

Growth hormone networks are regulated during stress responses to coordinate growth (Haina and Uwe, 2017). Brassinosteroids (BRs) are positive growth regulators that merge signals from biotic stress with growth and developmental plant programs. Thus, BRs are regulators of trade-offs between disease resistance and plant growth (De Bruyne et al., 2014). BRs also link abiotic signals to growth. During drought or carbon starvation, the *BRI 1-EMS-SUPPRESSOR 1* (*BES1*), a transcription factor part of the BRs signalling, is degraded affecting the normal plant growth rate. This mechanism favours the plant survival under these stress conditions at the cost of plant growth (Nolan et al., 2017). Gibberellic acid is also a positive growth phytohormone; its signalling is repressed by DELLA proteins (DELLAs). DELLAs are transcription factors, with growth repressing effects enhanced by stress conditions as salt (Silverstone et al., 1997; Achard et al., 2006; Sun, 2010).

The abiotic stress caused by shortage of nutrients such as Zn is generally characterized by chlorosis and stunted growth among other symptoms, which increase with the severity of the stress and time of exposure (Cakmak, 2008; Alloway, 2009; Marschner and Marschner, 2012; Yruela, 2013; Campos, 2015; Mattiello et al., 2015). Tolerance to Zn deficiency stress is variable among *Arabidopsis* natural accessions (Campos et al., 2017), which could be expressed in terms of ionome equilibrium, sufficient Zn concentration (Chapter 4) or less severity of the



Zn deficiency symptoms in the plant (Hacisalihoglu and Kochian, 2003; Cakmak, 2008; Alloway, 2009; Campos et al., 2017). In Chapter 4, after applying a GWAS, I found an overrepresentation of *HEAVY METAL-ASSOCIATED ISOPRENYLATED PLANT PROTEINS* (*HIPP*) genes harbouring SNPs associated with the ionome of Arabidopsis natural accessions grew upon sufficient or deficient Zn supply.

*HIPPs* are involved in biotic and especially in abiotic stress responses. Cold affects the expression of *HIPP24*, *HIPP26*, *HIPP23*, *HIPP25* and *HIPP27* (Barth et al., 2009), drought and abscisic acid affect the expression of *HIPP3* (Zschiesche et al., 2015). *HIPPs* role has been mainly related to tolerance to toxic elements like Cd. The expression of *HIPP26* is induced by cold, drought, salt, and Cd (Barth et al., 2009; Gao et al., 2009), and its overexpression induces tolerance to Cd (Gao et al., 2009). In a similar way, *HIPP6* overexpression confers tolerance to Cd and its expression is induced by Cd, Mercury (Hg), Fe, and Cu (Suzuki et al., 2002). The triple mutant loss of function *hipp20/hipp21/hipp22* is highly sensitive to Cd compared to wild-type plants (Tehseen et al., 2010). As a common pattern, stress conditions change the *HIPPs* gene expression and are involved in the tolerance to the non-essential heavy metal Cd.

I performed functional analyses in five *HIPPs* not described at the moment, which were detected in the GWAS of Chapter 4, and are part of an intriguing cluster of tandemly arrayed genes. Mutants of these genes showed increased tolerance to Zn deficiency (Chapter 5). However, after testing several stress conditions, I found out that their function is not specific for Zn deficiency. Mutants of this cluster of tandemly arrayed *HIPPs* also showed increase tolerance to Zn excess, Fe excess, and especially to Fe deficiency. The expression of these genes is induced upon Zn deficiency or Fe deficiency in wild-type plants. The overexpression lines of one of these genes showed to be as sensitive as the wild type, and in some cases even more sensitive than wild type to deficient or excess Fe or Zn supply. In addition, members of this cluster are higher expressed in the acetylation mutant *naa25* when compared to wild type. The *naa25* mutant is more sensitive to Fe deficiency than the wild type (Chapter 3) and has a disturbed Zn deficiency response. These results suggest the role of the five members of the cluster of tandemly arrayed *HIPPs* in adverse Zn and Fe supply.

The five genes from this cluster had not been characterized to the moment, due to sequence similarities they are related to metallochaperons (Tehseen et al., 2010; de Abreu-Neto et al., 2013). The heavy metal domain of these *HIPPs* contains the general sequence of a heavy metal

binding domain but lacks its core motif (Tehseen et al., 2010), the reason why this could be a heavy metal-associated like domain (Chapter 5). HIPPs like *HIPP3*, *HIPP7* and *HIPP26* have been experimentally shown to bind heavy metals (Dykema et al., 1999; Achard et al., 2006; Gao et al., 2009). However, it is not known if this domain is functional or not in the five members of the cluster of tandemly arrayed HIPPs. If it is functional, it could be involved in buffering metals in the symplast, trafficking metals in the cell (Wintz and Vulpe, 2002; Robinson and Winge, 2010; Pang et al., 2013) or sensing metals concentrations, which is the case of metalloregulatory proteins (Giedroc and Arunkumar, 2007; Kim et al., 2007; Lee and Helmann, 2007; Waldron et al., 2009; Caballero et al., 2011).

Functional analyses of the cluster of tandemly array HIPPs suggest a role in gene transcription regulation. Members of this cluster, positively regulates the expression of the other members of the same cluster upon Fe deficiency, either by direct or indirect interactions. When genes participate in similar pathways, their cross-regulation can become a necessary mechanism to ensure that all the components of a process be present at the same moment, especially if they interact among them (Gómez-Mena et al., 2005; Immink et al., 2009). The interaction among members of the cluster of tandemly array HIPPs is a feasible hypothesis, because these HIPPs have some common interactors among them, suggesting their work as a complex of proteins. HIPPs interact with several nuclear-localized proteins. And HIPPs interaction partners show interactions among them as well, which indicates that these HIPPs belong to a highly connected network of proteins.

The processes, in which these HIPPs are involved can be inferred by the function of their interaction partners. The proteins with which HIPPs interact are: NO APICAL MERISTEM/ARABIDOPSIS TRANSCRIPTION ACTIVATION FACTOR/CUP-SHAPED COTYLEDON DOMAIN CONTAINING PROTEIN 001 (NAC001), NAC13, NAC016, NAC069, NAC089, MEMBRANE-BOUND NAC 8 (NTL8), NTL9, bHLH112, ZINC FINGER HOMEBOX PROTEIN 4 (ZFHD4), ETHYLENE RESPONSE FACTOR 120 (ERF120), HYPERSENSITIVITY TO LOW PI-ELICITED PRIMARY ROOT SHORTENING 1 HOMOLOGUE 1 (HHO1), REGULATORS OF AXILLARY MERISTEMS 3 (RAX3), TRF5, ASIL1, DOF2, BEL1, GOLDEN2-LIKE 1 (GLK1), GLK2, F15L12, AT3G54390, ETHYLENE INSENSITIVE 2 NUCLEAR-ASSOCIATED PROTEIN 1 (ENAP1) and ENAP2. The HIPPs interaction partners have regulatory functions and several of them link stress signals to plant growth and development. The stress signals they link come

from high or low nutrients supply (Tan and Irish, 2006; Kasajima and Fujiwara, 2007; Cheng et al., 2012; Medici et al., 2015; Pan et al., 2015; Liu et al., 2017), salinity (Kim et al., 2008; Kim et al., 2013; He et al., 2015; Liu et al., 2015; Sakuraba et al., 2016), and drought (Liu et al., 2015). And those signals affect processes as germination (Kim et al., 2008; Rueda-Romero et al., 2012; He et al., 2015), growth (Kim et al., 2007; Cheng et al., 2012; Pan et al., 2015; Zhang et al., 2016; Liu et al., 2017; Zhang et al., 2017; Zhang et al., 2018), meristem initiation (Müller et al., 2006), senescence (Sakuraba et al., 2016), and cell death (Klein et al., 2012; De Clercq et al., 2013). Notably, members of the cluster of tandemly arrayed HIPPs and some of their interactors show a similar pattern, which consisted in gene expression induced by stress, loss of function of the genes increases tolerance to stress, and the overexpression of genes decreased growth. Which is similar to the negative-plant-growth regulators DELLAs (Achard et al., 2006).

All the results obtained from the cluster of tandemly arrayed HIPPs suggest their role as negative-plant-growth regulators induced by stress. The HIPP genes came to my hands in a study looking for genes involved in tolerance to Zn deficiency. Indeed, these genes show to be involved in Zn deficiency tolerance. However, they are not specific for Zn deficiency, their loss of function provide tolerance to adverse Zn and Fe supply, and maybe to more stress conditions than the ones tested in this research. Still, many aspects of the function of these HIPPs need to be studied, such as the genes whose expressions they may affect, trade-offs of their loss of function, and signal molecules in their regulatory activity. These genes have the potential to be used later on to improve crop tolerance and the information obtained in this thesis can be only the tip of the iceberg their potential.

### **Final remarks**

Zn deficiency response is a complex trait constituted by several components, among them Zn transporters, mainly in charged to increase the Zn symplast concentration. The expression of Zn transporters is induced only six hours after exposure to Zn deficiency indicating the existence of a mechanism in charge to sense the shortage of Zn and regulate gene expression. The transcription factors bZIP19 and bZIP23 induce the expression of several Zn transporters during Zn deficiency. Furthermore, we do not know for sure about other levels of regulation of the Zn homeostasis. Probably, the acetylation of bZIP19 and bZIP23 is a required step to allow the proper function of these transcription factors. The phenotypes of Zn transporters induced by deficiency are difficult to detect, mainly due to functional redundancy among some of them.

This characteristic complicates the detection of Zn transporter mutants in forward genetic approaches. The genes, in which mutation causes significant changes in several elements of the plant ionome upon Zn deficiency, were identified by forward genetics using the ionome natural variation, as well as genes, in which mutation significantly improved the tolerance to Zn deficiency, Zn excess, Fe deficiency and Fe excess were identified by forward genetics using the ionome natural variation.

A deep understanding of the genetic architecture of Zn deficiency is a key step in improving the crops efficient use of nutrients and increasing the Zn content of the edible parts of crops, through plant breeding strategies.





# References

- Achard P, Cheng H, De Grauwe L, Decat J, Schoutteten H, Moritz T, Van Der Straeten D, Peng J, Harberd NP** (2006) Integration of Plant Responses to Environmentally Activated Phytohormonal Signals. *Science* **311**: 91-94
- Achard P, Genschik P** (2009) Releasing the brakes of plant growth: how GAs shutdown DELLA proteins. *Journal of Experimental Botany* **60**: 1085-1092
- Achard P, Renou J-P, Berthomé R, Harberd NP, Genschik P** (2008) Plant DELLAs Restrains Growth and Promote Survival of Adversity by Reducing the Levels of Reactive Oxygen Species. *Current Biology* **18**: 656-660
- Ackland ML, Michalczyk AA** (2016) Zinc and infant nutrition. *Archives of Biochemistry and Biophysics* **611**: 51-57
- Ahn SJ, Shin R, Schachtman DP** (2004) Expression of KT/KUP Genes in Arabidopsis and the Role of Root Hairs in K<sup>+</sup> Uptake. *Plant Physiology* **134**: 1135-1145
- Aksnes H, Drazic A, Marie M, Arnesen T** (2016) First Things First: Vital Protein Marks by N-Terminal Acetyltransferases. *Trends in Biochemical Sciences* **41**: 746-760
- Al-Shehbaz IA, O'Kane SL** (2002) Taxonomy and Phylogeny of Arabidopsis (Brassicaceae). *The Arabidopsis Book / American Society of Plant Biologists* **1**: e0001
- Allen RS, Li J, Stahle MI, Dubroué A, Gubler F, Millar AA** (2007) Genetic analysis reveals functional redundancy and the major target genes of the Arabidopsis miR159 family. *Proceedings of the National Academy of Sciences* **104**: 16371-16376
- Alloway BJ** (2009) Soil factors associated with zinc deficiency in crops and humans. *Environmental Geochemistry and Health* **31**: 537-548
- Alonso-Blanco C, Aarts MGM, Bentsink L, Keurentjes JJB, Reymond M, Vreugdenhil D, Koornneef M** (2009) What has natural variation taught us about plant development, physiology, and adaptation? *Plant Cell* **21**: 1877-1896
- Anderegg G, Ripperger H** (1989) Correlation between metal complex formation and biological activity of nicotianamine analogues. *Journal of the Chemical Society, Chemical Communications*: 647-650
- Anders S, Pyl PT, Huber W** (2015) HTSeq—a Python framework to work with high-throughput sequencing data. *Bioinformatics* **31**: 166-169
- Andreini C, Banci L, Bertini I, Rosato A** (2006) Counting the Zinc-Proteins Encoded in the Human Genome. *Journal of Proteome Research* **5**: 196-201
- Andrés-Colás N, Perea-García A, Puig S, Peñarrubia L** (2010) Deregulated Copper Transport Affects Arabidopsis Development Especially in the Absence of Environmental Cycles. *Plant Physiology* **153**: 170-184



- Araki R, Shikanai T** (2014) Analysis of photosynthetic electron transport in *Arabidopsis thaliana* under iron deficiency. *Journal of Crop Research* **59**: 11-15
- Arosio P, Ingrassia R, Cavadini P** (2009) Ferritins: A family of molecules for iron storage, antioxidation and more. *Biochimica et Biophysica Acta (BBA) - General Subjects* **1790**: 589-599
- Arrivault S, Senger T, Krämer U** (2006) The *Arabidopsis* metal tolerance protein AtMTP3 maintains metal homeostasis by mediating Zn exclusion from the shoot under Fe deficiency and Zn oversupply. *Plant Journal* **46**: 861-879
- Assunção AGL, Herrero E, Lin YF, Huettel B, Talukdar S, Smaczniak C, Immink RGH, Van Eldik M, Fiers M, Schat H, Aarts MGM** (2010) *Arabidopsis thaliana* transcription factors bZIP19 and bZIP23 regulate the adaptation to zinc deficiency. *Proceedings of the National Academy of Sciences of the United States of America* **107**: 10296-10301
- Assunção AGL, Persson DP, Husted S, Schjørring JK, Alexander RD, Aarts MGM** (2013) Model of how plants sense zinc deficiency. *Metallomics* **5**: 1110-1116
- Assunção AGL, Schat H, Aarts MGM** (2003) *Thlaspi caerulescens*, an attractive model species to study heavy metal hyperaccumulation in plants. *New Phytologist* **159**: 351-360
- Atwell S, Huang YS, Vilhjalmsón BJ, Willems G, Horton M, Li Y, Meng D, Platt A, Tarone AM, Hu TT, Jiang R, Mulyati NW, Zhang X, Amer MA, Baxter I, Brachi B, Chory J, Dean C, Debieu M, de Meaux J, Ecker JR, Faure N, Kniskern JM, Jones JDG, Michael T, Nemri A, Roux F, Salt DE, Tang C, Todesco M, Traw MB, Weigel D, Marjoram P, Borevitz JO, Bergelson J, Nordborg M** (2010) Genome-wide association study of 107 phenotypes in *Arabidopsis thaliana* inbred lines. **465**: 627-631
- Avicé J-C, Etienne P** (2014) Leaf senescence and nitrogen remobilization efficiency in oilseed rape (*Brassica napus* L.). *Journal of Experimental Botany* **65**: 3813-3824
- Azimzadeh J, Nacry P, Christodoulidou A, Drevensek S, Camilleri C, Amiour N, Percy F, Pastuglia M, Bouchez D** (2008) *Arabidopsis* TONNEAU1 Proteins Are Essential for Preprophase Band Formation and Interact with Centrin. *The Plant Cell* **20**: 2146-2159
- Aznar A, Chen NWG, Rigault M, Riache N, Joseph D, Desmaële D, Mouille G, Boutet S, Soubigou-Taconnat L, Renou J-P, Thomine S, Expert D, Dellagi A** (2014)

## References

---

- Scavenging Iron: A Novel Mechanism of Plant Immunity Activation by Microbial Siderophores. *Plant Physiology* **164**: 2167-2183
- Aznar A, Chen NWG, Thomine S, Dellagi A** (2015) Immunity to plant pathogens and iron homeostasis. *Plant Science* **240**: 90-97
- Barak P, Helmke PA** (1993) The Chemistry of Zinc. *In* AD Robson, ed, Zinc in Soils and Plants: Proceedings of the International Symposium on 'Zinc in Soils and Plants' held at The University of Western Australia, 27–28 September, 1993. Springer Netherlands, Dordrecht, pp 1-13
- Barberon M, Geldner N** (2014) Radial Transport of Nutrients: The Plant Root as a Polarized Epithelium. *Plant Physiology* **166**: 528-537
- Barth O, Vogt S, Uhlemann R, Zschiesche W, Humbeck K** (2009) Stress induced and nuclear localized HIP26 from *Arabidopsis thaliana* interacts via its heavy metal associated domain with the drought stress related zinc finger transcription factor ATHB29. *Plant Molecular Biology* **69**: 213-226
- Bashir K, Rasheed S, Kobayashi T, Seki M, Nishizawa NK** (2016) Regulating Subcellular Metal Homeostasis: The Key to Crop Improvement. *Frontiers in Plant Science* **7**: 1192
- Baxter I, Brazelton JN, Yu D, Huang YS, Lahner B, Yakubova E, Li Y, Bergelson J, Borevitz JO, Nordborg M, Vitek O, Salt DE** (2010) A Coastal Cline in Sodium Accumulation in *Arabidopsis thaliana* Is Driven by Natural Variation of the Sodium Transporter *AtHKT1;1*. *PLoS Genet* **6**: e1001193
- Baxter I, Hermans C, Lahner B, Yakubova E, Tikhonova M, Verbruggen N, Chao D-y, Salt DE** (2012) Biodiversity of Mineral Nutrient and Trace Element Accumulation in *Arabidopsis thaliana*. *PLoS ONE* **7**: e35121
- Baxter I, Muthukumar B, Park HC, Buchner P, Lahner B, Danku J, Zhao K, Lee J, Hawkesford MJ, Guerinot ML, Salt DE** (2008) Variation in Molybdenum Content Across Broadly Distributed Populations of *Arabidopsis thaliana* Is Controlled by a Mitochondrial Molybdenum Transporter (*MOT1*). *PLOS Genetics* **4**: e1000004
- Baxter IR, Vitek O, Lahner B, Muthukumar B, Borghi M, Morrissey J, Guerinot ML, Salt DE** (2008) The leaf ionome as a multivariable system to detect a plant's physiological status. *Proceedings of the National Academy of Sciences of the United States of America* **105**: 12081-12086
- Beal T, Massiot E, Arsenault JE, Smith MR, Hijmans RJ** (2017) Global trends in dietary micronutrient supplies and estimated prevalence of inadequate intakes. *PLOS ONE* **12**: e0175554

- Bellaoui M, Pidkowich MS, Samach A, Kushalappa K, Kohalmi SE, Modrusan Z, Crosby WL, Haughn GW** (2001) The Arabidopsis BELL1 and KNOX TALE Homeodomain Proteins Interact through a Domain Conserved between Plants and Animals. *The Plant Cell* **13**: 2455-2470
- Beneš I, Schreiber K, Ripperger H, Kircheiss A** (1983) Metal complex formation by nicotianamine, a possible phytosiderophore. *Experientia* **39**: 261-262
- Benjamini Y, Hochberg Y** (1995) Controlling the False Discovery Rate: A Practical and Powerful Approach to Multiple Testing. *Journal of the Royal Statistical Society. Series B (Methodological)* **57**: 289-300
- Bird AJ, McCall K, Kramer M, Blankman E, Winge DR, Eide DJ** (2003) Zinc fingers can act as Zn<sup>2+</sup> sensors to regulate transcriptional activation domain function. *The EMBO journal* **22**: 5137-5146
- Biswas KK, Ooura C, Higuchi K, Miyazaki Y, Van Nguyen V, Rahman A, Uchimiya H, Kiyosue T, Koshiba T, Tanaka A, Narumi I, Oono Y** (2007) Genetic Characterization of Mutants Resistant to the Antiauxin p-Chlorophenoxyisobutyric Acid Reveals That AAR3, a Gene Encoding a DCN1-Like Protein, Regulates Responses to the Synthetic Auxin 2,4-Dichlorophenoxyacetic Acid in Arabidopsis Roots. *Plant Physiology* **145**: 773-785
- Black RE, Allen LH, Bhutta ZA, Caulfield LE, de Onis M, Ezzati M, Mathers C, Rivera J** (2008) Maternal and child undernutrition: global and regional exposures and health consequences. *The Lancet* **371**: 243-260
- Blindauer CA, Schmid R** (2010) Cytosolic metal handling in plants: Determinants for zinc specificity in metal transporters and metallothioneins. *Metallomics* **2**: 510-529
- Bonferroni CE** (1935) Il calcolo delle assicurazioni su gruppi di teste. *Tipografia del Senato*
- Bradshaw HD** (2005) Mutations in CAX1 produce phenotypes characteristic of plants tolerant to serpentine soils. *New Phytologist* **167**: 81-88
- Briat J-F, Rouached H, Tissot N, Gaymard F, Dubos C** (2015) Integration of P, S, Fe, and Zn nutrition signals in Arabidopsis thaliana: potential involvement of PHOSPHATE STARVATION RESPONSE 1 (PHR1). *Frontiers in Plant Science* **6**
- Buescher E, Achberger T, Amusan I, Giannini A, Ochsenfeld C, Rus A, Lahner B, Hoekenga O, Yakubova E, Harper JF, Guerinot ML, Zhang M, Salt DE, Baxter IR** (2010) Natural Genetic Variation in Selected Populations of Arabidopsis thaliana is Associated with Ionomics Differences. *PLoS ONE* **5**: e11081

## References

---

- Buljan M, Bateman A** (2009) The evolution of protein domain families. *Biochemical Society Transactions* **37**: 751-755
- Caballero HR, Campanello GC, Giedroc DP** (2011) Metalloregulatory Proteins: Metal Selectivity and Allosteric Switching. *Biophysical chemistry* **156**: 103-114
- Cailliatte R, Schikora A, Briat J-F, Mari S, Curie C** (2010) High-Affinity Manganese Uptake by the Metal Transporter NRAMP1 Is Essential for Arabidopsis Growth in Low Manganese Conditions. *The Plant Cell* **22**: 904-917
- Cakmak I** (2008) Enrichment of cereal grains with zinc: Agronomic or genetic biofortification? *Plant and Soil* **302**: 1-17
- Campos ACAL** (2015) Study of natural variation for Zn deficiency tolerance in *Arabidopsis thaliana*. Wageningen University, Wageningen
- Campos ACAL, Kruijer W, Alexander R, Akkers RC, Danku J, Salt DE, Aarts MGM** (2017) Natural variation in *Arabidopsis thaliana* reveals shoot ionome, biomass, and gene expression changes as biomarkers for zinc deficiency tolerance. *Journal of Experimental Botany* **68**: 3643-3656
- Castaings L, Caquot A, Loubet S, Curie C** (2016) The high-affinity metal Transporters NRAMP1 and IRT1 Team up to Take up Iron under Sufficient Metal Provision. **6**: 37222
- Caulfield LE, Black RE** (2004) Zinc deficiency. Comparative Quantification of Health Risks: Global and Regional Burden of Disease Attributable to Selected Major Risk Factors: 257-279
- Chao D-Y, Baraniecka P, Danku J, Koprivova A, Lahner B, Luo H, Yakubova E, Dilkes B, Kopriva S, Salt DE** (2014) Variation in Sulfur and Selenium Accumulation Is Controlled by Naturally Occurring Isoforms of the Key Sulfur Assimilation Enzyme ADENOSINE 5'-PHOSPHOSULFATE REDUCTASE2 across the *Arabidopsis* Species Range. *Plant Physiology* **166**: 1593-1608
- Chao D-Y, Chen Y, Chen J, Shi S, Chen Z, Wang C, Danku JM, Zhao F-J, Salt DE** (2014) Genome-wide Association Mapping Identifies a New Arsenate Reductase Enzyme Critical for Limiting Arsenic Accumulation in Plants. *PLoS Biol* **12**: e1002009
- Chao D-Y, Silva A, Baxter I, Huang YS, Nordborg M, Danku J, Lahner B, Yakubova E, Salt DE** (2012) Genome-Wide Association Studies Identify Heavy Metal ATPase3 as the Primary Determinant of Natural Variation in Leaf Cadmium in *Arabidopsis thaliana*. *PLoS Genet* **8**: e1002923

- Chen X, Ludewig U** (2018) Biomass increase under zinc deficiency caused by delay of early flowering in *Arabidopsis*. *Journal of Experimental Botany* **69**: 1269–1279
- Chen Y-Y, Wang Y, Shin L-J, Wu J-F, Shanmugam V, Tsednee M, Lo J-C, Chen C-C, Wu S-H, Yeh K-C** (2013) Iron Is Involved in the Maintenance of Circadian Period Length in *Arabidopsis*. *Plant Physiology* **161**: 1409-1420
- Cheng M-C, Hsieh E-J, Chen J-H, Chen H-Y, Lin T-P** (2012) *Arabidopsis* RGLG2, Functioning as a RING E3 Ligase, Interacts with AtERF53 and Negatively Regulates the Plant Drought Stress Response. *Plant Physiology* **158**: 363-375
- Cheung M-Y, Li X, Miao R, Fong Y-H, Li K-P, Yung Y-L, Yu M-H, Wong K-B, Chen Z, Lam H-M** (2016) ATP binding by the P-loop NTPase OsYchF1 (an unconventional G protein) contributes to biotic but not abiotic stress responses. *Proceedings of the National Academy of Sciences* **113**: 2648-2653
- Choi J, Choi D, Lee S, Ryu C-M, Hwang I** Cytokinins and plant immunity: old foes or new friends? *Trends in Plant Science* **16**: 388-394
- Clarkson DT** (1993) Roots and the Delivery of Solutes to the Xylem. *Philosophical Transactions of the Royal Society of London. Series B: Biological Sciences* **341**: 5-17
- Claus J, Bohmann A, Chavarria-Krauser A** (2013) Zinc uptake and radial transport in roots of *Arabidopsis thaliana*: A modelling approach to understand accumulation. *Annals of Botany* **112**: 369-380
- Clough SJ, Bent AF** (1998) Floral dip: A simplified method for *Agrobacterium*-mediated transformation of *Arabidopsis thaliana*. *Plant Journal* **16**: 735-743
- Clouse SD** (2011) Brassinosteroid Signal Transduction: From Receptor Kinase Activation to Transcriptional Networks Regulating Plant Development. *The Plant Cell* **23**: 1219-1230
- Colangelo EP, Guerinot ML** (2004) The Essential Basic Helix-Loop-Helix Protein FIT1 Is Required for the Iron Deficiency Response. *The Plant Cell* **16**: 3400-3412
- Connolly EL, Guerinot ML** (2002) Iron stress in plants. *Genome Biology* **3**: reviews1024.1021-reviews1024.1024
- Covington MF, Panda S, Liu XL, Strayer CA, Wagner DR, Kay SA** (2001) ELF3 Modulates Resetting of the Circadian Clock in *Arabidopsis*. *The Plant Cell* **13**: 1305-1316
- Curie C, Alonso JM, Le Jean M, Ecker JR, Briat JF** (2000) Involvement of NRAMP1 from *Arabidopsis thaliana* in iron transport. *Biochemical Journal* **347**: 749-755

- Curie C, Cassin G, Couch D, Divol F, Higuchi K, Le Jean M, Misson J, Schikora A, Czernic P, Mari S (2009) Metal movement within the plant: Contribution of nicotianamine and yellow stripe 1-like transporters. *Annals of Botany* **103**: 1-11
- de Abreu-Neto JB, Turchetto-Zolet AC, de Oliveira LFV, Bodanese Zanettini MH, Margis-Pinheiro M (2013) Heavy metal-associated isoprenylated plant protein (HIPP): characterization of a family of proteins exclusive to plants. *FEBS Journal* **280**: 1604-1616
- De Bruyne L, Höfte M, De Vleeschauwer D (2014) Connecting Growth and Defense: The Emerging Roles of Brassinosteroids and Gibberellins in Plant Innate Immunity. *Molecular Plant* **7**: 943-959
- De Clercq I, Vermeirssen V, Van Aken O, Vandepoele K, Murcha MW, Law SR, Inzé A, Ng S, Ivanova A, Rombaut D, van de Cotte B, Jaspers P, Van de Peer Y, Kangasjärvi J, Whelan J, Van Breusegem F (2013) The Membrane-Bound NAC Transcription Factor ANAC013 Functions in Mitochondrial Retrograde Regulation of the Oxidative Stress Response in Arabidopsis. *The Plant Cell* **25**: 3472-3490
- de Folter S, Immink RGH (2011) Yeast Protein–Protein Interaction Assays and Screens. *In* L Yuan, SE Perry, eds, *Plant Transcription Factors: Methods and Protocols*. Humana Press, Totowa, NJ, pp 145-165
- de Folter S, Immink RGH, Kieffer M, Pařenicová L, Henz SR, Weigel D, Busscher M, Kooiker M, Colombo L, Kater MM, Davies B, Angenent GC (2005) Comprehensive Interaction Map of the Arabidopsis MADS Box Transcription Factors. *The Plant Cell* **17**: 1424-1433
- de Nadal E, Ammerer G, Posas F (2011) Controlling gene expression in response to stress. *Cell* **12**: 833-845
- Deinlein U, Weber M, Schmidt H, Rensch S, Trampeczynska A, Hansen TH, Husted S, Schjoerring JK, Talke IN, Krämer U, Clemens S (2012) Elevated Nicotianamine Levels in Arabidopsis halleri Roots Play a Key Role in Zinc Hyperaccumulation. *The Plant Cell* **24**: 708-723
- Des Marais DL, Juenger TE (2010) Pleiotropy, plasticity, and the evolution of plant abiotic stress tolerance. *Annals of the New York Academy of Sciences* **1206**: 56-79
- Desbrosses-Fonrouge AG, Voigt K, Schröder A, Arrivault S, Thomine S, Krämer U (2005) Arabidopsis thaliana MTP1 is a Zn transporter in the vacuolar membrane which mediates Zn detoxification and drives leaf Zn accumulation. *FEBS Letters* **579**: 4165-4174

- Diaz-Mendoza M, Velasco-Arroyo B, Santamaria ME, González-Melendi P, Martinez M, Diaz I** (2016) Plant senescence and proteolysis: two processes with one destiny. *Genetics and Molecular Biology* **39**: 329-338
- Djamei A, Pitzschke A, Nakagami H, Rajh I, Hirt H** (2007) Trojan Horse Strategy in *Agrobacterium* Transformation: Abusing MAPK Defense Signaling. *Science* **318**: 453-456
- Dobin A, Davis CA, Schlesinger F, Drenkow J, Zaleski C, Jha S, Batut P, Chaisson M, Gingeras TR** (2013) STAR: ultrafast universal RNA-seq aligner. *Bioinformatics* **29**: 15-21
- Dosztányi Z, Mészáros B, Simon I** (2009) ANCHOR: web server for predicting protein binding regions in disordered proteins. *Bioinformatics* **25**: 2745-2746
- Dräger DB, Desbrosses-Fonrouge AG, Krach C, Chardonnens AN, Meyer RC, Saumitou-Laprade P, Krämer U** (2004) Two genes encoding *Arabidopsis halleri* MTP1 metal transport proteins co-segregate with zinc tolerance and account for high MTP1 transcript levels. *Plant Journal* **39**: 425-439
- Drevensek S, Goussot M, Duroc Y, Christodoulidou A, Steyaert S, Schaefer E, Duvernois E, Grandjean O, Vantard M, Bouchez D, Pastuglia M** (2012) The *Arabidopsis* TRM1–TON1 Interaction Reveals a Recruitment Network Common to Plant Cortical Microtubule Arrays and Eukaryotic Centrosomes. *The Plant Cell* **24**: 178-191
- Dubeaux G, Neveu J, Zelazny E, Vert G** (2018) Metal Sensing by the IRT1 Transporter-Receptor Orchestrates Its Own Degradation and Plant Metal Nutrition. *Molecular Cell* **69**: 953-964.e955
- Dunker AK, Lawson JD, Brown CJ, Williams RM, Romero P, Oh JS, Oldfield CJ, Campen AM, Ratliff CM, Hipps KW, Ausio J, Nissen MS, Reeves R, Kang C, Kissinger CR, Bailey RW, Griswold MD, Chiu W, Garner EC, Obradovic Z** (2001) Intrinsically disordered protein. *Journal of Molecular Graphics and Modelling* **19**: 26-59
- Durrett TP, Gassmann W, Rogers EE** (2007) The FRD3-Mediated Efflux of Citrate into the Root Vasculature Is Necessary for Efficient Iron Translocation. *Plant Physiology* **144**: 197-205
- Dykema PE, Sipes PR, Marie A, Biermann BJ, Crowell DN, Randall SK** (1999) A new class of proteins capable of binding transition metals. *Plant Molecular Biology* **41**: 139-150

- Eide D, Broderius M, Fett J, Guerinot ML** (1996) A novel iron-regulated metal transporter from plants identified by functional expression in yeast. *Proceedings of the National Academy of Sciences of the United States of America* **93**: 5624-5628
- Eide DJ** (2006) Zinc transporters and the cellular trafficking of zinc. *Biochimica et Biophysica Acta - Molecular Cell Research* **1763**: 711-722
- Eide DJ** (2009) Homeostatic and Adaptive Responses to Zinc Deficiency in *Saccharomyces cerevisiae*. *The Journal of Biological Chemistry* **284**: 18565-18569
- Eren E, Argüello JM** (2004) Arabidopsis HMA2, a divalent heavy metal-transporting P(1B)-type ATPase, is involved in cytoplasmic Zn<sup>2+</sup> homeostasis. *Plant Physiology* **136**: 3712-3723
- Essigmann B, Güler S, Narang RA, Linke D, Benning C** (1998) Phosphate availability affects the thylakoid lipid composition and the expression of SQD1, a gene required for sulfolipid biosynthesis in *Arabidopsis thaliana*. *Proceedings of the National Academy of Sciences* **95**: 1950-1955
- Evans GW** (1986) Zinc and its deficiency diseases. *Clinical Physiology and Biochemistry* **4**: 94-98
- Evrard A, Bargmann BOR, Birnbaum KD, Tester M, Baumann U, Johnson AAT** (2012) Fluorescence-Activated Cell Sorting for Analysis of Cell Type-Specific Responses to Salinity Stress in *Arabidopsis* and Rice. *Methods in molecular biology* (Clifton, N.J.) **913**: 265-276
- Feeney KA, Hansen LL, Putker M, Olivares-Yañez C, Day J, Eades LJ, Larrondo LF, Hoyle NP, O'Neill JS, van Ooijen G** (2016) Daily magnesium fluxes regulate cellular timekeeping and energy balance. *Nature* **532**: 375-379
- Ferrández-Ayela A, Micol-Ponce R, Sánchez-García AB, Alonso-Peral MM, Micol JL, Ponce MR** (2013) Mutation of an Arabidopsis NatB N-Alpha-Terminal Acetylation Complex Component Causes Pleiotropic Developmental Defects. *PLOS ONE* **8**: e80697
- Fisher RA** (1919) XV.—The Correlation between Relatives on the Supposition of Mendelian Inheritance. *Transactions of the Royal Society of Edinburgh* **52**: 399-433
- Fitter DW, Martin DJ, Copley MJ, Scotland RW, Langdale JA** (2002) GLK gene pairs regulate chloroplast development in diverse plant species. *The Plant Journal* **31**: 713-727



- Floris M, Mahgoub H, Lanet E, Robaglia C, Menand B** (2009) Post-transcriptional Regulation of Gene Expression in Plants during Abiotic Stress. *International Journal of Molecular Sciences* **10**: 3168-3185
- Fong JH, Shoemaker BA, Garbuzynskiy SO, Lobanov MY, Galzitskaya OV, Panchenko AR** (2009) Intrinsic Disorder in Protein Interactions: Insights From a Comprehensive Structural Analysis. *PLOS Computational Biology* **5**: e1000316
- Fournier-Level A, Korte A, Cooper MD, Nordborg M, Schmitt J, Wilczek AM** (2011) A map of local adaptation in *Arabidopsis thaliana*. *Science* **334**: 86-89
- Franks SJ** (2011) Plasticity and evolution in drought avoidance and escape in the annual plant *Brassica rapa*. *New Phytologist* **190**: 249-257
- Friso G, van Wijk KJ** (2015) Posttranslational Protein Modifications in Plant Metabolism. *Plant Physiology* **169**: 1469-1487
- Gabriel KR** (1971) The Biplot Graphic Display of Matrices with Application to Principal Component Analysis. *Biometrika* **58**: 453-467
- Gagne JM, Smalle J, Gingerich DJ, Walker JM, Yoo S-D, Yanagisawa S, Vierstra RD** (2004) *Arabidopsis* EIN3-binding F-box 1 and 2 form ubiquitin-protein ligases that repress ethylene action and promote growth by directing EIN3 degradation. *Proceedings of the National Academy of Sciences of the United States of America* **101**: 6803-6808
- Galbraith DW** (2014) Flow cytometry and sorting in *Arabidopsis*. *Methods in molecular biology* (Clifton, N.J.) **1062**: 509-537
- Galea CA, Wang Y, Sivakolundu SG, Kriwacki RW** (2008) Regulation of Cell Division by Intrinsically Unstructured Proteins; Intrinsic Flexibility, Modularity and Signaling Conduits. *Biochemistry* **47**: 7598-7609
- Gao W, Xiao S, Li H-Y, Tsao S-W, Chye M-L** (2009) *Arabidopsis thaliana* acyl-CoA-binding protein ACBP2 interacts with heavy-metal-binding farnesylated protein AtFP6. *New Phytologist* **181**: 89-102
- García MJ, Lucena C, Romera FJ, Alcántara E, Pérez-Vicente R** (2010) Ethylene and nitric oxide involvement in the up-regulation of key genes related to iron acquisition and homeostasis in *Arabidopsis*. *Journal of Experimental Botany* **61**: 3885-3899
- Gasber A, Klaumann S, Trentmann O, Trampczynska A, Clemens S, Schneider S, Sauer N, Feifer I, Bittner F, Mendel RR, Neuhaus HE** (2011) Identification of an *Arabidopsis* solute carrier critical for intracellular transport and inter-organ allocation of molybdate. *Plant Biology* **13**: 710-718
- Geldner N** (2013) Casparian strips. *Current Biology* **23**: R1025-R1026

- Ghandilyan A, Barboza L, Tisné S, Granier C, Reymond M, Koornneef M, Schat H, Aarts MGM** (2009) Genetic analysis identifies quantitative trait loci controlling rosette mineral concentrations in *Arabidopsis thaliana* under drought. *New Phytologist* **184**: 180-192
- Ghandilyan A, Kutman UB, Kutman BY, Cakmak I, Aarts MGM** (2012) Genetic analysis of the effect of zinc deficiency on *Arabidopsis* growth and mineral concentrations. *Plant and Soil* **361**: 227-239
- Ghandilyan A, Vreugdenhil D, Aarts MGM** (2006) Progress in the genetic understanding of plant iron and zinc nutrition. *Physiologia Plantarum* **126**: 407-417
- Gibbs DJ** (2015) Emerging Functions for N-Terminal Protein Acetylation in Plants. *Trends in Plant Science* **20**: 599-601
- Gibson G** (2010) Hints of hidden heritability in GWAS. **42**: 558-560
- Giedroc DP, Arunkumar AI** (2007) Metal sensor proteins: nature's metalloregulated allosteric switches. *Dalton Transactions*: 3107-3120
- Gilkerson J, Perez-Ruiz JM, Chory J, Callis J** (2012) The plastid-localized pfkB-type carbohydrate kinases FRUCTOKINASE-LIKE 1 and 2 are essential for growth and development of *Arabidopsis thaliana*. *BMC Plant Biology* **12**: 102
- Gómez-Mena C, de Folter S, Costa MMR, Angenent GC, Sablowski R** (2005) Transcriptional program controlled by the floral homeotic gene AGAMOUS during early organogenesis. *Development* **132**: 429-438
- Graham RD** (2008) Micronutrient Deficiencies in Crops and Their Global Significance. *In* BJ Alloway, ed, *Micronutrient Deficiencies in Global Crop Production*. Springer Netherlands, Dordrecht, pp 41-61
- Grotz N, Fox T, Connolly E, Park W, Guerinot ML, Eide D** (1998) Identification of a family of zinc transporter genes from *Arabidopsis* that respond to zinc deficiency. *Proceedings of the National Academy of Sciences of the United States of America* **95**: 7220-7224
- Grotz N, Guerinot ML** (2006) Molecular aspects of Cu, Fe and Zn homeostasis in plants. *Biochimica et Biophysica Acta - Molecular Cell Research* **1763**: 595-608
- Grundy J, Stoker C, Carré IA** (2015) Circadian regulation of abiotic stress tolerance in plants. *Frontiers in Plant Science* **6**
- Guerra AJ, Giedroc DP** (2012) Metal site occupancy and allosteric switching in bacterial metal sensor proteins. *Archives of Biochemistry and Biophysics* **519**: 210-222
- Gusev A, Bhatia G, Zaitlen N, Vilhjalmsen BJ, Diogo D, Stahl EA, Gregersen PK, Worthington J, Klareskog L, Raychaudhuri S, Plenge RM, Pasaniuc B, Price AL**

- (2013) Quantifying Missing Heritability at Known GWAS Loci. *PLOS Genetics* **9**: e1003993
- Gustin, J, E. LM, Donggiun K, Gunnam N, Marina T, E. SD** (2009) MTP1-dependent Zn sequestration into shoot vacuoles suggests dual roles in Zn tolerance and accumulation in Zn-hyperaccumulating plants. *The Plant Journal* **57**: 1116-1127
- Hacisalihoglu G, Kochian LV** (2003) How do some plants tolerate low levels of soil zinc? Mechanisms of zinc efficiency in crop plants. *New Phytologist* **159**: 341-350
- Haina Z, Uwe S** (2017) Differences and commonalities of plant responses to single and combined stresses. *The Plant Journal* **90**: 839-855
- Hausmann A, Aguilar Netz DJ, Balk J, Pierik AJ, Mühlenhoff U, Lill R** (2005) The eukaryotic P loop NTPase Nbp35: An essential component of the cytosolic and nuclear iron–sulfur protein assembly machinery. *Proceedings of the National Academy of Sciences of the United States of America* **102**: 3266-3271
- Haydon MJ, Bell LJ, Webb AAR** (2011) Interactions between plant circadian clocks and solute transport. *Journal of Experimental Botany* **62**: 2333-2348
- Haydon MJ, Cobbett CS** (2007) Transporters of ligands for essential metal ions in plants. *New Phytologist* **174**: 499-506
- Haydon MJ, Román Á, Arshad W** (2015) Nutrient homeostasis within the plant circadian network. *Frontiers in Plant Science* **6**: 299
- He L, Su C, Wang Y, Wei Z** (2015) ATDOF5.8 protein is the upstream regulator of ANAC069 and is responsive to abiotic stress. *Biochimie* **110**: 17-24
- Henriques R, Jásik J, Klein M, Martinoia E, Feller U, Schell J, Pais MS, Koncz C** (2002) Knock-out of Arabidopsis metal transporter gene IRT1 results in iron deficiency accompanied by cell differentiation defects. *Plant Molecular Biology* **50**: 587-597
- Hermans C, Conn SJ, Chen J, Xiao Q, Verbruggen N** (2013) An update on magnesium homeostasis mechanisms in plants. *Metallomics* **5**: 1170-1183
- Himelblau E, Amasino RM** (2001) Nutrients mobilized from leaves of Arabidopsis thaliana during leaf senescence. *Journal of Plant Physiology* **158**: 1317-1323
- Hindt MN, Guerinot ML** (2012) Getting a sense for signals: regulation of the plant iron deficiency response. *Biochimica et biophysica acta* **1823**: 1521-1530
- Ho C-H, Lin S-H, Hu H-C, Tsay Y-F** (2009) CHL1 Functions as a Nitrate Sensor in Plants. *Cell* **138**: 1184-1194

## References

---

- Hong S, Kim SA, Guerinot ML, McClung CR** (2013) Reciprocal Interaction of the Circadian Clock with the Iron Homeostasis Network in Arabidopsis. *Plant Physiology* **161**: 893-903
- Horstman A, Fukuoka H, Muino Acuna JM, Nitsch LMC, Guo C, Passarinho PA, Sanchez Perez GF, Immink RGH, Angenent GC, Boutilier KA** (2015) AIL and HDG proteins act antagonistically to control cell proliferation. *In*, Vol 142. Development, pp 454-464
- Horton MW, Hancock AM, Huang YS, Toomajian C, Atwell S, Auton A, Mulyati NW, Platt A, Sperone FG, Vilhjalmsen BJ, Nordborg M, Borevitz JO, Bergelson J** (2012) Genome-wide patterns of genetic variation in worldwide Arabidopsis thaliana accessions from the RegMap panel. **44**: 212-216
- Hruz T, Laule O, Szabo G, Wessendorp F, Bleuler S, Oertle L, Widmayer P, Gruissem W, Zimmermann P** (2008) Genevestigator V3: A Reference Expression Database for the Meta-Analysis of Transcriptomes. *Advances in Bioinformatics* **2008**: 5
- Huang C, Barker SJ, Langridge P, Smith FW, Graham RD** (2000) Zinc Deficiency Up-Regulates Expression of High-Affinity Phosphate Transporter Genes in Both Phosphate-Sufficient and -Deficient Barley Roots. *Plant Physiology* **124**: 415-422
- Huang DW, Sherman BT, Lempicki RA** (2008) Systematic and integrative analysis of large gene lists using DAVID bioinformatics resources. **4**: 44
- Huang DW, Sherman BT, Lempicki RA** (2009) Bioinformatics enrichment tools: paths toward the comprehensive functional analysis of large gene lists. *Nucleic Acids Research* **37**: 1-13
- Huang X-Y, Salt David E** (2016) Plant Ionomics: From Elemental Profiling to Environmental Adaptation. *Molecular Plant* **9**: 787-797
- Huot B, Yao J, Montgomery BL, He SY** (2014) Growth–Defense Tradeoffs in Plants: A Balancing Act to Optimize Fitness. *Molecular Plant* **7**: 1267-1287
- Hurst LD, Pál C, Lercher MJ** (2004) The evolutionary dynamics of eukaryotic gene order. **5**: 299
- Hussain D, Haydon MJ, Wang Y, Wong E, Sherson SM, Young J, Camakaris J, Harper JF, Cobbett CS** (2004) P-type ATPase heavy metal transporters with roles in essential zinc homeostasis in arabidopsis. *Plant Cell* **16**: 1327-1339
- Iakoucheva LM, Brown CJ, Lawson JD, Obradović Z, Dunker AK** (2002) Intrinsic Disorder in Cell-signaling and Cancer-associated Proteins. *Journal of Molecular Biology* **323**: 573-584

- Immink RGH, Tonaco IAN, de Folter S, Shchennikova A, van Dijk ADJ, Busscher-Lange J, Borst JW, Angenent GC** (2009) SEPALLATA3: the 'glue' for MADS box transcription factor complex formation. *Genome Biology* **10**: R24-R24
- Ishijima S, Shigemi Z, Adachi H, Makinouchi N, Sagami I** (2012) Functional reconstitution and characterization of the Arabidopsis Mg<sup>2+</sup> transporter AtMRS2-10 in proteoliposomes. *Biochimica et Biophysica Acta (BBA) - Biomembranes* **1818**: 2202-2208
- Jammes F, Lecomte P, de Almeida-Engler J, Bitton F, Martin-Magniette M-L, Renou JP, Abad P, Favery B** (2005) Genome-wide expression profiling of the host response to root-knot nematode infection in Arabidopsis. *The Plant Journal* **44**: 447-458
- Jin J, Xie X, Chen C, Park JG, Stark C, James DA, Olhovskiy M, Lindling R, Mao Y, Pawson T** (2009) Eukaryotic Protein Domains as Functional Units of Cellular Evolution. *Science Signaling* **2**: ra76-ra76
- Johnson C, Knight M, Kondo T, Masson P, Sedbrook J, Haley A, Trewavas A** (1995) Circadian oscillations of cytosolic and chloroplastic free calcium in plants. *Science* **269**: 1863-1865
- Jung J-H, Lee S, Yun J, Lee M, Park C-M** (2014) The miR172 target TOE3 represses AGAMOUS expression during Arabidopsis floral patterning. *Plant Science* **215-216**: 29-38
- Kammler M, Schön C, Hantke K** (1993) Characterization of the ferrous iron uptake system of Escherichia coli. *Journal of Bacteriology* **175**: 6212-6219
- Karve TM, Cheema AK** (2011) Small Changes Huge Impact: The Role of Protein Posttranslational Modifications in Cellular Homeostasis and Disease. *Journal of Amino Acids* **2011**
- Kasai K, Takano J, Miwa K, Toyoda A, Fujiwara T** (2011) High Boron-induced Ubiquitination Regulates Vacuolar Sorting of the BOR1 Borate Transporter in Arabidopsis thaliana. *Journal of Biological Chemistry* **286**: 6175-6183
- Kasajima I, Fujiwara T** (2007) Identification of novel Arabidopsis thaliana genes which are induced by high levels of boron. *Plant Biotechnology* **24**: 355-360
- Kasuga M, Liu Q, Miura S, Yamaguchi-Shinozaki K, Shinozaki K** (1999) Improving plant drought, salt, and freezing tolerance by gene transfer of a single stress-inducible transcription factor. *Nature Biotechnology* **17**: 287
- Kazan K, Lyons R** (2016) The link between flowering time and stress tolerance. *Journal of Experimental Botany* **67**: 47-60

- Kessler D, Papenbrock J** (2005) Iron–sulfur cluster biosynthesis in photosynthetic organisms. *Photosynthesis Research* **86**: 391-407
- Kim HS, Park BO, Yoo JH, Jung MS, Lee SM, Han HJ, Kim KE, Kim SH, Lim CO, Yun D-J, Lee SY, Chung WS** (2007) Identification of a Calmodulin-binding NAC Protein as a Transcriptional Repressor in Arabidopsis. *Journal of Biological Chemistry* **282**: 36292-36302
- Kim K-C, Lai Z, Fan B, Chen Z** (2008) Arabidopsis WRKY38 and WRKY62 Transcription Factors Interact with Histone Deacetylase 19 in Basal Defense. *The Plant Cell* **20**: 2357-2371
- Kim S-G, Kim S-Y, Park C-M** (2007) A membrane-associated NAC transcription factor regulates salt-responsive flowering via FLOWERING LOCUS T in Arabidopsis. *Planta* **226**: 647-654
- Kim S-G, Lee A-K, Yoon H-K, Park C-M** (2008) A membrane-bound NAC transcription factor NTL8 regulates gibberellic acid-mediated salt signaling in Arabidopsis seed germination. *The Plant Journal* **55**: 77-88
- Kim S, Plagnol V, Hu TT, Toomajian C, Clark RM, Ossowski S, Ecker JR, Weigel D, Nordborg M** (2007) Recombination and linkage disequilibrium in Arabidopsis thaliana. **39**: 1151-1155
- Kim W-Y, Ali Z, Park HJ, Park SJ, Cha J-Y, Perez-Hormaeche J, Quintero FJ, Shin G, Kim MR, Qiang Z, Ning L, Park HC, Lee SY, Bressan RA, Pardo JM, Bohnert HJ, Yun D-J** (2013) Release of SOS2 kinase from sequestration with GIGANTEA determines salt tolerance in Arabidopsis. *Nature Communications* **4**: 1352
- Kim Y-S, Sakuraba Y, Han S-H, Yoo S-C, Paek N-C** (2013) Mutation of the Arabidopsis NAC016 Transcription Factor Delays Leaf Senescence. *Plant and Cell Physiology* **54**: 1660-1672
- Klein P, Seidel T, Stöcker B, Dietz K-J** (2012) The membrane-tethered transcription factor ANAC089 serves as redox-dependent suppressor of stromal ascorbate peroxidase gene expression. *Frontiers in Plant Science* **3**: 247
- Knoth C, Eulgem T** (2008) The oomycete response gene LURP1 is required for defense against *Hyaloperonospora parasitica* in Arabidopsis thaliana. *The Plant Journal* **55**: 53-64
- Kobae Y, Uemura T, Sato MH, Ohnishi M, Mimura T, Nakagawa T, Maeshima M** (2004) Zinc transporter of Arabidopsis thaliana AtMTP1 is localized to vacuolar membranes and implicated in zinc homeostasis. *Plant and Cell Physiology* **45**: 1749-1758

- Konstantinopoulos PA, Karamouzis MV, Papavassiliou AG** (2007) Post-translational modifications and regulation of the RAS superfamily of GTPases as anticancer targets. *Nature Reviews Drug Discovery* **6**: 541
- Koornneef M, Alonso-Blanco C, Vreugdenhil D** (2004) Naturally occurring genetic variation in *Arabidopsis thaliana* *Annual Review of Plant Biology* **55**: 141-172
- Koornneef M, Meinke D** (2010) The development of *Arabidopsis* as a model plant. *The Plant Journal* **61**: 909-921
- Korshunova YO, Eide D, Clark WG, Guerinot ML, Pakrasi HB** (1999) The IRT1 protein from *Arabidopsis thaliana* is a metal transporter with a broad substrate range. *Plant Molecular Biology* **40**: 37-44
- Korshunova YO, Eide D, Gregg Clark W, Lou Guerinot M, Pakrasi HB** (1999) The IRT1 protein from *Arabidopsis thaliana* is a metal transporter with a broad substrate range. *Plant Molecular Biology* **40**: 37-44
- Korte A, Farlow A** (2013) The advantages and limitations of trait analysis with GWAS: a review. *Plant Methods* **9**: 29
- Korves TM, Bergelson J** (2003) A Developmental Response to Pathogen Infection in *Arabidopsis*. *Plant Physiology* **133**: 339-347
- Kovinich N, Kayanja G, Chanoca A, Riedl K, Otegui MS, Grotewold E** (2014) Not all anthocyanins are born equal: distinct patterns induced by stress in *Arabidopsis*. *Planta* **240**: 931-940
- Kremers G-J, Goedhart J, van Munster EB, Gadella TWJ** (2006) Cyan and Yellow Super Fluorescent Proteins with Improved Brightness, Protein Folding, and FRET Förster Radius. *Biochemistry* **45**: 6570-6580
- Krężel A, Maret W** (2006) Zinc-buffering capacity of a eukaryotic cell at physiological pZn. *JBIC Journal of Biological Inorganic Chemistry* **11**: 1049-1062
- Krężel A, Maret W** (2016) The biological inorganic chemistry of zinc ions. *Archives of Biochemistry and Biophysics* **611**: 3-19
- Kruijer W, Boer MP, Malosetti M, Flood PJ, Engel B, Kooke R, Keurentjes JJB, van Eeuwijk FA** (2015) Marker-Based Estimation of Heritability in Immortal Populations. *Genetics* **199**: 379-398
- Kuepper H, Fang Jie Z, McGrath SP** (1999) Cellular Compartmentation of Zinc in Leaves of the Hyperaccumulator *Thlaspi caerulescens*. *PLANT PHYSIOLOGY -ROCKVILLE PIKE BETHESDA-* **119**: 305-311

- Kwon K-C, Cho MH** (2008) Deletion of the chloroplast-localized AtTerC gene product in *Arabidopsis thaliana* leads to loss of the thylakoid membrane and to seedling lethality. *The Plant Journal* **55**: 428-442
- la Rosa NM-d, Sotillo B, Miskolczi P, Gibbs DJ, Vicente J, Carbonero P, Oñate-Sánchez L, Holdsworth MJ, Bhalerao R, Alabadí D, Blázquez MA** (2014) Large-Scale Identification of Gibberellin-Related Transcription Factors Defines Group VII ETHYLENE RESPONSE FACTORS as Functional DELLA Partners. *Plant Physiology* **166**: 1022-1032
- Law CW, Chen Y, Shi W, Smyth GK** (2014) voom: precision weights unlock linear model analysis tools for RNA-seq read counts. *Genome Biology* **15**: R29
- Lee J-W, Helmann JD** (2007) Functional specialization within the Fur family of metalloregulators. *BioMetals* **20**: 485
- Lee M-H, Jeon HS, Kim HG, Park OKC** (2017) An *Arabidopsis* NAC transcription factor NAC4 promotes pathogen-induced cell death under negative regulation by microRNA164. *New Phytologist* **214**: 343-360
- Li H-Y, Chye M-L** (2004) *Arabidopsis* Acyl-CoA-Binding Protein ACP2 Interacts With an Ethylene-Responsive Element-Binding Protein, AtEBP, via its Ankyrin Repeats. *Plant Molecular Biology* **54**: 233-243
- Li J, Zhang J, Wang X, Chen J** (2010) A membrane-tethered transcription factor ANAC089 negatively regulates floral initiation in *Arabidopsis thaliana*. *Science China Life Sciences* **53**: 1299-1306
- Li L, Tutone AF, Revel SMD, Gardner RC, Luan S** (2001) A Novel Family of Magnesium Transport Genes in *Arabidopsis*. *The Plant Cell* **13**: 2761-2775
- Li X, Zhang H, Ai Q, Liang G, Yu D** (2016) Two bHLH Transcription Factors, bHLH34 and bHLH104, Regulate Iron Homeostasis in *Arabidopsis thaliana*. *Plant Physiology* **170**: 2478-2493
- Li Y, Huang Y, Bergelson J, Nordborg M, Borevitz JO** (2010) Association mapping of local climate-sensitive quantitative trait loci in *Arabidopsis thaliana*. *Proceedings of the National Academy of Sciences* **107**: 21199-21204
- Liang G, Zhang H, Li X, Ai Q, Yu D** (2017) bHLH transcription factor bHLH115 regulates iron homeostasis in *Arabidopsis thaliana*. *Journal of Experimental Botany* **68**: 1743-1755



- Lin XY, Ye YQ, Fan SK, Jin CW, Zheng SJ** (2016) Increased Sucrose Accumulation Regulates Iron-Deficiency Responses by Promoting Auxin Signaling in Arabidopsis Plants. *Plant Physiology* **170**: 907-920
- Lin Y-F, Hassan Z, Talukdar S, Schat H, Aarts MGM** (2016) Expression of the ZNT1 Zinc Transporter from the Metal Hyperaccumulator *Noccaea caerulescens* Confers Enhanced Zinc and Cadmium Tolerance and Accumulation to *Arabidopsis thaliana*. *PLoS ONE* **11**: e0149750
- Lin Y-L, Tsay Y-F** (2017) Influence of differing nitrate and nitrogen availability on flowering control in Arabidopsis. *Journal of Experimental Botany* **68**: 2603-2609
- Lin YF, Liang HM, Yang SY, Boch A, Clemens S, Chen CC, Wu JF, Huang JL, Yeh KC** (2009) Arabidopsis IRT3 is a zinc-regulated and plasma membrane localized zinc/iron transporter. *New Phytologist* **182**: 392-404
- Linster E, Stephan I, Bienvenut WV, Maple-Grødem J, Myklebust LM, Huber M, Reichelt M, Sticht C, Møller SG, Meinel T, Arnesen T, Giglione C, Hell R, Wirtz M** (2015) Downregulation of N-terminal acetylation triggers ABA-mediated drought responses in Arabidopsis. *Nature Communications* **6**
- Liszcak G, Goldberg JM, Foyn H, Petersson EJ, Arnesen T, Marmorstein R** (2013) Molecular Basis for Amino-Terminal Acetylation by the Heterodimeric NatA Complex. *Nature structural & molecular biology* **20**: 1098-1105
- Liu W, Karemera NJU, Wu T, Yang Y, Zhang X, Xu X, Wang Y, Han Z** (2017) The ethylene response factor AtERF4 negatively regulates the iron deficiency response in *Arabidopsis thaliana*. *PLOS ONE* **12**: e0186580
- Liu W, Xie Y, Ma J, Luo X, Nie P, Zuo Z, Lahrmann U, Zhao Q, Zheng Y, Zhao Y, Xue Y, Ren J** (2015) IBS: an illustrator for the presentation and visualization of biological sequences. *Bioinformatics* **31**: 3359-3361
- Liu Y, Ji X, Nie X, Qu M, Zheng L, Tan Z, Zhao H, Huo L, Liu S, Zhang B, Wang YC** (2015) Arabidopsis AtbHLH112 regulates the expression of genes involved in abiotic stress tolerance by binding to their E-box and GCG-box motifs. *New Phytologist* **207**: 692-709
- Liu Y, Xie Y, Wang H, Ma X, Yao W, Wang H** (2017) Light and Ethylene Coordinately Regulate the Phosphate Starvation Response through Transcriptional Regulation of PHOSPHATE STARVATION RESPONSE1. *The Plant Cell* **29**: 2269-2284

- Long Y, Stahl Y, Weidtkamp-Peters S, Postma M, Zhou W, Goedhart J, Sánchez-Pérez M-I, Gadella TWJ, Simon R, Scheres B, Blilou I** (2017) In vivo FRET–FLIM reveals cell-type-specific protein interactions in Arabidopsis roots. *Nature* **548**: 97
- Lopez-Maury L, Marguerat S, Bahler J** (2008) Tuning gene expression to changing environments: from rapid responses to evolutionary adaptation. *9*: 583-593
- Loqué D, Ludewig U, Yuan L, von Wirén N** (2005) Tonoplast Intrinsic Proteins AtTIP2;1 and AtTIP2;3 Facilitate NH<sub>3</sub> Transport into the Vacuole. *Plant Physiology* **137**: 671-680
- Lozano-Durán R, Zipfel C** (2015) Trade-off between growth and immunity: role of brassinosteroids. *Trends in Plant Science* **20**: 12-19
- Lucena C, Waters BM, Romera FJ, García MJ, Morales M, Alcántara E, Pérez-Vicente R** (2006) Ethylene could influence ferric reductase, iron transporter, and H<sup>+</sup>-ATPase gene expression by affecting FER (or FER-like) gene activity. *Journal of Experimental Botany* **57**: 4145-4154
- Mach J** (2012) Plant Cortical Microtubule Arrays: Recruitment Mechanisms in Common with Centrosomes. *The Plant Cell* **24**: 2-2
- Maillard A, Diquélou S, Billard V, Lainé P, Garnica M, Prudent M, Garcia-Mina J-M, Yvin J-C, Ourry A** (2015) Leaf mineral nutrient remobilization during leaf senescence and modulation by nutrient deficiency. *Frontiers in Plant Science* **6**
- Manolio TA, Collins FS, Cox NJ, Goldstein DB, Hindorff LA, Hunter DJ, McCarthy MI, Ramos EM, Cardon LR, Chakravarti A, Cho JH, Guttmacher AE, Kong A, Kruglyak L, Mardis E, Rotimi CN, Slatkin M, Valle D, Whittemore AS, Boehnke M, Clark AG, Eichler EE, Gibson G, Haines JL, Mackay TFC, McCarroll SA, Visscher PM** (2009) Finding the missing heritability of complex diseases. *Nature* **461**: 747-753
- Mao Y-B, Xue X-Y, Tao X-Y, Yang C-Q, Wang L-J, Chen X-Y** (2013) Cysteine protease enhances plant-mediated bollworm RNA interference. *Plant Molecular Biology* **83**: 119-129
- Marjoram P, Zubair A, Nuzhdin SV** (2014) Post-GWAS: where next? More samples, more SNPs or more biology? *Heredity* **112**: 79-88
- Marschner H, Marschner P** (2012) Marschner's mineral nutrition of higher plants. Academic Press, London
- Martínez-Medina A, Van Wees SCM, Pieterse CMJCPCER** (2017) Airborne signals from Trichoderma fungi stimulate iron uptake responses in roots resulting in priming of

- jasmonic acid-dependent defences in shoots of *Arabidopsis thaliana* and *Solanum lycopersicum*. *Plant, Cell & Environment* **40**: 2691-2705
- Mäser P, Thomine S, Schroeder JI, Ward JM, Hirschi K, Sze H, Talke IN, Amtmann A, Maathuis FJM, Sanders D, Harper JF, Tchieu J, Gribskov M, Persans MW, Salt DE, Kim SA, Guerinot ML** (2001) Phylogenetic Relationships within Cation Transporter Families of *Arabidopsis*. *Plant Physiology* **126**: 1646-1667
- Mathilde S, Jean-François B, Grégory V, Catherine C** (2008) Cytokinins negatively regulate the root iron uptake machinery in *Arabidopsis* through a growth-dependent pathway. *The Plant Journal* **55**: 289-300
- Mattiello EM, Ruiz HA, Neves JCL, Ventrella MC, Araújo WL** (2015) Zinc deficiency affects physiological and anatomical characteristics in maize leaves. *Journal of Plant Physiology* **183**: 138-143
- Maurer-Stroh S, Eisenhaber F** (2005) Refinement and prediction of protein prenylation motifs. *Genome Biology* **6**: R55-R55
- Medici A, Marshall-Colon A, Ronzier E, Szponarski W, Wang R, Gojon A, Crawford NM, Ruffel S, Coruzzi GM, Krouk G** (2015) AtNIGT1/HRS1 integrates nitrate and phosphate signals at the *Arabidopsis* root tip. *Nature communications* **6**: 6274-6274
- Meier S, Bastian R, Donaldson L, Murray S, Bajic V, Gehring C** (2008) Co-expression and promoter content analyses assign a role in biotic and abiotic stress responses to plant natriuretic peptides. *BMC Plant Biology* **8**: 24
- Meijón M, Satbhai SB, Tsuchimatsu T, Busch W** (2014) Genome-wide association study using cellular traits identifies a new regulator of root development in *Arabidopsis*. *Nature genetics* **46**: 77-81
- Meinke DW, Cherry JM, Dean C, Rounsley SD, Koornneef M** (1998) *Arabidopsis thaliana*: a model plant for genome analysis. *Science (New York, N.Y.)* **282**: 662, 679-682
- Meinke DW, Meinke LK, Showalter TC, Schissel AM, Mueller LA, Tzafrir I** (2003) A Sequence-Based Map of *Arabidopsis* Genes with Mutant Phenotypes. *Plant Physiology* **131**: 409-418
- Meyers BC, Kozik A, Griego A, Kuang H, Michelmore RW** (2003) Genome-Wide Analysis of NBS-LRR-Encoding Genes in *Arabidopsis*. *The Plant Cell* **15**: 809-834
- Miller M, Song Q, Shi X, Juenger TE, Chen ZJ** (2015) Natural variation in timing of stress-responsive gene expression predicts heterosis in intraspecific hybrids of *Arabidopsis*. *Nature Communications* **6**: 7453

- Mills RF, Krijger GC, Baccarini PJ, Hall JL, Williams LE** (2003) Functional expression of AtHMA4, a P1B-type ATPase of the Zn/Co/Cd/Pb subclass. *The Plant Journal* **35**: 164-176
- Milner MJ, Seamon J, Craft E, Kochian LV** (2013) Transport properties of members of the ZIP family in plants and their role in Zn and Mn homeostasis. *Journal of Experimental Botany* **64**: 369-381
- Mitrophanov AY, Groisman EA** (2008) Positive feedback in cellular control systems. *BioEssays : news and reviews in molecular, cellular and developmental biology* **30**: 542-555
- Mittler R** (2002) Oxidative stress, antioxidants and stress tolerance. *Trends in Plant Science* **7**: 405-410
- Montanini B, Blaudez D, Jeandroz S, Sanders D, Chalot M** (2007) Phylogenetic and functional analysis of the Cation Diffusion Facilitator (CDF) family: improved signature and prediction of substrate specificity. *BMC Genomics* **8**: 107
- Moore RC, Grant SR, Purugganan MD** (2005) Molecular Population Genetics of Redundant Floral-Regulatory Genes in *Arabidopsis thaliana*. *Molecular Biology and Evolution* **22**: 91-103
- Morel M, Crouzet J, Gravot A, Auroy P, Leonhardt N, Vavasseur A, Richaud P** (2009) AtHMA3, a P1B-ATPase allowing Cd/Zn/Co/Pb vacuolar storage in *Arabidopsis*. *Plant Physiology* **149**: 894-904
- Müller D, Schmitz G, Theres K** (2006) Blind Homologous R2R3 Myb Genes Control the Pattern of Lateral Meristem Initiation in *Arabidopsis*. *The Plant Cell* **18**: 586-597
- Müller O, Krawinkel M** (2005) Malnutrition and health in developing countries. *CMAJ : Canadian Medical Association Journal* **173**: 279-286
- Murgia I, Vigani G** (2015) Analysis of *Arabidopsis thaliana* atfer4-1, atfh and atfer4-1/atfh mutants uncovers frataxin and ferritin contributions to leaf ionome homeostasis. *Plant Physiology and Biochemistry* **94**: 65-72
- Murmu J, Wilton M, Allard G, Pandeya R, Desveaux D, Singh J, Subramaniam R** (2014) *Arabidopsis* GOLDEN2-LIKE (GLK) transcription factors activate jasmonic acid (JA)-dependent disease susceptibility to the biotrophic pathogen *Hyaloperonospora arabidopsidis*, as well as JA-independent plant immunity against the necrotrophic pathogen *Botrytis cinerea*. *Molecular Plant Pathology* **15**: 174-184

- Nakashima K, Takasaki H, Mizoi J, Shinozaki K, Yamaguchi-Shinozaki K** (2012) NAC transcription factors in plant abiotic stress responses. *Biochimica et Biophysica Acta (BBA) - Gene Regulatory Mechanisms* **1819**: 97-103
- Nichols BA, Hopkins BG, Jolley VD, Webb BL, Greenwood BG, Buck JR** (2012) Phosphorus and zinc interactions and their relationships with other nutrients in maize grown in chelator-buffered nutrient solution. *Journal of Plant Nutrition* **35**: 123-141
- Nie P, Li X, Wang S, Guo J, Zhao H, Niu D** (2017) Induced Systemic Resistance against *Botrytis cinerea* by *Bacillus cereus* AR156 through a JA/ET- and NPR1-Dependent Signaling Pathway and Activates PAMP-Triggered Immunity in *Arabidopsis*. *Frontiers in Plant Science* **8**
- Nielsen FH** (2012) History of Zinc in Agriculture. *Advances in Nutrition* **3**: 783-789
- Nishida S, Kato A, Tsuzuki C, Yoshida J, Mizuno T** (2015) Induction of Nickel Accumulation in Response to Zinc Deficiency in *Arabidopsis thaliana*. *International Journal of Molecular Sciences* **16**: 9420
- Nolan TM, Brennan B, Yang M, Chen J, Zhang M, Li Z, Wang X, Bassham DC, Walley J, Yin Y** (2017) Selective Autophagy of BES1 Mediated by DSK2 Balances Plant Growth and Survival. *Developmental Cell* **41**: 33-46.e37
- Nordborg M, Weigel D** (2008) Next-generation genetics in plants. *Nature* **456**: 720-723
- O'Shea C, Kryger M, Stender Emil GP, Kragelund Birthe B, Willemoës M, Skriver K** (2015) Protein intrinsic disorder in *Arabidopsis* NAC transcription factors: transcriptional activation by ANAC013 and ANAC046 and their interactions with RCD1. *Biochemical Journal* **465**: 281-294
- Ogawa T, Nishimura K, Aoki T, Takase H, Tomizawa K-I, Ashida H, Yokota A** (2009) A Phosphofructokinase B-Type Carbohydrate Kinase Family Protein, NARA5, for Massive Expressions of Plastid-Encoded Photosynthetic Genes in *Arabidopsis*. *Plant Physiology* **151**: 114-128
- Page DR, Grossniklaus U** (2002) The art and design of genetic screens: *Arabidopsis thaliana*. *Nature Reviews Genetics* **3**: 124
- Pagni M, Ioannidis V, Cerutti L, Zahn-Zabal M, Jongeneel CV, Hau J, Martin O, Kuznetsov D, Falquet L** (2007) MyHits: improvements to an interactive resource for analyzing protein sequences. *Nucleic Acids Research* **35**: W433-W437
- Palmer CM, Hindt MN, Schmidt H, Clemens S, Guerinot ML** (2013) MYB10 and MYB72 Are Required for Growth under Iron-Limiting Conditions. *PLoS Genetics* **9**: e1003953

- Pan IC, Tsai H-H, Cheng Y-T, Wen T-N, Buckhout TJ, Schmidt W** (2015) Post-Transcriptional Coordination of the Arabidopsis Iron Deficiency Response is Partially Dependent on the E3 Ligases RING DOMAIN LIGASE1 (RGLG1) and RING DOMAIN LIGASE2 (RGLG2). *Molecular & Cellular Proteomics : MCP* **14**: 2733-2752
- Pang WL, Kaur A, Ratushny AV, Cvetkovic A, Kumar S, Pan M, Arkin AP, Aitchison JD, Adams MWW, Baliga NS** (2013) Metallochaperones Regulate Intracellular Copper Levels. *PLoS Computational Biology* **9**
- Park J-S, Wang M, Park S-J, Lee S-H** (1999) Zinc Finger of Replication Protein A, a Non-DNA Binding Element, Regulates Its DNA Binding Activity through Redox. *Journal of Biological Chemistry* **274**: 29075-29080
- Park J, Kim Y-S, Kim S-G, Jung J-H, Woo J-C, Park C-M** (2011) Integration of Auxin and Salt Signals by the NAC Transcription Factor NTM2 during Seed Germination in Arabidopsis. *Plant Physiology* **156**: 537-549
- Paulsen IT, Saier Jr MH** (1997) A novel family of ubiquitous heavy metal ion transport proteins. *Journal of Membrane Biology* **156**: 99-103
- Pérez-Pérez JM, Candela H, Micol JL** (2009) Understanding synergy in genetic interactions. *Trends in Genetics* **25**: 368-376
- Pérez-Pérez JM, Esteve-Bruna D, González-Bayón R, Kangasjärvi S, Caldana C, Hannah MA, Willmitzer L, Ponce MR, Micol JL** (2013) Functional Redundancy and Divergence within the Arabidopsis RETICULATA-RELATED Gene Family. *Plant Physiology* **162**: 589-603
- Persson DP, Chen A, Aarts MGM, Salt DE, Schjoerring JK, Husted S** (2016) Multi-element bioimaging of Arabidopsis thaliana roots. *Plant Physiology* **172**: 835-847
- Pesaresi P, Gardner NA, Masiero S, Dietzmann A, Eichacker L, Wickner R, Salamini F, Leister D** (2003) Cytoplasmic N-Terminal Protein Acetylation Is Required for Efficient Photosynthesis in Arabidopsis. *The Plant Cell* **15**: 1817
- Petricka JJ, Clay NK, Nelson TM** (2008) Vein patterning screens and the defectively organized tributaries mutants in Arabidopsis thaliana. *The Plant Journal* **56**: 251-263
- Pickett FB, Meeks-Wagner DR** (1995) Seeing double: appreciating genetic redundancy. *The Plant Cell* **7**: 1347-1356
- Pineau C, Loubet S, Lefoulon C, Chalies C, Fizames C, Lacombe B, Ferrand M, Loudet O, Berthomieu P, Richard O** (2012) Natural Variation at the FRD3 MATE Transporter

- Locus Reveals Cross-Talk between Fe Homeostasis and Zn Tolerance in *Arabidopsis thaliana*. *PLoS Genetics* **8**
- Polevoda B, Sherman F** (2000) N $\alpha$ -terminal Acetylation of Eukaryotic Proteins. *Journal of Biological Chemistry* **275**: 36479-36482
- Polevoda B, Sherman F** (2003) Composition and function of the eukaryotic N-terminal acetyltransferase subunits. *Biochemical and Biophysical Research Communications* **308**: 1-11
- Prasad AS** (2003) Zinc deficiency : Has been known of for 40 years but ignored by global health organisations. *BMJ : British Medical Journal* **326**: 409-410
- Prasad AS** (2012) Discovery of human zinc deficiency: 50 years later. *Journal of Trace Elements in Medicine and Biology* **26**: 66-69
- Prasad AS, Miale A, Jr., Farid Z, Sandstead HH, Schultert AR** (1963) Zinc Metabolism in Patients with the Syndrome of Iron Deficiency Anemia, Hepatosplenomegaly, Dwarfism, and Hypogonadism. *Journal of Laboratory and Clinical Medicine* **61**: 537-549
- Printz B, Lutts S, Hausman J-F, Sergeant K** (2016) Copper Trafficking in Plants and Its Implication on Cell Wall Dynamics. *Frontiers in Plant Science* **7**
- Provart NJ, Alonso J, Assmann SM, Bergmann D, Brady SM, Brkljacic J, Browse J, Chapple C, Colot V, Cutler S, Dangl J, Ehrhardt D, Friesner JD, Frommer WB, Grotewold E, Meyerowitz E, Nemhauser J, Nordborg M, Pikaard C, Shanklin J, Somerville C, Stitt M, Torii KU, Waese J, Wagner D, McCourt P** (2016) 50 years of *Arabidopsis* research: Highlights and future directions. *New Phytologist* **209**: 921-944
- Pruneda-Paz JL, Breton G, Nagel DH, Kang SE, Bonaldi K, Doherty CJ, Ravelo S, Galli M, Ecker JR, Kay SA** (2014) A genome-scale resource for the functional characterization of *Arabidopsis* transcription factors. *Cell reports* **8**: 622-632
- Przedpelska-Wasowicz E, Wasowicz P** (2013) Does zinc concentration in the substrate influence the onset of flowering in *Arabidopsis arenosa* (Brassicaceae)? *Plant Growth Regulation* **69**: 87-97
- Puig S, Peñarrubia L** (2009) Placing metal micronutrients in context: transport and distribution in plants. *Current Opinion in Plant Biology* **12**: 299-306
- Ragel P, Ródenas R, García-Martín E, Andrés Z, Villalta I, Nieves-Cordones M, Rivero RM, Martínez V, Pardo JM, Quintero FJ, Rubio F** (2015) The CBL-Interacting

## References

---

- Protein Kinase CIPK23 Regulates HAK5-Mediated High-Affinity K(+) Uptake in Arabidopsis Roots. *Plant Physiology* **169**: 2863-2873
- Ravet K, Touraine B, Boucherez J, Briat J-F, Gaymard F, Cellier F** (2009) Ferritins control interaction between iron homeostasis and oxidative stress in Arabidopsis. *The Plant Journal* **57**: 400-412
- Reed JW, Nagpal P, Bastow RM, Solomon KS, Dowson-Day MJ, Elumalai RP, Millar AJ** (2000) Independent Action of ELF3 and phyB to Control Hypocotyl Elongation and Flowering Time. *Plant Physiology* **122**: 1149-1160
- Regalla LM, Lyons TJ** (2006) Zinc in yeast: mechanisms involved in homeostasis. *Topics in current genetics* **14**: 37-58
- Reyt G, Boudouf S, Boucherez J, Gaymard F, Briat J-F** (2015) Iron- and Ferritin-Dependent Reactive Oxygen Species Distribution: Impact on Arabidopsis Root System Architecture. *Molecular Plant* **8**: 439-453
- Riboni M, Robustelli Test A, Galbiati M, Tonelli C, Conti L** (2014) Environmental stress and flowering time: The photoperiodic connection. *Plant Signaling & Behavior* **9**: e29036
- Riggs JW, Callis J** (2016) Studies of the PfkB Family of Proteins in Arabidopsis thaliana. *The FASEB Journal* **30**: 1164
- Robinson NJ, Winge DR** (2010) Copper metallochaperones. *In Annual Review of Biochemistry*, Vol 79, pp 537-562
- Robinson WD, Carson I, Ying S, Ellis K, Plaxton WC** (2012) Eliminating the purple acid phosphatase AtPAP26 in Arabidopsis thaliana delays leaf senescence and impairs phosphorus remobilization. *New Phytologist* **196**: 1024-1029
- Rockman MV** (2012) The QNT program and the alleles that matter for evolution: all that's gold does not glitter *Evolution* **66**: 1-17
- Roohani N, Hurrell R, Kelishadi R, Schulin R** (2013) Zinc and its importance for human health: An integrative review. *Journal of Research in Medical Sciences : The Official Journal of Isfahan University of Medical Sciences* **18**: 144-157
- Roskoski R** (2003) Protein prenylation: a pivotal posttranslational process. *Biochemical and Biophysical Research Communications* **303**: 1-7
- Rueda-Romero P, Barrero-Sicilia C, Gómez-Cadenas A, Carbonero P, Oñate-Sánchez L** (2012) Arabidopsis thaliana DOF6 negatively affects germination in non-after-ripened seeds and interacts with TCP14. *Journal of Experimental Botany* **63**: 1937-1949



- Sakuraba Y, Han S-H, Lee S-H, Hörtensteiner S, Paek N-C** (2016) Arabidopsis NAC016 promotes chlorophyll breakdown by directly upregulating STAYGREEN1 transcription. *Plant Cell Reports* **35**: 155-166
- Salt DE, Baxter I, Lahner B** (2008) Ionomics and the Study of the Plant Ionome. *Annual Review of Plant Biology* **59**: 709-733
- Sanda S, Leustek T, Theisen MJ, Garavito RM, Benning C** (2001) Recombinant Arabidopsis SQD1 Converts UDP-glucose and Sulfite to the Sulfolipid Head Group Precursor UDP-sulfoquinovose in Vitro. *Journal of Biological Chemistry* **276**: 3941-3946
- Sanz-Fernández M, Rodríguez-Serrano M, Sevilla-Perea A, Pena L, Mingorance MD, Sandalio LM, Romero-Puertas MC** (2017) Screening Arabidopsis mutants in genes useful for phytoremediation. *Journal of Hazardous Materials* **335**: 143-151
- Sappl PG, Heisler MG** (2013) Live-imaging of plant development: Latest approaches. *Current Opinion in Plant Biology* **16**: 33-40
- Schat H, Vooijs R, Kuiper E** (1996) Identical major gene loci for heavy metal tolerances that have independently evolved in different local populations and subspecies of *Silene vulgaris*. *Evolution* **50**: 1888-1895
- Schlichting CD** (1986) The Evolution of Phenotypic Plasticity in Plants. *Annual Review of Ecology and Systematics* **17**: 667-693
- Schmalenbach I, Zhang L, Reymond M, Jiménez-Gómez JM** (2014) The relationship between flowering time and growth responses to drought in the Arabidopsis Landsberg erecta x Antwerp-1 population. *Frontiers in Plant Science* **5**: 609
- Schneeberger K, Ossowski S, Lanz C, Juul T, Petersen AH, Nielsen KL, Jørgensen JE, Weigel D, Andersen SU** (2009) SHOREmap: Simultaneous mapping and mutation identification by deep sequencing. *Nature Methods* **6**: 550-551
- Schneider CA, Rasband WS, Eliceiri KW** (2012) NIH Image to ImageJ: 25 years of image analysis. *Nature Methods* **9**: 671
- Scholz G, Becker R, Pich A, Stephan UW** (1992) Nicotianamine - a common constituent of strategies I and II of iron acquisition by plants: A review. *Journal of Plant Nutrition* **15**: 1647-1665
- Schrader EK, Harstad KG, Matouschek A** (2009) Targeting proteins for degradation. *Nature chemical biology* **5**: 815-822

## References

---

- Scott Reid T, Terry KL, Casey PJ, Beese LS** (2004) Crystallographic Analysis of CaaX Prenyltransferases Complexed with Substrates Defines Rules of Protein Substrate Selectivity. *Journal of Molecular Biology* **343**: 417-433
- Shalem O, Dahan O, Levo M, Martinez MR, Furman I, Segal E, Pilpel Y** (2008) Transient transcriptional responses to stress are generated by opposing effects of mRNA production and degradation. *Molecular Systems Biology* **4**: 223-223
- Shanmugam V, Lo JC, Wu CL, Wang SL, Lai CC, Connolly EL, Huang JL, Yeh KC** (2011) Differential expression and regulation of iron-regulated metal transporters in *Arabidopsis halleri* and *Arabidopsis thaliana* - the role in zinc tolerance. *New Phytologist* **190**: 125-137
- Shannon P, Markiel A, Ozier O, Baliga NS, Wang JT, Ramage D, Amin N, Schwikowski B, Ideker T** (2003) Cytoscape: A Software Environment for Integrated Models of Biomolecular Interaction Networks. *Genome Research* **13**: 2498-2504
- Shimada TL, Shimada T, Hara-Nishimura I** (2010) A rapid and non-destructive screenable marker, FAST, for identifying transformed seeds of *Arabidopsis thaliana*: TECHNICAL ADVANCE. *Plant Journal* **61**: 519-528
- Silverstone AL, Mak PYA, Martinez EC, Sun T** (1997) The New Rga Locus Encodes a Negative Regulator of Gibberellin Response in *Arabidopsis Thaliana*. *Genetics* **146**: 1087-1099
- Sinclair SA, Krämer U** (2012) The zinc homeostasis network of land plants. *Biochimica et Biophysica Acta - Molecular Cell Research* **1823**: 1553-1567
- Sinclair SA, Sherson SM, Jarvis R, Camakaris J, Cobbett CS** (2007) The use of the zinc-fluorophore, Zinpyr-1, in the study of zinc homeostasis in *Arabidopsis* roots: Rapid report. *New Phytologist* **174**: 39-45
- Sivitz AB, Hermand V, Curie C, Vert G** (2012) *Arabidopsis* bHLH100 and bHLH101 Control Iron Homeostasis via a FIT-Independent Pathway. *PLoS ONE* **7**: e44843
- Smaczniak C, Immink RGH, Muiño JM, Blanvillain R, Busscher M, Busscher-Lange J, Dinh QD, Liu S, Westphal AH, Boeren S, Parcy F, Xu L, Carles CC, Angenent GC, Kaufmann K** (2012) Characterization of MADS-domain transcription factor complexes in *Arabidopsis* flower development. *Proceedings of the National Academy of Sciences* **109**: 1560-1565
- Smyth Gordon K** (2004) Linear Models and Empirical Bayes Methods for Assessing Differential Expression in Microarray Experiments. *In* *Statistical Applications in Genetics and Molecular Biology*, Vol 3

- Solovieff N, Cotsapas C, Lee PH, Purcell SM, Smoller JW** (2013) Pleiotropy in complex traits: challenges and strategies. *Nature Reviews Genetics* **14**: 483-495
- Somerville C** (1999) Plant Functional Genomics. *Science* **285**: 380-383
- Sommer AL, Lipman CB** (1926) EVIDENCE ON THE INDISPENSABLE NATURE OF ZINC AND BORON FOR HIGHER GREEN PLANTS. *Plant Physiology* **1**: 231-249
- Song H-R** (2012) Interaction between the Late Elongated hypocotyl (LHY) and Early flowering 3 (ELF3) genes in the Arabidopsis circadian clock. *Genes & Genomics* **34**: 329-337
- Song WY, Choi KS, Kim DY, Geisler M, Park J, Vincenzetti V, Schellenberg M, Kim SH, Lim YP, Noh EW, Lee Y, Martinoia E** (2010) Arabidopsis PCR2 is a zinc exporter involved in both zinc extrusion and long-distance zinc transport. *Plant Cell* **22**: 2237-2252
- Spinner L, Pastuglia M, Belcram K, Pegoraro M, Goussot M, Bouchez D, Schaefer DG** (2010) The function of TONNEAU1 in moss reveals ancient mechanisms of division plane specification and cell elongation in land plants. *Development* **137**: 2733-2742
- Stes E, Depuydt S, De Keyser A, Matthys C, Audenaert K, Yoneyama K, Werbrouck S, Goormachtig S, Vereecke D** (2015) Strigolactones as an auxiliary hormonal defence mechanism against leafy gall syndrome in *Arabidopsis thaliana*. *Journal of Experimental Botany* **66**: 5123-5134
- Sun T-p** (2010) Gibberellin-GID1-DELLA: A Pivotal Regulatory Module for Plant Growth and Development. *Plant Physiology* **154**: 567-570
- Suzuki N, Yamaguchi Y, Koizumi N, Sano H** (2002) Functional characterization of a heavy metal binding protein Cdl19 from *Arabidopsis*. *The Plant Journal* **32**: 165-173
- Swarbreck D, Wilks C, Lamesch P, Berardini TZ, Garcia-Hernandez M, Foerster H, Li D, Meyer T, Muller R, Ploetz L, Radenbaugh A, Singh S, Swing V, Tissier C, Zhang P, Huala E** (2008) The Arabidopsis Information Resource (TAIR): gene structure and function annotation. *Nucleic Acids Research* **36**: D1009-D1014
- Takahashi R, Ishimaru Y, Senoura T, Shimo H, Ishikawa S, Arao T, Nakanishi H, Nishizawa NK** (2011) The OsNRAMP1 iron transporter is involved in Cd accumulation in rice. *Journal of Experimental Botany* **62**: 4843-4850
- Tan QKG, Irish VF** (2006) The Arabidopsis Zinc Finger-Homeodomain Genes Encode Proteins with Unique Biochemical Properties That Are Coordinately Expressed during Floral Development. *Plant Physiology* **140**: 1095-1108

## References

---

- Tanaka M, Wallace IS, Takano J, Roberts DM, Fujiwara T** (2008) NIP6;1 Is a Boric Acid Channel for Preferential Transport of Boron to Growing Shoot Tissues in Arabidopsis. *The Plant Cell* **20**: 2860-2875
- Tarantino D, Santo N, Morandini P, Casagrande F, Braun H-P, Heinemeyer J, Vigani G, Soave C, Murgia I** (2010) AtFer4 ferritin is a determinant of iron homeostasis in Arabidopsis thaliana heterotrophic cells. *Journal of Plant Physiology* **167**: 1598-1605
- Tehseen M, Cairns N, Sherson S, Cobbett CS** (2010) Metallochaperone-like genes in Arabidopsis thaliana. *Metallomics* **2**: 556-564
- Tester M, Leigh RA** (2001) Partitioning of nutrient transport processes in roots. *Journal of Experimental Botany* **52**: 445-457
- The Arabidopsis Genome I** (2000) Analysis of the genome sequence of the flowering plant Arabidopsis thaliana. *Nature* **408**: 796
- Tian G-W, Mohanty A, Chary SN, Li S, Paap B, Drakakaki G, Kopec CD, Li J, Ehrhardt D, Jackson D, Rhee SY, Raikhel NV, Citovsky V** (2004) High-Throughput Fluorescent Tagging of Full-Length Arabidopsis Gene Products in Planta. *Plant Physiology* **135**: 25-38
- Todd WR, Elvehjem CA, Hart EB** (1980) Zinc in the nutrition of the rat. *Nutrition Reviews* **38**: 151-154
- Todesco M, Balasubramanian S, Hu TT, Traw MB, Horton M, Eppl P, Kuhns C, Sureshkumar S, Schwartz C, Lanz C, Laitinen RAE, Huang Y, Chory J, Lipka V, Borevitz JO, Dangl JL, Bergelson J, Nordborg M, Weigel D** (2010) Natural allelic variation underlying a major fitness tradeoff in Arabidopsis thaliana. *Nature* **465**: 632-636
- Tomatsu H, Takano J, Takahashi H, Watanabe-Takahashi A, Shibagaki N, Fujiwara T** (2007) An Arabidopsis thaliana high-affinity molybdate transporter required for efficient uptake of molybdate from soil. *Proceedings of the National Academy of Sciences of the United States of America* **104**: 18807-18812
- Tsugama D, Liu S, Takano T** (2012) A bZIP Protein, VIP1, Is a Regulator of Osmosensory Signaling in Arabidopsis. *Plant Physiology* **159**: 144-155
- Uversky VN, Gillespie JR, Fink AL** (2000) Why are “natively unfolded” proteins unstructured under physiologic conditions? *Proteins: Structure, Function, and Bioinformatics* **41**: 415-427
- van de Mortel JE, Almar Villanueva L, Schat H, Kwekkeboom J, Coughlan S, Moerland PD, Ver Loren van Themaat E, Koornneef M, Aarts MGM** (2006) Large Expression

- Differences in Genes for Iron and Zinc Homeostasis, Stress Response, and Lignin Biosynthesis Distinguish Roots of *Arabidopsis thaliana* and the Related Metal Hyperaccumulator *Thlaspi caerulescens*. *Plant Physiology* **142**: 1127-1147
- van der Lee R, Buljan M, Lang B, Weatheritt RJ, Daughdrill GW, Dunker AK, Fuxreiter M, Gough J, Gsponer J, Jones DT, Kim PM, Kriwacki RW, Oldfield CJ, Pappu RV, Tompa P, Uversky VN, Wright PE, Babu MM** (2014) Classification of Intrinsically Disordered Regions and Proteins. *Chemical Reviews* **114**: 6589-6631
- Van Roey K, Gibson TJ, Davey NE** (2012) Motif switches: decision-making in cell regulation. *Current Opinion in Structural Biology* **22**: 378-385
- van Wersch R, Li X, Zhang Y** (2016) Mighty Dwarfs: *Arabidopsis* Autoimmune Mutants and Their Usages in Genetic Dissection of Plant Immunity. *Frontiers in Plant Science* **7**: 1717
- Varotto C, Maiwald D, Pesaresi P, Jahns P, Salamini F, Leister D** (2002) The metal ion transporter IRT1 is necessary for iron homeostasis and efficient photosynthesis in *Arabidopsis thaliana*. *The Plant Journal* **31**: 589-599
- Vellosillo T, Martínez M, López MA, Vicente J, Cascón T, Dolan L, Hamberg M, Castresana C** (2007) Oxylipins Produced by the 9-Lipoxygenase Pathway in *Arabidopsis* Regulate Lateral Root Development and Defense Responses through a Specific Signaling Cascade. *The Plant Cell* **19**: 831-846
- Verma V, Ravindran P, Kumar PP** (2016) Plant hormone-mediated regulation of stress responses. *BMC Plant Biology* **16**: 86
- Vert G, Briat JF, Curie C** (2001) *Arabidopsis* IRT2 gene encodes a root-periphery iron transporter. *Plant Journal* **26**: 181-189
- Vert G, Chory J** (2009) A Toggle Switch in Plant Nitrate Uptake. *Cell* **138**: 1064-1066
- Vinocur B, Altman A** (2005) Recent advances in engineering plant tolerance to abiotic stress: achievements and limitations. *Current opinion in biotechnology* **16**: 123-132
- Waldron KJ, Rutherford JC, Ford D, Robinson NJ** (2009) Metalloproteins and metal sensing. *Nature* **460**: 823
- Wang N, Cui Y, Liu Y, Fan H, Du J, Huang Z, Yuan Y, Wu H, Ling H-Q** (2013) Requirement and Functional Redundancy of Ib Subgroup bHLH Proteins for Iron Deficiency Responses and Uptake in *Arabidopsis thaliana*. *Molecular Plant* **6**: 503-513
- Waters BM, Chu HH, DiDonato RJ, Roberts LA, Eisley RB, Lahner B, Salt DE, Walker EL** (2006) Mutations in *Arabidopsis* Yellow Stripe-Like1 and Yellow Stripe-Like3

## References

---

- reveal their roles in metal ion homeostasis and loading of metal ions in seeds. *Plant Physiology* **141**: 1446-1458
- Waters MT, Wang P, Korkaric M, Capper RG, Saunders NJ, Langdale JA** (2009) GLK Transcription Factors Coordinate Expression of the Photosynthetic Apparatus in *Arabidopsis*. *The Plant Cell* **21**: 1109-1128
- Weber K, Burow M** (2018) Nitrogen – essential macronutrient and signal controlling flowering time. *Physiologia Plantarum* **162**: 251-260
- Weigel D** (2012) Natural variation in *Arabidopsis*: From molecular genetics to ecological genomics. *Plant Physiology* **158**: 2-22
- Weigel D, Mott R** (2009) The 1001 Genomes Project for *Arabidopsis thaliana*. *Genome Biology* **10**: 107-107
- Weis-Garcia F, Bandura D, Baranov V, Ornatsky O, Tanner S** (2013) The Means: Cytometry and Mass Spectrometry Converge in a Single Cell Deep Profiling Platform. *Journal of Biomolecular Techniques : JBT* **24**: S12-S12
- Williams RJP** (1984) Zinc: what is its role in biology? *Endeavour* **8**: 65-70
- Winter D, Vinegar B, Nahal H, Ammar R, Wilson GV, Provart NJ** (2007) An “Electronic Fluorescent Pictograph” Browser for Exploring and Analyzing Large-Scale Biological Data Sets. *PLOS ONE* **2**: e718
- Wintz H, Fox T, Wu Y-Y, Feng V, Chen W, Chang H-S, Zhu T, Vulpe C** (2003) Expression Profiles of *Arabidopsis thaliana* in Mineral Deficiencies Reveal Novel Transporters Involved in Metal Homeostasis. *Journal of Biological Chemistry* **278**: 47644-47653
- Wintz H, Vulpe C** (2002) Plant copper chaperones. *Biochemical Society Transactions* **30**: 732-735
- Wolters H, Jürgens G** (2009) Survival of the flexible: hormonal growth control and adaptation in plant development. **10**: 305
- Woodroffe CC, Masalha R, Barnes KR, Frederickson CJ, Lippard SJ** (2004) Membrane-Permeable and -Impermeable Sensors of the Zinpyr Family and Their Application to Imaging of Hippocampal Zinc In Vivo. *Chemistry & Biology* **11**: 1659-1666
- Wright PE, Dyson HJ** (1999) Intrinsically unstructured proteins: re-assessing the protein structure-function paradigm. *Journal of Molecular Biology* **293**: 321-331
- Wu H, Chen C, Du J, Liu H, Cui Y, Zhang Y, He Y, Wang Y, Chu C, Feng Z, Li J, Ling H-Q** (2012) Co-Overexpression FIT with AtbHLH38 or AtbHLH39 in *Arabidopsis*-Enhanced Cadmium Tolerance via Increased Cadmium Sequestration in Roots and Improved Iron Homeostasis of Shoots. *Plant Physiology* **158**: 790-800

- Wu Y, Zhao Q, Gao L, Yu X-M, Fang P, Oliver DJ, Xiang C-B** (2010) Isolation and characterization of low-sulphur-tolerant mutants of Arabidopsis. *Journal of Experimental Botany* **61**: 3407-3422
- Xu F, Huang Y, Li L, Gannon P, Linster E, Huber M, Kapos P, Bienvenut W, Polevoda B, Meinnel T, Hell R, Giglione C, Zhang Y, Wirtz M, Chen S, Li X** (2015) Two N-Terminal Acetyltransferases Antagonistically Regulate the Stability of a Nod-Like Receptor in Arabidopsis. *The Plant Cell* **27**: 1547-1562
- Xu J, Li H-D, Chen L-Q, Wang Y, Liu L-L, He L, Wu W-H** (2006) A Protein Kinase, Interacting with Two Calcineurin B-like Proteins, Regulates K<sup>+</sup>-Transporter AKT1 in Arabidopsis. *Cell* **125**: 1347-1360
- Yan JY, Li CX, Sun L, Ren JY, Li GX, Ding ZJ, Zheng SJ** (2016) A WRKY Transcription Factor Regulates Fe Translocation under Fe Deficiency. *Plant Physiology* **171**: 2017-2027
- Yang J, Benyamin B, McEvoy BP, Gordon S, Henders AK, Nyholt DR, Madden PA, Heath AC, Martin NG, Montgomery GW, Goddard ME, Visscher PM** (2010) Common SNPs explain a large proportion of the heritability for human height. *Nature genetics* **42**: 565-569
- Yang Z, Tian L, Latoszek-Green M, Brown D, Wu K** (2005) Arabidopsis ERF4 is a transcriptional repressor capable of modulating ethylene and abscisic acid responses. *Plant Molecular Biology* **58**: 585-596
- Yosef N, Regev A** (2011) Impulse control: Temporal dynamics in gene transcription. *Cell* **144**: 886-896
- Yruela I** (2013) Transition metals in plant photosynthesis. *Metallomics* **5**: 1090-1109
- Yu J-H, Hamari Z, Han K-H, Seo J-A, Reyes-Domínguez Y, Scazzocchio C** (2004) Double-joint PCR: a PCR-based molecular tool for gene manipulations in filamentous fungi. *Fungal Genetics and Biology* **41**: 973-981
- Yu Q, Tian H, Yue K, Liu J, Zhang B, Li X, Ding Z** (2016) A P-Loop NTPase Regulates Quiescent Center Cell Division and Distal Stem Cell Identity through the Regulation of ROS Homeostasis in Arabidopsis Root. *PLOS Genetics* **12**: e1006175
- Yuan Y, Wu H, Wang N, Li J, Zhao W, Du J, Wang D, Ling H-Q** (2008) FIT interacts with AtbHLH38 and AtbHLH39 in regulating iron uptake gene expression for iron homeostasis in Arabidopsis. **18**: 385-397

- Zamioudis C, Hanson J, Pieterse CMJC** (2014)  $\beta$ -Glucosidase BGLU42 is a MYB72-dependent key regulator of rhizobacteria-induced systemic resistance and modulates iron deficiency responses in Arabidopsis roots. *New Phytologist* **204**: 368-379
- Zamioudis C, Korteland J, Van Pelt JA, van Hamersveld M, Dombrowski N, Bai Y, Hanson J, Van Verk MC, Ling H-Q, Schulze-Lefert P, Pieterse CMJ** (2015) Rhizobacterial volatiles and photosynthesis-related signals coordinate MYB72 expression in Arabidopsis roots during onset of induced systemic resistance and iron-deficiency responses. *The Plant Journal* **84**: 309-322
- Zhang F, Qi B, Wang L, Zhao B, Rode S, Riggan ND, Ecker JR, Qiao H** (2016) EIN2-dependent regulation of acetylation of histone H3K14 and non-canonical histone H3K23 in ethylene signalling. *Nature Communications* **7**: 13018
- Zhang F, Wang L, Ko EE, Shao K, Qiao H** (2018) Histone Deacetylases SRT1 and SRT2 Interact with ENAP1 to Mediate Ethylene-Induced Transcriptional Repression. *The Plant Cell* **30**: 153-166
- Zhang F, Wang L, Qi B, Zhao B, Ko EE, Riggan ND, Chin K, Qiao H** (2017) EIN2 mediates direct regulation of histone acetylation in the ethylene response. *Proceedings of the National Academy of Sciences* **114**: 10274-10279
- Zhang J, Liu B, Li M, Feng D, Jin H, Wang P, Liu J, Xiong F, Wang J, Wang HB** (2015) The bHLH transcription factor bHLH104 interacts with IAA-LEUCINE RESISTANT3 and modulates iron homeostasis in Arabidopsis. *Plant Cell* **27**: 787–805
- Zhang X, Huai J, Shang F, Xu G, Tang W, Jing Y, Lin R** (2017) A PIF1/PIF3-HY5-BBX23 Transcription Factor Cascade Affects Photomorphogenesis. *Plant Physiology* **174**: 2487-2500
- Zhang Y, Goritschnig S, Dong X, Li X** (2003) A Gain-of-Function Mutation in a Plant Disease Resistance Gene Leads to Constitutive Activation of Downstream Signal Transduction Pathways in suppressor of npr1-1, constitutive 1. *The Plant Cell* **15**: 2636-2646
- Zhao H, Eide DJ** (1997) Zap1p, a metalloregulatory protein involved in zinc-responsive transcriptional regulation in *Saccharomyces cerevisiae*. *Molecular and Cellular Biology* **17**: 5044-5052
- Zhu J-K** (2016) Abiotic Stress Signaling and Responses in Plants. *Cell* **167**: 313-324
- Zschiesche W, Barth O, Daniel K, Böhme S, Rausche J, Humbeck KC** (2015) The zinc-binding nuclear protein HIP3 acts as an upstream regulator of the salicylate-dependent plant immunity pathway and of flowering time in *Arabidopsis thaliana*. *New Phytologist* **207**: 1084-1096



- Zumajo-Cardona C, Pabón-Mora N** (2016) Evolution of the APETALA2 Gene Lineage in Seed Plants. *Molecular Biology and Evolution* **33**: 1818-1832



# Summary

Zn is an essential element for life and the second most abundant transition element in all organisms. Zn deficiency is one of most widespread micronutrient deficiencies in soils and plants need to cope with it. Plants are able to sense the shortage of Zn supply and adjust their Zn homeostasis accordingly. In this thesis, I explored the genetic architecture of the Zn deficiency response of *Arabidopsis thaliana*. I initiated functional analyses on some of the Zn transporter genes long known to be transcriptionally induced by Zn deficiency, but so far not investigated in much detail. Soon after the exposure to Zn deficiency the expression of these transporters is first induced in roots and later in shoots. Each Zn transporter gene is expressed in one, or more, specific root cell layer(s), which location may differ, depending on the root part. These transporters showed partial functional redundancy among them, which makes it difficult, if not impossible, to detect particular Zn deficiency phenotypes in single Zn transporter mutants (**Chapter 2**). Considering that the effect of mutations on Zn transporter genes is difficult to detect, the Zn deficiency response can be studied from the perspective of their regulatory components. In the search of these regulators I found that the disruption of the *N-ALPHA-TERMINAL ACETYLTRANSFERASE 25 (NAA25)* gene, involved in N-terminal-acetylation of proteins, causes a strong Fe deficiency sensitivity and a slightly, but consistently, higher expression of several Zn deficiency responsive genes upon Zn sufficiency, when compared to wild-type plants. The causes for the unusual expression pattern of these genes still remain unknown. One hypothesis I postulate is that the lack of N-terminal acetylation of the Zn deficiency regulators bZIP19 and bZIP23, which are possible targets N-terminal acetylation, alters their regulatory activity (**Chapter 3**).

To identify more unconventional genetic players underlying the Zn deficiency response, that is not the known suspects involved in Zn homeostasis, such as the transporter genes, the bZIP19/23 transcription factors or the genes involved in Zn chelation, I investigated the natural variation for the Arabidopsis ionome of plants grown under Zn deficiency, in a genome wide association approach (**Chapter 4**). The loss of function of seven genes, identified in this approach, each causes an increase in ionome profile changes due to Zn deficiency, some of the element concentrations significantly affected by the loss of function of these genes are those for Fe, Mn and Cu. The identified genes are involved in various, diverse, functions such as microtubule organization during cell division, defence against pathogens, control of the circadian clock, Fe storage and phosphorylation of carbohydrates. Thus, their role in Zn deficiency response can be direct or mediated. The genome wide association study also identified a cluster of five tandemly arrayed genes, encoding for HEAVY METAL-

ASSOCIATED ISOPRENYLATED PLANT PROTEINS (HIPPs). Functional analyses of these HIPPs suggest they function as negative plant-growth regulators induced by Zn and Fe deficiency (**Chapter 5**). Single *hipp* mutant lines are tolerant to Zn and especially Fe deficiency, while constitutive overexpression of HIPP10 reduces plant size. Yeast 2-hybrid analysis identified several transcription factors to interact with one or more HIPPs, suggesting these HIPPs to be part of a regulatory network controlling plant growth in response to adverse Zn and Fe supply.

In conclusion, this thesis contributes to our understanding of the complexity of the Arabidopsis Zn deficiency response, with analysis of obvious and much less obvious genetic factors contributing to the Zn deficiency response. While again a small part of the puzzle is completed, several new leads are uncovered in this thesis, which would be of great interest to follow up on. Such investigations are likely to bring us one step further in improving the Zn content of plant products and the Zn deficiency tolerance of crops.



## Acknowledgments

Seven years ago I moved to The Netherlands to pursue a Master's degree, and afterwards I decided to stay doing my PhD. Time flew, and I could not have accomplished this journey without all the wonderful people around me.

I would like to thank my promotor Mark for helping me to learn and understand so much during my PhD. Mark, you always found time to discuss my results or doubts about the experiments. I truly appreciate your guidance, encouragement and patience, along the ups and downs during my PhD. I also would like to thank my co-promotor Maarten for the comments and advice on my research. Maarten, your positive attitude and kindness were very motivating.

The experiments showed in this thesis could not have been done without the help of several people. Thanks Henk, Corrie, Frank, Ana Carolina, Ana A, and Joost v/d H from the Laboratory of Genetics; Richard, Alice, and Tjitske from the Laboratory of Biosciences; Patrick from the Laboratory of Entomology; Eric and Markus from the University of Heidelberg; and David, Paula and John from the University of Nottingham, for your contribution to this thesis in the experiments and data analysis. I also had the opportunity to supervise PhD, MSc and BSc students, who helped me to perform several experiments. Jeroen, María, Aron, Cindy, Aaliya and Jos thanks for the effort and enthusiasm while working with me in this thesis.

The Genetics group has been a great place to work due to all its members. Thanks Ana Carolina, Andrew, Anneloes, Arjan, Bas, Bertha, Charles, Cris, Duur, Diego, Edouard, Erik, Florian, Fons, Gabriella, Hans, Jelle, Jitpanu, Jose, Justin, Klaas, Krithi, Kim, Lennart, Margo, Mathijs, Mark Z, Mina, Mohamed, Pádraic, Pingping, Ramón, René, Roel, Ross, Roxanne, Sijmen, Sabine, Sarah, Tom, Tina, Vanessa and Yanli for making my time in the Genetics group really enjoyable, for all conversation over lunches, coffee breaks, all the fun in our “lab-uitjes”, Christmas dinners, and other social events.

Wyske and Corrie, thank you for being there for me every time I needed you during these years. Robert and Tânia, my two post-docs, it was such a pleasure to meet you both. I am grateful for your friendship, guidance, and our chats. In addition, we could always comfort each other about the struggles with our hydroponics experiments.

During my PhD I met wonderful people and made great friends. Aina, Alex, Alexander, Ana, Ana Paula, André, Amalia, Aranka, Chara, Elise, Eric, Giovanni, Greice, Jianhua, Jose H, Jose M, Paola, and Phoung, thanks for the fun and the time shared during dinners, picnics, trips, tennis training, races, game nights, and so much more.

Bea, Claudio, Lidia, Tânia, and Luchito, thank you for your invaluable friendship, companionship, advice, and laughs. Ineke and Martien, I was very lucky to live in your house. You made me feel at home, not just in a house. I truly enjoyed our dinners and long chats. You were all like family to me in a country where I had none. I will keep you all in my heart.

Finally, I would like to thank my family for being always there for me somehow. Dani, thank you for your help in my experiments and for your support especially during this last stretch of my PhD. I am happy you decided to come with me to Ecuador and I look forward to our years ahead. Maricela, Germán y Edwin gracias por su cariño y compañía en los veranos y navidades en España, me hicieron sentir en casa aun estando tan lejos de ella. A mis padres, Elena y Juan, gracias por el amor, apoyo y confianza incondicional que siempre me han dado. Todo lo que he alcanzado en la vida se lo debo a ustedes. Por eso con todo mi cariño les dedico esta tesis.



## Curriculum Vitae

Andrea Valeria Ochoa Tufiño was born on 24 August, 1984 in Pallatanga, Ecuador. She spent her childhood in her grandparents farm, where her fascination for plants began. In 2002 she obtained her high school degree at Colegio Nacional Natalia Jarrín in Cayambe and moved to San Rafael to study Biotechnology Engineering. In her graduation research, Valeria studied the genetic variation of *Polylepis*, a high-altitude native tree. In 2008, Valeria graduated at Universidad de las Fuerzas Armadas-ESPE, and started to work as a lecturer and research assistant. In 2011, after obtaining a scholarship to study abroad, she decide to pursue a Master's degree in Plant Biotechnology at Wageningen University. Her master's research was conducted in the laboratory of Genetics, and it was about the characterization of a gene involved in heavy metals tolerance and accumulation in *Noccaea caerulescens*. In 2013, she obtained a grant for her PhD research and started it in Wageningen University, at the Laboratory of Genetics under the supervision of Prof. Dr Mark Aarts and Prof. Dr Maarten Koorneef, which has led to this thesis.

## Publications

**Ochoa, V.**, Jadán, M., Jiménez, P., Segovia, C. and Proaño, K. (2008). Population genetics of *Polylepis pauta* and *Polylepis incana* in Papallacta with ISSRs. *Ciencia y Tecnología* 1:71-79.

**Ochoa AV**, Almira M, van Duynhoven A, Aarts MGM. Uncovering Zn transporters induced by Zn deficiency. *In preparation*

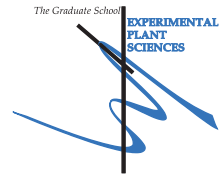
**Ochoa AV**, Campos AC, van den Heuvel J, Assunção AGL, Linster E, Wirtz M, Aarts MGM. Disruption of N-terminal-acetylation disturbs mineral homeostasis in *Arabidopsis thaliana*. *In preparation*

**Ochoa AV**, Campos AC, van den Heuvel J, Wolfkamp J, Danku J, Salt DE, Aarts MGM. Exploring *Arabidopsis thaliana* natural genetic variation to identify genes underlying the Zn deficiency response. *In preparation*

**Ochoa AV**, Aaliya K, Meeussen J, Aarts MGM. A conserved cluster of tandemly arrayed HIPP genes affects tolerance to Fe and Zn deficiency in *Arabidopsis thaliana*. *In preparation*

# Education Statement of the Graduate School

## Experimental Plant Sciences



Issued to: **Andrea Valeria Ochoa Tufiño**  
 Date: **05 October 2018**  
 Group: **Laboratory of Genetics**  
 University: **Wageningen University & Research**

1) Start-up phase	<u>date</u>
► <b>First presentation of your project</b> Analysis of the regulatory network of Zn in <i>Arabidopsis thaliana</i>	Jan 2014
► <b>Writing or rewriting a project proposal</b> Analysis of the regulatory network of Zn in <i>Arabidopsis thaliana</i>	Dec 2013
► <b>Writing a review or book chapter</b>	
► <b>MSc courses</b>	
► <b>Laboratory use of isotopes</b>	

Subtotal Start-up Phase 6.5 credits \*

2) Scientific Exposure	<u>date</u>
► <b>EPS PhD student days</b> EPS PhD student day 'Get2Gether', Soest, The Netherlands EPS PhD student day 'Get2Gether', Soest, The Netherlands	29-30 Jan 2015 28-29 Jan 2016
► <b>EPS theme symposia</b> EPS Theme 3 Symposium 'Metabolism and Adaptation', Wageningen, The Netherlands EPS Theme 4 Symposium 'Genome Biology', Wageningen, The Netherlands EPS Theme 3 Symposium 'Metabolism and Adaptation', Wageningen, The Netherlands EPS Theme 4 Symposium 'Genome Biology', Amsterdam, The Netherlands EPS Theme 3 Symposium 'Metabolism and Adaptation', Amsterdam, The Netherlands EPS Theme 3 Symposium 'Metabolism and Adaptation', Wageningen, The Netherlands	11 Mar 2014 03 Dec 2014 10 Feb 2015 15 Dec 2015 23 Feb 2016 14 Mar 2017
► <b>National meetings (e.g. Lunteren days) and other National Platforms</b> Annual meeting 'Experimental Plant Sciences', Lunteren, The Netherlands Annual meeting 'Experimental Plant Sciences', Lunteren, The Netherlands Annual meeting 'Experimental Plant Sciences', Lunteren, The Netherlands Annual meeting 'Experimental Plant Sciences', Lunteren, The Netherlands	14-15 Apr 2014 13-14 Apr 2015 11-12 Apr 2016 10-11 Apr 2017
► <b>Seminars (series), workshops and symposia</b> <i>Startsymposium:</i> Plant Developmental Biology, Wageningen, The Netherlands <i>Seminar Series:</i> Genetic Seminar Series (weekly) <i>Seminar:</i> Ionomics - Genomics of mineral nutrients and trace elements in plant - David Salt, Amsterdam, The Netherlands <i>Seminar:</i> On Bees, Pollination and Food Security - Koos Biesmeijer, Wageningen, The Netherlands <i>Seminar:</i> Genetics and epigenetics: a complex relationship - Ortrun Mittelsten Scheid, Wageningen, The Netherlands <i>Seminar:</i> The evolutionary significance of gene and genome duplications - Yves van de Peer, Wageningen, The Netherlands <i>Seminar:</i> Identification of a new sensory neuron membrane gene and why phylogenomics is important - Alexie Papanicolaou, Wageningen, The Netherlands <i>Seminar:</i> Dynamics of Adaptation and Genome Evolution in a Long-Term Experiment - John Hanna, Wageningen, The Netherlands	14 Oct 2013 2013-2017 23 Oct 2014 18 Dec 2014 19 Nov 2014 03 Feb 2015 22 Jun 2017 31 Aug 2017
► <b>Seminar plus</b>	
► <b>International symposia and congresses</b> Agronomic, Molecular Genetics and Human Nutrition Approaches for Improving the Nutritional Quality and Safety of Food Crops Conference, Antalya, Turkey LOCOMET international network (GDRI CNRS) meeting, Lille, France 26th International Conference on Arabidopsis Research (ICAR), Paris, France 4th International Zinc Symposium: Improving Crop Production and Human Health, Sao Paulo, Brazil 27th International Conference on Arabidopsis Research (ICAR), Gyeongju, South Korea LOCOMET international network (GDRI CNRS) meeting, Lille, France XVIII International Plant Nutrition Colloquium (IPNC), Copenhagen, Denmark	17-19 Mar 2014 02-04 Jul 2014 05-09 Jul 2015 15-17 Sep 2015 29 Jun-03 Jul 2016 07-08 Jul 2016 21-24 Aug 2017

<b>► Presentations</b> <i>Poster:</i> Agronomic, Molecular Genetics and Human Nutrition Approaches for Improving the Nutritional Quality and Safety of Food Crops Conference, Antalya, Turkey <i>Poster:</i> Annual meeting 'Experimental Plant Sciences', Lunteren, The Netherlands <i>Poster:</i> 26th International Conference on Arabidopsis Research (ICAR), Paris, France <i>Poster:</i> 27th International Conference on Arabidopsis Research (ICAR), Gyeongju, South Korea <i>Talk:</i> 4th International Zinc Symposium: Improving Crop Production and Human Health, Sao Paulo, Brazil <i>Talk:</i> LOCOMET international network (GDRI CNRS) meeting, Lille, France <i>Talk:</i> EPS Theme 3 Symposium 'Metabolism and Adaptation', Wageningen, The Netherlands <i>Talk:</i> Annual meeting 'Experimental Plant Sciences', Lunteren, The Netherlands <i>Talk:</i> XVIII International Plant Nutrition Colloquium (IPNC), Copenhagen, Denmark <b>► IAB interview</b> <b>► Excursions</b>	17-19 Mar 2014 13-14 Apr 2015 05-09 Jul 2015 29 Jun-03 Jul 2016 15-17 Sep 2015 07-08 Jul 2016 14 Mar 2017 10-11 Apr 2017 21-24 Aug 2017
--	---

*Subtotal Scientific Exposure*      25.1 credits \*

<b>3) In-Depth Studies</b> <b>► EPS courses or other PhD courses</b> Transcription Factors and Transcriptional Regulation, Wageningen, The Netherlands School of Plant Metallomics, Copenhagen, Denmark Introduction to R for Statistical Analysis, Wageningen, The Netherlands Genome Assembly, Wageningen, The Netherlands Basic Statistics, Wageningen, The Netherlands Linear Models, Wageningen, The Netherlands Generalized Linear Models, Wageningen, The Netherlands Mixed Linear Models, Wageningen, The Netherlands Image Analysis for Plant Phenotyping, Wageningen, The Netherlands <b>► Journal club</b> Group of Plant Genetics <b>► Individual research training</b>	<u>date</u> 17-19 Dec 2013 27-31 Jan 2014 23-24 Oct 2014 28-29 Apr 2015 20-27 May 2015 08-10 Jun 2015 15-16 Jun 2015 22-23 Jun 2015 12-15 Jul 2016  2013-2016
--	--

*Subtotal In-Depth Studies*      9.5 credits \*

<b>4) Personal development</b> <b>► Skill training courses</b> PhD Competence Assessment, Wageningen, The Netherlands Techniques for Writing and Presenting a Scientific Paper, Wageningen, The Netherlands Scientific Writing, Wageningen, The Netherlands Adobe Indesign Essential Training, Wageningen, The Netherlands <b>► Organisation of PhD students day, course or conference</b> <b>► Membership of Board, Committee or PhD council</b>	<u>date</u> 04-19 Nov 2014 14-17 Oct 2014 Nov 2016 - Jan 2017 09-10 Oct 2017
--	--

*Subtotal Personal Development*      3.7 credits \*

<b>TOTAL NUMBER OF CREDIT POINTS</b>	<b>44.8 credits *</b>
Herewith the Graduate School declares that the PhD candidate has complied with the educational requirements set by the Educational Committee of EPS which comprises of a minimum total of 30 ECTS credits	
* A credit represents a normative study load of 28 hours of study.	



The research described in this thesis was carried out at Laboratory of Genetics at Wageningen University, Wageningen, The Netherlands, and was financially supported by the Ecuadorian government through SENESCYT (Secretaría de Educación Superior, Ciencia, Tecnología e Innovación) and Universidad de las Fuerzas Armadas-ESPE.

## **Colophon**

Cover design and thesis layout by: Andrea Valeria Ochoa Tufiño

Printed by: ProefschriftMaken